Synthesis, characterization and thermal studies of cyclometalated palladium and platinum complexes derived from chalcogen ligands

By

Siddhartha Kolay

(CHEM01200904004)

BHABHA ATOMIC RESEARCH CENTRE

A thesis submitted to the

Board of Studies in Chemical Sciences

In partial fulfillment of requirements

For the degree of

DOCTOR OF PHILOSOPHY

of

HOMI BHABHA NATIONAL INSTITUTE

August 2016

Homi Bhabha National Institute

Recommendations of the Viva Voce Board

As members of the Viva Voce Board, we certify that we have read the dissertation prepared by **Siddhartha Kolay** entitled "**Synthesis, characterization and thermal studies of cyclometalated palladium and platinum complexes derived from chalcogen ligands**" and recommend that it may be accepted as fulfilling the dissertation requirement for the Degree of Doctor of Philosophy.

Date:

Chairman: Dr. S. Kannan

Date:

Guide: Dr. V. K. Jain 12/8/2016

Date:

Co-guide Dr. D. Das 12/8/2016

Date:

Member 1: Dr. S. R. Bharadwaj 12/8/2016

Date:

Member 2: Dr. Sunil Ghosh 12/8/2016

Date:

Member 3: Dr. Sandip Dey 12.08.2016

Date:

External Reviewer: Prof. H. B. Singh

Final approval and acceptance of this dissertation is contingent upon the candidate's submission of the final copies of the dissertation to HBNI.

I hereby certify that I have read this dissertation prepared under my direction and recommend that it may be accepted as fulfilling the dissertation requirement.

Guide: Dr. V. K. Jain 12/8/2016 Date:

Co-guide: Dr. D. Das 12/8/2016 Date:

STATEMENT BY AUTHOR

This dissertation has been submitted in partial fulfilment of requirements for an advanced degree at Homi Bhabha National Institute (HBNI) and is deposited in the Library to be made available to borrowers under rules of the HBNI.

Brief quotations from this dissertation are allowable without special permission, provided that accurate acknowledgement of source is made. Requests for permission for extended quotation from or reproduction of this manuscript in whole or in part may be granted by the Competent Authority of HBNI when in his or her judgment the proposed use of the material is in the interests of scholarship. In all other instances, however, permission must be obtained from the author.

Siddhartha Kolay

(Siddhartha Kolay)

DECLARATION

I, hereby declare that the investigations presented in this Thesis has been carried out by me. The work is original and has not been submitted earlier in whole or part for a degree / diploma to this or any other Institution / University.

Siddhartha Kolay

(Siddhartha Kolay)

Dedicated to...

Family

Acknowledgements

As I have completed my thesis work, it is a pleasure to thank those who knowingly or unknowingly contributed to make this thesis possible. First and foremost, I am thankful from the bottom of my heart and soul, to my guide Prof. (Dr.) V. K. Jain, Head, Chemistry Division, whose constant encouragement, guidance and support throughout the study enabled me to develop an understanding of the subject and pursue it. His constant motivation, fruitful suggestions and excellent guidance, inspired me to carry out and complete this work. Without his support, encouragement and guidance, this work would have not been possible. I take this opportunity to thank Dr. B. N. Jagatap, Director, Chemistry Group for his constant encouragement to carry out this work.

My research work would not have taken the present form without guidance, help and support from my co-guide Dr. D. Das.

I am thankful to my senior colleagues, Dr. G. Kedarnath, Dr. Liladhar Kumbhare, Dr. Goutam Kolay, Dr. S. Dey, Dr. Prasad Phadnis and Dr. Manideepa Basu for their constant support.

I express my sincere thanks to Shri Amey Wadawale, Chemistry Division, BARC, Dr. Mukesh Kumar, Solid State Physics Division, BARC, Dr. S. N. Achary, Chemistry Division, BARC for providing X-ray crystallographic analyses. I am grateful to Dr. R. B. Sunoj, IIT, Mumbai, Dr. C. Majumder, Chemistry Division, BARC, Dr. S. Nigam, Chemistry Division, BARC and Mr. H. K. Kisan, IIT, Mumbai for the theoretical calculations for characterizations of some complexes.

I am also thankful to my friends Adish, Vivek, Dilip, Pravin, Ninad, Rakesh and Rohit for keeping the spirits high in lab. I am also thankful to Mr. P. B. Sonowane, Mr. A. D. Parmar, Mr. Gopal, Supriya madam for their crucial help in laboratory upkeep and Chemistry Division office staffs for their administrative support.

I express my sincere gratitude to Mr. Kamal Chaudhari,Mr. Manoj Pal, and Mrs. Nisha Kushwah for recording NMR spectra. I owe a lot to Mr. Amey Wadawale, for solving crystal structures. I am thankful to Mrs. Alpa Shah, Mr. Suresh Chopade for elemental analysis of the studied complexes. I am thankful to Dr. S. R. Bharadwaj and Dr. K. Bhattacharyya for recording the XPS data of one sample.

I wish to thank doctoral committee members for their help and suggestions.

Finally, I convey my heartfelt gratitude to my parents, wife, brother and sister who have always encouraged me. Their inspiration, encouragement, blessings and support have helped me to achieve what I am today.....

Siddhartha Kolay

(Siddhartha Kolay)

Abbreviations

PPh_3	=	triphenylphosphine
OAc	=	acetate
E	=	nitrogen, phosphorus, arsenic, sulfur, selenium, tellurium
X	=	halogen
Mes	=	mesityl (2, 4, 6-trimethylphenyl)
Ph	=	phenyl
o-tol	=	$2\text{-}MeC_6H_4$
Epy	=	pyridine-2-chalcogenolate

Publications

Journal papers

1. Binuclear orthometalated N, N-dimethylbenzylamine complexes of palladium(II): Synthesis, structure and thermal behavior
   Siddhartha Kolay, N. Ghavale, A. Wadawale, D. Das and V. K. Jain,
   Phosphorus, Sulfur, and Silicon and the Related Elements, 188 (2013) 1449-1461.

2. Cyclopalladation of dimesityl selenide: syntheis, reactivity, structural characterization, isolation of an intermediate complex with C-H…Pd intra-molecular interaction and computational studies
   Siddhartha Kolay, A. Wadawale, D. Das, H. K. Kisan, R. B. Sunoj and V. K. Jain, *Dalton Trans.*, 42 (2013) 10828-10837.

3. Cyclopalladation of telluro ether ligands: Synthesis, reactivity and structural characterization
   Siddhartha Kolay, M. Kumar, A. Wadawale, D. Das and V. K. Jain,
   Dalton Trans., 43 (2014) 16056-16065.

4. Role of anagostic interactions in cycloplatination of telluro ethers: Synthesis and structural characterization
   Siddhartha Kolay, M. Kumar, A. Wadawale, D. Das and V. K. Jain,
   J. Organometal. Chem., 794 (2015) 40-47.

5. Platinum mediated activation of coordinated organonitriles by telluroethers in THF: Isolation, structural characterization and DFT analysis of intermediate complexes
   Siddhartha Kolay, A. Wadawale, S. Nigam, M. Kumar, C. Majumder, D. Das and V. K. Jain,
   Inorg. Chem. 54 (2015) 11741−11750.

6. Synthesis, structures and thermal behaviour of cyclopalladated 1,1′-dithiolate complexes
   Siddhartha Kolay, A. Wadawale, D. Das and V. K. Jain,
   Manuscript under preparation

Conferences

1. Cyclopalladation of telluro ether: Synthesis and structural investigation
   Siddhartha Kolay, M. Kumar, A. Wadawale, D. Das and V. K. Jain
   5th Interdisciplinary Symposium on Materials Chemistry, December 9-13, 2014, Bhabha Atomic Research Centre, Mumbai, Page: 460.

2. Cyclometalation of seleno and telluro ether ligands
   Siddhartha Kolay, A. Wadawale, D. Das and V. K. Jain
   National Conference on Chemistry of Chalcogens and Related Topics (NC3-2015), Defence Institute of Advanced Technology (DIAT), Pune; 12-13 January, 2015.

3. Synthesis and thermochemical studies of platinum group metal complexes derived from organochalcogen ligands
   Siddhartha Kolay and D. Das
   27th Research Scholars Meet-2015; Indian Chemical Society (Mumbai Branch) and Sathaya College, Mumbai, 20-21 February, 2015.

Table of contents

Synopsis

Homi Bhabha National Institute

Ph. D. PROGRAMME

1.	**Name of the Student:**	**Siddhartha Kolay**
2.	**Name of the Constituent Institution:**	Bhabha Atomic Research Centre
3.	**Enrolment No. :**	CHEM01200904004
4.	**Title of the Thesis:**	**Synthesis, characterization and thermal studies of cyclometalated palladium and platinum complexes derived from chalcogen ligands**
5.	**Board of Studies:**	Chemical Sciences, HBNI

Synopsis

The chemistry of platinum group metal complexes has witnessed a rapid growth in the last half century owing to the ease of synthesis, rich reaction chemistry and wide applications in diverse areas. Among them cyclometalated compounds represent an interesting family of organometallic compounds [1]. Since the early study of Cope and Siekman in 1965, cyclometalation of organic ligands has emerged as one of the most important reactions in organometallic chemistry and provide a straightforward entry to organometallic compounds that feature a metal-carbon σ-bond. The growing interest in these compounds may be attributed to their applications in organic synthesis [2], catalysis (e.g. $[Pd_2(\mu\text{-}OAc)_2\{o\text{-}tol_2PC_6H_4CH_2\text{-}o\}_2]$ (*o*-tol = *ortho*-tolyl)) [3], materials science [4] as well as due to their rich reaction chemistry [1]. The cyclometalated complexes are also encountered as reaction

intermediates in many organic transformations. Over a period, a myriad of internally functionalized organic compounds containing the neutral donor atom (e.g. N, P, As, O, S) have been utilized for cyclometalation reactions leading to the formation of, in general, a four electron C-anionic donor ligand (C⌒Y). Although several mechanisms have been proposed for the cyclometalation reaction, it is generally believed that initially a ligand is coordinated to the metal centre through a neutral donor atom and in this intermediate species, the C-H bond is activated only when it is within the metal coordination plane (Scheme-1) [5]. Although such intermediates are seldom isolated, their existence can be inferred.

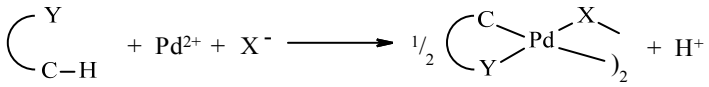

(X = Cl or OAc; Y = N, P, As, S donor atoms;
C-H = sp, sp^2, sp^3 carbon)

Scheme 1. Cyclopalladation of organic ligands

The utility of cyclometaladed complexes in materials science, particularly as mesogens, luminescence materials and single source precursors for phase pure inorganic materials, is growing rapidly. The progress for the latter application has however been hampered due to non-availability of suitable precursors as well as lack of understanding of thermo-physical properties of such complexes. In view to develop precursors for metal chalcogenides, cyclometalation reactions of chalcogen ligands have been investigated and the thermo-physical properties for some representative complexes have been studied during this doctoral program. Among group 16 donors, metalation of oxygen and sulfur compounds are well documented. However, with heavier chalcogen compounds, metalation of only a few organo-selenium ligands (Bu^tSeCH_2Ph [6]) has been described recently, whereas there is hardly any report on metalation of tellurium ligands.

The thesis is divided into four chapters, *viz.*, introduction, experimental, results and discussion and summary and conclusions, followed by references.

Chapter 1: Introduction

This chapter deals with a general introduction about palladium and platinum and their chemistry. A short discussion about cyclometalation reactions followed by suitable reaction conditions for cyclometalation and their applications as luminescent and liquid crystal materials, in catalysis and biology are given. A brief overview about the chalcogen series is also mentioned. A brief overview about the thermal decomposition of organochalcogen complexes relevant to the preparation of Pd/Pt metal chalcogenides is also included followed by the scope and plan of the present work. Relevant literature references are given in bibliography at the end of the thesis.

Chapter 2: Experimental

In this chapter, materials and methods used during the present study are described followed by discussion on analytical and instrumental techniques, *e.g.* IR, UV-vis, NMR, elemental analysis, XPS, TG-DTA, powder X-ray and single crystal X-ray diffraction analyses used during the course of the present investigation. Synthesis of various chalcogen ligands and palladium and platinum precursors used in the present work is described. Synthesis of new palladium and platinum complexes is presented in five sub-sections.

Chapter 3: Results and discussion

This chapter deals with the results obtained during the present investigation and include discussion on these findings. The chapter is divided into five sections. All the complexes have been characterized by elemental analysis, NMR (^{1}H, $^{13}C\{^{1}H\}$, $^{31}P\{^{1}H\}$,

$^{77}Se\{^{1}H\}$, $^{125}Te\{^{1}H\}$ and $^{195}Pt\{^{1}H\}$) spectroscopy and in some cases by IR, UV-vis absorption spectroscopy. Molecular structures of several complexes have been established unambiguously by single crystal X-ray diffraction analyses. The thermal decomposition of some complexes into metal chalcogenide nano-materials has also been carried out and the resulting products have been characterized by powder X-ray analysis.

The section **3.1** deals with the cyclopalladation of dimesityl selenide and its reactivity with thio- and seleno-pyridine (Scheme-2). The mechanistic path for the formation of cyclopalladated complex via the *ortho* C-H bond activation has been discussed together with the isolation of the intermediates. Mes_2Se on reaction with $[PdCl_2(PhCN)_2]$ in toluene yields chloro-bridged binuclear complex, $[Pd_2Cl_2(\mu\text{-}Cl)_2(Mes_2Se)_2]$ whereas with Na_2PdCl_4 in refluxing ethanol affords cyclometalated complex, $[Pd_2(\mu\text{-}Cl)_2\{MesSeC_6H_2(Me_2)CH_2\}_2]$. The latter can also be obtained from the former in refluxing ethanol. The molecular structures of both the complexes (Figure 1) were established by single crystal X-ray diffraction analysis. From the molecular structure it is evidence that the intra-molecular C–H···Pd agostic interaction ($d_{M\text{-}H}$: 2.75Å and $<_{C\text{-}H\cdots Pd}$: 111.23°) in $[Pd_2Cl_2(\mu\text{-}Cl)_2(Mes_2Se)_2]$ facilitates activation of C–H (sp^3) bond leading to metalation.

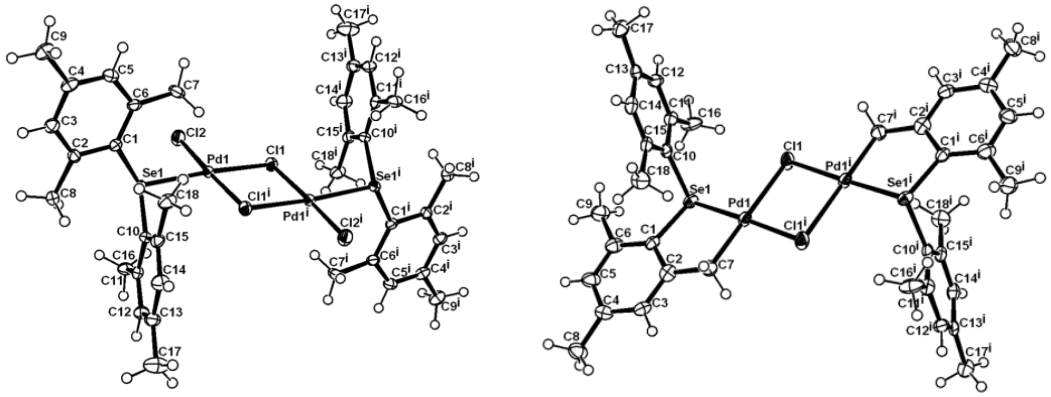

Figure 1. ORTEP drawing of (a) $[Pd_2Cl_2(\mu\text{-}Cl)_2(Mes_2Se)_2]$ and

(b) $[Pd_2(\mu\text{-}Cl)_2\{MesSeC_6H_2(Me_2)CH_2\}_2]$

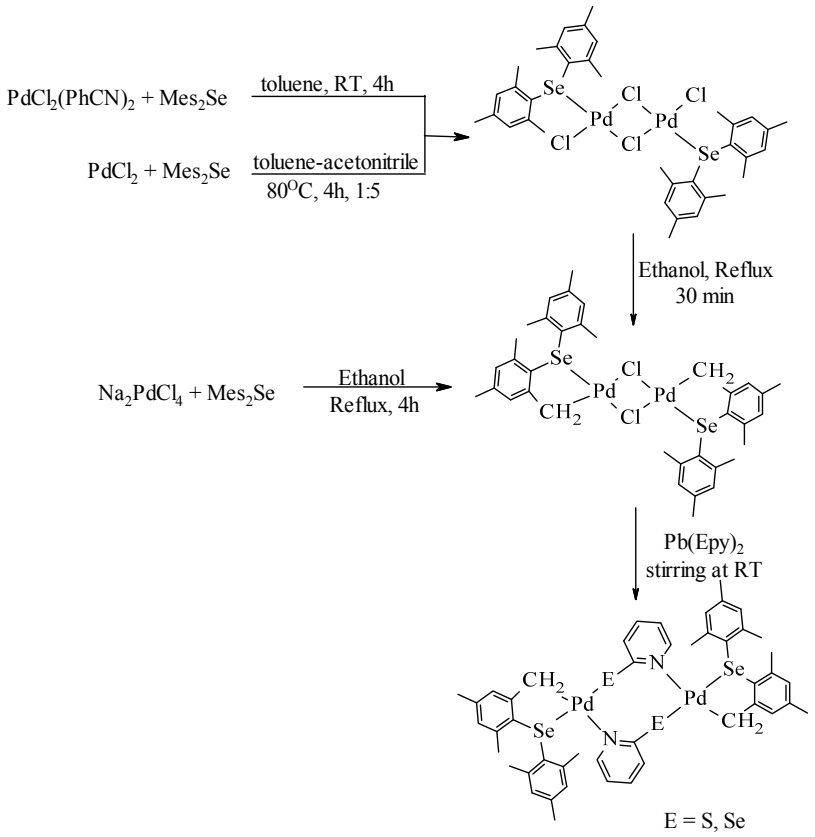

Scheme-2

The section **3.2** deals with the isolation of a number of complexes form in the reaction of telluro ethers with palladium precursors (Schemes-3 and 4). By subtle variation in reaction conditions a variety of complexes, such as addition complexes (e.g. *trans*-$[PdCl_2(TeMes_2)_2]$), complexes showing secondary Pd···H interactions (e.g. $[Pd_2(\mu\text{-}Cl)_2Cl_2(TeMes_2)_2]$), cyclometalated complexes (e.g. $[Pd_2(\mu\text{-}OAc)_2\{CH_2C_6H_2(4,6\text{-}Me_2)TeMes\}_2]$), complexes formed by Te-C bond cleavage (e.g. $[Pd(\mu\text{-}OAc)(\mu\text{-}TeMes)]_4$) have been isolated and structurally characterized. The complex with Pd···H secondary interaction on refluxing in polar solvent converts into cyclometalated product. It has been further observed that Mes_2Te, MesTetol-*o* and MesTePh all leads to cyclopalladated complexes when $[Pd(OAc)_2]_3$ is used as the palladating agent. In contrast, only Mes_2Te undergoes cyclometalation when Na_2PdCl_4 is used as the palladating agent. Thus telluroethers having at least one mesityl ring are

sufficient for cyclometalation with $[Pd(OAc)_2]_3$ via *ortho* C-H bond activation whereas comparatively bulky telluroether like Mes_2Te is required for Na_2PdCl_4. It has also been observed that the stability of $[Pd_2(\mu\text{-}Cl)_2\{CH_2C_6H_2(Me_2\text{-}4,6)TeMes\}_2]$ depends on temperature and leads to $[PdCl_2\{MesTeCH_2C_6H_2(4,6\text{-}Me_2)TeMes\}]$ on refluxing for 2 hr in polar solvent via Te-C bond cleavage. The molecular arrangement of $[PdCl_2\{MesTeCH_2C_6H_2(4,6\text{-}Me_2)TeMes\}]$ and $[Pd_2(\mu\text{-}OAc)_2\{CH_2C_6H_2(4,6\text{-}Me_2)Tetol\text{-}o\}_2]$ (Figure 2) have been determined by single crystal X-ray analysis.

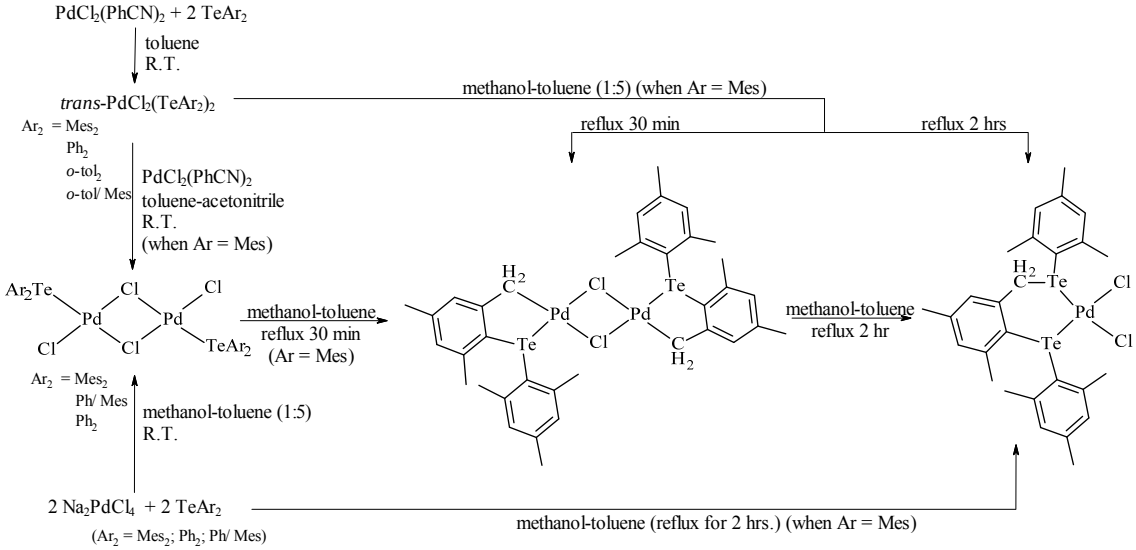

Scheme-3

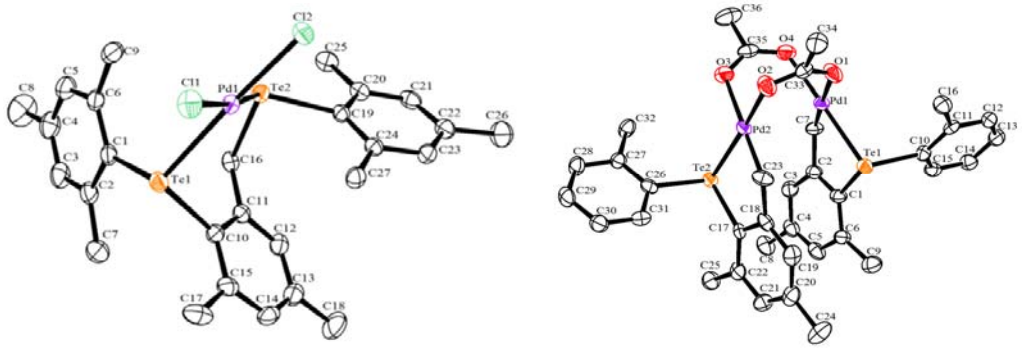

(a) (b)

Figure 2. ORTEP diagram of (a) $[PdCl_2\{MesTeCH_2C_6H_2(4,6\text{-}Me_2)TeMes\}]$ and (b) $[Pd_2(\mu OAc)_2\{CH_2C_6H_2(4,6\text{-}Me_2)Tetol\text{-}o\}_2]$

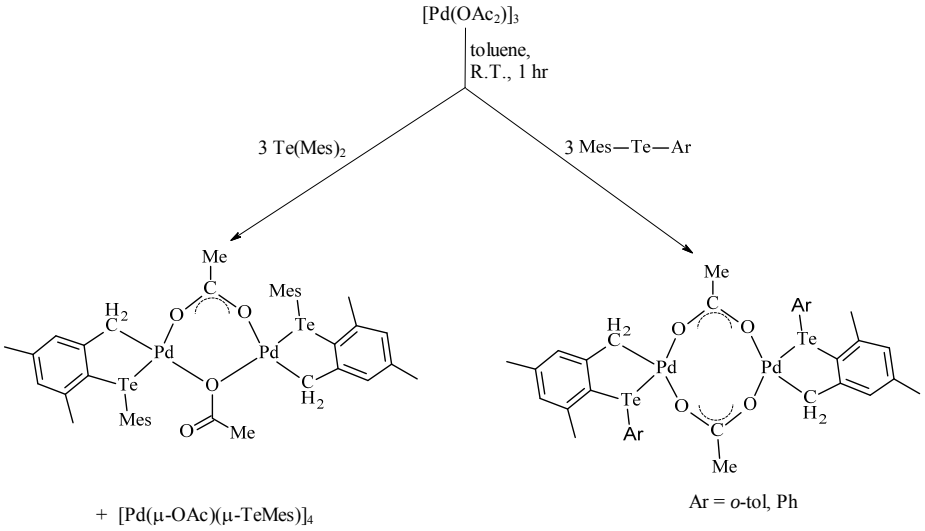

Scheme-4

The section **3.3** describes the role of anagostic interaction in the cycloplatination of telluroethers (Scheme-5). The reaction of K_2PtCl_4 with various telluro ethers in water-acetone mixture yields normal substitution product, $[PtCl_2(TeArAr')_2]$ (Ar/Ar′ = Ph_2, *o*-tol_2, Mes_2, Ph/Mes, *o*-tol/Mes). Among all the above mentioned complexes, only $[PtCl_2(TeMes_2)_2]$ in refluxing THF undergoes cyclometalation into mononuclear $[PtCl\{(CH_2C_6H_2Me_2$-4,6)TeMes$\}(TeMes_2)]$ via benzylic C-H (sp3) bond activation while all other complexes did not show any changes under identical reaction conditions. The molecular structures of *trans*-$[PtCl_2(TeMes_2)_2]$ (Figure 3(a), *trans*-$[PtCl_2(PhTeMes)_2]$, *trans*-$[PtCl_2(o$-tolTeMes$)_2]$, $[PtCl\{(CH_2C_6H_2Me_2$-4,6)TeMes$\}(TeMes_2)]$ (Figure 3(b)) have been determined by single crystal X-ray diffraction analyses. It has been noticed from the structures that with increasing steric demand of the telluroether the Pt···H distance decreases from 4.77Å (in case of MesTePh) to 2.45Å (in case of Mes_2Te). Hence, Pt···H interaction characterized as anagostic interaction is more prominent with sterically demanding telluroether and this interaction leads to the *ortho* C-H bond activation in case of Mes_2Te.

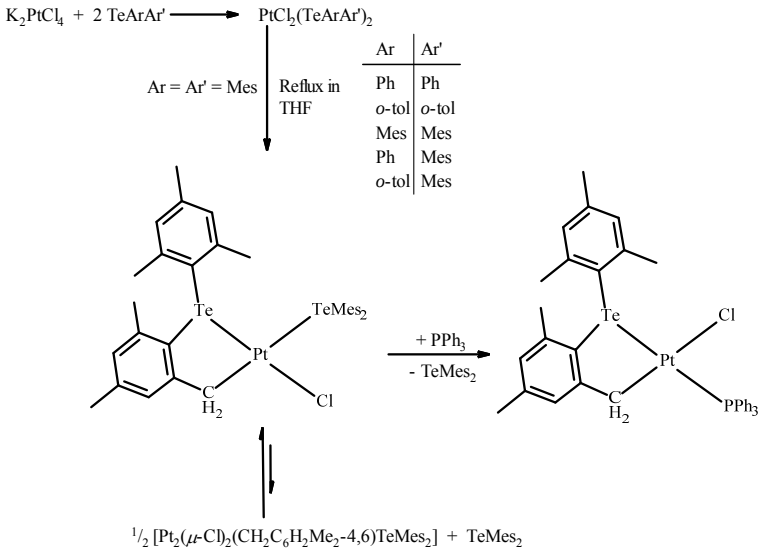

Scheme-5

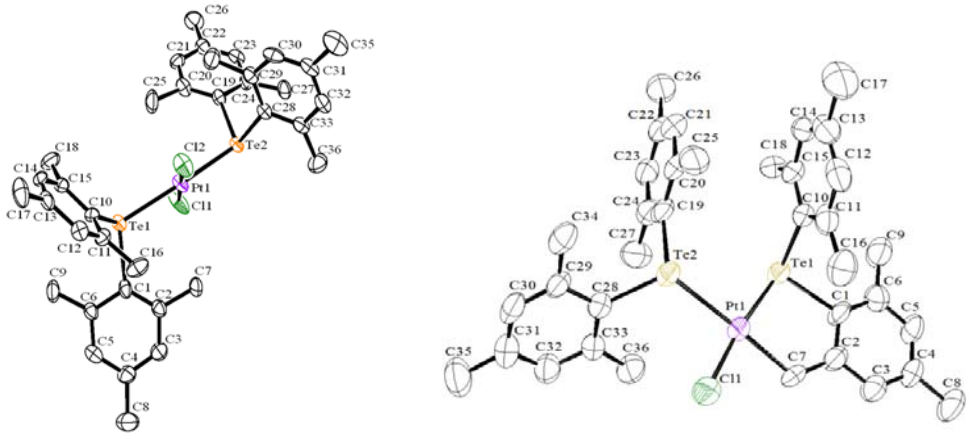

(a) (b)

Figure 3. ORTEP drawing of (a) $[PtCl_2(TeMes_2)_2]$ and (b) $[PtCl\{(CH_2C_6H_2Me_2\text{-}4,6)TeMes\}(TeMes_2)]$

The section **3.4** deals with platinum mediated activation of coordinated organonitriles by telluroethers in THF (Scheme-6). The reaction of $PtCl_2(PhCN)_2$ with various telluroethers (Mes_2Te, MesTetol-*o*) in dichloromethane yields the expected $[PtCl_2(TeArAr')_2]$. The reaction proceeds through a completely different path on changing the solvent from dichloromethane to THF. The reaction of $[PtCl_2(PhCN)_2]$ with $TeMes_2$ yields different

products depending on the duration of the reaction which was monitored by ^{125}Te NMR spectroscopy. The time dependent complexation chemistry indicates that initial reaction of telluroether takes place at the coordinated benzonitrile rather than at platinum centre leading to the formation of $[PtCl_2\{NC(O)Ph(TeMes_2)\}_2]$ followed by stepwise rearrangement into $[PtCl_2(TeMes_2)\{NC(O)Ph(TeMes_2)\}]$ and finally into $[PtCl_2(TeMes_2)_2]$. The above reactions path is also evaluated with other telluroethers like MesTetol-*o* and MesTePh and also with other organonitriles, $[PtCl_2(RCN)_2]$ (R = Me, 4-MeC_6H_4, 4-$CF_3C_6H_4$) differing in the nature of organic substituents. It has been further observed that these intermediate complexes can be isolated and characterized with only sterically demanding telluroether whereas with non-steriaclly hindered telluroethers, such intermediates might have formed, could not be detected and only the substitution products, *trans*-$[PtCl_2(TeArAr')_2]$ can be isolated. The XPS study on these intermediates indicates the presence of Te(IV) with strong secondary interaction with platinum (J(^{195}Pt-^{125}Te) = 309-347 Hz) and with carbonyl oxygen. The molecular structures of *trans*-$[PtCl_2\{NC(O)Ph(TeMes_2)\}_2]$ and *trans*-$[PtCl_2(TeMes_2)\{NC(O)Ph(TeMes_2)\}]$ (Figure 4) have been determined by single crystal X-ray diffraction analyses.

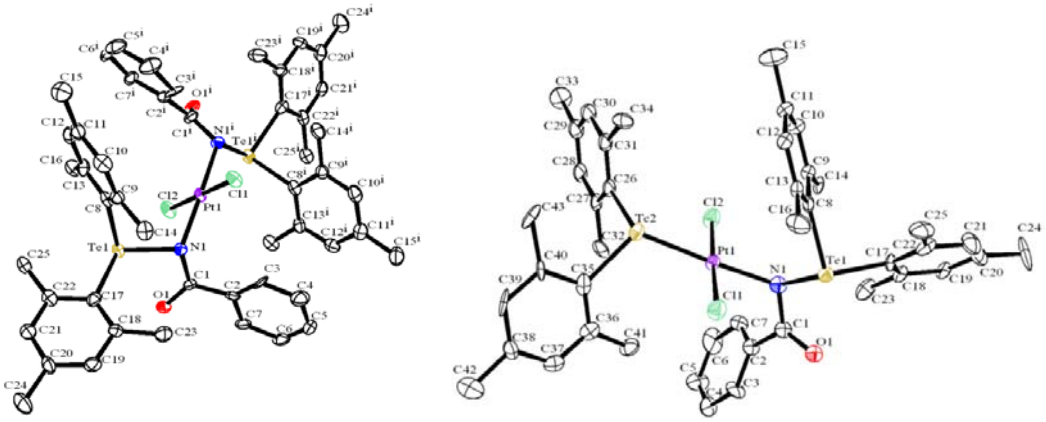

(a) (b)

Figure 4. ORTEP drawing of (a) *trans*-$[PtCl_2\{NC(O)Ph(TeMes_2)\}_2]$ and (b) *trans*-$[PtCl_2(TeMes_2)\{NC(O)Ph(TeMes_2)\}]$

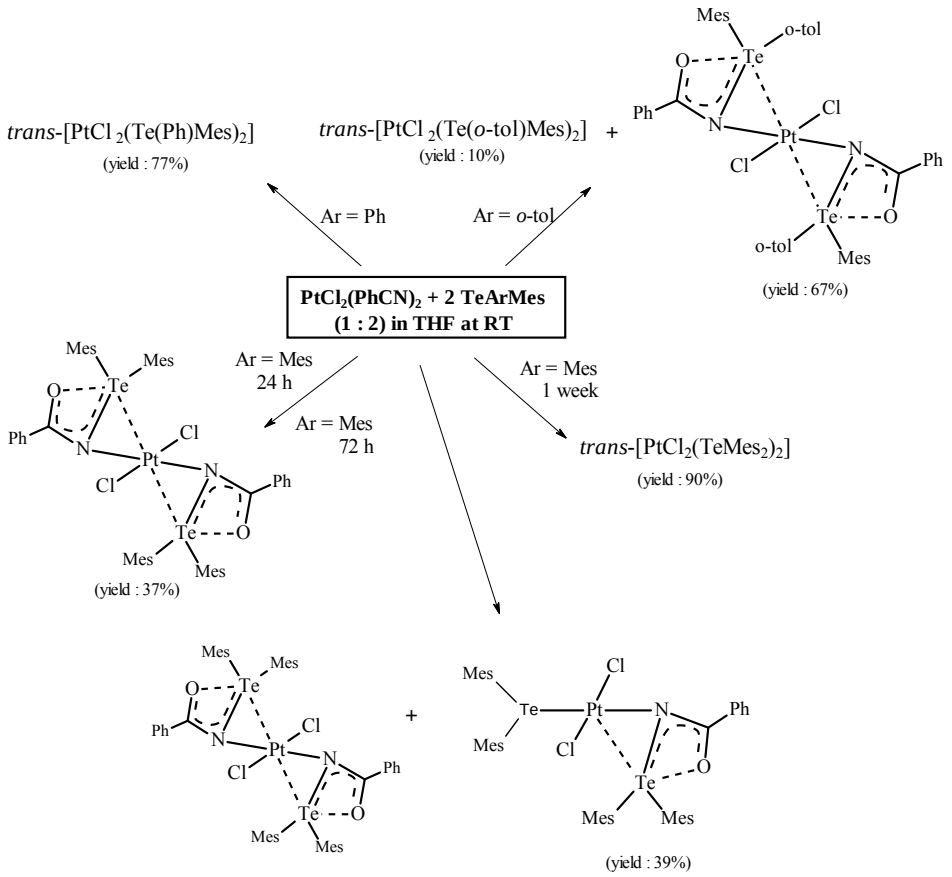

Scheme-6

The section **3.5** describes preparation of palladium chalcogenide nano-particles at low temperature by thermal decomposition of some of the cyclometalated complexes. The pyridylchalcogenolate bridged complexes, $[Pd_2(\mu\text{-}Epy)_2(Me_2NCH_2C_6H_4\text{-}C,N)_2]$ decomposed at ~220°C under inert atmosphere into a single phasic Pd_4S (in-case of E = S) and $Pd_{17}Se_{15}$ (in-case of E = Se) as confirmed from powder XRD analysis. The complex *trans*-$PdCl_2(TeMes_2)_2$ decomposed into Pd_7Te_3 on refluxing in xylene (Figure 5). Preparation of mixed ternary $PdSe_{0.51}S_{0.49}$ (Figure 6) material has also been discussed. The complex $[Pd_2(\mu\text{-}Cl)_2\{MesSeC_6H_2(Me_2\text{-}4,6)CH_2\}_2]$ gave $Pd_{17}Se_{15}$ at ~280°C on decomposition while the xanthate derivative, $[Pd\{CH_2C_6H_2(Me_2)SeMes\}(S_2CO^iPr)]$ yielded $PdSe_{0.51}S_{0.49}$ (Figure 6b) at ~ 300°C.

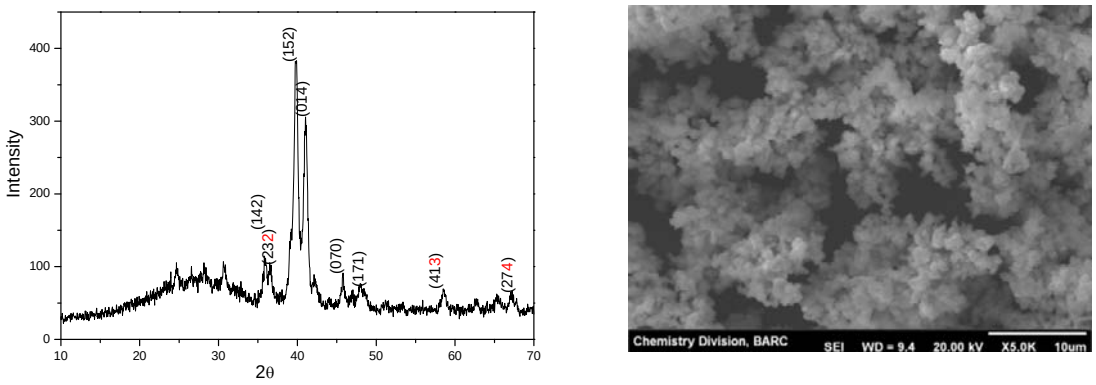

(a) (b)

Figure 5. (a) XRD pattern and (b) SEM image of Pd_7Te_3 obtained from *trans*-$PdCl_2(TeMes_2)_2$ in refluxing xylene

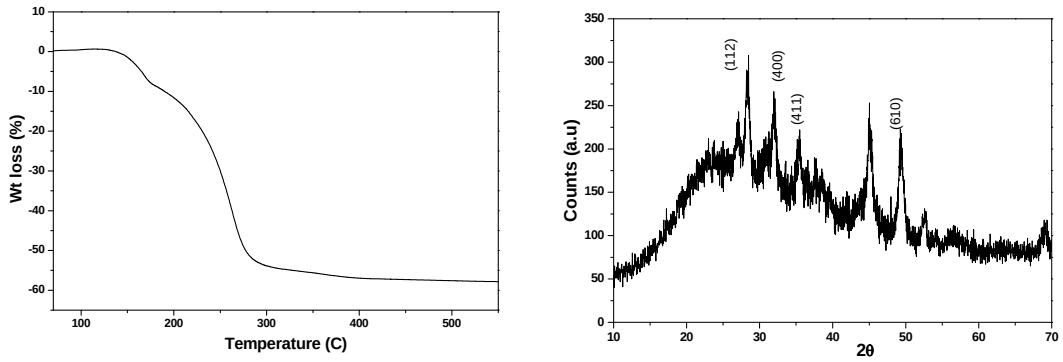

(a) (b)

Figure 6. (a) TG curve of [Pd{$CH_2C_6H_2(Me_2)SeMes$}(S_2CO^iPr)], (b) XRD pattern of $PdSe_{0.5}S_{0.5}$

Chapter 4: Summary and conclusions

This chapter gives summary and conclusions of the present investigation. The role of anagostic interaction prior to cyclometalation has been recognized. Such complexes have been isolated and structurally characterized. The facile cleavage of Te-C linkage has led to isolation of several other products while such derivates did not have any parallel with the organoselenium compounds. The reactions of $[PtCl_2(RCN)_2]$ with telluroether proceed

differently depending on the reaction medium. In THF such reactions proceed initially by the attack of telluroether on coordinated organonitrile to give an imide derivative in which tellurium and platinum show secondary interactions as revealed by the presence of platinum – tellurium coupling in the NMR spectra. Several of these complexes can be used as single source molecular precursors for the synthesis of palladium chaclcogenides. Precursors for ternanary systems have also been developed.

References

1. V. K. Jain and L. Jain, *Coord. Chem. Rev.*, 249 (2005) 3075-3197.
2. I.Omae, *J. Organomet. Chem.*, 692 (2007) 2608-2632.
3. M. Beller, H. Fischer, W. A. Herrmann, K. Öfele and C. Brossmer, *Angew. Chem., Int. Ed. Engl.*, 34 (1995) 1848-1849.
4. M. Ghedini, I. Aiello, A. Crispini, A. Golemme, M. La Deda and D. Pucci, *Coord. Chem. Rev.,* 250 (2006) 1373-1390.
5. J. Dupont, C. S. Consorti and J. Spencer, *Chem. Rev.,* 105 (2005) 2527-2571.
6. Q. Yao, E.P. Kinney and C. Zheng, *Org. Lett.,* 6 (2004) 2997-2999.

A part of the work reported in this thesis has already been published to secure the priority of the work in the field. The details of the publications are as follow:

Journal papers

1. Binuclear orthometalated N, N-dimethylbenzylamine complexes of palladium(II): Synthesis, structure and thermal behavior
   Siddhartha Kolay, N. Ghavale, A. Wadawale, D. Das and V. K. Jain,
   *Phosphorus, Sulfur, and Silicon and the Related Element*s, 188 (2013) 1449-146.

2. Cyclopalladation of dimesityl selenide: Synthesis, reactivity, structural characterization, isolation of an intermediate complex with C-H…Pd intra-molecular interaction and computational studies
   Siddhartha Kolay, A. Wadawale, D. Das, H. K. Kisan, R. B. Sunoj and V. K. Jain,
   Dalton Trans., 42 (2013) 10828-10837.

3. Cyclopalladation of telluro ether ligands: Synthesis, reactivity and structural characterization
   Siddhartha Kolay, M. Kumar, A. Wadawale, D. Das and V. K. Jain,
   Dalton Trans., 43 (2014) 16056-16065.

4. Role of anagostic interactions in cycloplatination of telluro ethers: Synthesis and structural characterization
   Siddhartha Kolay, M. Kumar, A. Wadawale, D. Das and V. K. Jain,
   J. Organomet. Chem., 794 (2015) 794, 40-47.

5. Platinum mediated activation of coordinated organonitriles by telluroethers in THF: Isolation, structural characterization and DFT analysis of intermediate complexes
   Siddhartha Kolay, A. Wadawale, S. Nigam, M. Kumar, C. Majumder, D. Das and V. K. Jain,
   Inorg. Chem., (*Under revision),*

6. Synthesis, structures and thermal behaviour of cyclopalladated 1,1′-dithiolate complexes
   Siddhartha Kolay, A. Wadawale, D. Das and V. K. Jain,
   M.S. Under preparation

Conferences/Symposia

1. Cyclopalladation of telluro ether: Synthesis and structural investigation;
   Siddhartha. Kolay, M. Kumar, A. Wadawale, D. Das and V. K. Jain;
   5th Interdisciplinary Symposium on Materials Chemistry, December 9-13, 2014, Bhabha Atomic Research Centre, Mumbai, India; Page: 460.

2. Cyclometalation of seleno and telluro ether ligands;
   Siddhartha. Kolay, A. Wadawale, D. Das and V. K. Jain; National Conference on Chemistry of Chalcogens and Related Topics (NC3-2015), Defence Institute of Advanced Technology (DIAT), Pune; 12-13 January, 2015.

3. Synthesis and thermochemical studies of platinum group metal complexes derived from organochalcogenligands;
Siddhartha Kolay and Dasarathi Das;
27th Research Scholars Meet-2015; Indian Chemical Society (Mumbai Branch) and Sathaya College, Mumbai, 20-21 February, 2015, (Presenter).

Siddhartha Kolay, 24/11/2015
Signature of the candidate

Doctoral Committee

S. No.	Name	Designation	Signature	Date
1.	Dr. S. Kannan	Chairman		24.11.15
2.	Prof. V. K. Jain	Guide and convener		24.11.2015
3.	Dr. D. Das	Co-guide		24.11.2015
4.	DR. S. R. Bharadwaj	Member		24.11.2015
5.	Dr. Sunil Ghosh	Member		24.11.2015
6.	Dr. Sandip Dey	Member		

List of Figures

Figure 13. (a) ORTEP diagram of $[Pd(\mu\text{-}OAc)(\mu\text{-}TeMes)]_4$ (25% probability). Hydrogen atoms are omitted for clarity (b and c) orientations of atomic planes within the molecule

Figure 14. $^{125}Te\{^1H\}$ NMR spectrum of *trans*-$[PtCl_2\{Te(Ph)Mes\}_2]$ in $CDCl_3$

Figure 15. $^{195}Pt\{^1H\}$ NMR spectrum of *trans*-$[PtCl_2\{Te(o\text{-}tol)Mes\}_2]$ in $CDCl_3$

Figure 16. $^{125}Te\{^1H\}$ NMR spectrum of$[PtCl\{(CH_2C_6H_2Me_2\text{-}4,6)TeMes\}(TeMes_2)]$ in $CDCl_3$

Figure 17. $^{125}Te\{^1H\}$ NMR spectrum of $[PtCl\{(CH_2C_6H_2Me_2\text{-}4,6)TeMes\}(PPh_3)]$ in $CDCl_3$

Figure 18. ORTEP drawing of *trans*-$[PtCl_2(TeMes_2)_2]$ with atomic numbering (H atoms omitted for clarity)

Figure 19. ORTEP drawing of *trans*-$[PtCl_2\{Te(Ph)Mes\}_2]$ with atomic numbering scheme (H atoms omitted for clarity)

Figure 20. ORTEP drawing of *trans*-$[PtCl_2\{Te(o\text{-}tol)Mes\}_2]$ with atomic numbering scheme(H atoms omitted for clarity)

Figure 21. ORTEP drawing of $[PtCl\{(CH_2C_6H_2Me_2\text{-}4,6)TeMes\}(TeMes_2)]$ with atomic numbering scheme (H atoms omitted for clarity)

Figure 22. ORTEP drawing of $[PtCl\{(CH_2C_6H_2Me_2\text{-}4,6)TeMes\}(PPh_3)]$ with atomic numbering scheme (H atoms omitted for clarity)

Figure 23. ^{125}Te NMR spectra of a reaction between $[PtCl_2(PhCN)_2]$ and $TeMes_2$ in 1:2 molar ratio in THF monitored with time (a) 24 Hrs, (b) 3 days and (c) 7 days. Spectra were recorded in $CDCl_3$

Figure 24. ^{125}Te NMR spectrum of a reaction between $[PtCl_2(MeCN)_2]$ and $TeMes_2$ in 1:2 molar ratio in THF (after 60 Hrs). Spectra were recorded in $CDCl_3$

Figure 25. ^{125}Te NMR spectrum of a reaction between $[PtCl_2(4\text{-}MeC_6H_4CN)_2]$ and $TeMes_2$ in 1:2 molar ratio in THF (after 65 Hrs). Spectra were recorded in $CDCl_3$

Figure 26. ^{125}Te NMR spectrum of a reaction between $[PtCl_2(4\text{-}CF_3C_6H_4CN)_2]$ and $TeMes_2$ in 1:2 molar ratio in THF (after 135 Hrs). Spectra were recorded in $CDCl_3$

Figure 27. Te **3d** and Pt **4f** X-ray photoelectron spectrum of *trans*-$[PtCl_2\{NC(O)Ph(TeMes_2)\}_2]$

Figure 28. ORTEP drawing of *trans*-$[PtCl_2(PhCN)\{NC(O)Ph(TeMestol\text{-}o)\}]$ with atomic numbering scheme (drawn with 25% probablility ellipsoids and H atoms omitted for clarity)

Figure 29. ORTEP drawing of *trans*-$[PtCl_2\{NC(O)Ph(TeMes_2)\}_2].4H_2O$ with atomic numbering scheme (drawn with 25% probablility ellipsoids and H atoms and solvent molecules are omitted for clarity)

Figure 30. ORTEP drawing of *trans*-$[PtCl_2\{NC(Ph)C_4H_7O\}\{NC(O)Ph(TeMes_2)\}]$ with atomic numbering scheme (drawn with 25% probablility ellipsoids and H atoms omitted for clarity)

Figure 31. ORTEP drawing of *trans*-$[PtCl_2\{NC(O)Ph\{Te(tol\text{-}o)Mes\}\}_2]$ with atomic numbering scheme (drawn with 25% probablility ellipsoids and H atoms omitted for clarity)

Figure 32. ORTEP drawing of *trans*-$[PtCl_2(TeMes_2)\{NC(O)Ph(TeMes_2)\}]$ with atomic numbering scheme (drawn with 25% probablility ellipsoids and H atoms omitted for clarity)

Figure 33. ORTEP drawing of *trans*-$[PtCl_2\{NC(O)Me(TeMes_2)\}_2].2CH_2Cl_2$ with atomic numbering scheme (drawn with 25% probablility ellipsoids and H atoms omitted for clarity)

Figure 34. (a) ORTEP drawing of $[PtCl(o\text{-}tolTe)\{NC(O)Ph\}_2].CH_2Cl_2$ (drawn with 25% probablility ellipsoids). H atoms and Solvent molecule omitted for clarity (b) inter molecular interaction π-π stacking

Figure 35. ORTEP drawing of $[Pd_2(\mu\text{-}Spy)_2(Me_2NCH_2C_6H_4\text{–}C,N)_2]$.

Figure 36. ORTEP drawing of $[Pd_2(\mu\text{-}Sepy)_2(Me_2NCH_2C_6H_4\text{–}C,N)_2]$.

Figure 37. (a) TG-DTG curve of $[Pd_2(\mu\text{-}Spy)_2(Me_2NCH_2C_6H_4\text{–}C,N)_2]$; **(b)** XRD pattern of Pd_4S obtained from $[Pd_2(\mu\text{-}Spy)_2(Me_2NCH_2C_6H_4\text{–}C,N)_2]$.

Figure 38(a). TG-DTG curve of $[Pd_2(\mu\text{-}Cl)(\mu\text{-}SPh)(Me_2NCH_2C_6H_4\text{-}C,N)_2]$; **(b)** XRD of TG residue (Pd_4S, JCPDS -73-1387) obtained from $[Pd_2(\mu\text{-}Cl)(\mu\text{-}SPh)(Me_2NCH_2C_6H_4\text{-}C,N)_2]$.

Figure 39(a). TG-DTG curve of $[Pd_2(\mu\text{-}Cl)(\mu\text{-}SMes)(Me_2NCH_2C_6H_4\text{-}C,N)_2]$; **(b)** XRD of TG residue (Pd_4S, JCPDS -73-1387) obtained from $[Pd_2(\mu\text{-}Cl)(\mu\text{-}SMes)(Me_2NCH_2C_6H_4\text{-}C,N)_2]$.

Figure 40(a). TG-DTG curve of $[Pd_2(\mu\text{-}SePh)_2(Me_2NCH_2C_6H_4\text{-}C,N)_2]$; **(b)** XRD of TG residue (Pd_7Se_4, JCPDS 44-0875) obtained from $[Pd_2(\mu\text{-}SePh)_2(Me_2NCH_2C_6H_4\text{-}C,N)_2]$.

Figure 41(a). TG-DTG curve of $[Pd_2(\mu\text{-}SeMes)_2(Me_2NCH_2C_6H_4\text{-}C,N)_2]$; **(b)** XRD of TG residue obtained from $[Pd_2(\mu\text{-}SeMes)_2(Me_2NCH_2C_6H_4\text{-}C,N)_2]$

Figure 42(a). TG-DTG curve of $[Pd_2(\mu\text{-}Sepy)_2(Me_2NCH_2C_6H_4\text{–}C,N)_2]$; **(b)** XRD pattern of $Pd_{17}Se_{15}$ obtained from $[Pd_2(\mu\text{-}Sepy)_2(Me_2NCH_2C_6H_4\text{–}C,N)_2]$.

Figure 43. ORTEP drawing of $[Pd(S_2COPr^i)\{(CH_2C_6H_2Me_2\text{-}4,6)SeMes\}]$, elipsoids are drawn with 25% probability.

Figure 44. TG-DTG curve of $[Pd_2(\mu\text{-}Cl)_2\{MesSeC_6H_2(Me_2)CH_2\}_2]$.

Figure 45. (a) XRD of $Pd_{17}Se_{15}$ (JCPDS -73-1424) and (**b**) XRD of Pd_7Se_4 (JCPDS: 31-0939) obtained from $[Pd_2(\mu\text{-}Cl)_2\{MesSeC_6H_2(Me_2)CH_2\}_2]$ in TG and in diphenyl ether at 250°C, respectively.

Figure 46. (a) TG-DTG curve of $[Pd(S_2COEt)\{(CH_2C_6H_2Me_2\text{-}4,6)SeMes\}]$ and **(b)** TG-DTG curve of $[Pd(S_2CO^iPr)\{(CH_2C_6H_2Me_2\text{-}4,6)SeMes\}]$.

Figure 47. Powder XRD pattern of the TG-residue modelled with structural model of $Pd_{17}Se_{15}$ (black sphere: observed data; red and black continuous lines: calculated pattern and difference between observed and calculated data; vertical ticks: Bragg positions).

Figure 48. EDAX data of the residue obtained from the solvothermal decomposition of $[Pd(S_2CO^iPr)\{(CH_2C_6H_2Me_2\text{-}4,6)SeMes\}]$ in diphenyl ether at 250°C.

List of Tables

Table 12. ^{1}H and $^{77}Se\{^{1}H\}$ NMR data for palladium complexes in $CDCl_3$.

Table 13. Selected bond lengths (Å) and angles (°) of $[Pd_2Cl_2(\mu\text{-}Cl)_2(Mes_2Se)_2]$

Table 14. Selected bond lengths (Å) and angles (°) of $[Pd_2(\mu\text{-}Cl)_2\{MesSeC_6H_2(Me_2)CH_2\}_2]$.

Table 15. Selected bond lengths (Å) and angles (°) of $[Pd_2(\mu\text{-}Spy)_2\{MesSeC_6H_2(Me_2)CH_2\}_2]$.

Table 16. Selected bond lengths (Å) and angles (°) of $[Pd_2(\mu\text{-}Sepy)_2\{MesSeC_6H_2(Me_2)CH_2\}_2]$.

Table 17. ^{1}H, $^{13}C\{^{1}H\}$ and $^{125}Te\{^{1}H\}$ NMR data in CDCl3 of palladium telluroether complexs.

Table 18. Selected bond lengths (Å) and bond angles (°) for monoclinic form of *trans*-$[PdCl_2(TeMes_2)_2]$.2MeCN

Table 19. Selected bond lengths (Å) and bond angles (°) for triclinic form of *trans*-$[PdCl_2(TeMes_2)_2]$.toluene

Table 20. Selected bond lengths (Å) and bond angles (°) for $[Pd_2(\mu\text{-}Cl)_2Cl_2(TeMes_2)_2]$.2acetone.

Table 21. Selected bond lengths (Å) and bond angles (°) for *cis*-$[PdCl_2\{MesTeCH_2C_6H_2(4,6\text{-}Me_2)TeMes\}]$.

Table 22. Selected bond lengths (Å) and bond angles (°) for $[Pd_2(\mu\text{-}OAc)_2\{CH_2C_6H_2(4,6\text{-}Me_2)TeMes\}_2]$.toluene.

Table 23. Selected bond lengths (Å) and bond angles (°) for $[Pd_2(\mu\text{-}OAc)_2\{CH_2C_6H_2(4,6\text{-}Me)_2Tetol\text{-}o\}_2]$.

Table 24. Selected bond lengths (Å) and bond angles (°) of $[Pd(\mu\text{-}OAc)(\mu\text{-}TeMes)]_4$

Table 25. ^{1}H, $^{125}Te\{^{1}H\}$ and $^{195}Pt\{^{1}H\}$ NMR data of platinu telluroether complexes in $CDCl_3$.

Table 26. Selected inter-atomic parameters (Å, °) for*trans*-$[PtCl_2(TeMes_2)_2]$

Table 27. Selected bond length (Å) and angles (°) of *trans*-[$PtCl_2${Te(Ph)Mes}$_2$] and *trans*-[$PtCl_2${Te(*o*-tol)Mes}$_2$]

Table 28. Selected bond length (Å) and angles (°) for [PtCl{($CH_2C_6H_2Me_2$-4,6)TeMes}(TeMes$_2$)]

Table 29. Selected bond length (Å) and angles (°) for[PtCl{($CH_2C_6H_2Me_2$-4,6)TeMes}(PPh_3)]

Table 30. Secondary C-H···M interactions with the metal centre(Å/°)

Table 31. ^{1}H, $^{125}Te\{^{1}H\}$ and $^{195}Pt\{^{1}H\}$ NMR data of platinum telluroether complexes recorded in $CDCl_3$.

Table 32. Selected interatomic parameters (Å / °) for *trans*-[$PtCl_2$(PhCN){NC(O)Ph[Te(tol-*o*)Mes]}]

Table 33. Selected interatomic parameters (Å / °) for *trans*-[$PtCl_2${NC(O)Ph(TeMes$_2$)}$_2$]

Table 34. Selected interatomic parameters (Å / °) for *trans*[$PtCl_2${NC(Ph)C_4H_7O}{NC(O)Ph(TeMes$_2$)}]

Table 35. Selected interatomic parameters (Å / °) for *trans*-[$PtCl_2${NC(O)Ph[Te(tol-*o*)Mes}$_2$]

Table 36. Selected interatomic parameters (Å / °) for *trans*-[$PtCl_2$(TeMes$_2$){NC(O)Ph(TeMes$_2$)}]

Table 37. Selected interatomic parameters (Å / °) for *trans*-[$PtCl_2${NC(O)Me(TeMes$_2$)}$_2$]

Table 38. Selected inter-atomic parameters (Å / °) for [PtCl(Tetol-*o*){NC(O)Ph}$_2$]

Table 39. ^{1}H and $^{77}Se\{^{1}H\}$ NMR data for cyclopalladated complexes in $CDCl_3$

Table 40. Selected bond lengths (Å) and angles (°) for [Pd_2(μ-Spy)$_2$($Me_2NCH_2C_6H_4$–C,N)$_2$]

Table 41. Selected bond lengths (Å) and angles (°) for [Pd_2(μ-Sepy)$_2$($Me_2NCH_2C_6H_4$–C,N)$_2$]

Table 42. Selected bond lengths (Å) and angles (°) of [Pd(S_2COPr^i){($CH_2C_6H_2Me_2$-4,6)SeMes}]

Chapter 1

Introduction

1.1 General introduction about palladium and platinum

The platinum group metals consist of six elements, viz. ruthenium, rhodium, palladium, osmium, iridium and platinum and occupy the 5^{th} and 6^{th} periods of groups 8, 9 and 10 in the Periodic Table. These six elements have similar physical and chemical properties and tend to occur together in nature with abundance in the earth's crust ~0.01 ppm. Out of them palladium and platinum are the most widely studied. Growing interest in the chemistry of palladium and platinum is reflected by a recent analysis of the non-patent scientific literature by Gavin [1] during the year 1998-2008. In fact, the chemistry of these two elements played a crucial role in the development of the organometallic and coordination chemistry. Soon after the discovery of Zeise´s salt ($K[PtCl_3(CH_2{=}CH_2)]$) (the first organometallic compound reported as early as in 1820 [2]), several complexes were synthesized such as *cis*-$[PtCl_2(NH_3)_2]$ in mid 1850s (now used as antitumor drug) [3] and $[PtCl_2(CO)]_2$ (the first metal carbonyl) in 1868 [4]. The progress was further accelerated in the twentieth century with the isolation of the first transition metal-alkyl complex $[PtMe_3I]_4$ in 1907 [5], discovery of *trans* effect in 1920s [6] and applications of palladium complexes in homogenous catalysis in the mid-twentith century (e.g. Wacker process [7]).

Platinum was discovered by a Spanish scientist Antonio de Ulloa in 1735 while palladium was discovered by a British chemist W.H. Wollaston in 1803. Both palladium and platinum are lustrous silvery-white metals which are sufficiently ductile and malleable to roll into sheet or to draw into wire and are resistant to corrosion. They have the similar physical and chemical properties and occur in the same mineral deposits [8]. Some of their main physical and chemical properties are summarized in Table-1[9-11].

Table 1. Some physical and chemical properties of palladium and platinum [9-11]

Properties	Palladium	Platinum
Abundance in earth's crust (by weight) (ppm)	0.015	0.01
Atomic number/ atomic weight	46/106.4	78/195.08
Ground state electronic configuration	$[Kr]4d^{10}5s^{0}$	$[Xe]5d^{9}6s^{1}$
Melting point (°C)	1554.9	1768.3
Boiling point (°C)	2963	3825
Lattice structure	*fcc*	*fcc*
Density (g cm^{-3})	12.02	21.45
Thermal conductivity (W/cm/K)	0.711	0.711
Specific heat (at 0°C), J/g/K	0.2443	0.1313
Pauling's electronegativity	2.2	2.2
Radius (Å): Atomic	1.375	1.387
M(0) Covalent	1.39	1.36
M(II) Covalent	1.28	1.29
Ionic (II)	0.86	0.80
Ionization potentials (eV)		
$M^{\circ} \rightarrow M^{+}$; $M \rightarrow M^{+2}$	8.33; 27.75	9.0; 27.56
$M^{\circ} \rightarrow M^{+3}$; $M \rightarrow M^{+4}$	60.67; 109.47	56.06; 97.16
$M^{+} \rightarrow M^{+2}$; $M^{+2} \rightarrow M^{+3}$	19.42; 32.92	18.56; 28.50
$M^{+3} \rightarrow M^{+4}$; $M^{+4} \rightarrow M^{+5}$	48.80; 66.00	41.10; 55.00
Oxidation potential (eV)		
$M^{\circ} \rightleftharpoons M^{2+} + 2e$	–0.92	–1.2
$M^{II} \rightleftharpoons M^{4+} + 2e$	–1.26	–0.77
Naturally occurring isotopes (% abundance, spin (I))	^{102}Pd (1.0, 0) ^{104}Pd (11.1, 0) ^{105}Pd (22.2, 5/2) ^{106}Pd (27.3, 0) ^{108}Pd (26.5, 0) ^{110}Pd (11.7, 0)	^{190}Pt (0.01, 0) ^{192}Pt (0.8, 0) ^{194}Pt (32.9, 0) ^{195}Pt (33.8, 1/2) ^{196}Pt (25.3, 0) ^{198}Pt (7.2, 0)

Resistance to chemical attack, excellent high temperature performance and electrical properties, and significant catalytic activities of platinum make its frequent use is employed in many industrial applications. One of the most important applications of metallic palladium is hydrogen absorption. Metallic palladium can absorb upto 900 times of its own volume,

greater than any other metal. The absorption process is reversible and highly selective for H_2 and D_2. This property provides a method to purify H_2 on industrial scale just by passing the impure H_2 through a palladium membrane at controlled temperature [12].

1.2 A brief coverage on palladium and platinum chemistry

Generally the chemistry of palladium and platinum is very similar. The difference in their chemistry is reflected mainly in their kinetics of reaction. The palladium complexes are more labile than the analogues platinum complexes. In fact, palladium complexes react about10^6 times faster than the platinum complexes. The differences are due to the difference in their crystal field stabilization energy. The difference in the kinetics is reflected in their application. Thus where palladium complexes are frequently used for catalytic applications, platinum complexes due to their kinetic inertness are used for elucidation of the reaction mechanism.

The ground state valence shell electronic configuration of palladium and platinum metals are [Kr]$4d^{10}5s^0$ and [Xe]$5d^96s^1$, respectively. In platinum because of lanthanide contraction imperfect shielding of the outer most electrons from the nuclear charge by the intermediately placed 4f sub-shell electronsits ionic radius is essentially similar to that of palladium. Due to the similar energy of the valence orbitals both palladium and platinum show variable oxidation states ranging from zero to six with different geometries as shown in Table 2 [11-20].

Table 2. Stereochemistry of palladium and platinum complexes in various oxidation states and coordination numbers (C. N.) of the metal ion [11-20].

Oxidation state	C. N.	Geometry	Examples
0	2	Linear	$[Pt(PPh_3)_2]$, $K_2[Pd(C{=}CR)_2]$
	3	Trigonal planar	$[Pd(PPh_3)_3]$, $[Pt(SO_2)(PCy_3)_2]$ [11]
		Distorted planar	$[PtX(PPh_3)_2]$ (X = O_2, C_2H_4, CS_2) [11]
	4	Tetrahedral	$[Pt(PF_3)_4]$, $[Pt(CO)(PPh_3)_3]$
I	4	Square planar	$[M_2X_2(\mu\text{-dppm})_2]$ [13]
	5	Trigonalbipyramidal	$[Pt_3(SnCl_3)_2(C_8H_{12})_3]$ [14]
II	3	T-shaped	$[Pd(Br)(Ph)(P^tBu_3)]$ [15]
	4	Tetrahedral	$[Pd(EDM)_2]I_2$ (EDM = N, N′ ethylene dimorpholine)
	4	Square planar	All authenticated four coordinated complexes
	5	Trigonal bipyramidal	$[Pt(SnCl_3)_5]^{3-}$, $[Pd(QAs)I]^+$
			$[Pd(Me_4[14]aneP_4]Br_2{\cdot}6H_2O$,
		Square pyramidal	$[PtMeCl(AsMe_3)_2(CF_3C{\equiv}CCF_3)]$[16];$[Pt(Me_4[14]aneP_4]Br_2{\cdot}4H_2O$ [17]
		Distorted square- pyramid	$[Pd(triphos)Cl]^+$
	6	Octahedral	$[Pd(diars)_2I_2]$
III	4	Square planar	$[Bu_4N]\{Pt(C_6Cl_5)_4]$ [18]
	6	Octahedral	$K_2[Pt_2(SO_4)_4(H_2O)_2]$ [19]
IV	6	Octahedral	$[PtL_6]^{2-}$; L = X, SCN; $[PtMe_3I]_4$
	8	Piano-stool	$[Pt(\eta^5\text{-}C_5H_5)Me_3]$
V	6	Octahedral	$[PtF_6]^-$
VI	6	Octahedral	$[PtF_6]$

The most common oxidation state exhibited by these metals is II with a square-planar geometry around the metal centre, although other geometries like T-shaped (e.g. [Pd(Br)(Ph)(P^tBu_3)] [15], tetrahedral (e.g. $[Pd(EDM)_2]I_2$ (EDM = N, N'-ethylene dimorpholine), square pyramidal (e.g. $[PtMeCl(AsMe_3)_2(CF_3C{\equiv}CCF_3)]$ [16, 17]), etc are also reported. The stability of higher coordinated complexes depends on the presence of π accepting ligand like $SnCl_3^-$, NO^+ so that the excess negative charge accumulated on the metal center due to the coordinating ligands is neutralized by the π acceptor ligands.

The complexes in zero oxidation sate are stabilized by strong σ–donor and π–acceptor ligands such as carbonyls, isocynide, acetylene, phosphine, phosphite and arsines, etc. These complexes exhibit geometries ranging from linear (e.g., $[Pt(PPh_3)_2]$) to tetrahedral (e.g., $[Pt(PPh_3)_4]$). Though both palladium and platinum complexes in +1 and +3 oxidation states are known but their chemistry is not as diverse as that of 0, +2 and +4 state. The chemistry in mono- and tri-valent palladium and platinum is gradually evolving [21, 22]. Although they have d^9 (+1) and d^7 (+3) electronic configuration, the complexes are diamagnetic due to the formation of metal-metal bond and hence exist as dimer. Chemistry of Pd(IV) and Pt(IV) is now well established. The work on Pd(IV) is relatively less explored as compared to Pt(IV). The higher ionization potential of Pd(IV) as compared to Pt(IV) is responsible for poor stability of palladium(IV) complexes which tend to reduce to Pd(II). Only platinum shows +5 (e.g., PtF_5) and +6 (e.g., PtF_6) oxidation states, but these are very reactive and highly unstable. Neither platinum nor palladium forms any compound in which they exhibit oxidation states either in excess of +6 or in negative.

There is a sustained and growing interest in palladium and platinum chemistry as evident from several books, monographs, and review articles published time to time [11, 12, 23-30]. The chemistry of palladium and platinum, in general, is similar except that the reactivity of palladium is higher by more than a million times than platinum. An important

feature exhibited by square planar palladium(II) and platinum(II) complexes is *cis*-*trans* isomerism and many pairs of *cis* and *trans* isomer of platinum(II) complexes have been isolated due to their kinetic inertness over palladium(II). At the same time palladium complexes offer a balance between thermodynamic and kinetic labiality enabling product selectivity and specificity during the reactions. Generally the formation of *trans* isomer is entropically more favorable than the *cis* isomer. However, the formation of *cis* isomer is enthalpicaly more favorable in the presence of π-bonding ligand because in the *cis* isomer the two π-bonding ligand can utilize different metal *d*-orbital for bonding whereas in *trans* geometry they have to share the same metal *d*-orbital.

A ligand in square-planar palladium and platinum complexes can be replaced by another in several ways [31, 32]. In substitution reactions, one of the coordinated ligand is substituted by another ligand (Eq. 1).

$$MA_3X + Y^- \longrightarrow MA_3Y + X^- \qquad ...(1)$$

The substitution of one ligand by another one can proceed either by electrophilic substitution (electron poor late transition metals like Pd(II), Pt(II)) or by nucleophilic substitution. The substitution reactions of platinum(II) complexes generally occur at a fairly slow rate, so that they are ideal for kinetic studies. Ligands substitution reactions of square-planar platinum(II) complexes occur stereo-specifically with retention of configuration. The rate and mode of substitution reactions is dependent on the *trans*-effect which can be defined in the following way: "In compounds with square planar structure, the rate of substitution of an atom or molecule linked to central atom is determined by the nature of substituent at the opposite end of diagonal. Thus stability of bond between this (central atom) and any substituent is little effected by character of neighboring atom or molecules, but is greatly influenced by those more distant, in trans position, on diagonal of the square" [31, 32]. The intensity of *trans* effect (as measured by an increase in the rate of substitution of the *trans*

ligand) can follow the sequence: F^-, H_2O, OH^-< NH_3<Py<Cl^-< Br^-< I^-, SCN^-, NO_2^-, $SC(NH_2)_2$, Ph^-, < SO_3^{2-}< PR_3, AsR_3, SR_2, CH_3^- , H^-, NO, CO, CN^-, C_2H_4.

In oxidative addition reactions, the oxidation state along with the coordination number usually changes by two units. Therefore, with both palladium and platinum a wide range of oxidative addition chemistry is available in both the oxidation state of 0 and II. The reverse of this reaction is known as reductive elimination. Oxidative addition reactions with square-planar d^8 metal complexes are of special interest as it is one of the key steps in homogeneous catalysis.

Palladium and platinum form a myriad of classical and organometallic complexes with a variety of ligands conataining Groups 14-17 donor atoms. Among organometallic complexes, cyclometalated derivatives represent an interesting and important family of organometallic compounds that find numerours applications in organic synthesis, catalysis and materials science. In fact these compounds remained in forefront ever since their intial isolation in the mid 1960s by Cope and Siekman [33]. A brief coverage on these compounds is included here.

1.3 Cyclometalation reactions

The term “cyclometalation” was first introduced by Trofimenko [34]. The process is transition metal mediated activation of C-H bond leading to the formation of, in general, a four-electron C-anionic donor ligand complexing with a new metal-carbon σ-bond (Scheme 1).

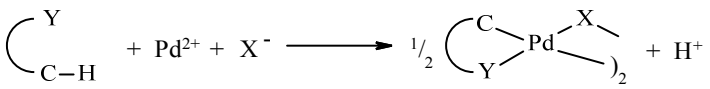

(X = Cl or OAc; Y = N, P, As, S donor atoms;
C-H = sp, sp^2, sp^3 carbon)

Scheme 1. Cyclometalation of organic ligands

It is generally believed that the reaction consists of two consecutive steps: initial coordination of the metal center via a neutral donor atom like N, P, As, S, etc and subsequently intra-molecular activation of C-H bond leading to cyclometalated product with release of a proton. Thus, in true sense, cyclometalated complexes are not metalacycle [35]. So far, though the major portion of the cyclometalation reactions take place through the activation of C-H bond, examples with carbon-carbon, carbon-oxygen and carbon-silicon bond are also reported. Since the early study of Cope and Siekman [33], cyclometalated complexes have been of considerable interest and are described in a number of reviews, book chapters [36-47]. Although nearly all the transition metals undergo cyclometalation reactions, the platinum group metals have received the most attention with predominance by palladium.

Cyclometalation has received a significant attention due to its mildest route for activation of inert and stable C-H and C-R bond. In spite of incomplete knowledge in the reaction mechanism, cyclometalation is a highly attractive and versatile route for creating organometallic complexes with wide applicationsin organic synthesis [47, 48], catalysis [49-52], materials science [53, 54], etc. Apart from these, cyclometalated complexes have gained attention in various other domains, for example, as active unit in sensors [55, 56], as photophysical devices in organometallic light-emitting diodes [57-59], for light harvesting and energy transfer such as in photovoltaic cells [60], anticancer agents and for other biological applications [61-64].

1.3.1 General Principles of Cyclometalation

Generally, metal-carbon σ-bond formation occurs by direct interaction of ligands (E$^{\frown}$CR) and the metal substrate followed by elimination of R by combination with a suitable leaving group. Therefore, the whole process of cyclometalation reaction can be split into two

steps, the coordination of the metal center by neutral donor atom, E (N, P, S, Se, etc) and the intra-molecular activation of C-R bond. Arranging the C-E bond and the metal center in close proximity is pivotal for reducing the entropic and enthalpic costs of the subsequent bond-activation step before the metalacycle ring closure. In most cases, though the intermediates are seldom isolated, their existence can be inferred. Pre-coordination of the ligand modify the electron density as well as steric environment around the metal center. The success of the cyclometalation reaction depends on both steric and electronic factors which depend on the nature of metal precursor, the donor site E, and the C-R bond to be activated.

1.3.2 Effect of metal precursor

The prerequisite for the metal center for cyclometalation is the presence of one vacant coordination site so that hetero atom can coordinate the metal center via M-E bond [65]. Various precursors capable of easily generating one vacant coordination site, like $[MCl(cod)]_2$ (M = Ir, Rh, cod = 1,5-cyclooctadiene), $[PdCl_2(PhCN)_2]$, $[PtCl_2(SEt_2)_2]$, $[Pd(OAc)_2]_3$, Na_2PdCl_4, K_2PtCl_4, etc. have been well studied. It has been noticed that the second step, i.e.; the activation of the C-R bond is facilitated by the presence of strongly basic ligands like alkoxide, alkyl or hydride attached to metal center. In that case the proton abstraction from the ligand leads to the formation of unreactive alcohol, alkane or hydrogen and hence supplies the thermodynamic driving force for the bond activation. It is well documented that because of flexible coordination mode of acetate (OAc^-) (κ^1, κ^2-chelating, κ^2-bridging), a vacant coordination site at the metal center is generated in solution [66]. In addition to that, the conjugated acid HOAc, resulted from the abstraction of H from C-H bond activation is weak and does not interfere with the formed C-M bond. Moreover, the κ^2-bridging mode may generate a cyclic transition state involving metal coordination via one oxygen and interaction of the oxygen with the C-H entity. This configuration preorganizes

the reactants and places the metal in close proximity to the carbon that participates in the C-H bond activation [67]. Because of these remarkable properties, acetate (AcO^-) has emerged as one of the most promising ligand for cyclopalladation.

1.3.3 Effect of Donor (E)

A plethora of organic compounds containing N, P, As, S donor atoms have been utilized for cyclometalation reactions. Since the first step of cyclometalation is the coordination of the ligand to the metal center, the nature of the donor group attached to the ligand plays a very important role to the success of the reaction. The effect can be classified on the basis of its basicity and steric demand where both are mutually diverging. The effect of the donor group can be explained from Scheme 2.

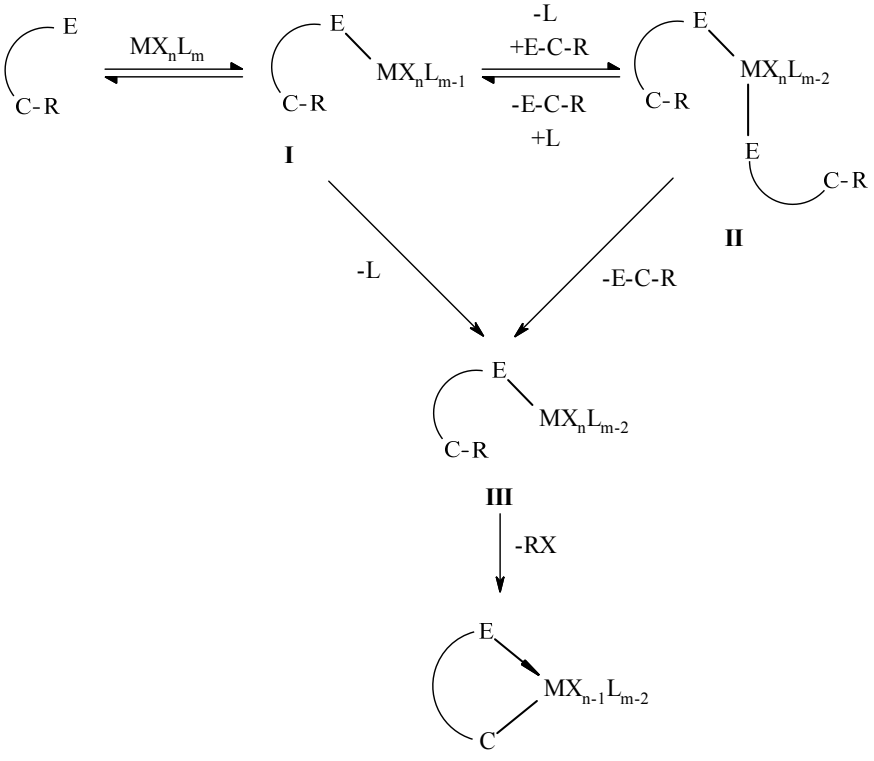

Scheme 2. Steps involved in cyclometalation

Initial coordination of the ligand leads to a complex $MX_n(E\text{-}CR)(L_{m-1})$ (**I**). On reaction with another molecule of ligand lead to complex $MX_n(E\text{-}CR)_2(L_{m-2})$ (**II**) via the substitution of the weakly bound ligand. The coordinatively unsaturated intermediate $MX_n(E\text{-}CR)(L_{m-2})$ (**III**), which is the key intermediate for the reaction, is formed from either **I** or **II** via decoordination of a ligand. The thermodynamic driving force for the formation of complex **III** depends on the strength of the M-E bond. Thus too strong and too stable bonding decreases the chance of ligand dissociation from **II**, while too weak bonding leads to the formation of the starting material, MX_nL_m. Since both steric and electronic factors govern the strength of the M-E bond and these effects are mutually diverging, the nature of E plays a very crucial role in the reaction. It has been observed that the cyclometalation with high-valent early transition metals is most successful when the donor atoms are hard, as with alkoxides, aryloxides, or amines. On the other hand, soft transition metals like platinum group metals favor bonding to phosphines and sulfides as soft Lewis bases. Though hard-soft principle provides a guidelines, numerous examples are reported where comparatively soft donor atoms are used in cyclometalation with hard metals like pyridine with Zr(IV) [68] and hard amine donor with soft palladium(II) [69]. It has been reported that the steric crowding played a very important role in cyclometalation. Amine with larger substituent ($E= NR_2$), weaken metal coordination substantially [70]. Thus, dimethylamino group ($E = NMe_2$) has proven to be particularly suitable [71], while on further increasing the steric crowding around nitrogen, like NEt_2 or N^iPr_2 much weaker complexes are formed. In some cases, even nitrogen fails to coordinate to the metal center due to excessive shielding of the nitrogen's lone pair of electrons. Cyclometalation of primary amine is more difficult as the cyclometalation is prevented from the formation of more stable coordination compounds of type **II** (Scheme 2), and therefore, care has to be taken to keep a 1:1 ligands/ metal ratio to maximize the formation of compound **I** [72].

Metal coordination is well documented with bulky substituent for softer donor like phosphine or sulfide. Thus Dunina et. al. reported successful cyclopalladation with bulky $P(^tBu)_3$ [73]. Though the strength of the Pd-P bond is significantly strong, the steric crowding by bulky substituentensures here that the M-P bond does not become too strong. Similar effect has also been observed with $P(o\text{-}tol)_3$ [74]. The beneficial outcome of steric effect has been explained by Shaw [75]. It has been noticed that the cyclometalation with sterically demanding phosphines is favored due to entropic and enthalpic factors.

1.3.4 Nature of metalacycle

It has been observed that the size of the metalacycle can vary from three to eight but with different preferences. It has also been observed that there is a clear cut tendency of majority of the ligands to form five-membered metalacycle. For example, for a series of amine of the type $Ph(CH_2)_nNMe_2$ (n = 0-3), only benzylamine is cyclometalated leading to the formation of five-membered metalacycle while all others form only the simple coordination complexes (Scheme 3) [76]. Preferences towards the five-membered metalacycle has also been noticed in the reaction of 1-arylazonaphthalenes with Pd(II) [77-79]. It is obvious from the structure (Scheme 4) of the ligand that cyclometalated complexes can form with the four different type of ring closer due to the presence of two different types of nitrogen and two different types of aromatic ring.

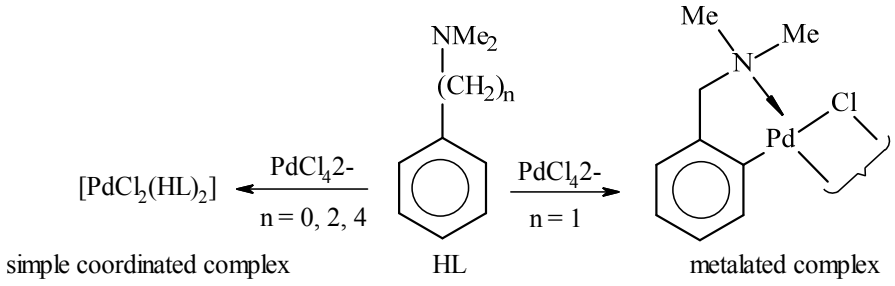

Scheme 3. Effect of ring size on cyclometalation

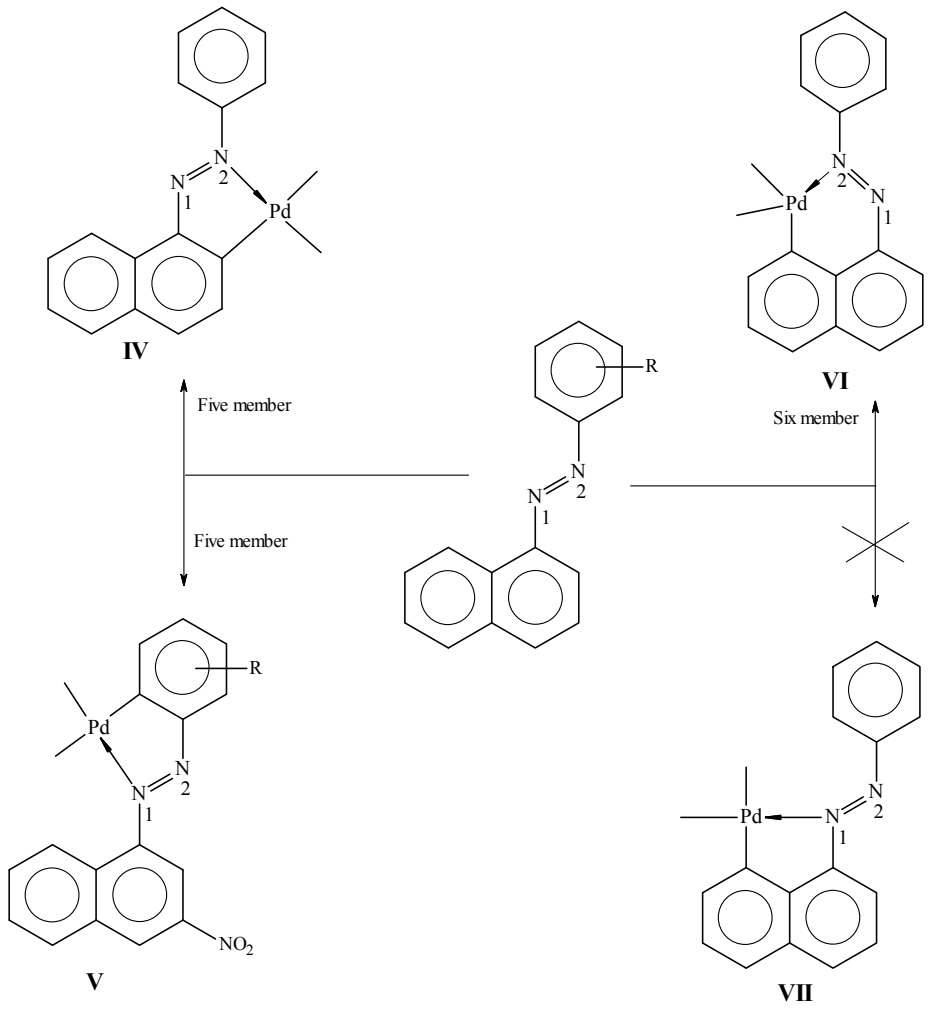

Scheme 4. Cyclometalation of 1-arylazonaphthalen: Showing the preference of five-membered metalacycle

The greater accessibility of nitrogen atom for initial coordination along with the greater nucleophilicity of naphthalene ring as compared to benzene ring leads to cyclopalladation into C(2) position. In contrast, on introducing strong electron-accepting substituent like NO_2 at the thired position of naphthalene ring and electron-donating substituent at the benzene ring, cyclopalladation into the benzene ring become possible (**V**). In both the cases, a five-membered metalacycle is formed. However, when all the possibilities for forming the five-membered metalacycle was completely blocked by methyl

groups, i.e. 2' and 6'-position in the benzene ring and 2 position in naphthalene are blocked, six-membered metalacycle (**VI**) is formed. The coordination of palladium by nitrogen was confirmed by ^{15}N NMR spectroscopy [77]. The preference of the metal center for five-membered metalacycle is explained on the basis of the tendency of the metal center to maintain the E-M-metalated carbon angle close to 90°. This preferred angle can be maintained by the formation of five- member metalacycle with the square-planar geometry around the metal center [78, 80]. Four- membered metalacycles are also reported [81-84] though their numbers are significantly less as compared to the number of five- and six-member metalacycles.

1.3.5 Effect of the State of Metalating Carbon Atom

The effect of the state of the carbon atom undergoing metalation is mainly based on steric hindrance. Therefore, on the ground of steric crowding, the ease of the cyclometalation of saturated carbon atom decreases in the sequence primary> secondary > tertiary. This order can be justified with the following example. When 8-alkylquinolines were used for cyclopalladation, the palladation occurs readily only when 8-positions contains methyl group and more slowly for ethyl group. But the metalation fails in the case of isopropyl, instead form only the simple coordination complex [85, 86]. In contrary to the above result, it has been reported that the metalation at tertiary carbon take place very readily provided that the carbanion formed after proton abstraction is stabilized by the presence of electron withdrawing group attached to the tertiary carbon [87, 88]. Thus, it can be concluded that the tendency towards metalation decreases after the addition of the substituent in carbon atom undergoing metalation, but results go in the opposite direction when such substituents are strong electron withdrawing and hence metalation facilitated by the increase of the acidity of the C-H bond.

1.3.6 Effect of Other Experimental Conditions

Apart from the above mentioned effects in cyclometalation, other experimental conditions like nature of solvent, reaction time and reaction temperature are also quite important in the course of cyclometalation. The solvent commonly used for this type of reaction is the polar solvent like methanol [69, 85, 89-91]. The presence of polar solvent in the reaction helps in creating the vacant coordination sites in the coordination sphere of the metal through solvation. The effect of the presence of polar solvent can be observed in the cyclopalladation of 8-methylquinoline-2-carboxaldimine (Scheme 5). It was observed that the cyclopalladation takes place only in methanol whereas only coordination complex is formed in chloroform even at elevated temperature [85]. The role of methanol was explained that once the vacant coordination site was formed in the coordination sphere of Pd(II), methanol facilitate bidentate coordination of the ligand to the metal and hence ensure the equatorial position of the 8-methyl group, necessary for cyclopalladation.

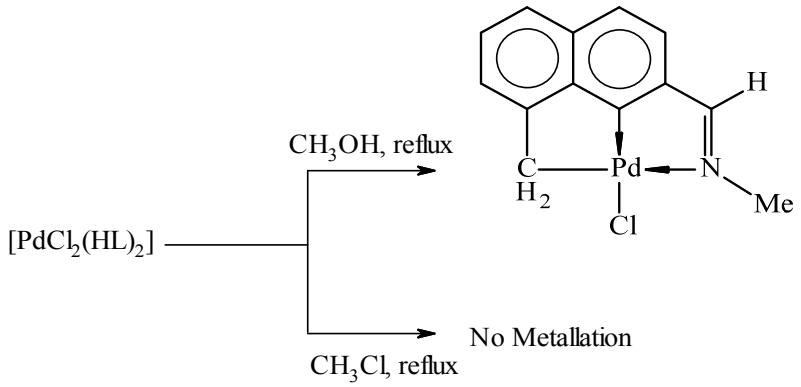

HL = 8-methylquinoline-2-carboxaldimine

Scheme 5. Effect of solvent on cyclometallation

Similar solvent effect was also observed incase of hexamethylphosphoramide [92]. Apart from polar solvents, many reactions have been reported where the cyclometalation has been observed in weakly coordinating solvent of low polarity like benzene [93] and

chloroform [94]. The reaction with palladium acetate is conventionally carried out in glacial acetic acid. The requirement for the correct selection of the solvent can be observed with the following example. 2-Pivaloylpyridine on reacting with $Pd(OAc)_2$ in glacial acetic acid yields the expected cyclopalladated complex (Scheme 6). Whereas when the reaction is carried out in methanol or in aqueous THF, bis-chelate complexe is formed. The reaction time and temperature necessary for the metalation are determined by many factors like the nature of the ligand as well as the metalating agent, the nature of the solvent, etc.

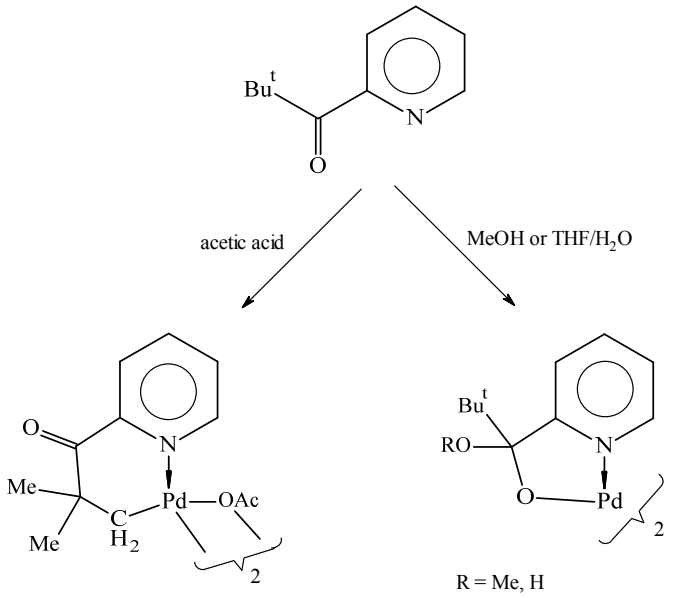

Scheme 6. Effect of solvent in cyclometallation

1.3.7 Methods of Cyclometalation:

A number of excellent reviews have summaraized various methods for C-H bond activation leading to cyclometalation [65, 71, 95, 96]. The three major pathways for the reaction include (i) electrophilic C-H bond activation, (ii) oxidative addition and (iii) σ-bond metathesis. Though for most cyclometalation process, the exact mechanism is far from the understanding, the electronic structure of the metal center together with the nature of the C-H bond to some extent give an idea about the nature of the reaction path.

1.3.7.1 Electrophilic C-H bond activation

This path of activation is generally observed with electron-poor late transition metals like palladium(II), platinum(II). This path of activation is analogus to the aromatic electrophilic substitution reaction as it was observed that the rate of C-H bond activation increases upon introduction of electron withdrawing group into the organic ring. It was concluded by theoretical calculation that actually the bond activation takes place through the interaction of C-H bond with metal center after the formation of the initial coordination complex as shown in Scheme 7.

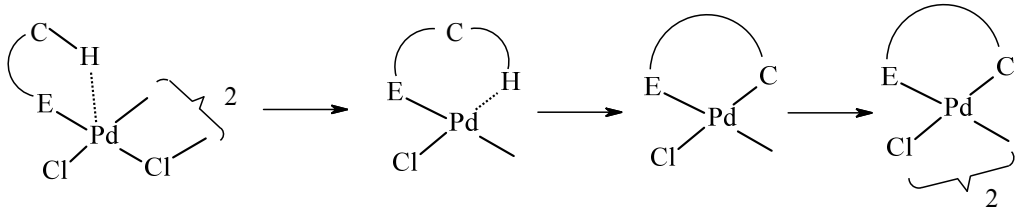

Scheme 7. Schematic diagram for electrophilic C-H bond activation

The M···H-C interactions play a crucial role in cyclometalation reactions [97-100]. These interactions are reported as agostic [97], hydrogen bonding and anagostic [101] and are shown in Scheme 8. To distinguish attaractive agostic interactions from sterically enforced M···H-C contacts in square planar d^8 palladium and platinum complexes, Lippand and coworkers [101] coined the term anagostic interaction. The axial M···C-H contacts in square planar complexes can be either repulsive anagostic (3c-4e) interactions or attractive hydrogen bonds (3c-4e) where metal atom acts as a hydrogen bond acceptor. Both these interactions require axially oriented fully occupied metal-dz^2 orbital, whereas pre-agostic rely on metal-dxz, yz-σ*(C-H)π back donation. The pre-agostic interactions are considered as a route to becoming agostic. The M···H distance in agostic interaction lies in the range 1.8-2.3Å while for anagostic it is much longer (2.3-2.9Å). The M···H-C angel for agostic and anagostic interaction falls in the region, ~90-140° and ~ 110-170°, respectively [97].

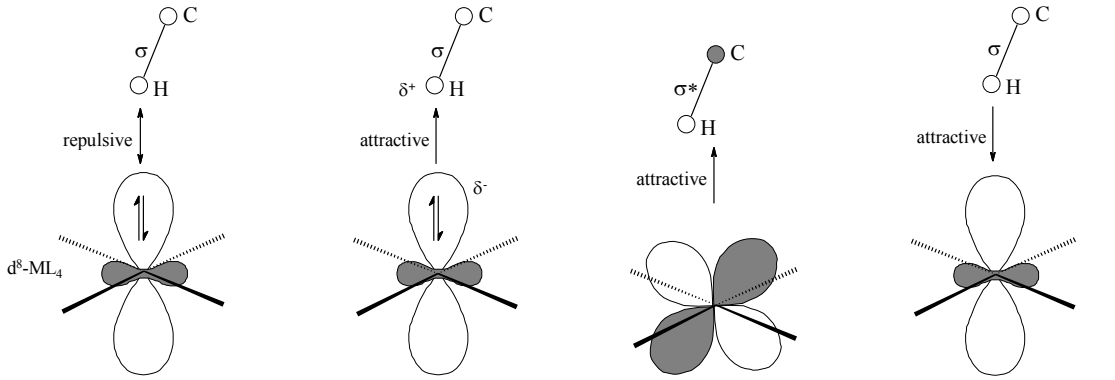

(a) **anagostic** 3-center-4-electron Filled $M(dz^2)$

(b) **hydrogen bond** 3-center-4-electron σ-back donation

(c) **preagostic** 3-center-2-electron π-back donation

(d) **σ-agostic** 3-center-2-electron partly empty $M(dz^2)$

Scheme 8. Schematic representation of agostic and anagostic interaction [97]

1.3.7.2 Oxidative addition

This path of activation normally takes place with electron-rich metal center like iridium(I), rhodium(I), osmium(II), and with late transition metals. Here the ligand acts as an accepter in contrast to the electrophilic path and the anti-bonding σ* orbital of the C-H bond get populated through two-electron transfer from the metal. In this path the final cyclometalated products are obtained through the reductive elimination as shown in Scheme 9.

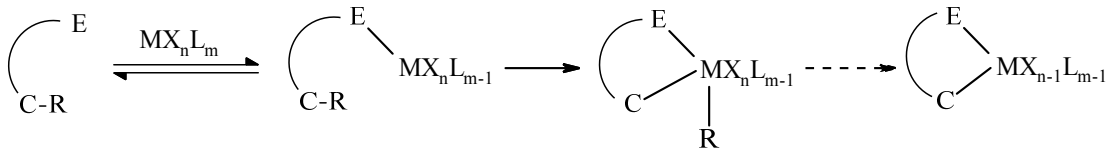

Scheme 9. Schematic diagram for C-H bond activation via oxidative addition

1.3.7.3 σ-bond metathesis

Cyclometalation through this pathway usually takes place with electron-poor late metal centers. The schematic of the process is shown in Scheme 10.

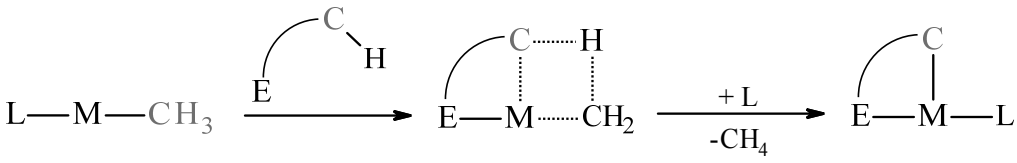

Scheme 10. Schematic diagram for C-H bond activation via σ-bond metathesis

Apart from the above mentioned three pathways, the other widely used pathway by the metals centers is *trans*-cyclometalation where one metalated ligand is exchanged with other ligand as exemplified in Scheme 11.

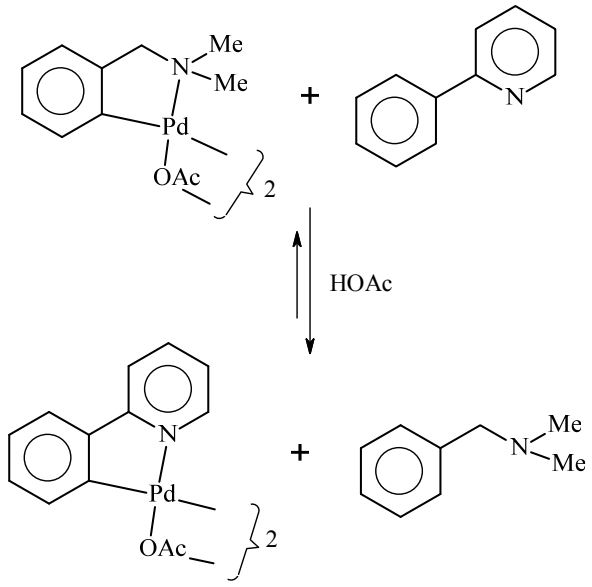

Scheme 11. Cyclometalation via transcyclometalation

1.4 Applications of cyclometalated complexes

Cyclometalated complexes are of considerable interest [102]. There are several obvious reasons for this sustained interest in these complexes which can be attributed to their

outstanding applications as catalysts (e.g., $[Pd_2(\mu\text{-}OAc)_2\{tol_2PC_6H_4CH_2\text{-}o\}_2]$ applied by Herrmann and coworkers [48]) in organic synthesis [47, 48, 52], remarkable metallomesogenic [103] and intriguing photophysical properties [104], and applications in materials science [52] besides their rich reaction chemistry [102, 105].

1.4.1 Luminescent properties

The last decade has witnessed a phenomenal surge of interest in electronic device based on photo- and electro-luminescence materials. Now days, the organic light emitting diodes and light emitting electrochemical cells are the most promising alternative of liquid crystals. Because of this high potential, a significant part of the present research is devoted into the studies of luminescence materials where cyclometalated complexes have played a crucial role. Cyclometalated complexes of d^6-heavy metals has emerged as the most versatile candidates [106-109], several examples of square-planer d^8 palladium(II) and platinum(II) complexes exhibiting the luminescence properties are well documented [110-113]. $Ir(ppy)_3$ is the first and the most popular green-emitting phosphor used in OLEDs [114]. The metalacycle exhibing the luminescence properties mainly contain aromatic carbon donor atom along with nitrogen donor atoms in bidentate C^N or tridentate C^N^N or N^C^N or C^N^C fashion. Some of the luminescent metalacycles are shown in Scheme 12.

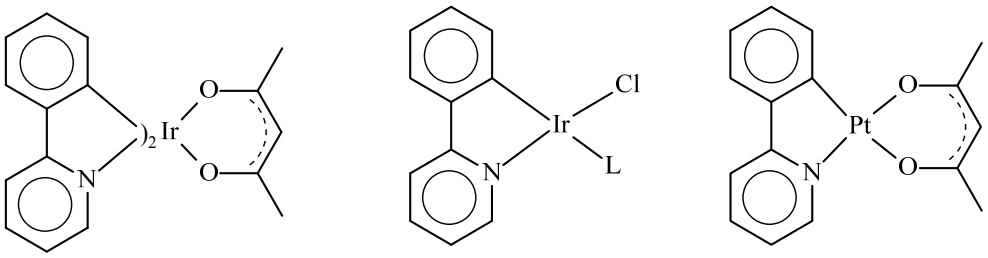

Scheme 12. Metalacycles with luminescent properties

1.4.2 Liquid crystals

One of the important applications of cyclometalated complexes are in liquid crystal industry. The mesogenic palladacyles have received much attention over the last few years [115, 116]. The cyclometalated complexes of palladium and platinum are predominant and are dimeric. They contain mainly five-membered cyclometalated ring and show high thermal stability which make them very promising candidates for LCD applications. Scheme 13 present some of the palladacycle exhibiting the mesomorphic properties.

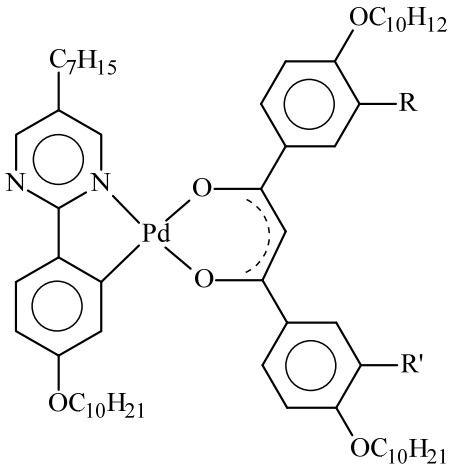

R = R' = H
R = $OC_{10}H_{21}$, R' = H
R = $OC_{10}H_{21}$, R' = $OC_{10}H_{21}$

Scheme 13. Palladacycles with mesogenic properties

1.4.3 Catalysis

The significant achievement of cyclometalated complex is in the field of organic synthesis where cyclopalladated complexes act as a catalyst. The application of this class of complexes in catalysis was evidenced since its discovery by Cope and Seikman [33]. The major drawback for organic synthesis leading to higher alkane through C-C bond formation is the chemical inertness of C-H bond. The problem of chemical inertness can be overcome

through cyclometalation. In the last decade palladacycles have emerged as a very promising family of organometallic catalyst and it is proposed that the palladium catalysed organic transformation take place through the formation of palladacycle. However, the role of palladacycles in cross-coupling reactions truly began in 1995 after the discovery of the cyclopalladated $[Pd_2(\mu\text{-}OAc)_2\{tol_2PC_6H_4CH_2\text{-}o\}_2]$ by Herrmann and coworkers [48] and its involvement in the Heck [48] and Suzuki – Miyaura [48] reactions. Rapid enhancements in activity and stability observed on orthometallation led to the preparation of a wide variety of phosphorous-, nitrogen-, sulfur- and oxygen-based palladacycles as well as cyclopalladated pincer complexes of the type PCP, PCS and NCN, and their application in various C-C and C-heteroatom coupling reaction. Scheme 14 shows some the cyclopalladated complexes acts as catalyst. Apart from the usual scope of Heck, Suzuki and related reactions, palladacycles find applications in many other areas of organic transformation [52]. Palladacycles derived from oxazoles, 2-phenylpyridine and quinoline have been reported as effective catalysts for the oxidation of primary and secondary alcohols to the corresponding aldehydes and ketones under an atmospheric pressure of air without the addition of any other re-oxidants [117-119].

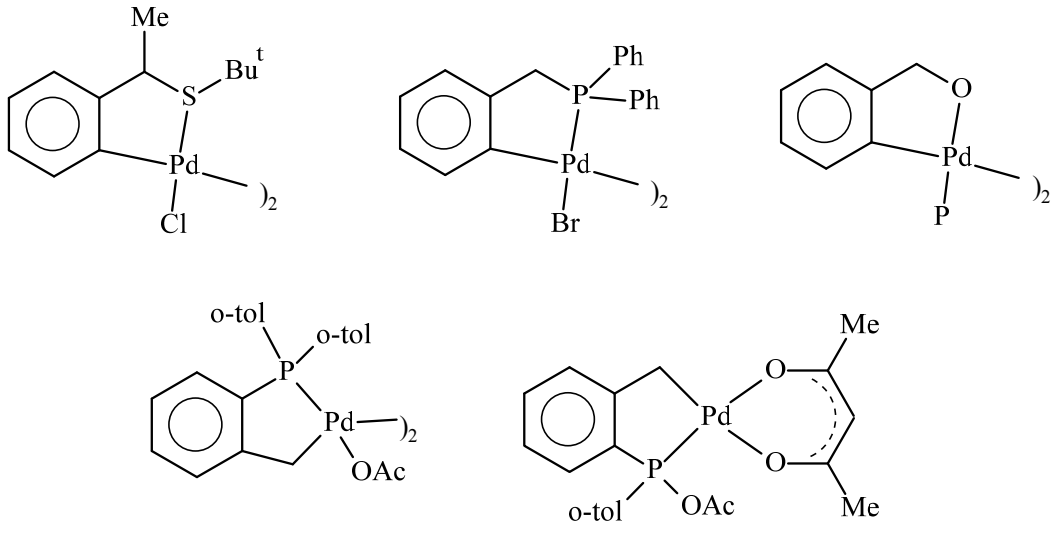

Scheme 14. Palladacycles with with catalytic activity

1.5 Chemistry with chalcogen ligands

The chemistry of chalcogen ligands with platinum group metals has been one of the active areas of research for the past several decades due to their wide structural diversity, relevance in catalysis, applications in materials science and biology. A plethora of chalcogen ligands, such as chalcogenoethers, chalcogenolate, chalcogenides, etc., have been used to prepare metal complexes. The chemistry of platinum group metal complexes with chalcogen ligands has been dominated by sulfur ligands while havier chalcogens (Se or Te) have received scant attention.

Monodentate, chelating bi-/ tri-dentate and hybrid chalcogenoethers incorporating N, O, S hetero donor atoms have been used for the synthesis of metal complexes. A number of reviews pertaining to specific aspects of the chemistry of these compounds have been published [120-125]. The metal complexes are usually isolated in a single step reaction between metal halides with the free ligand in an appropriate solvent. The metal complexes are usually obtained by stirring either an aqueous solution of metal salts with a chalcogenoether or a solution of a metal complex containing labile ligands such organonitriles, olefins, etc. with a chalcogenoether in an organic solvent. Organochalcogeno ether-based binuclear palladium and platinum complexes of general formula, $[M_2X_4(R_2E)_2]$ (M = Pd or Pt; E = S, Se, Te) are prepared in several ways [126-128] and the one involving reaction of $MCl_2(R_2E)_2$ with Na_2MX_4 in ethanol is commonly employed. Thioethers have a greater π-acceptor capacity than nitrogen donor ligands but less than PR_3 or AsR_3. Inversion at pyrimidylchalcogen atom in several metal complexes has been investigated by NMR spectroscopy and in general it is a facile process [125]. The barrier of inversion increases with increasing size of the chalcogen atom and follows the order Te>Se > S [125]. Inversion barrier in platinum complexes is higher than those in the corresponding palladium complexes. Chalcogenoether complexes undergo a variety of reactions; and to name a few are, Te-C

bond cleavage, trans-metalation and cyclometalation reactions. The latter reactions with selenium or tellurium ligands have met with little success.

1.6 Scope of the present work

The above discussion on palladium and platinum chemistry clearly indicates that there are several areas which offer new opportunities for further investigations. In particular organometallic derivatives derived from cyclometalation are of particular interest. Cyclometalation of seleno and telluro ligands, which has hardly been elucidated or when investigated has met with little success, is worth pursuing. Thermo-chemical aspects of organometallic compounds have also been little explored, although their applications in organic synthesis, catalysis, materials science and biology are well documented. So it is proposed to examine cyclometalation reactions of seleno- and telluro-ethers and study thermochemical behavior of the resulting organometallic complexes. All the complexes have been characterized by elemental analyses, IR, NMR (^{1}H, ^{13}C, ^{31}P, ^{77}Se, ^{125}Te, ^{195}Pt), UV-Vis, mass spectrometry. In several cases structures have been established unambiguously by single crystal X-ray diffraction analyses. For the sake of convenience and clarity the present work is sub-divided as follows:

- Cyclopalladation of selenoethers
- Cyclopalladation of telluroethers
- Cycloplatination of telluroethers
- Reactivity of telluoroethers with coordinated organonitrile with platinum(II)
- Thermochemical behaviour of cyclopalladated complexes

Chapter 2

Experimental

2.1 Materials and methods

Glassware of Pyrex quality with interchangeable ground joints were used during this investigation. The moisture and air sensitive reactions were carried out in special type of glass-wares like Schlenk tubes, two necked flasks with appropriate joints were used. The precipitates were filtered through G-2/ G-3 sintered discs. All the glass-wares were thoroughly cleaned by keeping them overnight in an alkali bath [5% NaOH in ethanol-water (1:1 v/v) mixture], and were washed with water and then rinsed with acetone and dried at 120-130°C in an electric oven for 3-4 h and subsequently kept in a desiccator containing fused $CaCl_2$ for cooling prior to use.

All the solvents and reagents were of AR grade and were dried and purified by standard procedures [129]. Diethyl ether (C_2H_5-O-C_2H_5) (b.p. 34.6°C) and tetrahydrofuran (THF) (b.p.: 66°C) were distilled over P_2O_5 and were dried by refluxing over sodium metal and benzophenone and distilled under argon when blue color persisted. Toluene (b.p.: 111°C) was dried by refluxing over sodium metal and benzophenone, followed by distillation under argon. Methanol (b.p.: 65°C) was dried by refluxing with magnesium methoxide (prepared from magnesium turnings and methanol in the presence of catalytic amount of iodine) for 2-3 h and distilled under argon. Dichloromethane (b. p.: 40 °C) was dried over calcium chloride followed by decantation and distillation. Hexane (b.p.: 67-68°C) was dried by refluxing over sodium metal using benzophenone as an indicator. Elemental selenium (99.99%, SMP Hyderabad), tellurium (99.99%, SMP Hyderabad), sodium borohydride (Aldrich) were obtained from commercial sources and used as such. The compounds, N,N-dimethylbenzylamine, PhSH, MesSH (Mes = mesityl or 2,4,6-$Me_3C_6H_2$), Ph_2Se_2, pySH, 2-bromo mesitylene, bromo-benzene, 2-bromo-toluene, 2,4,6-tri methyl aniline were obtained from commercial sources and were used without further purification.

2.2 Experimental techniques

Melting points were determined in one end sealed capillary tube and are uncorrected. The elemental analysis for C, H, N and S was carried out on a Thermo Fischer Flash EA 1112 CHNS micro-analyser. The IR spectra were recorded as Nujol mulls between CsI (range: 200-4000 cm^{-1}) or KBr (range: 400-40000 cm^{-1}) plates on a Bomen MB-102 or Jasco (model FT-IR-6100) FT-IR spectrometer with a resolution of 4 cm^{-1}. The spectra were calibrated using polystyrene film. Electronic spectra were recorded in a suitable solvent on a Chemito Spectroscan UV-2600 double beam UV-vis spectrophotometer using quartz cuvettes with a diameter of 1 cm. The wavelength range covered in the spectrometer is 200-1100 nm with a resolution of ~1 nm.

The ^{1}H, $^{13}C\{^{1}H\}$, $^{31}P\{^{1}H\}$, $^{77}Se\{^{1}H\}$, $^{125}Te\{^{1}H\}$ and $^{195}Pt\{^{1}H\}$ NMR spectra were recorded on a Bruker Avance-II, 300MHz NMR spectrometer (in 5 mm thin-walled NMR tubes) operating at 300.1, 75.5, 121.49, 57.24, 94.7 and 64.5 MHz, respectively and Bruker Ascend TM-400 (400, 100.61, 161.97, 76.33, 126.24, 86.02 MHz, respectively) NMR spectrometer. The chemical shifts are relative to the internal chloroform peak at δ 7.26 ppm for ^{1}H and δ 77.0 ppm for ^{13}C and external 85% H_3PO_4 for ^{31}P; and Me_2Se for ^{77}Se (secondary reference Ph_2Se_2δ 463 ppm); external Me_2Te for ^{125}Te (secondary reference Ph_2Te_2, δ 421 ppm in C_6D_6) and external Na_2PtCl_6 in D_2O. A 90^0 pulse was used in every case. The physical characteristics of some of the spin ½ nuclei are given in Table 3 [130].

Mass spectra were recorded in a MS-500 Ion Trap (IT) Varian mass spectrometer at Sophisticated Analytical Instrumentation Facility (SAIF), Indian Institute of Technology-Bombay, Mumbai. Powder XRD patterns were recorded on a Philips PW 1820 using Cu-K_α radiation. TG curves were recorded on a Setsys Evolution 1750 instrument at a heating rate of 5°C/min under flowing argon atmosphere. X-ray photoelectron spectra (XPS) were recorded on a SPECS instrument with 385 W, 13.85 kV and 175.6 nA (sample current) Al Kα (1486.6

eV) duel anode, with a PHOBIOS 100/150 Delay Line Detector (DLD). The XPS was recorded with pass energy of 50. The C 1S peak (284.6 eV) was used as an internal reference for the absolute binding energy calculation. SEM were recorded on SERON INC South Korea made (model no. ATS 2100) instrument and EDAX were recorded on Oxford Instrumentation UK (model no. INCAE 350), using highly polished Co metal as reference.

Table 3. Physical characteristics of some spin ½ nuclei [130]

Nucleus	Natural abundance (%)	γ- values (10^{-7} rad $T^{-1}s^{-1}$)	Receptivity D^p	Magnetic moment (μ/μ_N)
Hydrogen (^{1}H)	99.98	26.75	1.000	4.837
Carbon (^{13}C)	1.11	6.73	$1.76x10^{-4}$	1.216
Phosphorus (^{31}P)	100	10.83	0.066	1.958
Selenium (^{77}Se)	7.58	5.10	5.26×10^{-4}	0.922
Tellurium (^{125}Te)	6.99	–8.453	2.21×10^{-3}	–1.528
Platinum (^{195}Pt)	33.80	5.75	3.36×10^{-3}	1.0398

Single Crystal X-Ray Crystallography

The single crystal X-ray structural analyses of a number of complexes were carried out on Rigaku AFC 7S (using graphite monochromated Mo Kα, λ = 0.71069 Å radiation), Bruker APEX-II CCD (using graphite monochromated Mo Kα, λ = 0.71069 Å radiation) or SuperNova CCD (using graphite monochromated Cu-K_α, λ= 1.54184 Å radiation) diffractmeters [131]. The crystals were directly mounted on the diffractometer after examining the quality of crystal under a polarizing microscope. In some cases, crystals were cut to the desired size before mounting. All the data were corrected for Lorentz and polarization effects. The structures were solved by direct methods using SHELX-97 [132]

and refined by full matrix least square method [132, 133] on F^2 using data correction for absorption effects using empirical procedures [134]. All the non-hydrogen atoms were refined anisotropically and hydrogen atoms were placed in their geometrically idealized positions with coordinate and thermal parameters riding on host atoms. All the calculations were performed using a crystal structure crystallographic software package [135, 136]. The molecular structures were drawn using ORTEP [137-139]. Crystallographic and refinement details of some of the synthesized complexes are given in Tables 4-11.

Table 4. Crystallographic and structural determination data for $[Pd_2Cl_2(\mu\text{-}Cl)_2(Mes_2Se)_2]$, $[Pd_2(\mu\text{-}Cl)_2\{MesSeC_6H_2(Me_2)CH_2\}_2]$, $[Pd_2(\mu\text{-}Spy)_2\{Mes\ SeC_6H_2(Me_2)CH_2\}_2]$ and $[Pd_2(\mu\text{-}Sepy)_2\{Mes\ SeC_6H_2(Me_2)CH_2\}_2]$

Complex	$[Pd_2Cl_2(\mu\text{-}Cl)_2(Mes_2Se)_2]$	$[Pd_2(\mu\text{-}Cl)_2\{Mes\ SeC_6H_2(Me_2)CH_2\}_2]$	$[Pd_2(\mu\text{-}Spy)_2\{Mes\ SeC_6H_2(Me_2)CH_2\}_2]$	$[Pd_2(\mu\text{-}Sepy)_2\{Mes\ SeC_6H_2(Me_2)CH_2\}_2]$
Empirical formula	$C_{36}H_{44}Cl_4Pd_2Se_2$	$C_{36}H_{42}Cl_2Pd_2Se_2$	$C_{46}H_{50}N_2Pd_2S_2Se_2$	$C_{46}H_{50}N_2Pd_2Se_4$
Formula weight	989.24	916.32	1065.72	1159.52
Diffractometer	Agilent SuperNova	Agilent SuperNova	Bruker APEX-II CCD	Bruker APEX-II CCD
Radiation (λ/Å)	Cu-K_α (1.54184Å)	Cu-K_α (1.54184Å)	Mo-K_α (0.71073Å)	Mo-Kα (0.71073Å)
Temperature(K)	100 (2)	100 (2)	296 (2)	298 (2)
Crystal size (mm)	0.12×0.05×0.02	0.03×0.03×0.01	0.25×0.15×0.15	0.20×0.15×0.10
Crystal system	Triclinic	Monoclinic	Triclinic	Monoclinic
Space group	P ī	$P2_{1/}c$	Pī	C2/c
a (Å)	8.5654(5)	15.1293(5)	8.735(5)	24.997(5)
b (Å)	11.1973(8)	15.0902(5)	10.919(5)	9.941(5)
c (Å)	11.5045(6)	15.1702(4)	23.272(5)	18.149(5)
α (°)	110.442(6)	90.00	98.092(5)	90.000(5)
β (°)	97.754(5)	97.287(3)	93.574(5)	97.153(5)
γ (°)	109.719(6)	90.00	96.018(5)	90.000(5)
Volume ($Å^3$)	932.46(12)	3435.45(18)	2178.7(17)	4475(3)
ρ_{calcd} (g cm^{-3})	1.762	1.772	1.625	1.721
Z	1	4	2	4

μ (mm^{-1})/F(000)	12.829/ 488	12.475/1808	2.626/1064	4.090/ 2272
θ range (°)	4.2772–66.4884	4.1459–66.4852	2.78–26.48	2.43–24.98
Index range	-10≤h≤10 -13≤k≤13 -13≤l≤13	-18≤h≤17 -17≤k≤17 -18≤l≤12	-10≤h≤10 -13≤k≤13 -27≤l≤29	-32≤h≤33 -13≤k≤12 -24≤l≤23
Reflections collected/Unique	13045/3294	10027/4265	33744/8908	35367/5556
Data/Restraints/Parameters	3294/0/205	5990/0/389	8908/0/497	5556/0/250
Final R_1, ωR_2 indices	0.0291/0.0631	0.0446/0.0895	0.0253/0.0683	0.0333/0.0606
R_1, ωR_2 (all data)	0.0407/0.0676	0.0723/0.1016	0.0370/0.0779	0.0781/0.0725
Goodness of fit on F^2	1.021	0.983	1.101	0.994

Table 5. Crystallographic and structural determination data for *trans*-[$PdCl_2(TeMes_2)_2$].2 MeCN, *trans*-[$PdCl_2(TeMes_2)_2$].toluene, [$Pd_2(\mu$-$Cl)_2Cl_2(TeMes_2)_2$]. 2 acetone and *cis*-[$PdCl_2\{MesTeCH_2C_6H_2(4,6\text{-}Me_2)TeMes\}$].

	trans-[$PdCl_2(TeMes_2)_2$]. 2 MeCN	*Trans*-[$PdCl_2(TeMes_2)_2$]. toluene	[$Pd_2(\mu$-$Cl)_2Cl_2(TeMes_2)_2$]. 2acetone	*cis*-[$PdCl_2\{MesTeCH_2C_6H_2(4,6\text{-}Me_2)TeMes\}$]
Empirical formula	$C_{36}H_{44}Cl_2PdTe_2$. $2CH_3CN$	$C_{36}H_{44}$ $Cl_2PdTe_2.C_7H_8$	$C_{36}H_{44}Cl_4Pd_2Te_2$. $C_6H_{12}O_2$	$C_{27}H_{32}Cl_2PdTe_2$
Formula weight	991.32	1001.35	1202.67	789.03
Diffractomete	Agilent SuperNova	Agilent SuperNova	Agilent SuperNova	Bruker APEX-II CCD
Radiation (λ/Å)	Cu K/α (1.5418)	Cu K/α (1.5418)	Cu K/α (1.5418)	Mo K/α (0.71073)
Temperature (K)	298 (2)	298 (2)	298 (2)	298 (2)
Crystal size (mm)	0.15 0.05 x 0.02	0.1 x 0.1 x 0.05	0.15 x 0.13 x 0.10	0.14 x 0.05 x 0.01
Crystal system	Monoclinic	Triclinic	Monoclinic	Monoclinic
Space group	$P2_1/n$	*P*-1	$P2_1/c$	$P2_1/c$
Unit cell dimensions				
a (Å)	8.8514(16)	11.3836(8)	9.9444(3)	12.8111(3)
b (Å)	10.3908(17)	12.8965(7)	22.0756(8)	19.8187(4)
c (Å)	23.3718(5)	16.0242(9)	10.5502(4)	12.0377(2)
α (°)	90.00	87.937(5)	90.00	90.00
β (°)	100.804(18)	78.771(5)	95.709(3)	114.103(10)
γ (°)	90.00	67.794(6)	90.00	90.00
Volume ($Å^3$)	2111.47(7)	2134.5(2)	2304.58(13)	2789.89(10)
Z	2	2	2	4
ρ_{calcd} (g cm^{-3})	1.559	1.558	1.733	1.879

μ (mm^{-1})/F(000)	15.596/ 976	15.421/ 988	18.466/ 1176	2.920/ 1512
Limiting indices	$-9 \leq h \leq 10$ $-12 \leq k \leq 12$ $-28 \leq l \leq 28$	$-13 \leq h \leq 12$ $-14 \leq k \leq 15$ $-19 \leq l \leq 18$	$-11 \leq h \leq 11$ $-26 \leq k \leq 26$ $-6 \leq l \leq 12$	$-16 \leq h \leq 15$ $-24 \leq k \leq 24$ $-15 \leq l \leq 15$
θ for data collection (°)	3.85 – 69.91	2.81 – 70.04	4.01 – 69.90	1.74 – 26.39
no. of reflns collected	3981	7925	4259	5696
no. of independent reflns	3585	5758	3132	5053
Data/restraints/parameters	3981/0/221	7925/0/447	4259 /0 /235	5696/ 0/ 298
Final R_1, wR_2 indices	0.0459/0.1302	0.0507/0.1151	0.0674/ 0.1643	0.0238/ 0.0645
R_1, wR_2 (all data)	0.0504/0.1344	0.0773/0.1281	0.0958/ 0.1747	0.0297/ 0.0755
Goodness of fit on F^2	1.130	1.057	1.189	1.176

Table 6. Crystallographic and structural determination data for $[Pd_2(\mu\text{-}OAc)_2\{CH_2C_6H_2(4,6\text{-}Me_2)TeMes\}_2]$.toluene, $[Pd_2(\mu\text{-}OAc)_2\{CH_2C_6H_2(4,6\text{-}Me_2)Tetol\text{-}o\}_2]$ and $[Pd(\mu\text{-}OAc)(\mu\text{-}TeMes)]_4$

	$[Pd_2(\mu\text{-}OAc)_2\{CH_2C_6H_2(4,6\text{-}Me_2)TeMes\}_2]$.toluene	$[Pd_2(\mu\text{-}OAc)_2\{CH_2C_6H_2(4,6\text{-}Me_2)Tetol\text{-}o\}_2]$	$[Pd(\mu\text{-}OAc)(\mu\text{-}TeMes)]_4$
Empirical formula	$C_{40}H_{48}O_4Pd_2Te_2.C_7H_8$	$C_{36}H_{40}O_4Pd_2Te_2$	$C_{44}H_{56}O_8Pd_4Te_4$
Formula weight	1152.92	1004.68	1648.89
Diffractometer	Agilent SuperNova	Agilent SuperNova	Agilent SuperNova
Radiation (λ/Å)	Cu K/α (1.5418)	Cu K/α (1.5418)	Cu K/α (1.5418)
Temperature (K)	130 (10)	298(2)	298(2)
Crystal size (mm)	0.20 x 0.15 x 0.10	0.12 x 0.10 x 0.05	0.18 x 0.05 x 0.05
Crystal system	Monoclinic	Monoclinic	Triclinic
Space group	$P2_1/n$	$P2_1/n$	*P*-1
Unit cell dimensions			
a (Å)	11.1936(3)	12.2913(3)	8.2911(4)
b (Å)	33.0163(13)	17.9732(5)	12.0292(5)
c (Å)	11.9487(3)	16.5408(5)	13.7289(6)
α (°)	90.00	90.00	72.307(4)
β (°)	92.641(2)	101.904(3)	72.599(4)
γ (°)	90.00	90.00	89.423(4)
Volume ($Å^3$)	4411.2(2)	3575.50(18)	1239.86(10)
Z	4	4	1
ρ_{calcd} (g cm^{-3})	1.736	1.866	2.208

μ (mm^{-1})/F(000)	17.127/ 2264	21.018/ 1936	30.102/ 776
Limiting indices	$-13 \leq h \leq 7$ $-33 \leq k \leq 39$ $-14 \leq l \leq 13$	$-14 \leq h \leq 14$ $-21 \leq k \leq 20$ $-13 \leq l \leq 20$	$-9 \leq h \leq 10$ $-14 \leq k \leq 14$ $-16 \leq l \leq 16$
θ for data collection (°)	3.94 – 70.24	3.675 – 69.879	3.56-70.07
no. of reflns collected	8254	6614	4648
no. of independent reflns	6016	4494	3616
Data/restraints/parameters	8254/37/490	6614/ 0 /405	4648/ 0/ 279
Final R_1, wR_2 indices	0.0739/0.1838	0.0704/ 0.1732	0.0376/ 0.0846
R_1, wR_2 (all data)	0.1009/0.2024	0.1110/ 0.1972	0.0600/ 0.0948
Goodness of fit on F^2	1.047	1.066	1.042

Table 7. Crystallographic and Structural Refinement data for *trans*-[$PtCl_2${Te(R)Mes}$_2$] (R =Mes, Ph, *o*-tol), [PtCl{($CH_2C_6H_2Me_2$-4,6)TeMes}($TeMes_2$)] and [PtCl{($CH_2C_6H_2Me_2$-4,6)TeMes}PPh_3]

	trans-[$PtCl_2${Te(Ph)Mes}$_2$]	*trans*-[$PtCl_2${Te(*o*-tol)Mes}$_2$]	*trans*-[$PtCl_2${TeMes}$_2$]	[PtCl{($CH_2C_6H_2Me_2$-4,6)TeMes}($TeMes_2$)]	[PtCl{($CH_2C_6H_2Me_2$-4,6)TeMes}(PPh_3)]
Empirical formula	$C_{30}H_{32}Cl_2PtTe_2$	$C_{32}H_{36}Cl_2PtTe_2$	$C_{36}H_{44}Cl_2PtTe_2$	$C_{36}H_{43}ClPtTe_2$	$C_{36}H_{36}ClPPtTe$
Formula weight	913.74	941.80	997.90	961.44	857.76
Diffractometer	Agilent SuperNova	Agilent SuperNova	Agilent SuperNova	Agilent SuperNova	Agilent SuperNova
Radiation (λ/Å)	Cu K/α (1.5418)	Cu K/α (1.5418)	Cu K/α (1.5418)	Cu K/α (1.5418)	Cu K/α (1.5418)
Temperature (K)	298 (2)	298 (2)	298 (2)	298 (2)	298 (2)
Crystal size(mm)	0.73 x 0.45 x 0.12	0.20 x 0.20 x 0.10	0.078 x 0.180 x 0.400	0.27 x 0.15 x 0.08	0.19 x 0.39 x 0.87
Crystal system	Triclinic	Monoclinic	Triclinic	Monoclinic	Triclinic
Space group	$P\bar{1}$	$P2_1/c$	$P\bar{1}$	$P2_1/n$	$P\bar{1}$
a(Å)	8.3863(7)	12.2222(7)	12.2279(4)	12.3617 (3)	9.2579(3)
b(Å)	8.8308(9)	9.8439(6)	15.9978(5)	15.0672(3)	18.5589(8)
c(Å)	11.8748(15)	14.6962(9)	18.9292(6)	18.7395(4)	20.6306(9)
α(°)	68.588(11)	-	84.313(3)	-	106.161(4)
β(°)	76.008(9)	113.953(7)	83.183(3)	100.793(2)	97.925(3)
γ(°)	68.321(9)	-	86.493(3)	-	101.363(3)
Volume ($Å^{3)}$	754.98(16)	1615.88(19)	3654.1(2)	3428.60(13)	3267.2(2)
Z	1	2	4	4	4
ρ_{calcd} (g cm^{-3})	2.010	1.936	1.814	1.863	1.744

μ (mm^{-1})/F(000)	25.378/428	23.737/888	21.034/1904	21.689/1832	16.317/1656
θ for data collection/^{o}	4.0580 to 69.3280	3.958 to 70.405	2.779 to 70.106	3.791 to 69.987	2.841to 69.969
Limiting indices	$-10 \leq h \leq 9$ $-10 \leq k \leq 10$ $-14 \leq l \leq 14$	$-14 \leq h \leq 12$ $-11 \leq k \leq 11$ $-12 \leq l \leq 17$	$-14 \leq h \leq 14$ $-19 \leq k \leq 18$ $-22 \leq l \leq 17$	$-14 \leq h \leq 12$ $-17 \leq k \leq 18$ $-22 \leq l \leq 19$	$-11 \leq h \leq 8$ $-22 \leq k \leq 22$ $-25 \leq l \leq 23$
No. of unique reflns	2784	3028	13593	6364	12159
No. of obsd reflns with $I > 2\sigma(I)$	1745	2659	10182	5045	8245
Data/restraints/parameters	2784/0/165	3028/0/173	13593/6/764	6364/0/372	12159 / 0 /731
Final R_1, ωR_2 indices	0.0872/0.2304	0.0707/0.2022	0.0877/0.2597	0.0763/0.2246	0.1158/ 0.3000
R_1, ωR_2 (all data)	0.1237/0.2778	0.0759/0.2068	0.1102/ 0.2790	0.0891/0.2351	0.1436/ 0.3379
Goodness of fit on F^2	1.022	1.075	1.064	1.077	1.160
Largest diff. peak and hole ($e.Å^{-3}$)	2.629 and -2.121	3.698 to -1.831	4.711 to -2.702	3.950 to -2.023	4.681 to -4.816

Table 8. Crystallographic and structural determination data for *trans*-[$PtCl_2$(PhCN){NC(O)Ph[Te(tol-*o*)Mes]}], *trans*-[$PtCl_2${NC(O)Ph($TeMes_2$)}$_2$].4H_2O, *trans*-[$PtCl_2${NC(Ph)C_4H_7O}{NC(O)Ph($TeMes_2$)}] and *trans*-[$PtCl_2${NC(O)Ph[Te(tol-*o*)Mes]}$_2$],

Complex	*trans*-[$PtCl_2$(PhCN){NC(O)Ph[Te(tol-*o*)Mes]}]	*trans*-[$PtCl_2${NC(O)Ph($TeMes_2$)}$_2$] . 4H_2O	*trans*-[$PtCl_2${NHC(Ph)C_4H_7O}{NC(O)Ph($TeMes_2$)}]	*trans*-[$PtCl_2${NC(O)Ph[Te(tol-*o*)Mes]}$_2$]
Empirical formula	$C_{30}H_{28}Cl_2N_2OPtTe$	$C_{50}H_{54}Cl_2N_2O_2PtTe_2$. 4$H_2O$	C_{36} H_{40} Cl_2 N_2 O_2 Pt Te	$C_{46}H_{46}Cl_2N_2O_2PtTe_2$
Formula weight	826.13	1308.14	926.29	1180.04
Diffractometer	Agilent SuperNova	Rigaku AFC 75	Agilent SuperNova	Agilent SuperNova
Radiation (λ/Å)	Cu-Kα (1.54184Å)	Mo- Kα (0.71069Å)	Cu-Kα (1.54184Å)	Cu-Kα (1.54184Å)
Temperature (K)	298 (2)	298 (2)	298 (2)	298 (2)
Crystal size (mm)	0.40 x 0.10 x 0.1	0.30 x 0.10 x 0.10	0.33 x 0.14 x 0.08	0.25 x 0.16 x 0.12
Crystal system	Triclinic	Monoclinic	Triclinic	Monoclinic
Space group	$P\bar{1}$	$C2_1/c$	$P\bar{1}$	$P2_1/n$
a (Å)	10.6997(8)	15.561(6)	9.2752(7)	13.8807 (16)
b (Å)	10.8569(9)	26.713(9)	12.7816(8)	12.3488(7)
c (Å)	14.5674(9)	13.146(9)	16.1748(15)	25.5038(16)
α(º)	98.279(6)	90	73.237(7)	90
β(º)	105.843(6)	110.75(4)	73.350(8)	96.456(9)
γ(º)	110.015(7)	90	77.950(6)	90
Volume ($Å^3$)	1475.9(2)	5110(4)	1742.4(3)	4343.916
ρ_{calcd} (g cm^{-3})	1.859	1.690	1.764	1.804

Z	2	4	2	4
μ (mm^{-1})/F(000)	18.395/788	4.017 / 2528	15.679 / 900	17.864 / 2272
θ range(°)	3.268-70.060	2.632-27.518	2.940-69.951	3.472-42.586
Index range	$-12 \leq h \leq 13$ $-13 \leq k \leq 12$ $-14 \leq l \leq 17$	$-20 \leq h \leq 18$ $0 \leq k \leq 34$ $-9 \leq l \leq 17$	$-9 \leq h \leq 11$ $-10 \leq k \leq 15$ $-19 \leq l \leq 19$	$-5 \leq h \leq 9$ $-10 \leq k \leq 9$ $-22 \leq l \leq 14$
Reflections collected/unique	8940 / 5403	7056 / 5878	10887 / 6437	3127 / 2063
Data/restraints/parameter	5403 / 42 / 338	5878 / 0 / 280	6437 / 30 / 404	2063 / 309/ 383
Final R1, ωR_2 indices	0.0847 / 0.2201	0.0709 / 0.1624	0.0838 / 0.2081	0.0815 / 0.2026
R_1, ωR_2 (all data)	0.1150 / 0.2407	0.1410 / 0.1910	0.1342 / 0.2513	0.0867 / 0.2121
Goodness of fit on F^2	1.046	1.059	1.036	1.080

Table 9. Crystallographic and structural determination data for *trans*-[$PtCl_2(TeMes_2)\{NC(O)Ph(TeMes_2)\}$], *trans*-[$PtCl_2\{NC(O)Me(TeMes_2)\}_2$].$2CH_2Cl_2$ and [$PtCl(Tetol\text{-}o)\{NC(O)Ph\}_2$].$CH_2Cl_2$

Complex	*trans*-[$PtCl_2(TeMes_2)\{NC(O)Ph(TeMes_2)\}$]	[$PtCl(Tetol\text{-}o)\{NC(O)Ph\}_2$]	*trans*-[$PtCl_2\{NC(O)Me\ (TeMes_2)\}_2$]. $2CH_2Cl_2$
Empirical formula	$C_{43}H_{49}Cl_2NOPtTe_2$	$C_{21}H_{17}ClN_2O_2PtTe.CH_2Cl_2$	$C_{40}H_{50}C_2N_2O_2PtTe_2.2CH_2Cl_2$
Formula weight	1117.02	772.43	1281.86
Diffractometer	Rigaku AFC 75	Rigaku AFC 75	Rigaku AFC 75
Radiation (λ/Å)	Mo- Kα (0.71069Å)	Mo-Kα (0.71069Å)	Mo-Kα (0.71069Å)
Temperature (K)	298 (2)	298 (2)	298 (2)
Crystal size (mm)	0.15 x 0.15 x 0.05	0.20 x 0.20 x 0.20	0.15 x 0.10 x 0.05
Crystal system	Triclinic	Monoclinic	Triclinic
Space group	$P\bar{1}$	$P2_1/n$	$P\bar{1}$
a (Å)	12.208(2)	11.7651(16)	9.111(5)
b (Å)	12.602(4)	11.1423(14)	12.324(4)
c (Å)	14.752(5)	19.900(3)	12.961(11)
α(º)	71.33(2)	90	105.69(4)
β(º)	89.58(2)	106.190(12)	107.79(5)
γ(º)	86.273(19)	90	107.96(5)
Volume ($Å^3$)	2145.5(11)	2505.2(6)	1206.6(14)
ρ_{calcd} ($g\ cm^{-3}$)	1.729	2.048	1.764
Z	2	4	1
μ (mm^{-1})/F(000)	4.759 / 1076	7.083 / 1448	4.459 / 620

θ range(°)	2.560-27.501	2.567 - 27.493	2.596 - 27.491
Index range	$-15 \leq h \leq 15$ $-9 \leq k \leq 16$ $-18 \leq l \leq 19$	$-14 \leq h \leq 15$ $-14 \leq k \leq 0$ $-25 \leq l \leq 14$	$-6 \leq h \leq 11$ $-15 \leq k \leq 15$ $-16 \leq l \leq 16$
Reflections collected/unique	11824 / 9837	6833 / 5744	6715 / 5528
Data/restraints/parameter	9837 / 96 / 380	5744 / 28 / 309	5528 / 1 / 242
Final R1, ωR_2 indices	0.0936 / 0.1481	0.0583 / 0.1202	0.0767 / 0.1281
R_1, ωR_2 (all data)	0.1956/ 0.3635	0.1570 / 0.1531	0.1762/ 0.2649
Goodness of fit on F^2	0.808	0.956	0.952

Table 10. Crystallographic and structural determination data for $[Pd_2(\mu\text{-}Spy)_2(Me_2NCH_2C_6H_4\text{-}C,N)_2]$ and $[Pd_2(\mu\text{-}Sepy)_2(Me_2NCH_2C_6H_4\text{-}C,N)_2]$

Complex	$[Pd_2(\mu\text{-}Spy)_2(Me_2NCH_2C_6H_4\text{-}C,N)_2]$	$[Pd_2(\mu\text{-}Sepy)_2(Me_2NCH_2C_6H_4\text{-}C,N)_2]$
Empirical formula	$C_{28}H_{32}N_4Pd_2S_2$	$C_{28}H_{32}N_4Pd_2Se_2$
Formula weight	701.56	795.30
Diffractometer	Rigaku AFC 75	Rigaku AFC 75
Radiation (λ/Å)	Mo-K_α (.07107)	Mo-K_α (.07107)
Temperature (K)	298 (2)	298 (2)
Crystal size (mm)	0.20×0.20×0.20	0.40×0.20×0.05
Crystal system	Triclinic	Monoclinic
Space group	P $\bar{1}$	C2/c
a (Å)	10.333(3)	16.131(9)
b (Å)	11.294(10)	9.812(8)
c (Å)	13.794(6)	18.867(11)
α (^{0})	70.62(5)	-
β (^{0})	72.560(17)	110.03(5)
γ (^{0})	79.50(5)	-
volume (Å^3)	1442.6(14)	2806(3)
ρ_{calcd} (g cm^{-3})	1.615	1.883
Z	2	4
μ (mm^{-1}) / F(000)	1.415 / 704	3.901 / 1552
θ range of data collection(°)	2.51–27.61	2.53–27.50
Index ranges	$-13 \le h \le 7$ $-14 \le k \le 14$ $-17 \le l \le 17$	$-11 \le h \le 20$ $-12 \le k \le 7$ $-24 \le l \le 23$
Reflection collected / Unique	6583 / 3231	3217 / 1291
Data/restraints/parameters	6583 / 0 / 323	3217 / 0 / 165
Final R_1, ωR_2 indices	0.0551 , 0.1081	0.0600 , 0.1002
R_1, ωR_2 (all data)	0.1760 , 0.1455	0.2326 , 0.1407
Goodness of fit on F^2	0.973	0.929
Largest difference in peak and hole (e A$^{\circ -3}$)	0.959 & -0.967	0.844 & -1.555

Table 11. Crystallographic and structural determination data for [Pd{$MesSeC_6H_2(Me_2)CH_2$}(S_2COPr^i)]

Empirical formula	$C_{22}H_{28}OPdS_2Se$
Formula weight	557.92
Diffractometer	Rigaku AFC7S
Radiation (λ/Å)	Mo-K_α (.07107)
Temperature (K)	298(2)
Crystal size (mm)	0.15×0.05×0.05
Crystal system	Triclinic
Space group	P $\bar{1}$
a (Å)	7.861(6)
b (Å)	11.800(8)
c (Å)	14.059(7)
α (^{0})	112.55(4)
β (^{0})	91.57(5)
γ (^{0})	104.02(6)
volume (Å^3)	1158.0(14)
ρ_{calcd} (g cm^{-3})	1.600
Z	2
μ (mm^{-1}) / F(000)	2.563 / 560
θ range of data collection(°)	2.695 - 27.510
Index ranges	$-10 \le h \le 5$ $-14 \le k \le 15$ $-18 \le l \le 18$
Reflection collected / Unique	6509 / 5327
Data/restraints/parameters	5327 / 0 / 251
Final R_1, ωR_2 indices	0.0678 / 0.1096
R_1, ωR_2 (all data)	0.2110 / 0.1456
Goodness of fit on F^2	0.960
Largest difference in peak and hole (e A$^{\circ -3}$)	

2.3 Synthesis of ligands and metal precursors

2.3.1 Synthesis of ligands

Dimesityldisulfide (Mes_2S_2)

Dimesityldisulfide was prepared by the reaction of MesMgBr (prepared from MesBr (17.50 g, 87.90 mmol) and magnesium turnings (2.14 g, 88.06 mmol)) with sulfur powder (2.80 g, 87.32 mmol) in diethyl ether at –78 °C. After completion of the reaction, the reaction mixture was brought to room temperature and alkaline aqueous $K_3[Fe(CN)_6]$ (28.85 g, 87.62 mmol) were added. The organic fraction was extracted with diethylether and dried over anhydrous $MgSO_4$. The solvent was removed under vacuum and the residue was recrystallised from ethylacetate as bright yellow crystals (yield: 5.3 g, 39%); m.p.: 105 ºC (Lit. 109 ºC [140]). Anal. Calcd. for $C_{18}H_{22}S_2$: C, 71.1; H, 7.2; S, 21.1 %. Found: C, 71.1; H, 7.2; S, 27.2 %.

Dimesityldiselenide (Mes_2Se_2)

Synthesized following the similar procedure as for Mes_2S_2 and recrystallized from diethyl ether as bright orange crystals (yield: 45%); m.p.: 109 °C [141]. ^{1}H NMR ($CDCl_3$) δ: 2.25 (s, 6H, 2,6-Me); 2.28 (s, 3H, 4-Me); 6.85 (s, 2H, 3,5-H). $^{13}C\{^1H\}$ NMR (CDCl3) δ: 20.9 (s, 4-CMe); 24.1 (s, 2,6-CMe); 128.3 (s, 3,5-C); 128.9 (s, 1-C); 139.1 (s, 4-C); 143.7 (s, 2,6-C).$^{77}Se\{^1H\}$ NMR ($CDCl_3$) δ: 371 ppm.

Bis(2-pyridyl)diselenide ($SeC_5H_4N)_2$

To an aqueous solution of Na_2Se_2 (prepared by the reaction of selenium powder (5.00 g, 63.3 mmol) with sodium borohydride (2.40 g, 63.4 mmol)) 2-bromo-pyridine (10.00g, 63.3 mmol) was added drop-wise. The reaction mixture was refluxed for 6 h and then cooled to room temperature. The organic fraction was extracted with dichloromethane and dried over anhydrous $MgSO_4$. The organic fraction was concentrated and the compound was separated as yellow crystals (yield: 5.0g, 50%) at 0-5°C; m.p.: 48°C [142]. ^{1}H NMR ($CDCl_3$) δ: 7.07 (t,

J = 5.55 Hz, 1 H), 7.53 (t, *J* = 7.35 Hz, 1 H), 7.78 (d, *J* = 7.8 Hz, 1 H), 8.44 (d, *J* = 3.6 Hz, 1 H). $^{77}Se\{^{1}H\}$ NMR ($CDCl_3$) *δ*: 426 ppm.

Dimesityl selenide ($SeC_{18}H_{22}$)

This was prepared by the reaction of an aqueous solution of Na_2Se (prepared by the reaction of selenium powder (6.46g, 81.8 mmol) with sodium borohydride (6.20g, 163.9 mmol)) with diazonium salt of 2,4,6-trimethyl aniline (prepared by the reaction of 2,4,6-trimetyl aniline (22.15g, 163.8 mmol) with $NaNO_2$ (12.0g, 173.9 mmol) in aqueous medium followed by the drop-wise addition of HCl (30 ml) at -7°C. The reaction mixture was stirred at -7°C for 2 h and then stirred at room temperature for additional 3 h. The reaction was freeze by adding 40 ml of petroleum ether. The organic fraction was extracted by dichloromethane and dried over anhydrous $MgSO_4$.The solution was concentrated and the title compound was separated at 0-5°C as needle shape colorless crystals (yield: 15.0 g, 60%); m.p.: 105°C.Analysis Calcd. for $C_{18}H_{22}Se$: C, 68.13; H, 6.99. Found: C, 68.3; H, 6.8%. ^{1}H NMR ($CDCl_3$) δ: 2.24 (s, 3H, 4-Me); 2.26(s, 6H, 2,6 -Me); 6.85 (s, 2H ,3,5 –H). ^{77}Se $\{^{1}H\}$ NMR ($CDCl_3$) δ: 234 ppm.

Dimesityldiselluride (Mes_2Te_2)

To a THF solution of MesMgBr (prepared from MesBr (20.82 g, 104 mmol) and magnesium turnings (2.52 g, 104 mmol) in 50 ml THF), a freshly grind tellurium powder (13.34 g, 104 mmol) was added under nitrogen atmosphere with stirring which continued overnight. The contents were exposed to air for 2 h with stirring and the solvent was evaporated under reduced pressure. The residue was extracted with diethyl ether (3 x 50 ml) and filtered. The filtrate was concentrated to 50 ml which on slow evaporation afforded red crystals of the title compound (yield: 15.00 g, 58%); m.p.: 120°C (lit. 125-127°C) [143]. Anal. Calcd. for $C_{18}H_{22}Te_2$: C, 43.8; H, 4.5 %. Found: C, 43.7; H, 4.3 %. ^{1}H NMR ($CDCl_3$) δ: 2.33 (s, Me-4), 2.37 (s, Me-2,6), 6.88 (s, 3, 5-CH). $^{13}C\{^{1}H\}$ NMR ($CDCl_3$)*δ*: 20.9 (4-Me);

30.1 (2,6-Me); 112.0 (Te-C); 126.9 (3, 5-CH); 139.3, 146.1 ppm. ^{125}Te {^{1}H} NMR ($CDCl_3$) = 200 ppm.

Diphenylditelluride (Ph_2Te_2)

Synthesized following the similar procedure as for Mes_2Te_2 and recrystallized from diethyl ether as bright red crystals (yield: 62%); m.p.: 62°C. Anal. Calcd. for $C_{12}H_{10}Te_2$: C, 35.2; H, 2.5 %. Found: C, 35.6; H, 2.5 %. ^{1}H NMR ($CDCl_3$) δ: 7.19-7.27 (m, 3H), 7.83-7.84 (m, 2H). ^{13}C{^{1}H} NMR ($CDCl_3$)*δ*: 108.0 (Te-C); 127.9; 129.1, 137.5 ppm. ^{125}Te {^{1}H} NMR ($CDCl_3$) = 421 ppm.

Di-*o*-tolylditelluride (*o*-tol_2Te_2)

Synthesized following the similar procedure as for Mes_2Te_2 and recrystallized from diethyl ether as bright red crystals (yield: 54%). Anal. Calcd. for $C_{14}H_{14}Te_2$: C, 38.4; H, 2.2 %. Found: C, 38.5; H, 2.0 %. ^{125}Te{^{1}H} NMR ($CDCl_3$) = 282 ppm.

Dimesityltelluride (Mes_2Te)

To an ice cold solution (50 ml) of dimesitylditelluride (2.5 g, 5.06 mmol) bromine (0.261 ml) in 5 ml toluene was added drop wise. To this MesTeBr solution, a THF solution of MesMgBr (0.5M, 25 ml) was added drop wise with stirring whereupon a colorless solution was formed. After one hour of stirring at room temperature, water (50 ml) was introduced to the reaction flask. The organic layer was evaporated under reduced pressure and the compound was extracted with diethyl ether (20 ml x 4) from the aqueous phase. The organic phase was washed with aqueous NH_4Cl followed by saturated NaCl and dried over anhydrous $MgSO_4$. The solution was concentrated under reduced pressure and the title compound was separated as colorless crystals (yield: 3.12 g, 84%); m.p.: 110°C (lit. 123-125°C) [143]. Anal. Calcd for $C_{18}H_{22}Te$: C, 59.1; H, 6.1 %. Found: C, 58.2; H, 5.9 %. ^{1}H NMR ($CDCl_3$) *δ*: 2.28 (s, Me-4); 2.39 (s, 2, 6-Me); 6.91 (s, 3, 5-CH). ^{13}C{^{1}H} NMR ($CDCl_3$)*δ*: 20.8 (s, 4-Me); 28.2

(s, 2,6-Me); 119.1 (Te-C); 127.8 (3, 5-CH); 137.9, 144.2 ppm. $^{125}Te\{^{1}H\}$ NMR ($CDCl_3$) δ: 261 ppm [144].

Diphenyltelluride (Ph_2Te)

Prepared similar to Mes_2Te employing PhMgBr. The compound was purified by converting into Ph_2TeBr_2, by oxidation of the crude Ph_2Te with bromine, which was recrystallized from toluene as yellow crystals. The latter was reduced with $Na_2S.15H_2O$ in refluxing methanol for 15 min. The contents were diluted with water and methanol was evaporated under reduced pressure. The compound from the aqueous phase was extracted with diethyl ether (4 x 20 ml) and after processing gave cream colored oily liquid in 66 % yield. Anal. Calcd. for $C_{12}H_{10}Te$: C, 51.1; H, 3.6 %. Found: C, 50.5; H, 3.5 %. ^{1}H NMR ($CDCl_3$) δ: 7.23-7.36 (m); 7.74-7.77 (m) (Ph). $^{13}C\{^{1}H\}$ NMR ($CDCl_3$) δ: 114.8 (C-Te); 127.9; 129.6; 138.0 ppm. $^{125}Te\{^{1}H\}$ NMR ($CDCl_3$) δ: 693 ppm.

Di-*o*-tolyltelluride (*o*-tol_2Te)

Prepared and purified similar to diphenyl telluride and isolated as cream colored liquid in 60 % yield. Anal. Calcd. for $C_{14}H_{14}Te$: C, 54.3; H, 4.5 %. Found: C, 53.6; H, 4.5 %. ^{1}H NMR ($CDCl_3$) δ: 2.72 (s, Me); 7.22 (t, 6.8 Hz); 7.48 (br, m); 7.82 (d, 7.5 Hz). ^{13}C $\{^{1}H\}$ NMR ($CDCl_3$) δ: 26.7 (Me); 119.0 (C-Te); 127.3; 128.8; 129.8; 138.5; 142.8 (C-2) ppm. ^{125}Te $\{^{1}H\}$ NMR ($CDCl_3$) δ: 499 ppm.

Mesityl(phenyl)telluride (MesTePh)

Prepared by treatment of MesTeBr (prepared from Mes_2Te_2 (5.0g, 10.0 mmol) and bromine (1.62 g, 10.3 mmol) in THF) with PhMgBr (0.6 M, 40 ml) and processed in a way similar to Ph_2Te, and was isolated as cream color liquid in 49% yield. Anal. Calcd. for $C_{15}H_{16}Te$: C, 55.6; H, 5.0 %. Found: C, 55.5; H, 5.2 %. ^{1}H NMR ($CDCl_3$) δ: 2.36 (s, 4-Me); 2.60(s, 2, 6-Me); 7.06 (s, 3, 5-CH); 7.14-7.19 (m); 7.36-7.39 (m) (Ph). ^{125}Te $\{^{1}H\}$ NMR ($CDCl_3$) δ: 427 ppm.

Mesityl(*o*-tolyl)telluride (MesTe(tol-*o*))

Prepared from *o*-tolTeBr (prepared from *o*-tol_2Te_2 (5.0 g, 11.31 mmol) and bromine (1.83 g, 11.57 mmol) in THF) and MesMgBr (0.5 M, 50 ml) and processed in a way similar to Mes_2Te, and isolated as cream colored crystalline solid (yield: 5.2 g, 68%); m. p.: 50°C. Anal. Calcd. for $C_{16}H_{18}Te$: C, 56.9; H, 5.4 %. Found: C, 56.0; H, 5.6 %. ^1H NMR ($CDCl_3$) δ: 2.47; 2.52; 2.70 (each s, Me); 6.97-7.29 (m, 3, 5-CH of Mes, *o*-tol). $^{13}C\{^1H\}$ NMR ($CDCl_3$) δ: 21.0 (Me); 24.8 (Me); 29.3 (Me); 117.8; 120.1; 126.4; 126.6; 127.6; 129.3; 132.9; 139.3; 140.2; 145.6 ppm. ^{125}Te $\{^1H\}$ NMR ($CDCl_3$) δ: 337 ppm.

NaS_2COPr^i

To a solution of sodium iso-propoxide (prepared by dissolving sodium (2.0 g, 86.95 mmol) in 50 ml iso-propanol) carbon disulfide (5.0 ml) was added drop wise with stirring which continued for additional 1 h. The solution was dried under vacuum. The residue was washed with methanol and acetone (2 x 5 ml) and dried (yield 10.7 g, 78%); m. p.: 120-122°C [145]. ^1H NMR (DMSO-d_6) δ: 1.14 (d, 6.3Hz, 6H, Me); 5.43 (heptate, 6.3 Hz, CH). $^{13}C\{^1H\}$ NMR (DMSO-d_6) δ: 22.3 (s, Me), 73.0 (s, OCH), 229.8 (s, CS_2) ppm.

NaS_2COPr^n

The title compound was prepared using a procedure similar to NaS_2COPr^i and isolated as a light yellow powder in 66% yield; m. p.: 90°C. ^1H NMR (DMSO-d_6) δ: 0.85 (t, 7.5 Hz, 3H, Me); 1.57 (sextet, 7 Hz, CH_2); 4.11 (t, 7 Hz, OCH_2) ppm. $^{13}C\{^1H\}$ NMR (DMSO-d_6) δ: 11.1 (s, Me); 22.3 (s, CH_2); 72.7 (s, OCH_2); 230.5 (s, CS_2) ppm.

NaS_2COEt

The title compound was prepared following the procedure similar to NaS_2COPr^i and isolated as a light yellow powder in72% yield. m. p.: 180°C. ^1H NMR (DMSO-d_6) δ: 1.16 (t, 7 Hz, 3H, Me); 4.20 (q, 7 Hz, 2H, OCH_2) ppm. $^{13}C\{1H\}$ NMR (DMSO-d_6) δ: 14.9 (s, Me); 66.5 (s, OCH_2); 230.3 (s, CS_2) ppm.

NaS_2COMe

The title compound was prepared following the procedure similar to NaS_2COPr^i and isolated as a light yellow powder in 80% yield; m. p.: 140°C. ^1H NMR (DMSO-d_6) δ: 3.71 (s, Me) ppm. $^{13}C\{1H\}$ NMR (DMSO-d_6) δ: 58.1 (s, Me); 230.9 (s, CS_2) ppm.

$[Pb(SMes)_2]$

To a methanolic solution of NaSMes (prepared from the reaction of $NaBH_4$ (0.50 g, 13.2 mmol) with dimesityldisulfide (2.0 g, 6.6 mmol) in methanol), a methanolic solution of $Pb(OAc)_2$ (2.15 g, 6.6 mmol) was added and stirred for 3 h at room temperature whereupon a yellow-brown precipitate formed. The precipitate was filtered and washed with methanol, water, acetone and ether. The solid was dried under vacuum (yield: 1.62 g, 48%); m.p.: 247 °C [146]. Anal. Calcd. for $C_{18}H_{22}$ PbS_2: C, 42.4; H, 4.3; S, 12.6 %. Found: C, 42.3; H, 4.2; S, 12.8 %.

$[Pb(Spy)_2]$

To a methanolic solution of 2-mercaptopyridine (2.0 g, 18.0 mmol) 18 ml 1.01 (N) NaOMe was added and stirred for 10 min. To this solution methanolic solution of $Pb(OAc)_2$ (3.0 g, 9.2 mmol) was added and stirred for additional 2 h. The yellow precipitate was filtered and washed with methanol followed by acetone and dried under reduced pressure (yield: 1.95 g, 51%) [147]. Anal Calcd for $C_{10}H_8N_2PbS_2$: C, 28.1; H, 1.9; N, 6.5; S, 15.0 %. Found: C, 28.3; H, 2.1; N, 6.6; S, 15.2 %.

$[Pb(Sepy)_2]$

The title compound was prepared following the procedure similar to $Pb(SMes)_2$and isolated as a yellow powder (yield: 59%). Anal. Calcd for $C_{10}H_8N_2PbS_2$: C, 23.0; H, 1.5; N, 5.4 %. Found: C, 23.3; H, 1.5; N, 5.3 %.

2.3.2 Synthesis of metal precursors

$Na_2[PdCl_4]$ [148], $K_2[PtCl_4]$ [149], $[Pd(OAc)_2]_3$ [150], $PdCl_2(PhCN)_2$ [23], $PtCl_2(RCN)_2$ (R = Me, Ph, 4-MeC_6H_4, 4-$CF_3C_6H_4$) [11] were prepared according to literature methods.

$[Pd(\mu\text{-}Cl)(Me_2NCH_2C_6H_4\text{-}C,N)]_2$

To a methanolic solution of Na_2PdCl_4 (2.08 g, 7.07 mmol) N,N-dimethylbenzylamine (0.96 g, 7.1 mmol) was added followed by the addition of NaOAc (0.58 g, 7.07 mmol). The mixture was stirred for 24 h and the yellow precipitate was filtered through G2 and washed with distilled water and methanol. The precipitate was dried under vacuum (yield: 1.73 g, 89%); m. p.: 187°C [151]. Anal. Calcd for $C_{18}H_{24}Cl_2N_2Pd_2$: C, 39.1; H, 4.4; N, 5.1 %. Found: C, 39.0; H, 4.5; N, 5.0 %.

2.4 Synthesis of palladium complexes with selenoether

$[Pd_2Cl_2(\mu\text{-}Cl)_2(Mes_2Se)_2]$

(i) To a toluene solution (25ml) of Mes_2Se (0.21g, 0.65 mmol), $PdCl_2(PhCN)_2$ (0.23g, 0.61 mmol) was added and stired for 4 h at room temperature. The solution was dried under vacuum and the residue was washed thoroughly with diethyl ether and toluene. The complex was extracted with dichloromethane and recrystallized from dichloromethane-hexane (10:1 v/v) mixture at room temperature as red crystals (yield: 0.18 g, 60 %); m.P.: 193°C(dec)).Analysis Calcd. for $C_{36}H_{44}Cl_4Pd_2Se_2$: C, 43.71; H, 4.48; Found: C, 43.42; H, 4.44 %. ^{1}H NMR (500 MHz, $CDCl_3$) δ: 2.22, 2.24, 2.49, 2.65 (s, ratio 4:2:1:6, Me), 6.77, 6.83, 6.85, (s, C_6H_2); ^{77}Se {^{1}H} NMR ($CDCl_3$) δ: 322 ppm.

(ii) To a toluene-acetonitrile (5 : 25 ml) solution of Mes_2Se (0.45 g, 1.41 mmol), $PdCl_2$ (0.25 g, 1.41 mmol) was added and reflued for 4 h at 80°C whereupon a red precipitate formed which was filtered and washed with diethyl ether and toluene. The title complex was extracted with dichloromethane and dried under reduced pressure (yield : 540 mg, 77%). NMR data were consistent with the above preparation.

$[Pd_2(\mu\text{-}Cl)_2\{MesSeC_6H_2(Me_2)CH_2\}_2]$

To an ethanolic (25ml) solution of Na_2PdCl_4 (0.43g, 1.47 mmol), Mes_2Se (0.48g, 1.51 mmol) was added and refluxed for 4 h. The solvent was evaporated under reduced pressure and the residue was washed thoroughly with hexane and diethyl ether and was extracted with toluene and dried. The complex was recrystallized from acetone - diethyl ether mixture (10:1 v/v) as rod like orange crystals (yield: 0.41g, 61 %);m.p.: 165°C (dec)). Analysis Calcd. for $C_{36}H_{42}Cl_2Pd_2Se_2$: C, 47.19; H, 4.62. Found: C, 47.50; H, 4.31 %. ^{1}H NMR (500 MHz, $CDCl_3$) δ: 1.91 (s, 4-Me, non-metalated), 2.24, 2.26 (each s, 4- and 6-Me, metalated), 2.40 (br

s, 2,6-Me, non-metalated), 3.37 (AB pattern, CH_2, $\Delta\gamma_{AB}$ 46Hz, J_{AB}=12.6Hz), 6.75, 6.78 (each s, C_6H_2 metalated), 6.85 (s, C_6H_2 non-metalated) ppm. ^{77}Se {^{1}H} NMR ($CDCl_3$) δ: 408 ppm.

[Pd_2(μ-Spy)$_2${$MesSeC_6H_2(Me_2)CH_2$}$_2$]

To a dichloromethane solution of [Pd_2(μ-Cl)$_2$($C_{18}H_{21}Se$)$_2$] (0.10g, 0.11 mmol), Pb(Spy)$_2$ (0.05 g, 0.11mmol) was added and stirred overnight at room temperature. The solution was passed through Cellite and dried under reduced pressure to give a red residue. The residue was washed with hexane and diethyl ether and extracted with acetone. The solution was concentrated to 1 ml and the complex was recrystallized as yellow crystals (yield: 0.10 g, 84%) upon addition of few drops of diethyl ether; m.p.: 176°C. Anal. Calcd. for $C_{46}H_{50}N_2Pd_2S_2Se_2$: C, 51.84; H, 4.73; N, 2.63; S, 6.02. Found: C, 51.30; H, 4.72; N, 2.02; S, 5.78 %. ^{1}H NMR (300 MHz, acetone-d_6) δ: 1.93 (s, 4-Me, non-metalated), 2.22 (s, 4- and 6-Me, metalated), 2.43 (s, 2,6-Me, non-metalated), 3.46 (AX pattern, CH_2, $\Delta\gamma_{AX}$ 135Hz, J_{AX}=14Hz), 6.75 (s, C_6H_2 metalated), 6.88 (s, C_6H_2 non-metalated), 6.10 (t, CH-4, C_5H_4N), 6.81 (t, CH-5, C_5H_4N), 7.13 (d, 7.8 Hz, CH-3, C_5H_4N), 7.74 (d, 5 Hz, CH-6, C_5H_4N) ppm. ^{77}Se {^{1}H} NMR ($CDCl_3$) δ: 406 ppm.

[Pd_2(μ-Sepy)$_2${$MesSeC_6H_2(Me_2)CH_2$}$_2$]

To a dichloromethane solution of [Pd(μ-Cl){$MesSeC_6H_2(Me_2)CH_2$}]$_2$ (0.25g, 0.027 mmol), Pb(Sepy)$_2$ (0.14g, 0.027 mmol) was added and stirred for 6h. The solution was dried and the complex was washed with hexane (2 ×5 ml) and extracted with toluene. The complex was re-crystallized from acetone-hexane mixture as pale yellow crystals (yield: 0.17g, 55%); m.p: 155°C. Anal. Calcd. for $C_{46}H_{50}N_2Pd_2Se_4$: C, 47.65; H, 4.35; N, 2.42. Found: C, 48.37; H, 4.63; N, 2.32 . ^{1}H NMR (300 MHz, $CDCl_3$) δ: 0.80 - 2.33 (m), 2.69 - 4.01 (m), 6.12 (d, 7.2Hz), 6.45 (t, 6.2Hz), 6.66-6.87 (br, m), 7.38 (d, 4.8Hz), 7.59 (t, 7.6Hz), 8.02 (d, 7.8Hz) ppm. ^{77}Se {^{1}H} NMR ($CDCl_3$) δ: 341, 378, 380, 408.

[PdCl{MesSeC$_6$H$_2$(Me$_2$)CH$_2$}PPh$_3$]

To a dichloromethane solution of [Pd$_2$(μ-Cl$_2$){MesSeC$_6$H$_2$(Me$_2$)CH$_2$}$_2$] (0.10g, 0.011 mmol), PPh$_3$ (0.06g, 0.023 mmol) was added and stirred for 10 mins. The reaction mixture was dried under reduced pressure and the residue was washed with hexane and extracted with toluene. The toluene extract was dried under vacuum to yield a cream colored solid (yield: 0.11g, 71%); m.p.: >200^{o}C. Anal. Calcd. for $C_{36}H_{36}ClPdPSe$: C, 60.00; H, 5.04. Found: C, 59.71; H, 5.32 %. ^{1}H NMR (300 MHz, $CDCl_3$) δ: 1.95 (s, 4-Me,non-metalated), 2.17, 2.24 (each s, 4- and 6-Me, metalated), 2.69 (br, CH_2), 6.48, 6.70 (each s, 3-,5-H, metalated), 6.88 (s, 3-,5-H, non-metalated), 7.41-7.44 (br, Ph), 7.72-7.78 (br, Ph) ppm.^{31}P{^{1}H} (300 MHz, $CDCl_3$) δ: 31.7 ppm. ^{77}Se{^{1}H} NMR ($CDCl_3$) δ : 393 (d, ^{2}J(Se-P) = 167 Hz) ppm.

2.5 Synthesis of palladium complexes with telluroethers

***trans*-[$PdCl_2(TeMes_2)_2$]**

To a toluene solution of [$PdCl_2(PhCN)_2$] (0.30 g, 0.78 mmol), a toluene solution of Mes_2Te (0.57g, 1.56 mmol) was added and stirred for 4 h at room temperature whereupon an orange-red precipitate formed. The latter was filtered and washed with hexane and diethyl ether, and extracted with acetonitrile. The complex was recrystallized from acetonitrile solution containg few drops of diethyl ether on slow evaporation as orange-red color rectangular shaped crystals (yield: 0.55 g, 77%); m.p.: 178°C (dec). Anal calcd for $C_{36}H_{44}Cl_2PdTe_2$: C, 47.55; H, 4.88%. Found: C, 47.37; H, 4.86%. ^{1}H NMR ($CDCl_3$) δ: 2.23, 2.58 (s, Me); 6.86 (s, 3,5-CH). $^{13}C\{^1H\}$ NMR ($CDCl_3$) δ: 20.9, 27.2 (Me), 118.8 (Te-C), 129.3 (3,5-CH), 139.9, 143.6. $^{125}Te\{^1H\}$ NMR ($CDCl_3$) δ: 489 ppm.

***trans*-[$PdCl_2(TePh_2)_2$]**

Prepared similar to *trans*-[$PdCl_2(TeMes_2)_2$] and isolated as an orange–red crystalline solid in 74% yield; m.p.: 160°C (dec). Anal calcd for $C_{24}H_{20}Cl_2PdTe_2$: C, 38.90; H, 2.72%. Found: C, 38.71; H, 2.70%. ^{1}H NMR ($CDCl_3$) δ: 7.29-7.44 (m), 7.81 (d, 7.2 Hz) (Ph). $^{13}C\{^1H\}$ NMR ($CDCl_3$) δ: 117.9 (C-Te), 129.7, 130.0, 137.0. $^{125}Te\{^1H\}$ NMR (CDCl3) δ: 750 ppm.

[$PdCl_2${Te(*o*-tol)$_2$}$_2$]

Prepared similar to *trans*-[$PdCl_2(TeMes_2)_2$]and isolated in 58% yield; m. p.: 195°C (dec). Anal calcd for $C_{28}H_{28}Cl_2PdTe_2$: C, 42.19; H, 3.54%. Found: C, 42.40; H, 3.17%. ^{1}H NMR ($CDCl_3$) δ: 2.54 (s, Me), 7.10(t, 7.2 Hz) 7.25 (d) 7.34 (t, 7.2 Hz), 7.84 (d, 7.2 Hz) (*o*-tol). $^{13}C\{^1H\}$ NMR ($CDCl_3$) δ: 25.5 (Me), 119.8 (C-Te), 127.4, 130.2, 130.3, 138.4, 142.4 (*o*-tol). $^{125}Te\{^1H\}$ NMR ($CDCl_3$) δ: 637 ppm.

[$PdCl_2$(MesTetol-*o*)$_2$]

Prepared similar to *trans*-[$PdCl_2(TeMes_2)_2$]and isolated in 62% yield; m. p.: 183-184 °C (dec). Anal calcd for $C_{32}H_{36}Cl_2PdTe_2$: C, 45.05; H, 4.25%. Found: C, 45.52; H, 4.00%. ^{1}H NMR ($CDCl_3$) δ: 2.31, 2.46, 2.76 (each s, Me), 7.01(s), 7.15-7.25 (m).

[$Pd_2(\mu\text{-}Cl)_2Cl_2(TeMes_2)_2$]

(i) To a methanolic solution (5 ml) of Na_2PdCl_4 (0.10 g, 0.35 mmol), a toluene solution (25 ml) of Mes_2Te (0.13 g, 0.36 mmol) was added and stirred for 3 h at room emperature whereupon a dark-red precipitate formed which was filtered and washed with toluene. The complex was extracted with acetone and recrystallized from acetone-hexane mixture (5:1 v/v) at -5°C as red needle shaped crystals (yield: 0.15 g, 79%); m.p.: 178°C (dec). Anal calcd for $C_{36}H_{44}Cl_4Pd_2Te_2$: C, 39.79; H, 4.08%. Found: C, 39.71; H, 4.07%. ^{1}H NMR ($CDCl_3$) δ: 2.24 (s, 1Me); 2.65 (s, 2Me), 6.88 (s, 2H). $^{13}C\{^1H\}$ NMR ($CDCl_3$) δ: 20.9, 26.8 (Me), 116.8 (C-Te), 130.1 (3,5-CH), 141.0, 143.3. $^{125}Te\{^1H\}$ NMR ($CDCl_3$) δ: 575 ppm.

(ii) To a toluene-acetonitrile (1:1 v/v) solution of *trans*-[$PdCl_2(TeMes_2)_2$] (0.10 g, 0.11 mmol), $PdCl_2(PhCN)_2$ (0.04 g, 0.11 mmol) was added and stirred for 5 h at room temperature whereupon a red precipitate formed.The precipitate was filtered, washed with toluene and processed similar to (i) (yield: 71%). The NMR data were consistent with the above preparation.

[$Pd_2(\mu\text{-}Cl)_2Cl_2${Te(Ph)Mes}$_2$]

Prepared similar to [$Pd_2(\mu\text{-}Cl)_2Cl_2(TeMes_2)_2$] employing method (i) and isolated as brown crystalline solid from acetone-hexane mixture (10:1 v/v) at -5°C in 74% yield; m.p.: 174°C (dec). Anal calcd for $C_{30}H_{32}Cl_4Pd_2Te_2$: C, 35.95; H, 3.22%. Found: C, 35.86; H, 3.22%. ^{1}H NMR (CDCl3) δ: 2.34 (s,1Me), 2.81 (s, 2Me), 7.04 (s, 3,5-CH, Mes), 7.19-7.44 (m, Ph). $^{125}Te\{^1H\}$ NMR (CDCl3) δ: 704 ppm.

$[Pd_2(\mu\text{-}Cl)_2Cl_2(TePh_2)_2]$

Prepared in a manner similar to $[Pd_2(\mu\text{-}Cl)_2Cl_2(TeMes_2)_2]$ employing both methods (i) and modified (ii) under refluxing in toluene and was isolated as an orange-red crystalline solid from acetonitrile-diethyl ether mixture at room temperature in 66-73% yield, m.p: 142°C (dec). Anal calcd for $C_{24}H_{20}Cl_4Pd_2Te_2$: C, 31.39; H, 2.19%. Found: C, 31.32; H, 2.19%. ^{1}H NMR ($CDCl_3$) δ: 7.38 (t, 7.5 Hz), 7.49 (t, 7.2 Hz), 7.78 (d, 7.2 Hz). ^{125}Te{^{1}H} NMR ($CDCl_3$) δ: 823 ppm.

$[Pd_2(\mu\text{-}Cl)_2\{CH_2C_6H_2(4,6\text{-}Me_2)TeMes\}_2]$

A toluene-methanol (5:1 v/v; 50 ml) solution of *trans*-$[PdCl_2(TeMes_2)_2]$ (0.10 g, 0.11 mmol) was refluxed for 30 min with stirring under an argon atmosphere whereupon an orange-red solution faded to orange colour. The solvents were evaporated under vacuum and the residue was washed with petroleum ether, and then extracted with toluene. The solvent was reduced to 2 ml under vacuum and on addition of hexane (5 ml), the title complex precipitated out as an orange powder (yield: 0.04 g, 75%); m.p.: 164-169 °C (dec.). Anal calcd for $C_{36}H_{42}Cl_2Pd_2Te_2$: C, 42.66; H, 4.18%. Found: C, 42.52; H, 4.17%. ^{1}H NMR ($CDCl_3$) δ: 2.04 (s, 1Me), 2.25 (s, 1Me), 2.53 (s, 2Me), 3.38 (br, CH_2), 6.94 (s, 1H), 6.78 (s, 1H), 6.87 (s, 2H) (CH, Mes). ^{13}C{^{1}H} NMR ($CDCl_3$) δ: 20.9, 21.0, 22.9, 25.7, 27.2 (1Me), 29.7 (CH_2, metallated), 127.4, 128.8 (3/5- CH of metallated), 129.1 (3,5-CH non-metallated), 140.3, 140.8, 141.2, 143.9 (quaternary carbons). ^{125}Te{^{1}H} NMR ($CDCl_3$) δ: 644 ppm.

The complex, $[Pd_2(\mu\text{-}Cl)_2\{CH_2C_6H_2(4,6\text{-}Me_2)TeMes\}_2]$ could also be obtained when a toluene-methanol solution of $[Pd_2(\mu\text{-}Cl)_2Cl_2(TeMes_2)_2]$ was refluxed for 30 min (^{125}Te{^{1}H} NMR ($CDCl_3$) δ: 644 ppm).

***cis*-$[PdCl_2\{MesTeCH_2C_6H_2(4,6\text{-}Me_2)TeMes\}]$**

(i) A toluene-methanol solution of $[Pd_2(\mu\text{-}Cl)_2\{CH_2C_6H_2(4,6\text{-}Me_2)TeMes\}_2]$ was refluxed for 2 h. The solvents were evaporated under vacuum and the residue was

washed with petroleum ether and extracted with toluene. The complex was recrystallized from toluene-hexane (10:1 v/v) mixture on slow evaporation as dark-red crystals, m.p.: 185°C (dec). Anal calcd for $C_{27}H_{32}Cl_2PdTe_2$: C, 41.10; H, 4.09%. Found,C, 41.20; H, 3.96%. ^{1}H NMR ($CDCl_3$) δ: 2.02, 2.22, 2.27, 2.50 (each s, 1Me), 2.47, 2.63 (br, s, each 2Me, 2,6-Me of Mes), 3.55 (AX pattern, CH_2 metallated, $\Delta\nu_{AX}$ = 169 Hz, J_{AX} = 11 Hz), 6.25, 6.83 (each s, 1H, 3,5-CH, metallated), 6.93 (s, 3,5-CH, Mes). $^{13}C\{^1H\}$ NMR ($CDCl_3$) δ: 20.5, 20.8, 25.3, 26.5 (1Me), 27.5, 28.5 (br, 2Me), 117.0, 117.6 (C-Te), 129.0, 129.2, 130.4, 130.9, 140.6, 140.9, 141.1, 142.3, 142.7, 144.3 ppm. $^{125}Te\{^1H\}$ NMR ($CDCl_3$) δ: 428 ppm.

(ii) A toluene-methanol solution of *trans*-$[PdCl_2(TeMes_2)_2]$ (0.15 g, 0.16 mmol) was refluxed for 2 h which resulted into a dark-red solution. After processing in a similar way gave red crystals of the title complex (yield: 0.45 g, 35%). The NMR data were consistent with the product obtained in the above preparation.

(iii) To a methanolic solution of Na_2PdCl_4 (0.20 g, 0.68 mmol), a toluene solution of $TeMes_2$ (0.25 g, 0.69 mmol) was added with stirring and refluxed for 2 h. The solvents were evaporated under reduced pressure and the residue was washed with petroleum ether and extracted with toluene. The complex was recrystallized similarly as above (yield: 0.12 g, 23%). Analytical and NMR data were consistent to the product obtained through (i).

$[Pd_2(\mu\text{-}OAc)_2\{CH_2C_6H_2(4,6\text{-}Me_2)TeMes\}_2]$

To a toluene solution of palladium acetate (0.20 g, 0.30 mmol), a toluene solution of Mes_2Te (0.33 g, 0.89 mmol) was added with stirring which continued for 1 h at room temperature. The solution was passed through Celite to remove any decomposition products. The solution was concentrated to 5 ml and precipitated by adding petroleum ether. The precipitate was filtered out and washed with a small portion of petroleum ether and then

recrystallized from toluene-hexane mixture (1:1, v/v) at room temperature to afford two different types of crystals, *viz* yellow rectangular blocks (yield: 0.26 g, 55%); m. p.: 138-139°C (dec) and a few red needle shaped crystals. The two were separated manually. The yellow crystals were characterized as $[Pd_2(\mu\text{-}OAc)_2\{CH_2C_6H_2(4,6\text{-}Me_2)TeMes\}_2]$ while the red crystals could be characterized by single crystal X-ray diffraction analysis as a tetra-nuclear complex, $[Pd(\mu\text{-}OAc)(\mu\text{-}TeMes)]_4$. Anal. Calcd. for $[Pd_2(\mu\text{-}OAc)_2\{CH_2C_6H_2(4,6\text{-}Me_2)TeMes\}_2]$, $C_{40}H_{48}O_4Pd_2Te_2$: C, 45.29; H, 4.56%. Found: C, 44.00; H, 4.31%. ^{1}H NMR ($CDCl_3$, 400MHz) δ: 1.95-2.53 (overlapping singlets due to methyl groups of mesityl and acetate groups), 3.36 (AB pattern, CH_2 metallated, $\Delta\nu_{AB}$ = 71 Hz, J_{AB} = 13 Hz), 6.43, 6.60, 6.64, 6.77, 6.81, 6.86 (each br s of 3,5-CH of mesityl). ^{125}Te{^{1}H} NMR ($CDCl_3$) δ: 554 ppm.

$[Pd_2(\mu\text{-}OAc)_2\{CH_2C_6H_2(4,6\text{-}Me)_2Tetol\text{-}o\}_2]$

Prepared similar to $[Pd_2(\mu\text{-}OAc)_2\{CH_2C_6H_2(4,6\text{-}Me_2)TeMes\}_2]$and isolated as orange crystals from acetonitrile-diethyl ether at -5°C in 63% yield; m. p.: 140°C (dec). Anal. Calcd. for $C_{36}H_{40}O_4Pd_2Te_2$: C, 43.04; H, 4.01%. Found: C, 43.05; H, 3.84%. ^{1}H NMR ($CDCl_3$) δ: 1.88 (s, OAc), 2.04, 2.14, 2.29 (each s, 1Me), 3.09 (AB pattern, CH_2 metallated, $\Delta\nu_{AB}$ = 24.6 Hz, J_{AB} = 12.7 Hz), 6.60 (s, 3,5-CH, Mes), 6.70-6.91 (m), 7.18 (br) (o-tol). ^{13}C{^{1}H} NMR ($CDCl_3$) δ: 21.2, 22.2, 23.4, 24.0, 24.2, (for Me, CH_2), 118.9 (C-Te), 126.6, 127.2, 128.7, 128.9, 130.4, 132.6, 140.6, 141.0, 142.2, 179.8 (C=O);^{125}Te{^{1}H} NMR ($CDCl_3$) δ: 592 ppm

$[Pd_2(\mu\text{-}OAc)_2\{CH_2C_6H_2(4,6\text{-}Me_2)TePh\}_2]$

Prepared similar to $[Pd_2(\mu\text{-}OAc)_2\{CH_2C_6H_2(4,6\text{-}Me_2)TeMes\}_2]$ as a red powder in 45% yield; m. p.: 147°C (dec). The complex tends to decompose and hence gave variable analysis. ^{125}Te{^{1}H} NMR ($CDCl_3$) δ: 690 ppm.

2.6 Synthesis of platinum complexes with telluroethers

***trans*-[$PtCl_2(TePh_2)_2$]**

To an aqueous solution of K_2PtCl_4 (0.10 g, 0.24 mmol), a toluene-acetone solution of diphenyl telluride (0.14 g, 0.475 mmol) was added and stirred for 12 h at room temperature. The acetone was removed under vacuum and the organic layer was separated out and washed with distilled water and dried over anhydrous Na_2SO_4**.** The clear solution was passed through Cellite and concentrated to 5 ml. The title complex was precipitated as a greenish yellow powder by addition of hexane and then was washed with hexane and diethyl ether and dried, (yield: 0.12 g, 61%), m.p.: 196°C (dec). Anal. calcd. for $C_{24}H_{20}Cl_2PtTe_2$: C, 34.75; H, 2.42 %. Found: C, 34.31; H, 2.40 %. ^{1}H NMR ($CDCl_3$) δ: 7.22-7.27 (m), 7.35-7.40 (m), 7.61-7.64 (m) [Ph] ppm. ^{125}Te{^{1}H} NMR ($CDCl_3$) δ: 717 (major, $^1J(^{195}Pt\text{-}^{125}Te)$ = 1329 Hz) and 728 (minor) ppm. ^{195}Pt{^{1}H} NMR ($CDCl_3$) δ: -3650 (major), -3653 (minor) ppm. When a $CDCl_3$ solution of the complex is left for longer duration of acquisition additional peaks in the ^{125}Te{^{1}H} and ^{195}Pt{^{1}H} NMR spectra were observed which could be due to dissociation in solution.

***trans*-[$PtCl_2${$(Te(tol\text{-}o)_2\}_2$]**

Prepared similar to *trans*-[$PtCl_2(TePh_2)_2$] and recrystallized from dichloromethane–hexane as yellow needles (yield: 0.15 g, 73%); m. p.: >210°C. Anal. calcd. for $C_{28}H_{28}Cl_2PtTe_2$: C, 37.97; H, 3.19 %, Found: C, 37.23;H, 3.16.%. ^{1}H NMR ($CDCl_3$) δ: 2.25, 2.56 (each s); 7.08-7.15 (m), 7.24-7.36 (m); 7.79 (dd, 1.2, 7.5Hz); 7.88 (d,d, 1.2, 7.5 Hz) ppm. ^{125}Te{^{1}H} NMR ($CDCl_3$) δ: 622 ($^1J(^{195}Pt\text{-}^{125}Te)$ = 793 Hz) ppm; when this solution was left for overnight a new additional peak appeared in ^{125}Te NMR spectrum at δ: 605 ($^1J(^{195}Pt\text{-}^{125}Te)$ = 1357 Hz) ppm while ^{195}Pt{^{1}H} NMR ($CDCl_3$) showed two resonances at δ: -3717, -4324 ppm.

***trans*-[$PtCl_2(TeMes_2)_2$]**

Prepared similar to *trans*-[$PtCl_2(TePh_2)_2$]and recrystallized from dichloromethane-hexane in 64% yield as light orange crystalline solid; m.p.: 180°C. Anal. calcd. for $C_{36}H_{44}Cl_2PtTe_2$: C, 43.33; H, 4.44 %. Found: C, 43.64; H, 4.87 %. ^{1}H NMR ($CDCl_3$) δ: 2.24 (s, 4-Me); 2.61 (s, 2,6-Me); 6.85 (s, 3,5-CH). $^{13}C\{^1H\}$ NMR ($CDCl_3$)δ: 20.9, 26.8, 116.8 (Te-C), 129.3 (3,5-CH), 139.8, 143.6. $^{125}Te\{^1H\}$ NMR ($CDCl_3$) δ: 467 ($^1J(^{195}Pt\text{-}^{125}Te)$ = 379 Hz) ppm. $^{195}Pt\{^1H\}$ NMR ($CDCl_3$) δ : -3449 ($^1J(^{195}Pt\text{-}^{125}Te)$ = 359 Hz) ppm.

***trans*-[$PtCl_2$(PhTeMes)$_2$]**

Prepared similar to *trans*-[$PtCl_2(TePh_2)_2$] and recrystallized from dichloromethane-hexane in 75% yield as orange crystals; m. p.: 198°C (dec). Anal. calcd. for $C_{30}H_{32}Cl_2PtTe_2$: C, 39.43; H, 3.53 %. Found: C, 39.07; H, 3.45 %. ^{1}H NMR ($CDCl_3$) δ: 2.29 (s, 4-Me), 2.68 (s, 2,6-Me); 6.96 (s, 3,5-CH); 7.30 (br, m); 7.59 (br) (Ph). $^{125}Te\{^1H\}$ NMR ($CDCl_3$) δ: 575 ($^1J(^{195}Pt\text{-}^{125}Te)$ = 366 Hz), 576 (^1J(Pt-Te) = 369 Hz) ppm. $^{195}Pt\{^1H\}$ NMR ($CDCl_3$) δ: -3555, -3557 ppm.

***trans*-[$PtCl_2$(*o*-tolTeMes)$_2$]**

Prepared similar to *trans*-[$PtCl_2(TePh_2)_2$] and recrystallized from dichloromethane-hexane in 70% yield as orange crystals; m. p.: > 200°C. Anal. calcd. for $C_{32}H_{36}Cl_2PtTe_2$: C, 40.81; H, 3.85 %. Found: C,40.65; H, 3.78 %. ^{1}H NMR ($CDCl_3$) δ: 2.29, 2.30 (each s, 4-Me of Mes), 2.45, 2.48 (each s, 2-Me of tol); 2.72, 2.74 (each s, 2,6-Me of Mes); 6.95, 6.97 (each s, 3,5-CH of Mes); 7.02-7.22 (m, tol); 7.51, 7.64 (each d, 7.8 Hz, tol) ppm. $^{125}Te\{^1H\}$ NMR ($CDCl_3$) δ: 541; 543 ($^1J(^{195}Pt\text{-}^{125}Te)$ = 515 Hz) ppm. $^{195}Pt\{^1H\}$ NMR ($CDCl_3$) δ : -3611, -3615 ppm.

[PtCl{($CH_2C_6H_2Me_2$-4,6)TeMes}($TeMes_2$)]

A THF (~ 25 ml) solution of *trans*-[$PtCl_2(TeMes_2)_2$] (0.06 g, 0.06 mmol) was refluxed with stirring for 2 h under an argon atmosphere whereupon the initial orange colour

faded. After cooling the solution, the solvent was evaporated under reduced pressure to give a yellow residue which was washed with hexane and recrystallized from dichloromethane-hexane mixture as red prismatic crystals (yield: 0.04 g, 70%); m.p.: 182°C (dec). Anal. calcd. for $C_{36}H_{43}ClPtTe_2$: C, 44.97; H, 4.51 %. Found: C, 45.02; H, 4.61 %. ^{1}H NMR ($CDCl_3$) δ: 2.02, 2.19, 2.24, 2.27, 2.34, 2.53 (each s for Me); 4.0 (J_{AX} = 16.8, $\Delta\nu_{AX}$=105.8 Hz; metallated CH_2); 6.66 (s, 4,6-CH of Mes of metallated); 6.71 (s, 4,6-CH, Mes_2Te); 6.86, 7.04 (CH of metallated ring) ppm.^{125}Te{^{1}H} NMR ($CDCl_3$) δ: 336 ($^1J(^{195}Pt\text{-}^{125}Te)$ = 612 Hz); 592 ($^1J(^{195}Pt\text{-}^{125}Te)$ = 1528 Hz) ppm; for the dimer: 424 ($^1J(^{195}Pt\text{-}^{125}Te)$ = 788 Hz) and 600 ($^1J(^{195}Pt\text{-}^{125}Te)$ = 1192 Hz); 260(s, $TeMes_2$) ppm. ^{195}Pt{^{1}H} NMR ($CDCl_3$) δ: -4286 (minor); -4450 (major) ppm.

[PtCl{($CH_2C_6H_2Me_2$-4,6)TeMes}(PPh_3)]

To a dichloromethane solution of [PtCl{($CH_2C_6H_2Me_2$-4,6)TeMes}($TeMes_2$)] (0.04 mg, 0.047 mmol) a solution of triphenylphosphine (0.01 mg; 0.05mmol) was added with stirring under argon.After stirring the reactants for 3 h at room temperature, the solvent was evaporated under vacuum and the residue was washed with hexane. The complex on recrystallization from acetone –hexane (1:1 v/v) mixture at room temperature gave pale yellow rod like crystals (yield: 0.03 g, 67%); m. p.: 167°C. Anal. calcd. for $C_{36}H_{36}ClPPtTe$: C, 50.41; H, 4.23 %. Found: C, 50.63; H, 4.21 %. ^{1}H NMR ($CDCl_3$) δ:2.12, 2.26, 2.28 (each s, 1 Me); 2.58 (s, 2Me); 2.89 (br, CH_2); 6.47, 6.68 (each s; 1CH); 6.87 (s, 2CH); 7.44 (m, 7.74-7.81 (m) (Ph). ^{31}P{^{1}H} NMR ($CDCl_3$) δ: 23.6 ($^1J(^{195}Pt\text{-}^{31}P)$ = 3945Hz; $^2J(^{125}Te\text{-}^{31}P)$ = 456 Hz) ppm.^{125}Te{^{1}H} NMR ($CDCl_3$) δ: 555 ($^1J(^{195}Pt\text{-}^{125}Te)$ = 677 Hz; $^2J(^{125}Te\text{-}^{31}P)$ = 455 Hz) ppm.

2.7 Synthesis of platinum tellurimide complexes

2.7.1 Reaction between $[PtCl_2(PhCN)_2]$ and ArTeAr′ in 1:2 ratio in dichloromethane *cis*-$[PtCl_2(TePh_2)_2]$

To a dichloromethane solution (50 ml) of $[PtCl_2(PhCN)_2]$ (0.10 g, 0.21 mmol), Ph_2Te (0.12 g, 0.43 mmol) was added and stirred at room temperature for 48 h whereupon the colour of the solution changed from green to yellow. The clear solution was dried in vacuum and the residue was washed with acetone and extracted with dichloromethane. The complex was recrystallized from dichloromethane–hexane (5:1 v/v) mixture as light orange crystals, (yield: 0.14 g, 80%); m.p.: 195°C. Anal. calcd. for $C_{24}H_{20}Cl_2PtTe_2$: C, 34.75; H, 2.43 %, Found: C, 34.52; H, 2.41%.^{1}H NMR ($CDCl_3$) δ: 7.22-7.27 (m), 7.35-7.40 (m),7.61-7.65(m) [Ph] ppm. ^{125}Te{^{1}H} NMR ($CDCl_3$) δ: 717 ($^1J(^{195}Pt\text{-}^{125}Te)$ = 1355 Hz) ppm, 728 (trans isomer, ~5%) ppm.

***trans*-[$PtCl_2$(MesTePh)$_2$]**

Prepared similar to *cis*-$[PtCl_2(TePh_2)_2]$and recrystallized from dichloromethane-hexane (5:1 v/v) as orange crystals (yield: 83%); m.p.: 196 °C. Anal. calcd. for $C_{30}H_{32}Cl_2PtTe_2$: C, 39.43; H, 3.53 %, Found: C, 39.07; H, 3.45 %.^{1}H NMR ($CDCl_3$) δ: 2.29 (s, 3H), 2.68 (s, 6H). 6.96 (s, 2H), 7.23-7.31 (m, 3H), 7.56-7.61 (m, 2H) ppm. ^{125}Te{^{1}H} NMR ($CDCl_3$) δ: 575 ($^1J(^{195}Pt\text{-}^{125}Te)$ = 366 Hz), 576 ($^1J(^{195}Pt\text{-}^{125}Te)$ = 369 Hz) ppm.^{195}Pt{^{1}H} NMR($CDCl_3$) δ: -3555, -3557 ppm.

***cis*-[$PtCl_2${Te(tol-*o*)$_2$}$_2$]**

Prepared similar to *cis*-$[PtCl_2(TePh_2)_2]$ and recrystallized from dichloromethane-hexane (5:1 v/v) as cream colored needle shaped crystals (yield: 76%); m.p.: >200°C. Anal. calcd. for $C_{28}H_{28}Cl_2PtTe_2$: C, 37.97; H, 3.18 %, Found: C, 37.55; H, 3.16%.^{1}H NMR ($CDCl_3$)

δ: 2.24 (s, tol-Me); 7.07-7.15 (m); 7.29-7.34 (m); 7.79 (d, 7.5 Hz) (C_6H_4) ppm. $^{125}Te\{^1H\}$ NMR ($CDCl_3$) δ: 605 ($^1J(^{195}Pt\text{-}^{125}Te)$ = 1347 Hz) ppm; 622 (trans isomer, ~ 5%).

***trans*-[$PtCl_2${MesTe(tol-*o*)}$_2$]**

Prepared similar to *cis*-[$PtCl_2(TePh_2)_2$] and recrystallized from dichloromethane-hexane (5:1) as orange crystals in 66% yield; m.p.: >200°C. Anal. calcd. for $C_{32}H_{36}Cl_2PtTe_2$: C, 40.81; H, 3.85 %, Found: C, 40.76; H, 3.82 %.^{1}H NMR ($CDCl_3$) δ: 2.29, 2.30 (each s, 4-Me of Mes), 2.45, 2.47 (each s, 2-Me of tol); 2.72, 2.74 (each s, 2,6-Me of Mes); 6.95, 6.97 (each s, 3,5-CH of Mes); 7.02-7.22 (m, tol); 7.52, 7.64(each d, 7.8 Hz, tol) ppm.

***trans*-[$PtCl_2(TeMes_2)_2$]**

Prepared similar to *cis*-[$PtCl_2(TePh_2)_2$]and recrystallized from acetone-hexane (5:1 v/v) as orange crystal in 60% yield; m.p.: 182°C. Anal. calcd. for $C_{36}H_{44}Cl_2PtTe_2$: C, 43.33; H, 4.44 %, Found: C,43.37; H,4.32 %.^{1}H NMR ($CDCl_3$) δ: 2.24 (s, 4-Me), 2.59 (s, 2,6-Me), 6.83 (s, 3,5-CH) ppm. $^{125}Te\{^1H\}$ NMR ($CDCl_3$) δ: 467 ($^1J(^{195}Pt\text{-}^{125}Te)$ = 378 Hz) ppm.$^{195}Pt\{^1H\}$ NMR δ: -3453 ppm (a small signal due to unreacted $PtCl_2(PhCN)_2$ was noted at -2335 ppm).

2.7.2 Reactions between [$PtCl_2(PhCN)_2$] and MesTeAr in 1:1 ratio in THF (Ar = Ph, tol-*o*, Mes)

Reaction with MesTePh

To a THF solution of [$PtCl_2(PhCN)_2$] (0.10 g, 0.21 mmol) MesTePh (0.07 g, 0.22 mmol) was added and stirred for 6 h at room temperature. The solution was dried and washed with diethyl ether. The complex was extracted with dichloromethane and recrystallized from dichloromethane-hexane (5:1 v/v) mixture on slow evaporation (yield: 0.07 g, 38%). Microanalysis and NMR data are consistent with the complex prepared in CH_2Cl_2.

Reaction with MesTe(tol-*o*)

The reaction was carried out similar to MesTePh. The residue was extracted with diethylether and the insoluble part was identified as $[PtCl_2\{Te(o\text{-tol})Mes\}_2]$ (yield: ~ 5%) (by NMR data). The ether extract on evaporation afforded *trans*-$[PtCl_2(PhCN)\{NC(O)Ph[Te(tol\text{-}o)Mes]\}]$ (yield: 41%) which was recrystallized from acetone-hexane mixture as light yellow crystals. Anal. calcd. for $C_{30}H_{28}Cl_2N_2OPtTe$: C, 43.61; H, 3.42; N, 3.39%. Found: C, 43.52; H, 3.41; N, 3.45%. ^{1}H NMR ($CDCl_3$) δ: 2.29 (s, 4-Me of Mes), 2.38 (s, 2-Me of tol), 2.64 (s, 2,6-Me of Mes), 6.98 (s, 3,5-CH of Mes),7.38-7.86 (m), 8.73-8.77(m) (aryl) ppm. ^{125}Te{^{1}H} NMR ($CDCl_3$) δ: 937 (J(^{195}Pt-^{125}Te) = 317 Hz) ppm.

Reaction with $TeMes_2$

(i) *At room temperature*

The reaction was carried out similar to MesTePh and the residue was recrystallized from acetone-hexane mixture by slow evaporation. Orange crystals of *trans*-$[PtCl_2\{NC(O)Ph(TeMes_2)\}_2]$ (yield: 28%) were separated out and the mother liquor on further reduction of the solvent afforded crystals of *trans*-$[PtCl_2(TeMes_2)_2]$ (yield: < 5%) (characterized from NMR). The characterization data for *trans*-$[PtCl_2\{NC(O)Ph(TeMes_2)\}_2]$; m.p.: >200°C. Anal. calcd. for $C_{50}H_{54}Cl_2N_2O_2PtTe_2$: C, 48.58; H, 4.40; N, 2.27 %, Found: C, 48.25; H, 4.33; N, 2.30%.^{1}H NMR ($CDCl_3$) δ: 2.21 (s, 4-Me), 2.39 (s, 2,6-Me**$_2$**); 6.70 (s, 3,5-CH); 7.16 (t, 7.8 Hz), 7.36 (m), 8.24 (d, 7.2 Hz) ppm.^{13}C{^{1}H} NMR ($CDCl_3$): 21.0, 22.4 (s, Me), 127.4, 128.6, 130.2, 130.3, 130.7, 133.9 (56 Hz), 140.6, 143.6, 182.3 (C=O) ppm.^{125}Te{^{1}H} NMR ($CDCl_3$) δ: 959 (J(^{195}Pt-^{125}Te) = 347 Hz) ppm. ^{195}Pt{^{1}H} NMR ($CDCl_3$) δ : - 3079 ppm.

(ii) *Refluxed for 30 minutes*

The reaction between $[PtCl_2(PhCN)_2]$ (0.10 g, 0.21 mmol) and Mes_2Te (0.08 g, 0.21 mmol) was carried out similar to the above under reflux for 30 minutes in THF. After drying under vacuum, the residue was washed with hexane and extracted with diethylether. The solvent was evaporated in vacuum to give a pale yellow powder of *trans*-$[PtCl_2\{NC(Ph)C_4H_7O\}\{NC(O)Ph(TeMes_2)\}]$ (yield: 0.07 g, 35%); m.p.: 179-180°C. Anal. calcd. for $C_{36}H_{39}Cl_2N_2O_2PtTe$: C, 46.68; H, 4.25; N, 3.02 %, Found: C, 47.00; H, 4.20; N, 2.85%.^{1}H NMR ($CDCl_3$) δ: 2.21, 2.27 (each s, Me); 2.60 (br), 3.54-3.78 (m), 5.18 (br) (C_4H_7O); 6.95 (s, $C_6H_2Me_3$); 7.28-7.50 (m); 8.58-8.65 (m) (aryl) ppm. $^{125}Te\{^1H\}$ NMR ($CDCl_3$) δ: 946 ppm. $^{195}Pt\{^1H\}$ NMR ($CDCl_3$) δ : - 1861 ppm.

(iii) *Refluxed for 3 hrs*

The reaction between $[PtCl_2(PhCN)_2]$ (0.10 g, 0.21 mmol) and Mes_2Te (0.08 mg, 0.21 mmol) was carried out similar to the above under reflux for 3 h in THF. The solvent was evaporated under vacuum and the residue was extracted from diethyl ether leaving behind an insoluble part which was soluble in acetone.

The diethylether extract on evaporation gave an orange powder of $[PtCl(TeMes_2)\{Te(Mes)CH_2C_6H_2Me_2\}]$ which could be recrystallized from acetonitrile-diethyl ether mixture at room temperature (yield: 29%.), m.p.: 180°C. Anal. calcd. for $C_{36}H_{43}ClPtTe_2$: C, 44.97; H, 4.51 %, Found: C, 45.01; H, 4.53 %.^{1}H NMR ($CDCl_3$) δ: 2.02, 2.19, 2.24, 2.27, 2.34, 2.53 (each s for Me) , 4.0 (J_{AX} = 16.8, $\Delta\nu_{AX}$=105.8 Hz; metallated CH_2); 6.66 (s, 3,5-CH of Mes of metallated); 6.71 (s, 3,5-CH of $TeMes_2$); 6.86, 7.04 (CH of metallated ring) ppm. $^{125}Te\{^1H\}$ NMR ($CDCl_3$) δ: 336 ($^1J(^{195}Pt\text{-}^{125}Te)$ = 622 Hz), 592 ($^1J(^{195}Pt\text{-}^{125}Te)$ = 1545 Hz), 598 (~ 5% due to dimer), 259 ($TeMes_2$) ppm.

The acetone extract on evaporation gave a yellow powder comprising of $[Pt_2Cl_2(\mu\text{-}Cl)_2(TeMes_2)_2]$ and $[PtCl_2(PhCN)_2]$ as inferred from NMR data; $^{125}Te\{^1H\}$ NMR ($CDCl_3$) δ:

425 ($^{1}J(^{195}Pt\text{-}^{125}Te)$ = 1052Hz) ppm (due to $[Pt_2Cl_2(\mu\text{-}Cl)_2(TeMes_2)_2]$). $^{195}Pt\{^{1}H\}$ NMR ($CDCl_3$) δ : - 3083 (due to $[Pt_2Cl_2(\mu\text{-}Cl)_2(TeMes_2)_2]$) and -2336 (due to $[PtCl_2(PhCN)_2]$) ppm.

2.7.3 Reactions between $[PtCl_2(PhCN)_2]$ and MesTeAr in 1:2 ratio in THF

Reaction with MesTePh

The reaction was carried out in a manner similar to MesTePh of **2.7.2** using $[PtCl_2(PhCN)_2]$ (0.10 g, 0.21 mmol) and MesTePh (0.14 g, 0.43 mmol) in THF at room temperature and the product after recrystallization was characterized as $[PtCl_2\{Te(Ph)Mes\}_2]$ (yield: 0.15 g, 77%).

Reaction with MesTe(tol-*o*)

The reaction was carried out similar to MesTetol-*o* of**2.7.2**. The residue was extracted with diethylether and the insoluble part was identified as $[PtCl_2\{Te(o\text{-tol})Mes\}_2]$ (yield: ~ 10%) (NMR data were consistent with the sample prepared in CH_2Cl_2).The ether extract on evaporation afforded *trans*-$[PtCl_2(NC(O)Ph\{Te(tol\text{-}o)Mes\})_2]$ (yield 67%) and was recrystallized from acetone–hexane (8:1 v/v) mixture at room temperature as orange crystals; m.p.: 179°C. Anal. calcd. for $C_{46}H_{46}Cl_2N_2O_2PtTe_2$: C, 46.82; H, 3.93; N, 2.37 %, Found: C, 46.77; H, 4.00; N, 2.40%.^{1}H NMR ($CDCl_3$) δ: 2.13 (s, 4-Me of Mes), 2.18 (s, 2-Me of tol), 2.43 (s, 2,6-Me of Mes), 6.64 (s, 3,5-CH of Mes), 7.09-7.23 (m), 7.30-7.35 (m), 7.90 (d, 7.8Hz), 8.18 (d, 7.5Hz) [tol] ppm. $^{125}Te\{^{1}H\}$ NMR ($CDCl_3$) δ: 907 ppm. $^{195}Pt\{^{1}H\}$ NMR ($CDCl_3$) δ : -1525 ppm.

When *trans*-$[PtCl_2(NC(O)Ph\{Te(tol\text{-}o)Mes\})_2]$was left in acetone–hexane at room temperature in open for recrystallization, colorless crystals of $[PtCl(Tetol\text{-}o)\{NC(O)Ph\}_2]$ were isolated. Anal. calcd. for $C_{21}H_{17}ClN_2O_2PtTe$: C, 36.69; H, 2.49; N, 4.07 %, Found: C, 36.43; H, 2.53; N, 3.99 %.^{1}H NMR ($CDCl_3$) δ: 2.93 (s, 2-Me); 7.32; 7.38 (t, 7.5 Hz); 7.49 (t,

6.9 Hz, 4-CH of Ph and tol); 7.72 (d, 8.1 Hz, 2,6-CH of Ph); 8.22 (d, 7.8 Hz, 6-CH of tol) ppm.^{125}Te{^{1}H} NMR ($CDCl_3$) δ: 633 ppm. ^{195}Pt{^{1}H} NMR ($CDCl_3$) δ : -3188 ppm.

Reaction with $TeMes_2$

This reaction on stirring at room temperature gave different products depending on the duration of the reaction.

(i) *24 Hours reaction time*

The reactants $[PtCl_2(PhCN)_2]$ (0.10 g, 0.21 mmol) and Mes_2Te (0.16 g, 0.43 mmol) in THF were stirred for 24 h at room temperature. The solvent was evaporated under vacuum and the residue was extracted with diethyl ether from which *trans*-$[PtCl_2\{NC(O)Ph(TeMes_2)\}_2]$ (yield 37 %) was isolated and characterized by NMR spectroscopy. The supernantant exhibited ^{125}Te NMR spectrum showing resonance due to *trans*-$[PtCl_2(TeMes_2)_2]$,*trans*-$[PtCl_2\{NC(O)Ph(TeMes_2)\}_2]$ and *trans*-$[PtCl_2(TeMes_2)\{NC(O)Ph(TeMes_2)\}]$ together a small amount of $TeMes_2$.

(ii) *72 Hours reaction time*

The contents of another reaction were stirred for 72 h followed by evaporation of the solvent. The residue was washed with diethylether and extracted with acetone. The acetone extract on drying gave *trans*-$[PtCl_2(TeMes_2)\{NC(O)Ph(TeMes_2)\}]$ and was recrystallized from acetone-hexane (10:1 v/v) as colorless crystals (yield: 39%); m.p.: 190°C. Anal. calcd. for $C_{43}H_{49}Cl_2NOPtTe_2$: C, 46.23; H, 4.42; N, 1.25 %, Found: C, 46.31; H, 4.41; N, 1.27%.^{1}H NMR ($CDCl_3$) δ: 2.21 (s, 2,4,6-Me of –$NTeMes_2$), 2.29 (s, 4-Me of $TeMes_2$), 2.59 (br, s, 2,6-Me of $TeMes_2$)), 6.70 (s, 3,5-CH of $NTeMes_2$), 6.91 (s, 3,5-CH of $TeMes_2$), 7.41-7.54 (m, 3,4,5-CH of Ph), 8.49 (d, 7.2 Hz, 2,6-CH of Ph) ppm.^{13}C{^{1}H} NMR ($CDCl_3$) δ: 20.8, 21.0, 22.8, 26.1, 127.8, 128.9, 129.3, 130.2, 130.7, 134.7, 139.3, 141.5, 143.4, 183.4 (C=O) ppm.^{125}Te{^{1}H} NMR ($CDCl_3$) δ: 418 (^{1}J(^{195}Pt-^{125}Te) = 1638 Hz), 939 (J(^{195}Pt-^{125}Te) = 309 Hz) ppm. ^{195}Pt{^{1}H} NMR ($CDCl_3$) δ : - 2701 ppm.

(iii) *7 Days reaction time*

The contents of another reaction were stirred for 7 days followed by evaporation of the solvent. The residue was washed with hexane-diethylether (1:1 v/v) mixture and extracted with diethylether. The ether extract after drying under vacuum afforded *trans*-$[PtCl_2(TeMes_2)_2]$ as characterized by ^{125}Te NMR spectroscopy (δ^{125}Te NMR : 467 ppm; $^1J(^{195}Pt\text{-}^{125}Te) = 377$ Hz).

2.8 Synthesis of cyclopalladated complexes with sulfur and selenium ligands

$[Pd_2(\mu\text{-Spy})_2(Me_2NCH_2C_6H_4\text{-}C,N)_2]$

To a dichloromethane solution of $[Pd_2(\mu\text{-}Cl)_2(Me_2NCH_2C_6H_4\text{-}C,N)_2]$ (0.21 g, 0.38 mmol), [Pb(Spy)2] (0.17 g, 0.39 mmol) was added and stirred for 24 h. The solution was passed through Celite and the complex was precipitated as yellow powder upon addition of hexane. The powder was washed with diethyl ether and recrystallized from dichloromethane-hexane mixture (10:1 v/v) at -5°C as yellow crystals (yield: 0.18 g, 66%); m. p.: >195°C (dec). Anal. Calcd. for $C_{28}H_{32}N_4Pd_2S_2$: C, 47.9; H, 4.6; N, 8.0; S, 9.1. Found: C, 48.0; H, 4.7; N, 7.9; S, 8.9 %. Mass: m/z: 591 (M^{+}-Spy,). UV-vis at λ_{max}: 276, 337 nm.^{1}H NMR ($CDCl_3$) δ: 2.39, 2.55 (each s, NMe_2); 2.84–3.10 (AB pattern CH_2N); 6.65–6.69 (m), 6.91 (br, C_6H_4); 6.99 (t, 6.6 Hz, CH–5), 7.30 (d, 7.5Hz, CH–4), 7.66 (d, 7.5 Hz, CH–3), 8.60 (d, 6Hz, CH–6) (Spy).

$[Pd_2(\mu\text{-Sepy})_2(Me_2NCH_2C_6H_4\text{–}C,N)_2]$

To a toluene solution (20 ml) of NaSepy, prepared *in situ* by reduction of py_2Se_2 (0.11 g, 0.37 mmol) with methanolic $NaBH_4$ (0.03 g, 0.79 mmol), $[Pd(\mu\text{-Cl})(Me_2NCH_2C_6H_4\text{–}C,N)]_2$ (0.20 g, 0.36 mmol) dissolved in 10 ml toluene was added and stirred for 2 h. The reaction mixture was evaporated under vacuum. The complex was extracted with toluene and the solution was passed through Celite and dried under reduced pressure. The complex was washed with diethyl ether and recrystallized from dichloromethane-hexane mixture to give yellowish brown crystals (yield: 0.22 g; 78%); m.p.: 193 °C (dec.). Anal. Calcd. for $C_{28}H_{32}N_4Pd_2Se_2$: C, 42.3; H, 4.0; N, 7.0. Found: C, 42.2; H, 4.1; N, 7.2. Mass: m/z: 638 (M^+ - Sepy); 504 (M^+ - (N,N-dimethylbenzylamine + Sepy)). UV-vis at λ_{max}: 275, 287, 330 nm.^{1}H NMR (500 MHz) ($CDCl_3$) δ: (at room temperature) 2.53 (s, NMe_2), 2.97 (s), 3.13-3.37 (AB pattern) (NCH_2), 6.68 (br) 6.76 (t, 6 Hz), 6.87 (m), 6.94 (m), 7. 45 (d, 8 Hz), 7.69 (br), 8.73

(d, 5 Hz); (at -30 ºC): 2.49, 2.52 (each s, NMe_2), 2.97 (s) 3.05- 3.14 (AB pattern) (NCH_2), 6.68 (t, 1H, C_6H_4), 6.81 (t, 6.5 Hz,1H, C_5H_4N), 6.89 (t, 4.5 Hz, 2H, C_6H_4), 6.98 (t,7 Hz, 1H, C_5H_4N), 7.46 (d, 8 Hz, 1H, C_5H_4N), 7.75 (t,5 Hz, 1H, C_6H_4), 8.73 (d, 5Hz, 1H, C_5H_4N); $^{77}Se\{^1H\}$ NMR ($CDCl_3$) δ: 311 ppm.

[Pd_2(μ-Cl)(μ-SPh)($Me_2NCH_2C_6H_4$–C,N)$_2$]

To a toluene solution (20 ml) of [Pd(μ-Cl)($Me_2NCH_2C_6H_4$–C,N)]$_2$ (0.30 g, 0.54 mmol), PhSH (0.12 g, 1.09 mmol) in toluene (5 ml) was added. After stirring for 5 min, Et_3N (151 μL, 1.0 mmol) was added and the whole reaction mixture was further stirred for 2 h. The contents were passed through Celite and the clear filtrate was shaken first with distilled water (1 × 10 ml) and then with aqueous NaCl solution (2 × 5 ml) in a separating funnel and in both the cases the organic fraction was collected. The organic fraction was dried over anhydrous Na_2SO_4. The clear solution was decanted and passed through Celite. The filtrate was concentrated to 5 ml and the title complex was precipitated by adding hexane which was filtered, washed with diethyl ether and dried under vacuum. The complex was recrystallized from dichloromethane-hexane mixture (10:1 v/v) at 0-5°C as yellow crystalline solid. Yield: 0.25 g (yield: 74 %); m.p.: 185 °C (dec.). Anal. Calcd. for $C_{24}H_{29}ClN_2Pd_2S$: C, 46.0; H, 4.7; N, 4.5; S, 5.1. Found: C, 45.9; H, 4.6; N, 4.6; S, 4.9 %. Mass: m/z: 626 (M^+); 590 (M - Cl^-). UV-Vis : λ_{max}: 282, 339 nm. ^1H NMR ($CDCl_3$) δ: 2.77 (s, 12H, NMe_2); 3.89 (s, 4H, -CH_2-); 6.94–6.97 (m), 7.13 (m) (SPh); 7.60–7.63 (m),8.15–8.18 (m) (C_6H_4).

[Pd_2(μ-Cl)(μ-SMes)($Me_2NCH_2C_6H_4$–C,N)$_2$]

To a dichloromethane solution (15ml) of [Pd(μ-Cl)($Me_2NCH_2C_6H_4$–C,N)]$_2$ (0.26 mg, 0.47 mmol), solid [Pb(SMes)$_2$] (0.24 g, 0.47 mmol) was added with stirring. The yellow solution turned orange with appearance of a white precipitate. The reaction mixture was stirred for 2 h and the solution was passed through Celite. The clear filtrate was concentrated and the complex was precipitated by adding hexane. The precipitate was washed with diethyl

and recrystallized from dichloromethane-hexane mixture (10:1 v/v) as orange crystals (yield: 0.19g, 59%) at 0-5 °C; m.p.: 166 °C (dec). Anal. Calcd. for $C_{27}H_{35}ClN_2Pd_2S$: C, 48.5; H, 5.3; N, 4.2; S, 4.8. Found: C, 48.7; H, 5.2; N, 4.3; S, 4.5%. Mass: m/z: 668 (M^+); 632 (M^+-Cl) ; 517 (M^+- SMes). UV-vis at λ_{max}:279, 341 nm. ^{1}H NMR ($CDCl_3$) δ: 2.16 (s, 3H, 4-Me); 2.71 (s, 12H, NMe_2); 3.14 (s, 6H ,2,6-Me); 3.85 (s, 4H, -CH_2-); 6.44(s); 6.47 (s) ($C_6H_2Me_3$); 6.54–6.60 (m); 6.79–6.82 (m) (C_6H_4).

[Pd_2(μ-SePh)$_2$($Me_2NCH_2C_6H_4$–C,N)$_2$]

To a toluene solution (20 ml) of NaSePh, prepared *in situ* by reduction of Ph_2Se_2 (0.11 g, 0.36 mmol) with methanolic $NaBH_4$ (0.03 g, 0.79 mmol), [Pd(μ-Cl)($Me_2NCH_2C_6H_4$–C,N)]$_2$ (0.20 g, 0.36 mmol) dissolved in 20 ml toluene was added and stirred for 2 h. The solvents were evaporated under reduced pressure and the residue was extracted with benzene and passed through Celite, concentrated and precipitated by adding hexane. The precipitate was washed with diethyl ether and recrystallized from benzene-hexane mixture as red crystals (yield: 0.17 g, 61%); m.p.: 158 °C (dec)). Anal. Calcd. for $C_{30}H_{34}N_2Pd_2Se_2$: C, 45.4; H, 4.3; N, 3.5. Found: C, 45.1; H, 4.3; N, 3.2%. Mass: m/z: 793 (M^+), 659 (M^+-N,N-dimethylbenzylamine), 637 (M^+-SePh). UV-Vis : λ_{max} : 276, 335 nm. ^{1}H NMR ($CDCl_3$) δ: 2.76 (s, 12H, NMe_2); 3.91 (s, 4H, -CH_2-); 6.89–6.97 (m), 7.12–7.15 (m), 7.63 (d, 6.6 Hz); 8.81 (d, d, 1.8, 7.8 Hz) (Ph + C_6H_4). ^{77}Se {^{1}H} NMR ($CDCl_3$) δ: 181 ppm.

[Pd(S_2COPr^i){($CH_2C_6H_2Me_2$-4,6)SeMes}]

To a dichloromethane solution (50 ml) of [Pd_2(μ-Cl)$_2${$MesSeC_6H_2(Me_2)CH_2$}$_2$] (400 mg, 0.44 mmol), a methanolic solution (10 ml) of sodium *iso*-propyl xanthate (140 m g, 0.88 mmol) was added and the reaction mixture was stirred for 4 h. The solvents were evaporated under vacuum and the residue was washed with hexane (2 x 5 ml) and extracted with acetone. The solvent was evaporated and the residue was recrystallized as rectangular yellow crystals from acetone–hexane mixture on slow evaporation at room temperature (yield: 360 mg,

75%); m. p.: 65°C. Anal. Calcd. for $C_{22}H_{28}OPdSeS_2$: C, 47.3; H, 5.1; S, 11.5. Found: C, 47.2; H, 5.0; S, 11.7%. ^{1}H NMR ($CDCl_3$) δ: 1.40, 1.41 (each d, 6 Hz, OPr^i), 1.98, 2.24, 2.28, 2.45 (each singlet, Me), 3.42 (AB pattern, CH_2), 5.55 (septate, 6Hz, OCH), 6.72 (s, 1H, CH-5), 6.86 (s, 2H, 3,5-CH, mesityl), 6.95 (s, 1H, CH-3). ^{77}Se{^{1}H} NMR ($CDCl_3$) δ: 389 ppm.

[Pd(S_2COPr^n){($CH_2C_6H_2Me_2$-4,6)SeMes}]

This was prepared in a manner similar to [Pd(S_2COPr^i){($CH_2C_6H_2Me_2$-4,6)SeMes}] and isolated as reddish powder (yield: 53%); m. p.: 114°C. Anal. Calcd. for $C_{22}H_{28}OPdSeS_2$: C, 47.3; H, 5.1; S, 11.5. Found: C, 47.5; H, 5.3; S, 11.4 %.^{1}H NMR ($CDCl_3$) δ: 0.99 (t, 7.5Hz, Me, OPr^n),1.84 (Me, OPr^n),1.98, 2.24, 2.28, 2.45 (each s, Me), 3.42 (AB pattern, CH_2, $\Delta\gamma_{AB,}$ 27 Hz, J_{AB}=14.4Hz), 4.48 (t, OCH_2), 6.73 (s, 1H, CH-5), 6.86 (each s, 2H, CH-3, 5), 6.95 (s, 1H, CH-3) ppm. ^{13}C {^{1}H} NMR ($CDCl_3$) δ: 10.3, 20.4, 20.9, 21.7, 23.4, 23.7, 26.5, 73.5, 126.3, 127.1, 128.3, 129.0, 130.0, 139.4, 139.9, 140.9, 154.0, 233.8 (CS_2) ppm. ^{77}Se {^{1}H} NMR ($CDCl_3$) δ: 392 ppm.

[Pd(S_2COEt){($CH_2C_6H_2Me_2$-4,6)SeMes}]

This was prepared in a manner similar to [Pd(S_2COPr^i){($CH_2C_6H_2Me_2$-4,6)SeMes}] and isolated as reddish powder (yield: 69%); m. p.: 138°C. Anal. Calcd. for $C_{21}H_{26}OPdSeS_2$: C, 46.4; H, 4.8; S, 11.8. Found: C, 46.5; H, 5.0; S, 11.7%.^{1}H NMR ($CDCl_3$) δ: 1.43 (t, 7.2 Hz, Me, OEt), 1.98, 2.23, 2.27, 2.45 (each s, Me), 3.41 (AB pattern, CH_2, $\Delta\gamma_{AB}$ 26Hz, J_{AB}=14Hz), 4.59 (quartet, 7.2 Hz, OCH_2), 6.73 (s, 1H, CH-5), 6.86 (s, 2H, CH-3,5), 6.95 (s,1H, CH-3) ppm. ^{13}C {^{1}H} NMR ($CDCl_3$) δ: 14.0 (OCH_2Me), 20.5, 20.9, 23.5, 26.7 (each s, Me), 68.0 (OCH_2), 126.3, 127.1, 128.3, 129.1, 130.1, 139.4, 139.9, 140.9, 153.9, 233.5 (CS_2) ppm.^{77}Se {^{1}H} NMR ($CDCl_3$) δ: 390 ppm.

[Pd(S_2COMe){($CH_2C_6H_2Me_2$-4,6)SeMes}]

This was prepared in a manner similar to [Pd(S_2COPr^i){($CH_2C_6H_2Me_2$-4,6)SeMes}] and isolated as reddish powder (yield: 57%); m. p.: 120°C. Anal. Calcd. for $C_{20}H_{21}OPdSeS_2$:

C, 45.3; H, 4.5; S, 12.1. Found: C, 45.2; H, 4.6; S, 12.3 %.^{1}H NMR ($CDCl_3$) δ: 1.98, 2.24, 2.28, 2.45(each s, Me), 3.43 (AB pattern, CH_2, $\Delta\gamma_{AB}$27Hz, J_{AB}=14Hz), 4.12 (s, OMe), 6.73 (s, 1H, CH-5), 6.86 (s, 2H, CH-3, 5), 6.95 (s,1H, CH-3) ppm.

Chapter 3

Results and Discussion

3.1 Chemistry of palladium complexes with selenoether

Since the early study of Cope and Siekman, cyclometalated palladium complexes have been of considerable interest and have emerged as one of the most important families of organopalladium complexes. The sustained interest in these compounds can be attributed to their outstanding applications as catalysts in organic synthesis [47-49, 52], remarkable metallomesogenic and photophysical properties [103, 104] and their utility in material science [53, 54].

A plethora of organic compounds containing groups 15 and 16 donor atoms undergo cyclopalladation. There is an extensive literature on cyclopalladated complexes derived from groups 15 donor (N, P, As) ligands. Among the group 16 donor ligands, only sulfur compounds have been investigated [52, 102], and have also been used in C-C coupling reactions as catalysts [50]. Cyclopalladation of organoselenium ligands is rarely reported, $[Pd_2(\mu\text{-}OAc)_2(C_6H_4CH_2SeBu^t)_2]$ being the only complex described so far [51] where palladation takes place through aromatic C-H bond activation. The lack of studies on cyclometalation of organoselenium ligands could possibly be due to the formation of either simple coordination complexes, $[PdX_2(SeR_2)_2]$ or the cleavage of Se-C bond under cyclometalation conditions [152]. It is worthnoting that palladium complexes with selenoether ligands show better catalytic activity than the corresponding thio ligands [153]. Thus it was considered worthwhile to examine cyclopalladation of selenoethers.

Synthesis and spectroscopy

The reaction of dimesityl selenide with Pd(II) afforded a variety of complexes depending on the recation conditions and the palladium source (Scheme 15). The reaction of dimesityl selenide (Mes_2Se) with $PdCl_2(PhCN)_2$ in toluene at room temperature yielded a

chloro-bridged binuclear palladium complex, $[Pd_2Cl_2(\mu\text{-}Cl)_2(Mes_2Se)_2]$ as a brown powder in fairly good yield. Similarly, the complex $[Pd_2Cl_2(\mu\text{-}Cl)_2(Mes_2Se)_2]$ was formed on treatement of $PdCl_2$ with Mes_2Se in toluene-acetonitrile mixture under refluxing condition for 4 h at 80°C. The treatement of Na_2PdCl_4 with Mes_2Se in refluxing ethanol gave the cyclometalated complex, $[Pd_2(\mu\text{-}Cl)_2\{MesSeC_6H_2(Me_2)CH_2\}_2]$ (Scheme 15) as rod-like orange crystals from acetone-hexane mixture on slow evaporation. In some preparations, complex $[Pd_2(\mu\text{-}Cl)_2\{MesSeC_6H_2(Me_2)CH_2\}_2]$ in the former and complex $[Pd_2Cl_2(\mu\text{-}Cl)_2(Mes_2Se)_2]$ in the latter case were also formed in very poor yields (< 5%) and could be separated conveniently on the basis of their solubility. The complex $[Pd_2(\mu\text{-}Cl)_2\{MesSeC_6H_2(Me_2)CH_2\}_2]$ can also be obtained from $[Pd_2Cl_2(\mu\text{-}Cl)_2(Mes_2Se)_2]$ on refluxing it in ethanol. The conversion of $[Pd_2Cl_2(\mu\text{-}Cl)_2(Mes_2Se)_2]$ into $[Pd_2(\mu\text{-}Cl)_2\{MesSeC_6H_2(Me_2)CH_2\}_2]$ takes place via agostic interaction driven activation of *ortho* C-H bond. The complex $[Pd_2(\mu\text{-}Cl)_2\{MesSeC_6H_2(Me_2)CH_2\}_2]$ on treatement with lead salts of 2-pyridinechalcogenolates in dichloromethane afforded 2-pyridinechalcogenolate bridged binuclear complexes, $[Pd_2(\mu\text{-}Epy)_2\{MesSeC_6H_2(Me_2)CH_2\}_2]$ (E = S, Se) (Scheme 15) while on treatment with PPh_3 yielded the bridge-cleavaged mononuclear $[PdCl\{MesSeC_6H_2(Me_2)CH_2\}(PPh_3)]$ complex.

The ^1H NMR spectra of all the above complexes showed expected resonances (Table 12). The spectrum of $[Pd_2(\mu\text{-}Cl)_2\{MesSeC_6H_2(Me_2)CH_2\}_2]$ exhibited resonances attributable for the metallated and non-metalated mesityl group. The metalated CH_2 protons are anisotropic and appeared as a distinct AB pattern at a significant downfield, 3.37 ppm with $\Delta\gamma_{AB}$ = 46Hz, and J_{AB}=12.6 Hz (Figure 1). The appearance of metalated $-CH_2$ at such a deshielding region is due to the strong *trans* influence of the metalated carbon.

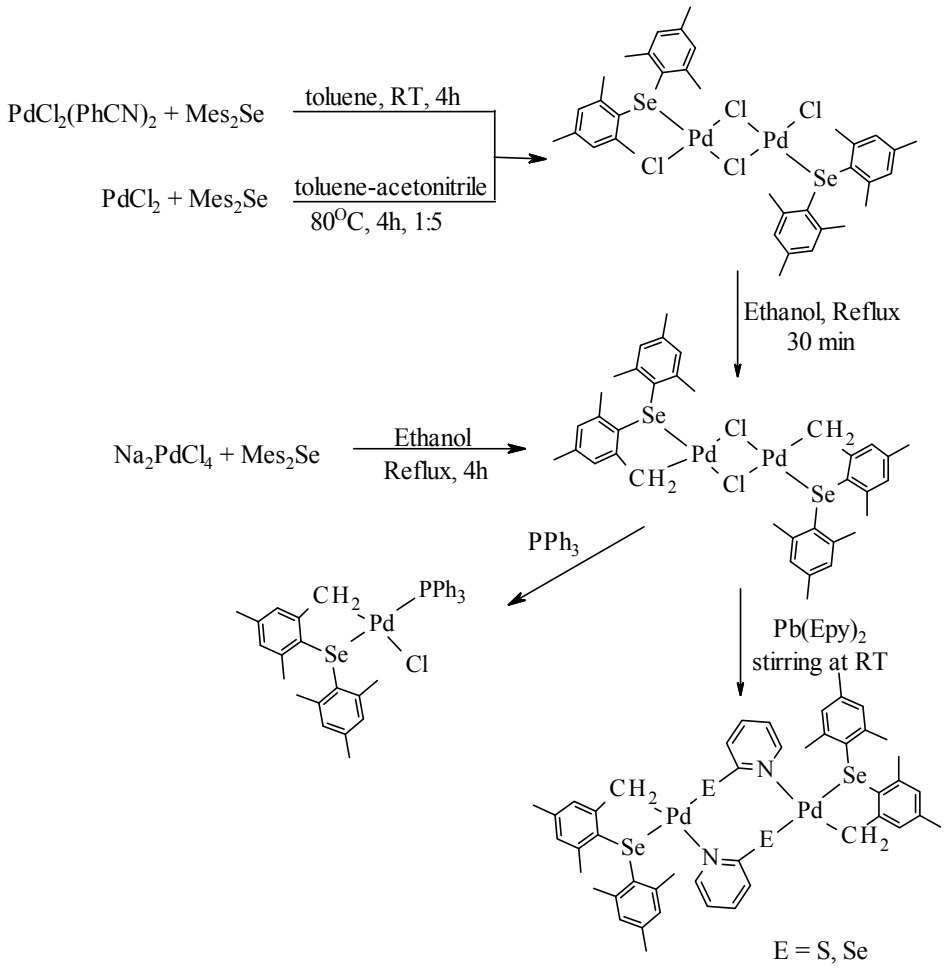

Scheme 15

On substituting the bridging chloride by bridging 2-pyridinechalcogenolates the nature of metalated $-CH_2$ changes from AB to AX pattern. Thus, in complex $[Pd_2(\mu\text{-}Spy)_2\{MesSeC_6H_2(Me_2)CH_2\}_2]$ the above mentioned metalated CH_2 showed a distinct AX pattern at 3.46 ppm with a larger chemical shift difference ($\Delta\gamma_{AX}$ =135Hz) and coupling constant, (J_{AX}=14Hz) in ^1H NMR spectra. The ^1H NMR spectrum of $[Pd_2(\mu\text{-}Sepy)_2\{MesSeC_6H_2(Me_2)CH_2\}_2]$ was quiet complex due to the existence of other isomeric species in solution which were also corroborated by the ^{77}Se NMR spectrum which displayed resonances attributable to two isomeric forms (*sym-cis* and *sym-trans*). However, only one isomeric form could be crystallized from solution. Such a dynamic behaviour of

cyclopalladated complexes is well documented. Thus, the cyclopalladated complexes, $[Pd_2(Me_2NCH_2C_6H_4)_2\{\mu\text{-}SC_5H_3(R)N\}_2]$ (R = H or Me) [154,155], are known to adopt different isomeric forms and in solution a dynamic equilibrium may exist between them [155].

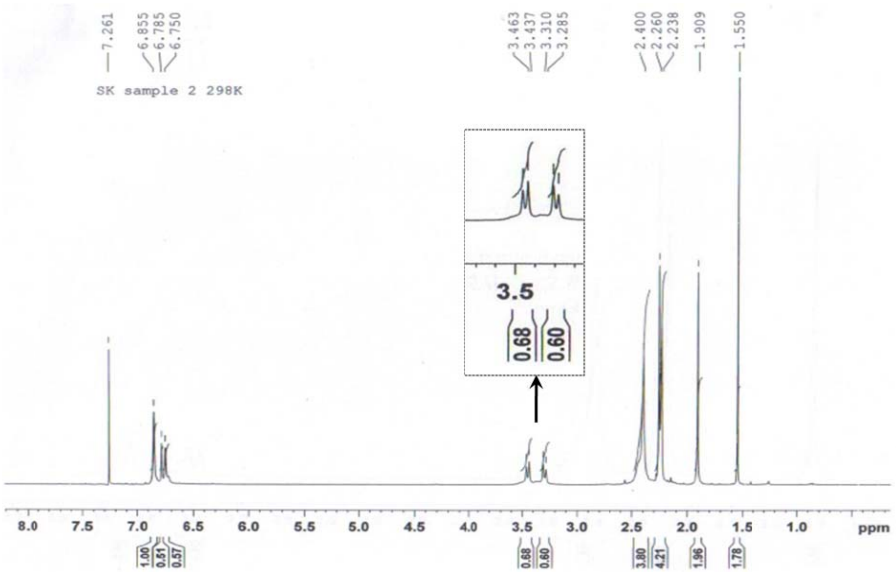

Figure 1. ^{1}H NMR sprectrum of $[Pd_2(\mu\text{-}Cl)_2\{MesSeC_6H_2(Me_2)CH_2\}_2]$

The ^{77}Se NMR spectra of these complexes displayed a single resonance (Table 12) which is deshielded with respect to the free ligand, Mes_2Se (δ 234 ppm). The ^{77}Se NMR resonance for complex $[Pd_2(\mu\text{-}Cl)_2\{MesSeC_6H_2(Me_2)CH_2\}_2]$ (δ 408 ppm) and $[Pd_2(\mu\text{-}Spy)_2\{MesSeC_6H_2(Me_2)CH_2\}_2]$ (δ 406 ppm) are considerably deshielded as compared to the simple coordination complex $[Pd_2Cl_2(\mu\text{-}Cl)_2(Mes_2Se)_2]$ (δ 322 ppm). Such a large deshielding could be due to the presence of a strong *trans* influencing group (CH_2) *cis* to selenium in the cyclometalated complexes $[Pd_2(\mu\text{-}Cl)_2\{MesSeC_6H_2(Me_2)CH_2\}_2]$ and $[Pd_2(\mu\text{-}Spy)_2\{MesSeC_6H_2(Me_2)CH_2\}_2]$ than the non-cyclometalated derivative $[Pd_2Cl_2(\mu\text{-}Cl)_2(Mes_2Se)_2]$ which has a weak *trans* influencing ligand (Cl).

Table 12. ^{1}H and $^{77}Se\{^{1}H\}$ NMR data for palladium complexes in $CDCl_3$.

Complex	^{1}H NMR δ in ppm	^{77}Se NMR δ in ppm
$[Pd_2Cl_2(\mu\text{-}Cl)_2(Mes_2Se)_2]$	2.22, 2.24, 2.49, 2.65 (s, ratio 4:2:1:6, Me), 6.77, 6.83, 6.85, (s, C_6H_2)	322
$[Pd_2(\mu\text{-}Cl)_2\{MesSeC_6H_2(Me_2)CH_2\}_2]$	1.91 (s, 4-Me, non-metalated), 2.24, 2.26 (each s, 4- and 6-Me, metalated), 2.40 (br s, 2,6-Me, non-metalated), 3.37 (AB pattern, CH_2, $\Delta\gamma_{AB}$ 46Hz, J_{AB}=12.6Hz), 6.75, 6.78 (each s, C_6H_2 metalated), 6.85 (s, C_6H_2 non-metalated)	408
$[Pd_2(\mu\text{-}Spy)_2\{MesSeC_6H_2(Me_2)CH_2\}_2]$	1.93 (s, 4-Me, non-metalated), 2.22 (s, 4- and 6-Me, metalated), 2.43 (s, 2,6-Me, non-metalated), 3.46 (AX pattern, CH_2, $\Delta\gamma_{AX}$ 135Hz, J_{AX}=14Hz), 6.75 (s, C_6H_2 metalated), 6.88 (s, C_6H_2 non-metalated), 6.10 (t, CH-4, C_5H_4N), 6.81 (t, CH-5, C_5H_4N), 7.13 (d, 7.8 Hz, CH-3, C_5H_4N), 7.74 (d, 5 Hz, CH-6, C_5H_4N)	406
$[Pd_2(\mu\text{-}Sepy)_2\{MesSeC_6H_2(Me_2)CH_2\}_2]$	0.80 – 2.33 (m), 2.69 - 4.01 (m), 6.12 (d, 7.2Hz), 6.45 (t, 6.2Hz), 6.66-6.87 (br, m), 7.38 (d, 4.8Hz), 7.59 (t, 7.6Hz), 8.02 (d, 7.8Hz)	341, 378, 380, 408.
$[PdCl\{MesSeC_6H_2(Me_2)CH_2\}(PPh_3)]$#	1.95 (s, 4-Me,non-metalated), 2.17, 2.24 (each s, 4- and 6-Me, metalated), 2.69 (br, CH_2), 6.48, 6.70 (each s, 3-,5-H, metalated), 6.88 (s, 3-,5-H, non-metalated), 7.41-7.44 (br, Ph), 7.72-7.78 (br, Ph)	393 (d, ^{2}J(Se-P) = 167 Hz)

$^{31}P\{^{1}H\}$ NMR δ: 31.7 ppm.

X-ray Crystallography

The molecular structures of complex $[Pd_2Cl_2(\mu\text{-}Cl)_2(Mes_2Se)_2]$, $[Pd_2(\mu\text{-}Cl)_2\{MesSeC_6H_2(Me_2)CH_2\}_2]$, $[Pd_2(\mu\text{-}Spy)_2\{MesSeC_6H_2(Me_2)CH_2\}_2]$ and $[Pd_2(\mu\text{-}Sepy)_2\{MesSeC_6H_2(Me_2)CH_2\}_2]$ were established by single crystal X–ray diffraction analyses. ORTEP drawings with the atomic numbering scheme are shown in Figures 2–5 and selected inter-atomic parameters are summarized in Tables 13-16. All the complexes are dimeric with the palladium atoms acquiring a distorted square planar configuration. The Pd–Se distances are well within the range reported in palladium selenolate complexes, such as $[PdCl(SeCH_2CH_2NMe_2)]_3$ [156], $[Pd(OAc)(SeCH_2CH_2CH_2NMe_2)]_2$ [157] and $[Pd(OAc)(SeC_6H_4Me\text{-}2)]_4$ [158].

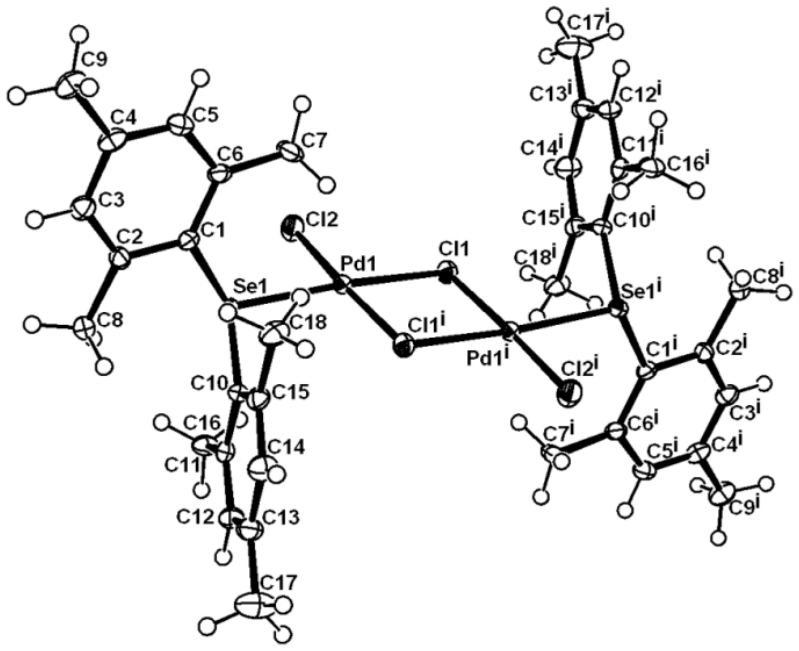

Figure 2. ORTEP drawing of $[Pd_2Cl_2(\mu\text{-}Cl)_2(Mes_2Se)_2]$, elipsoids are drawn with 25% probability.

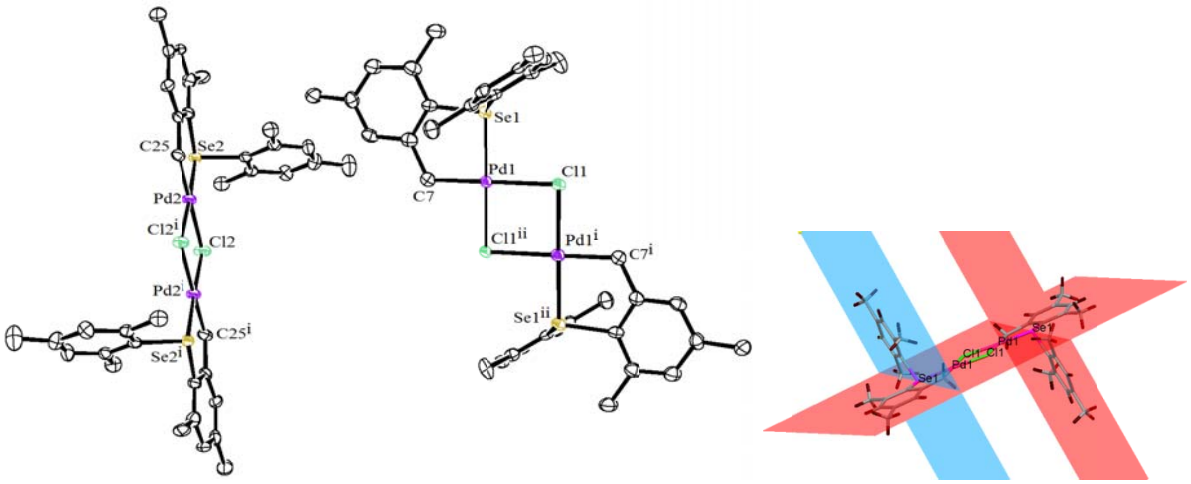

(a) **(b)**

Figure 3. (a) ORTEP drawing of $[Pd_2(\mu\text{-}Cl)_2\{MesSeC_6H_2(Me_2)CH_2\}_2]$; elipsoids are drawn with 50% probability, **(b)** Mutual orientation of the mesityl rings of two Mes_2Se.

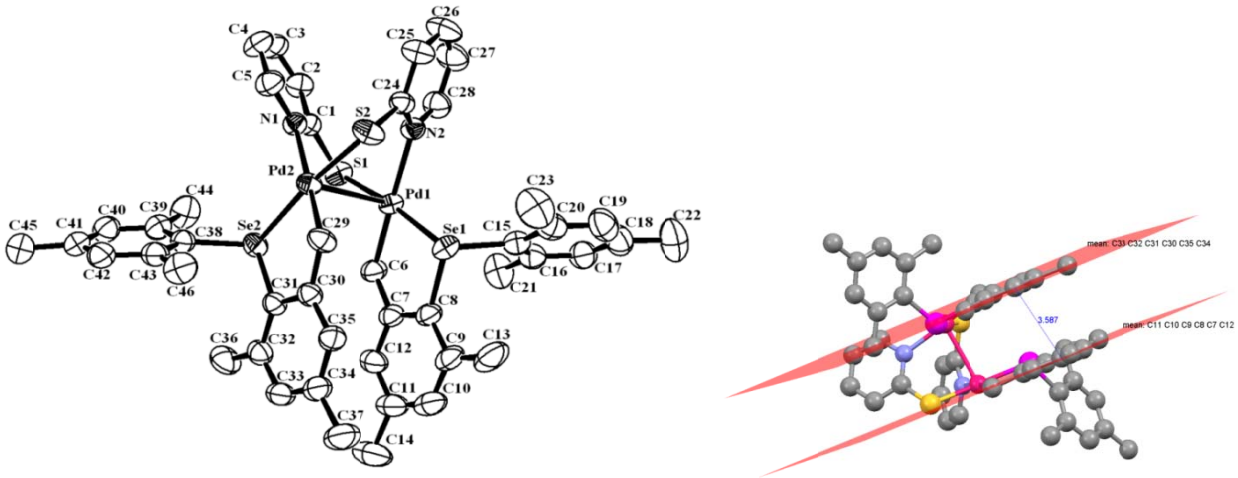

(a) (b)

Figure 4. (a) ORTEP drawing of $[Pd_2(\mu\text{-}Spy)_2\{MesSeC_6H_2(Me_2)CH_2\}_2]$; elipsoids are drawn with 25% probability, **(b)** π- π stacking between the mesityl rings.

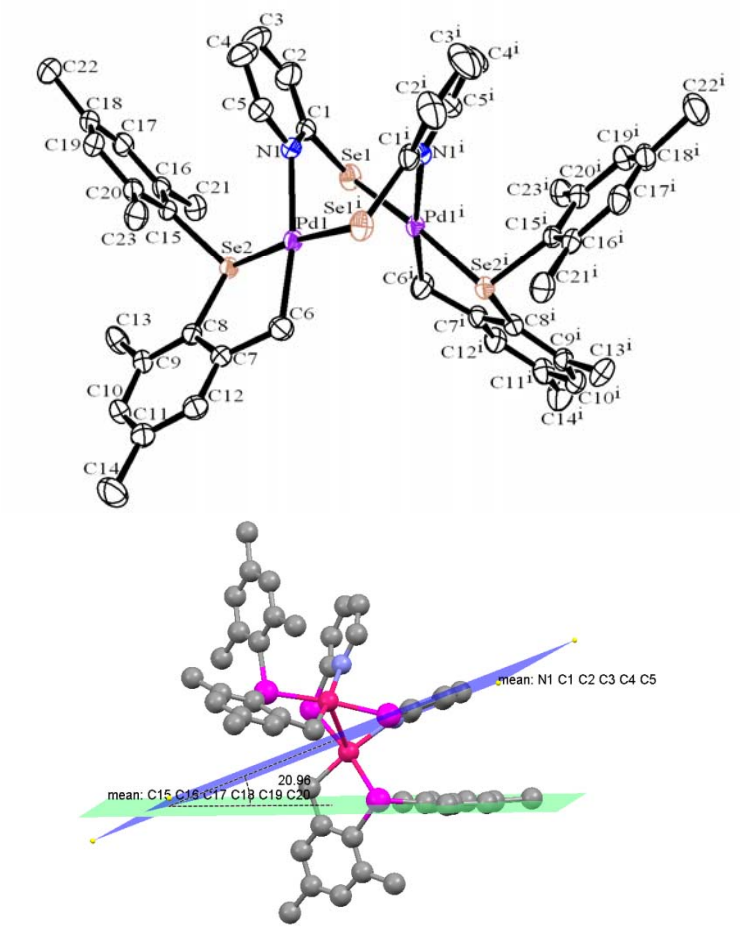

Figure 5. (a) ORTEP drawing of $[Pd_2(\mu\text{-Sepy})_2\{MesSeC_6H_2(Me_2)CH_2\}_2]$; elipsoids are drawn with 25% probability, **(b)** Mutual orientation of the mesityl rings of two Mes_2Se

Table 13. Selected bond lengths (Å) and angles (°) of $[Pd_2Cl_2(\mu\text{-}Cl)_2(Mes_2Se)_2]$

Se1 – Pd1	2.3837(5)	Pd1– Cl1	2.3504(9)
Pd1– $Cl1^i$	2.3307(10)	C1– Se1	1.947(4)
Pd1– Cl2	2.2810(10)	C10 – Se1	1.945(4)
		Pd···Pd	3.452
Cl1– Pd1– Se1	172.57(3)	Cl2 – Pd1 – $Cl1^i$	176.37(3)
$Cl1^i$ – Pd1– Se1	97.51(3)	C1 – Se1 – Pd1	116.04(11)
Cl2 – Pd1 – Se1	86.04(3)	C10 – Se1 – Pd1	103.38(11)
$Cl1^i$ – Pd1 – Cl1	84.96(3)	C10 – Se1 – C1	104.08(16)
Cl2 – Pd1 – Cl1	91.42(3)	Pd1 – Cl1 – $Pd1^i$	95.04(3)

Table 14. Selected bond lengths (Å) and angles (°) of $[Pd_2(\mu\text{-}Cl)_2\{MesSeC_6H_2(Me_2)CH_2\}_2]$.

Molecule a		**Molecule b**	
Pd1 – Se1	2.3438(8)	Pd2 – Se2	2.3342(9)
Pd1 – C7	2.024(7)	Pd2 – C25	2.039(7)
Pd1 – Cl1	2.4786(17)	Pd2 – Cl2	2.4833(17)
Pd1 – Cl1^{i}	2.3739(16)	Pd2 – Cl2^{i}	2.3713(17)
Se1 – C1	1.912(7)	Se2 – C19	1.925(7)
Se1 – C10	1.948(6)	Se2 – C28	1.946(7)
Pd1 – Pd1^{i}	3.472	Pd2 – Pd2^{i}	3.440
Se1 – Pd1 – Cl1	93.02(4)	Se2 – Pd2 – Cl2	92.72(5)
Se1 – Pd1 – Cl1^{i}	177.92(5)	Se2 – Pd2 – Cl2^{i}	176.84(5)
Se1 – Pd1 – C7	87.22(19)	Se2 – Pd2 – C25	87.0(2)
C7 – Pd1 – Cl1	179.7(2)	C25 – Pd2 – Cl2	179.3(2)
C7 – Pd1 – Cl1^{i}	91.1(2)	C25 – Pd2 – Cl2^{i}	90.5(2)
Cl1 – Pd1 – Cl1^{i}	88.67(6)	Cl2 – Pd2 – Cl2^{i}	89.78(6)
Pd1 – C7 – C2	117.0(5)	Pd2 – C25 – C20	117.4(5)
Pd1 – Se1 – C1	98.5(2)	Pd2 – Se2 – C19	98.6(2)
Pd1 – Se1 – C10	107.49(19)	Pd2 – Se2 – C28	107.62(19)
Pd1 – Cl1 – Pd1^{i}	91.33(6)	Pd2 – Cl2 – Pd2^{i}	90.22(6)

Table 15. Selected bond lengths (Å) and angles (°) of $[Pd_2(\mu\text{-}Spy)_2\{MesSeC_6H_2(Me_2)CH_2\}_2]$.

Pd1 – Se1	2.4005(12)	Pd2 – Se2	2.4184(6)
Pd1 – C6	2.037(3)	Pd2 – C29	2.025(3)
Pd1 – S1	2.3136(13)	Pd2 – S2	2.3218(9)
Pd1 – N2	2.179(2)	Pd2 – N1	2.171(2)
Se1 – C8	1.924(3)	Se2 – C31	1.919(3)
Se1 – C15	1.950(3)	Se2 – C38	1.949(3)
		Pd1 – Pd2	2.9288(9)
Se1 – Pd1 – S1	172.71(2)	Se2 – Pd2 – S2	172.12(2)
Se1 – Pd1 – C6	85.94(8)	Se2 – Pd2 – C29	85.05(8)
Se1 – Pd1 – N2	96.86(6)	Se2 – Pd2 – N1	96.85(6)
C6 – Pd1 – N2	174.19(11)	C29 – Pd2 – N1	176.47(10)
C6 – Pd1 – S1	86.89(9)	C29 – Pd2 – S2	87.70(8)
S1 – Pd1 – N2	90.40(6)	S2 – Pd2 – N1	90.55(7)
Pd1 – Se1 – C8	97.89(10)	Pd2 – Se2 – C31	97.09(9)
Pd1 – Se1 – C15	114.57(8)	Pd2 – Se2 – C38	118.57(8)
C8 – Se1 – C15	102.35(12)	C31 – Se2 – C38	103.39(12)
S1-Pd1-Pd2-S2	-122.78(3)	Se1-Pd1-Pd2-S2	64.56(3)
S1-Pd1-Pd2-Se2	64.91(2)	Se1-Pd1-Pd2-Se2	-107.749(19)

Table 16. Selected bond lengths (Å) and angles (°) of $[Pd_2(\mu\text{-Sepy})_2\{MesSeC_6H_2(Me_2)CH_2\}_2]$.

C6-Pd1	2.045(4)	C1-Se1	1.900(5)
N1-Pd1	2.154(3)	$Pd1^i$-Se1	2.4197(8)
$Pd1^i$-Pd1	3.1429(8)	C15-Se2	1.953(4)
$Se1^i$-Pd1	2.4197(8)	C8-Se2	1.934(4)
Se2-Pd1	2.4156(8)		
C6-Pd1-N1	171.26(16)	C15-Se2-Pd1	106.71(11)
C6-Pd1-$Pd1^i$	110.18(14)	C8-Se2-Pd1	95.84(12)
C6-Pd1-$Se1^i$	87.92(12)	C1-N1-Pd1	124.9(3)
C6-Pd1-Se2	84.15(13)	C5-N1-Pd1	115.4(3)
$Se1^i$-Pd1-$Pd1^i$	78.396(16)	N1-Pd1-$Pd1^i$	78.53(9)
Se2-Pd1-$Pd1^i$	104.033(16)	N1-Pd1-$Se1^i$	94.77(9)
Se2-Pd1-$Se1^i$	172.059(19)	N1-Pd1-Se2	93.13(9)
C1-Se1-$Pd1^i$	102.04(13)		
Se1-$Pd1^i$-Pd1-$Se1^i$	-142.25	$Se1^i$-Pd1-$Pd1^i$-$Se2^i$	45.50
Se2-Pd1-$Pd1^i$-$Se2^i$	-126.74	Se1-$Pd1^i$-Pd1-Se2	45.50

The complex $[Pd_2Cl_2(\mu\text{-}Cl)_2(Mes_2Se)_2]$ is a centrosymetric dimer and comprises of a chloro-bridged "$Pd_2(\mu\text{-}Cl)_2$" core. Coordinated selenoether ligands are mutually *trans*. The $Pd–Cl_{(bridging)}$ distances are longer than the terminal Pd–Cl distance. The $Pd–Cl_{bridging}$ *trans* to selenoether ligand is marginally longer than the one *trans* to the terminal chloride ligand. The C1–Se1–C10 angle is 104.08°. The mesityl ring lies at ~7° above the Pd_2Cl_2 plane so as to result in intra-molecular C–H···Pd interaction. The Pd···H7C distance and Pd···H7C-C7 angle are 2.75Å and 111.23° respectively. The bond distance and angle indicate that this interaction is agostic in nature. The Pd···H7C and Cl2···H7B distances are smaller than the sum of their van der Waals

radii, 2.75 vs 2.83Å and 2.86 vs 2.95Å, respectively. These interactions support involvement of metal–center in C–H (sp^3) bond activation leading to metalation.

The unit cell of the complex $[Pd_2(\mu\text{-}Cl)_2\{MesSeC_6H_2(Me_2)CH_2\}_2]$ comprises two independent half molecules which differ slightly in bond lengths, bond angles and torsion angles; as shown in the Figure 3. The molecule adopts a sym-*trans* configuration. In contrast to $[Pd_2Cl_2(\mu\text{-}Cl)_2(Mes_2Se)_2]$ where both the mesityl rings of the selenoether are near perpendicular to the central Pd_2Cl_2 plane, in $[Pd_2(\mu\text{-}Cl)_2\{MesSeC_6H_2(Me_2)CH_2\}_2]$ one of the mesityl ring comes into the central Pd_2Cl_2 plane to satisfy the square planar geometry around palladium, while the non-metalated mesityl rings remain at near perpendicular (86.17° for molecule **a** and 83.86° for molecule **b**) to the planar metalated PdCCCSe rings. The two five-membered planar metalated PdCCCSe rings are co-planar with the four-membered rectangular Pd_2Cl_2 ring. Coordination around each palladium atom is defined by two Cl atoms, a C and a Se atom of the metalated selenoether. The two bridging Pd–Cl distances are distinctly different. The one *trans* to metalated carbon atom is longer than the one *trans* to selenium, owing to the strong *trans* influence of the CH_2 group. This is well in agreement with the reported values (e.g. $[Pd_2(\mu\text{-}Cl)_2(py\text{-}C_6H_4)_2]$; Pd–Cl = 2.426 (1), 2.349 (2)Å [158]. The Pd–C [106, 158] and Pd–Se [153] distances are in conformity with the reported values (e.g., $[PdCl\{OC_6H_4C(Ph)=NCH_2CH_2SePh\}]$, Pd–Se = 2.3575 (6) Å) [153]. The Pd···Pd separation of ~3.45 Å is within the range observed in chloro-bridged cyclometalated palladium complexes (~3.5 Å) [102].

The two palladium atoms in $[Pd_2(\mu\text{-}Spy)_2\{MesSeC_6H_2(Me_2)CH_2\}_2]$ and $[Pd_2(\mu\text{-}Sepy)_2\{MesSeC_6H_2(Me_2)CH_2\}_2]$ are held together by bridging pyridyl chalcogenolate groups (Epy) forming an eight−membered ring which adopts a distorted twist boat conformation. The

chalcogen atoms of the Epy ligands are *trans* to the Se atoms of the metalated ligand resulting in an anti configuration which is generally observed for $Pd_2(\mu\text{-}Spy)_2L_4$ type of complexes [104, 159, 160]. The configuration around palladium in both the complexes is distorted square planar but the mutual orientation of the square planes are different for $[Pd_2(\mu\text{-}Spy)_2\{MesSeC_6H_2(Me_2)CH_2\}_2]$ and $[Pd_2(\mu\text{-}Sepy)_2\{MesSeC_6H_2(Me_2)CH_2\}_2]$. The angle between the square planes S1Pd1Se1N2 and S2Pd2Se2N1 is 20.97° in $[Pd_2(\mu\text{-}Spy)_2\{MesSeC_6H_2(Me_2)CH_2\}_2]$ and between $Se1Pd1^iN1^iSe2^i$ and $Se2Pd1Se1^iN1$ is 39.02° in $[Pd_2(\mu\text{-}Sepy)_2\{MesSeC_6H_2(Me_2)CH_2\}_2]$ resulting in different orientation of the metalated mesityl ring in the two complexes. The metalated mesityl rings of $[Pd_2(\mu\text{-}Spy)_2\{MesSeC_6H_2(Me_2)CH_2\}_2]$ display fairly good intra-molecular π-π stacking with an angle of 2.04° between the planes and average stacking separation of 3.587Å. Such type of interaction is absent in $[Pd_2(\mu\text{-}Sepy)_2\{MesSeC_6H_2(Me_2)CH_2\}_2]$. The Pd–S, Pd–N and Pd–C distances are in accord with those reported in $[Pd_3(\mu\text{-}Spy)_2(Me_2NCH_2C_6H_4\text{-}C,N)_3][BF_4]$ [155] and $[Pd_2(\mu\text{-}SCNCH_2CH_2NMe)_2(Bzq)_2]$ [104]. The Pd–Se distances can be compared with $[Pd_2(\mu\text{-}SePh)_2(C_{10}H_6NMe_2\text{-}C,N)_2]$ [105]. The Pd···Pd distance in $[Pd_2(\mu\text{-}Spy)_2\{MesSeC_6H_2(Me_2)CH_2\}_2]$ (2.9288 (9) Å) is within the generally acceptable range of intra-molecular Pd···Pd interaction (<3.00Å) while in the corresponding selenolate complex $[Pd_2(\mu\text{-}Sepy)_2\{MesSeC_6H_2(Me_2)CH_2\}_2]$ it is much longer (3.143 Å). In the complex $[Pd_2(\mu\text{-}Spy)_2\{MesSeC_6H_2(Me_2)CH_2\}_2]$ one of the mesityl rings on both selenium ligands are parallel to each other and is separated by 3.587 Å which may be attributed to π-stacking and are positioned on the opposite side of pyridine thiolate rings. In $[Pd_2(\mu\text{-}Sepy)_2\{MesSeC_6H_2(Me_2)CH_2\}_2]$ also one mesityl group on each of the $Se(Mes)_2$ ligands is almost but not exactly parallel to the Sepy rings.

3.2 Chemistry of palladium complexes with telluroethers

Although cyclopalladation of a wide variety of organic compounds containing nitrogen, phosphorus and sulfur has been extensively investigated [50, 52, 102, 161], there is hardly any report on metalation of organo-tellurium compounds. The absence of cyclometalation of organotellurium ligands can be attributed to the formation of coordination complexes, $[PdX_2(TeR_2)_2]$, cleavage of Te-C bond or even complete decomposition of the complexes under metalation conditions. In a recent attempt by Singh and co-workers to metalate di-*o*-tolyl telluride, cleavage of the Te-C bond has been noted [152]. They isolated $[Pd(OAc)_2\{(o\text{-tol})_2O\}]$ and $[o\text{-tol}_2Pd_3(\mu\text{-OAc})_4\{Te(o\text{-tol})_2\}_2]$ formed by cleavage of the Te-C bond of $o\text{-tol}_2Te$, rather than metalated complex.

In the light of the above, reactions of common palladium precursors Na_2PdCl_4, $PdCl_2(PhCN)_2$, $[Pd(OAc)_2]_3$ used in cyclopalladation reactions with diorganotellurides have been investigated and the results are included in this section.

Synthesis and spectroscopy

The reactions of Pd(II) with various telluroethers result in the formation of various complexes depending upon the reaction conditions, nature of telluroethers along with the steric crowding around the telluroethers and the source of Pd(II) (Schemes 16 and 17). Thus the reaction of $[PdCl_2(PhCN)_2]$ with diaryl telluride in 1:2 molar ratio in toluene at room temperature gave mononuclear palladium complexes, *trans*-$[PdCl_2(TeAr_2)_2]$ (Scheme 16) (Ar = Mes (Mes = 2,4,6-trimethylpheny), Ph, *o*-tol (*o*-tol = *ortho*-tolyl)) as orange crystalline solids in good yield. The complex, *trans*-$[PdCl_2(TeMes_2)_2]$ on treatement with one equivalent of $[PdCl_2(PhCN)_2]$ in toluene-acetonitrile mixture at room temperature afforded a chloro-bridged binuclear complex,

$[Pd_2(\mu\text{-}Cl)_2Cl_2(TeMes_2)_2]$. The latter can also be prepared by the reaction of Na_2PdCl_4 with $TeMes_2$ at room temperature as dark-red precipitate which was extracted with acetone and gave red-needle shaped crystals from slow diffusion of hexane in acetone at -5°C in 79% yield. Similarly, by employing the above method and using MesTePh and $TePh_2$, $[Pd_2(\mu\text{-}Cl)_2Cl_2(MesTePh)_2]$and $[Pd_2(\mu\text{-}Cl)_2Cl_2(TePh_2)_2]$ were also prepared as brown/orange crystals in more than 70% yield.

On refluxing *trans*-$[PdCl_2(TeMes_2)_2]$ in toluene-methanol solution for ~30 minutes cyclopalladated binuclear complex, $[Pd_2(\mu\text{-}Cl)_2\{CH_2C_6H_2(4, 6\text{-}Me_2)TeMes\}_2]$ (Scheme 16) was isolated as an orange powder in 75% yield. When refluxing was prolonged for 2h a mononuclear complex *cis*-$[PdCl_2\{MesTeCH_2C_6H_2(Me_2\text{-}4,6)TeMes\}]$ was formed which was extracted with toluene and crystallized from toluene–hexane mixture as dark-red crystals. The latter can also be prepared by refluxing *trans*-$[PdCl_2(TeMes_2)_2]$ in tolune-methanol solution or performing the reaction of Na_2PdCl_4 with $TeMes_2$ in toluene-methanol under refluxing condition for 2h. The formation of complex *cis*-$[PdCl_2\{MesTeCH_2C_6H_2(Me_2\text{-}4,6)TeMes\}]$ can be inferred by the nucleophilic attack of the tellurolate ion ($MesTe^-$), generated by Te-C bond cleavage, on methylene carbon of the cyclopalladated complex, $[Pd_2(\mu\text{-}Cl)_2\{CH_2C_6H_2(4, 6\text{-}Me_2)TeMes\}_2]$. The formation of tellurolate ion ($MesTe^-$) by Te-C bond cleavage has been observed previously and is well documented in the literature [162, 163]. The formation of tellurolate ion from a telluroether ligand has already been noted in the past [164] and also in the present study with the isolation of the complex and characterization crystalloghaphycally (see later, e.g. isolation of $[Pd(\mu\text{-}OAc)(\mu\text{-}TeMes)]_4$).

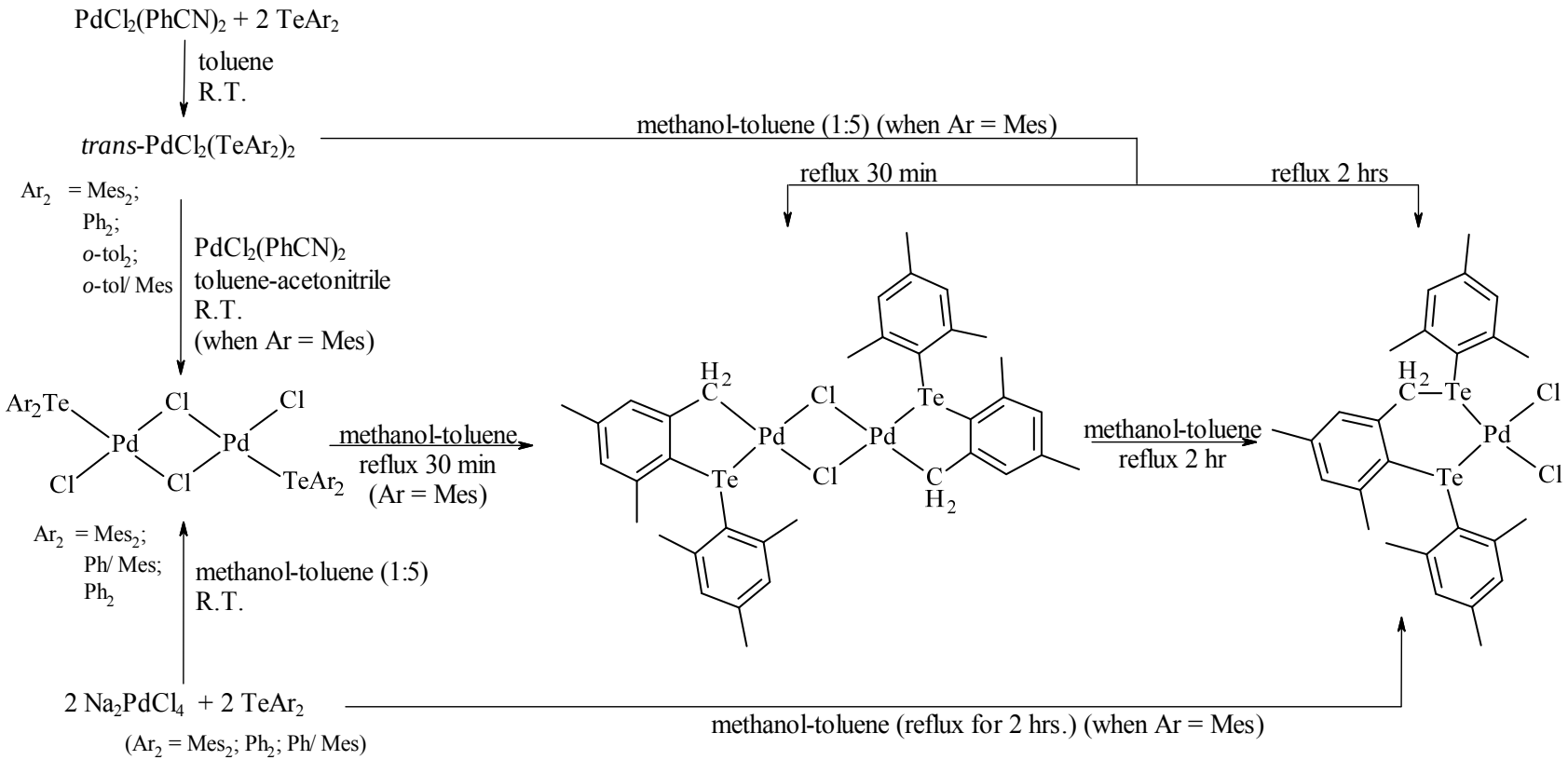

Scheme 16. Synthetic routes for palladium telluroether complexes

Attempt was also made to prepare similar cyclopalladated complexes with other telluroethers like *o*-tolTeMes, *o*-tol_2Te and Ph_2Te which were unsuccessful. The complex *trans*-$[PdCl_2(TeMes_2)_2]$ ended up into Pd_7Te_3 (Figures 6 and 7) which was indentified from powder X-ray diffraction pattern (JCPDS file no: 43-1294) on changing the solvent from toluene-methanol to xylene on refluxing for 2 h. The conversion of telluroether complexes of palladium, $[PdCl\{C_6H_5(2\text{-}HOC_6H_4)CHNH(CH_2)_3TeC_6H_4OMe\text{-}4\}]$, into Pd_3Te_2 nanoparticles has recently been reported by Singh and coworkers [165].

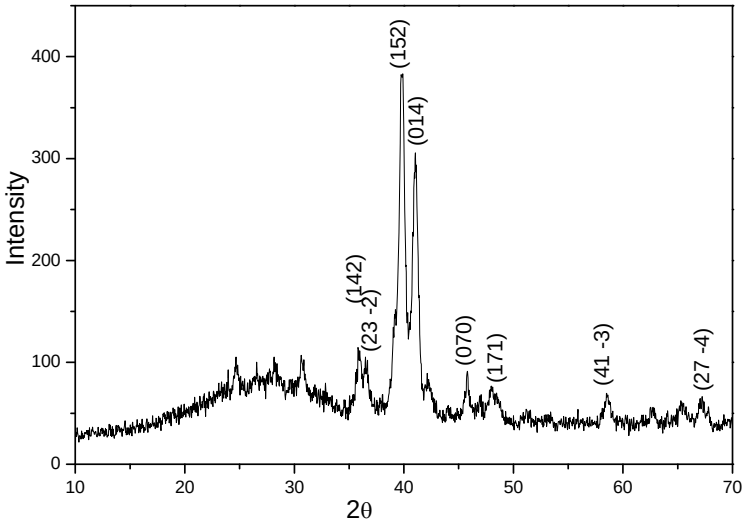

Figure 6. XRD pattern of Pd_7Te_3 obtained from *trans*-$[PdCl_2(TeMes_2)_2]$ in refluxing xylene.

On changing the palladating agent from chloride based to acetate based a completely different and interesting chemsity was evolved and the results are presented schematically in Scheme 17. Thus the reaction of palladium acetate with $TeMes_2$ in toluene at room temperature afforded an acetato-bridged analogue of $[Pd_2(\mu\text{-}Cl)_2\{CH_2C_6H_2(4,6\text{-}Me_2)TeMes\}_2]$, $[Pd_2(\mu\text{-}OAc)_2\{CH_2C_6H_2(4,6\text{-}Me_2)TeMes\}_2]$ as a yellow crystalline solid together with a very minor component, a tetra-nuclear complex, $[Pd(\mu\text{-}OAc)(\mu\text{-}TeMes)]_4$ formed by the cleavage of Te-C bond of Mes_2Te. This reaction with unsymmetrical

telluroether ligands, MesTeAr (Ar = *o*-tol, Ph) also yielded cyclopalladated complexes, $[Pd_2(\mu\text{-}OAc)_2\{CH_2C_6H_2(4,6\text{-}Me_2)TeAr\}_2]$ (Ar = *o*-tol, Ph) in which 2-methyl of the mesityl group of the telluroether ligand was exclusively metallated.

Cyclopalladation using telluroether ligands containing at least one meistyl group was quite facile when $[Pd(OAc)_2]_3$ was used as the palladating agent, whereas the same took place with Na_2PdCl_4 or $[PdCl_2(PhCN)_2]$ only in case of Mes_2Te. This could be due to the fact that in the latter case only with Mes_2Te due to steric crowding of two bulky mesityl rings, one of the *ortho* C-H bond falls into the coordination plane of palladium as is evidenced in the molecular structure of $[Pd_2(\mu\text{-}Cl)_2Cl_2(TeMes_2)_2]$ (see later, Figure 11 (b)) leading to metallation with the generation of HCl as by-product. On the other hand, with $[Pd(OAc)_2]_3$, in the reaction medium via η^2-bridging mode OAc^- give a cyclic transition state by coordinating palladium with one oxygen and at the same time bringing one of the *ortho* C-H bond of methyl group of mesityl into the close proximity of palladium using other oxygen atom through C-H···O interaction and leads to activation of the C-H bond with the generation of HOAc as the by-product. HOAc being a weak conjugate of OAc^- also makes the metalation energetically more feasible than strong acid; HCl generated in the case of Na_2PdCl_4 and have a strong interference with the formed M-C bond than HOAc.

The presence of acetate groups in the complex $[Pd_2(\mu\text{-}OAc)_2\{CH_2C_6H_2(4,6\text{-}Me_2)TeMes\}_2]$ and $[Pd_2(\mu\text{-}OAc)_2\{CH_2C_6H_2(4,6\text{-}Me_2)Tetol\text{-}o\}_2]$ have been inferred from the IR spectroscopy. The IR spectra showed absoptions at 1615, 1558 ($[Pd_2(\mu\text{-}OAc)_2\{CH_2C_6H_2(4,6\text{-}Me_2)TeMes\}_2]$)/ 1566 ($[Pd_2(\mu\text{-}OAc)_2\{CH_2C_6H_2(4,6\text{-}Me_2)Tetol\text{-}o\}_2]$) cm^{-1} attributable to the bridging acetate groups. The ^1H NMR spectra displayed expected resonances (Table 17). The methyl groups (at 2- and 6- positions) of the coordinated mesityl telluride were deshielded in the ^1H NMR spectra while they were shielded in the ^{13}C NMR spectra with reference to the corresponding free ligands. The cyclopalladated complexes showed a distinct AB pattern for

the Pd-CH_2 protons at a chemical shift significantly downfield from that of the mesityl methyl groups (3.38 ppm, br, 2H ($[Pd_2(\mu\text{-}Cl)_2\{CH_2C_6H_2(4,6\text{-}Me_2)TeMes\}_2]$); 3.36 ppm, 2H, $\Delta\nu_{AB}$ = 71 Hz, J_{AB} = 13 Hz ($[Pd_2(\mu\text{-}OAc)_2\{CH_2C_6H_2(4,6\text{-}Me_2)TeMes\}_2]$); 3.09 ppm, 2H, $\Delta\nu_{AB}$ = 24.6 Hz, J_{AB} = 12.7 Hz ($[Pd_2(\mu\text{-}OAc)_2\{CH_2C_6H_2(4,6\text{-}Me_2)Tetol\text{-}o\}_2]$)). Similar anisotropic behavior has been also noted for analogous selenium complex, $[Pd_2(\mu\text{-}Cl)_2\{CH_2C_6H_2(4,6\text{-}Me_2)SeMes\}_2]$ as mentioned in **3.1**. The CH_2 protons in *cis*-$[PdCl_2\{MesTeCH_2C_6H_2(Me_2\text{-}4,6)TeMes\}]$ are also anisotropic and appeared as an AX pattern at 3.55 ppm with significantly large chemical shift difference (2H, $\Delta\nu_{AX}$ = 169 Hz, J_{AX} = 11 Hz).

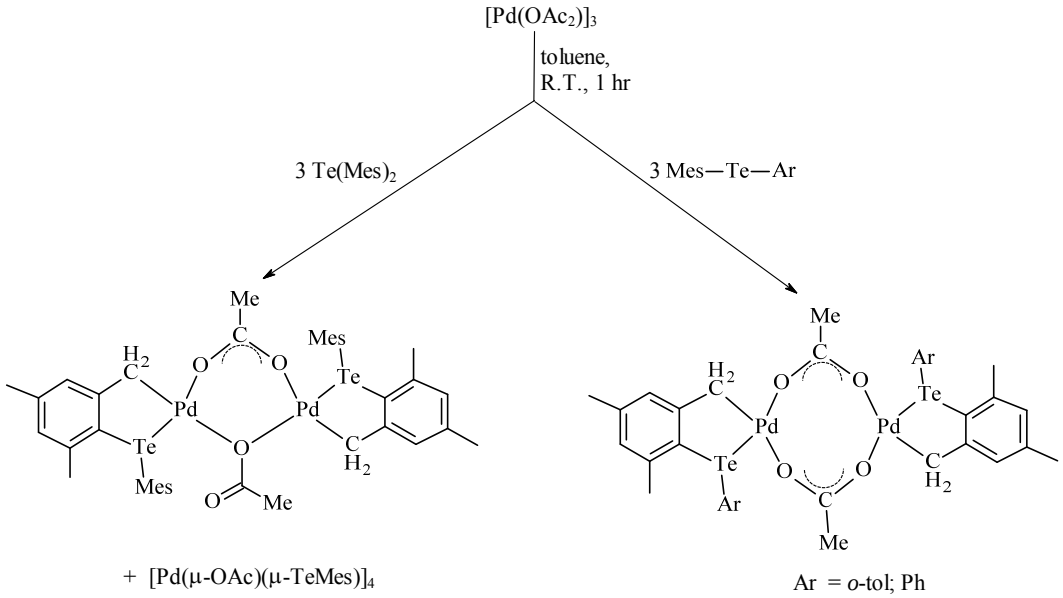

Scheme 17. Synthesis of acetato bridged cyclopladated telluroether complexes

The $^{125}Te\{^1H\}$ NMR spectra of these complexes displayed a single resonance which appeared at higher frequency (Table 17) with respect to the free ligands ($TeMes_2$, ^{125}Te δ = 260.8 ppm, Te(*o*-tol)$_2$, ^{125}Te δ = 499.3 ppm, $TePh_2$, ^{125}Te δ = 693.4 ppm, MesTe(*o*-tol) ^{125}Te δ = 336.8 ppm, MesTePh ^{125}Te δ = 427.2 ppm). The ^{125}Te NMR resonance was progressively

deshielded from mononuclear *trans*-[$PdCl_2(TeMes_2)_2$] (δ 489.1 ppm) to cyclopalladated derivative [$Pd_2(\mu\text{-}Cl)_2\{CH_2C_6H_2(4,6\text{-}Me_2)TeMes\}_2$] (δ 644.0 ppm) through the binuclear [$Pd_2(\mu\text{-}Cl)_2Cl_2(TeMes_2)_2$] (δ 575.0 ppm). Such a large deshielding (69 ppm) from binuclear complex [$Pd_2(\mu\text{-}Cl)_2Cl_2(TeMes_2)_2$] to cyclopalladated complex [$Pd_2(\mu\text{-}Cl)_2\{CH_2C_6H_2(4, 6\text{-}Me_2)TeMes\}_2$] has also been noted in the case of the corresponding mesityl selenoether derivatives (deshielded by 86 ppm in ^{77}Se resonance) and is mentioned in **section3.1**. The effect of bridging ligand as well as the nature of Ar group on Te is also evident in cyclopalladated complexes. There is shielding of ~90 ppm of the ^{125}Te NMR resonance on replacing bridging chloride in [$Pd_2(\mu\text{-}Cl)_2\{CH_2C_6H_2(4, 6\text{-}Me_2)TeMes\}_2$] (δ 644.0 ppm) by acetate group [$Pd_2(\mu\text{-}OAc)_2\{CH_2C_6H_2(4,6\text{-}Me_2)TeMes\}_2$] (δ 554.1 ppm). Replacement of mesityl group on Te in [$Pd_2(\mu\text{-}OAc)_2\{CH_2C_6H_2(4,6\text{-}Me_2)TeMes\}_2$] by *ortho*-tolyl or phenyl groups results in successive deshielding of the resonance ([$Pd_2(\mu\text{-}OAc)_2\{CH_2C_6H_2(4,6\text{-}Me_2)Tetol\text{-}o\}_2$], 592.2 ppm; [$Pd_2(\mu\text{-}OAc)_2\{CH_2C_6H_2(4,6\text{-}Me_2)TePh\}_2$], 690.4 ppm). Such changes could be attributed to the electron releasing methyl groups in the aryl ring which consequently increases electron density at the tellurium.

X-ray Crystallography

Molecular structures of *trans*-[$PdCl_2(TeMes_2)_2$], [$Pd_2(\mu\text{-}Cl)_2Cl_2(TeMes_2)_2$].2acetone, *cis*-[$PdCl_2\{MesTeCH_2C_6H_2(4,6\text{-}Me_2)TeMes\}$], [$Pd_2(\mu\text{-}OAc)_2\{CH_2C_6H_2(4,6\text{-}Me_2)TeMes\}_2$].toluene, [$Pd_2(\mu\text{-}OAc)_2\{CH_2C_6H_2(4,6\text{-}Me)_2Tetol\text{-}o\}_2$] and [$Pd(\mu\text{-}OAc)(\mu\text{-}TeMes)]_4$ were established by single crystal X-ray diffraction analyses and the ORTEP drawing along with the numbering schemes are shown in Figures 7-13. Selected inter-atomic parameters are summarized in Tables 18 - 24. Palladium atom in all these complexes acquires a distorted square planar configuration. The Pd-Te distances (2.47-2.59 Å) are well within the

range reported for palladium-telluroether complexes, [PdCl{$OC_9H_6C(Me)$ = $NCH_2CH_2TeC_6H_4OMe$-4}] (Pd-Te = 2.5025(7) Å [166], [$PdCl_2${4-$BrC_3H_2N_2CH_2CH_2TeC_6H_4OMe$-4}]] (Pd-Te = 2.512(6) Å [167], [$Pd(TePh)_2$(dppe)] (Pd-Te = 2.5871-2.6704(8) Å [168] and [$tol_2Pd_3(\mu$-$OAc)_4(Tetol_2$-o)$_2$] (Pd-Te = 2.5054 Å [152]. The Pd-C distances (~2.03 Å) are in accord with the values reported for cyclopalladated complexes such as [$Pd_2(\mu$-$Cl)_2${$CH_2C_6H_2$(4,6-Me_2)SeMes}$_2$] (Pd-C = ~2.03 Å [169] and [Pd(OCH-C_4H_3N)(Bzq)] (Bzq = 7,8-benzoquinolyl) (Pd-C = 1.993(3) Å [104]. The Te-C (~2.14Å) bond distances are in conformity with the range reported in organotellurium compounds (e.g. Mes_2Te (Te-C = 2.140(3) Å [144], Te{C_5H_3(Me-3)N}$_2$ (Te-C = 2.136(1) Å [163] and [$Cd(TeMes)_2]_n$ (Te-C = 2.164(12)Å [170].

The mononuclear complex, *trans*-[$PdCl_2(TeMes_2)_2$] (Figure 7) was isolated in a *trans* configuration and showed polymorphism depending on the crystallization solvents. The two polymorphs, viz rectangular block and needle shaped crystals were isolated from acetonitrile-diethyl ether (monoclinic form, Figure 7(a)) and toluene-hexane (triclinic form, Figure 7(b)) mixture, respectively. The two polymorphs essentially differ slightly in the inter-atomic parameters as well as in the relative orientation of the mesityl groups on tellurium. The Te-Pd-Te angle in the triclinic form is significantly reduced (~164°) from the ideal value of 180° while in the monoclinic form it is 180°. The Pd-Te-C angles in the monoclinic form are smaller than the triclinic form. The C-Te-C angle (~100° in the triclinic form and 102.5° in monoclinic form) are as observed in Mes_2Te (101.0(1)°) [144]. In the monoclinic form the mesityl rings (C1-C9) and ($C1^i$-$C9^i$) are coplanar and are almost perpendicular (85.60°) to the Pd square plane (Cl1Te1Pd1$Te1^i$$Cl1^i$), while the other mesityl rings (C10-C18) and ($C10^i$-$C18^i$) lie in plane parallel to each other which are nearly perpendicular to the Pd square plane (77.80°). The two mesityl rings attached to tellurium atom lie at an angel of 80.04°.

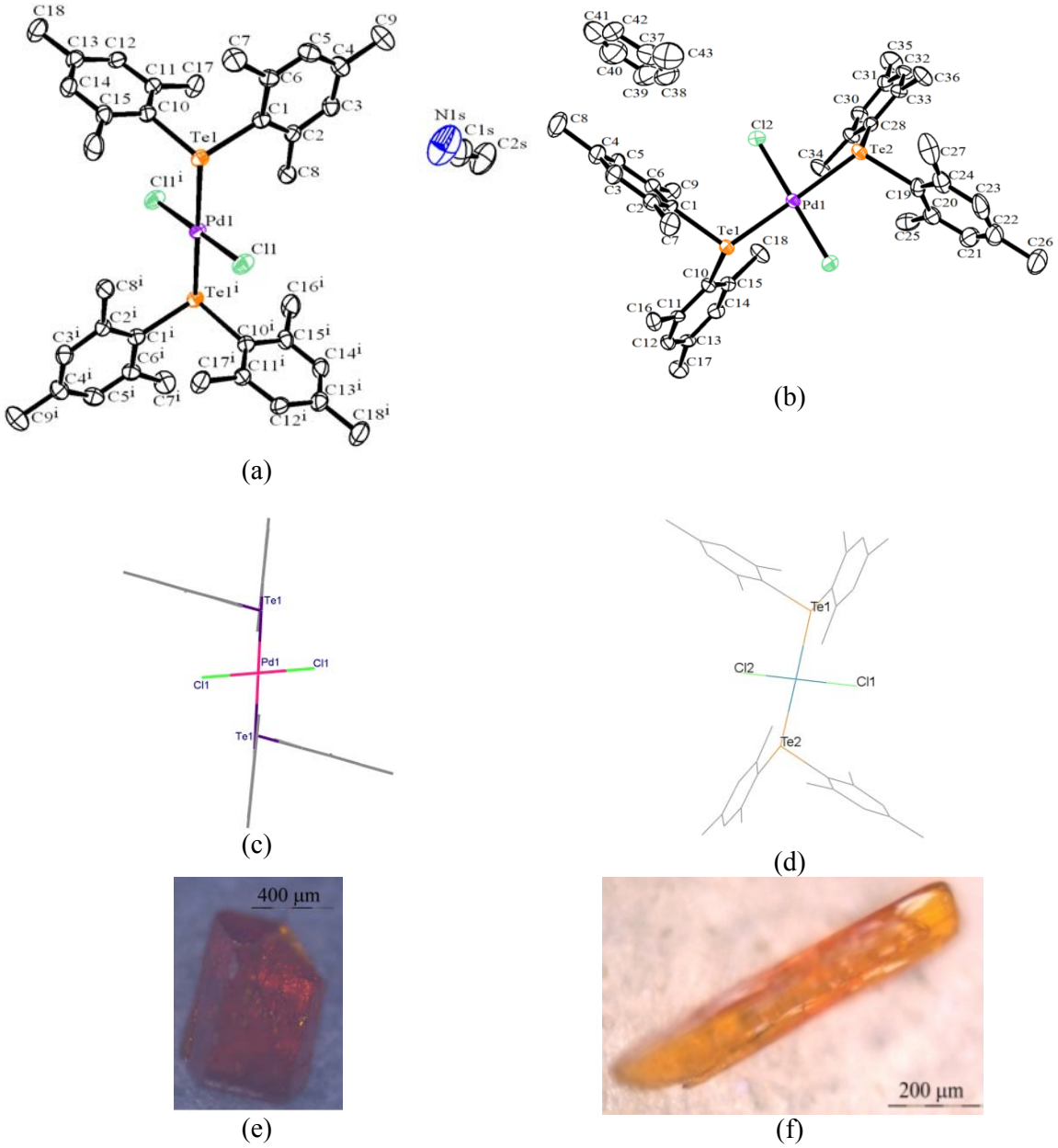

Figure 7. ORTEP diagram of **(a)** *trans*-$[PdCl_2(TeMes_2)_2]$.2MeCN **(b)** of *trans*-$[PdCl_2(TeMes_2)_2]$.toluene (25% probability). Hydrogen atoms are omitted for clarity, **(c)** and **(d)** view perpendicular to the Pd1 square plane, **(e)** and **(f)** Optical microscope imagesof **(a)** and **(b)** respectively.

There are weak secondary interaction between the chloride and the hydrogen atom of the acetonitrile molecule (Cl1…C25 = 2.719Å) as well as nitrogen and hydrogen (sp^2 (2.691Å) and sp^3 (2.718Å)) atom of nearby molecule (Figure 8). In the triclinic form the arrangement of the mesityl rings are completely different. The mesityl rings (C10-C18) and (C29-C36) are *syn* to the Pd square plane.

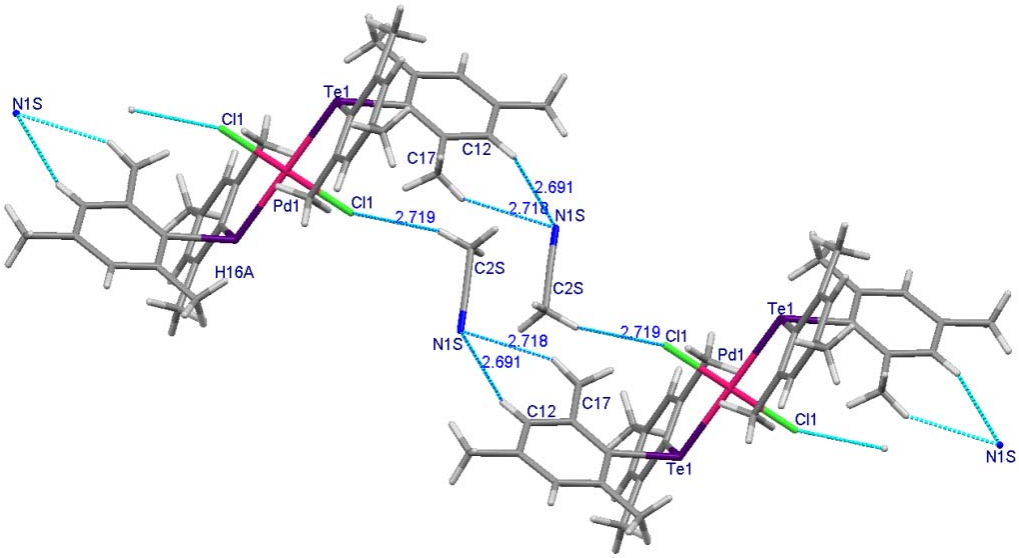

Figure 8. Short interactions between solvent acetonitrile and *trans*-$[PdCl_2(TeMes_2)_2]$ in *trans*-$[PdCl_2(TeMes_2)_2].2CH_3CN$

The binuclear complex, $[Pd_2(\mu\text{-}Cl)_2Cl_2(TeMes_2)_2]$ (Figure 9) crystallizes with two molecules of acetone and comprises of a rectangular planar four-membered chloro-bridged "$Pd_2(\mu\text{-}Cl)_2$" core; a configuration usually observed for the chloro-bridged complexes [102] with neutral monodentate group 16 ligands. Two telluroether ligands are mutually *trans*, forming a *sym-trans* dimeric structure. The terminal Pd-Cl distances are marginally shorter (2.290(4) Å) than the bridging Pd-Cl distances (2.310(4), 2.403(4)Å). The Pd-Te distance is shorter than the one noted for the mononuclear complex, *trans*-$[PdCl_2(TeMes_2)_2]$. This may

be attributed to the weak *trans* influencing effect of chloro ligand *trans* to it. The C-Te-C angle (97.64°) is also reduced significantly from the mononuclear complex. The Pd…H17A-C17 distance (2.377 Å), which is significantly shorter than the van der Waal radii (2.83 Å), and the C17-H17…Pd1 angle (171.19°) correspond to an anagostic interaction between palladium and the *ortho*-methyl hydrogen atom [97]. There is also a short contact between the terminal chloride and hydrogen atom (H17A) of *ortho* methyl group (Cl2...H17A-C17 = 2.925 Å).

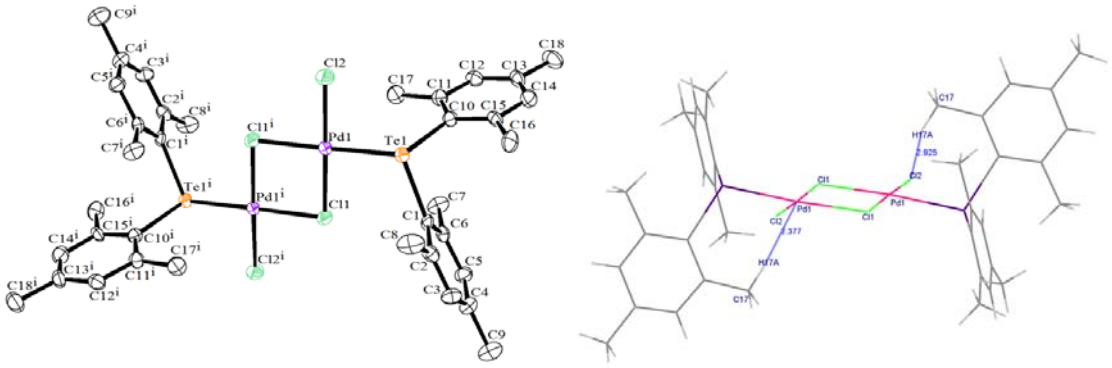

(a) (b)

Figure 9. (a) ORTEP diagram of $[Pd_2(\mu\text{-}Cl)_2Cl_2(TeMes_2)_2]$.2acetone (25% probability). Hydrogen atoms and solvent molecules are omitted for clarity, (b) intra molecular interactions

Table 17. ^{1}H, $^{13}C\{^{1}H\}$ and $^{125}Te\{^{1}H\}$ NMR data in CDCl3 of palladium telluroether complexs.

Complex	^{1}H NMR δ in ppm	$^{13}C\{^{1}H\}$ NMR δ in ppm	$^{125}Te\{^{1}H\}$ NMR δ in ppm
trans-$[PdCl_2(TeMes_2)_2]$	2.23, 2.58 (s, Me); 6.86 (s, 3,5-CH).	20.9, 27.2 (Me), 118.8 (Te-C), 129.3 (3,5-CH), 139.9, 143.6.	489
trans-$[PdCl_2(TePh_2)_2]$	7.29-7.44 (m), 7.81 (d, 7.2 Hz) (Ph).	117.9 (C-Te), 129.7, 130.0, 137.0.	750
trans-$[PdCl_2\{Te(o\text{-}tol)_2\}_2]$	2.54 (s, Me), 7.10(t, 7.2 Hz) 7.25 (d) 7.34 (t, 7.2 Hz), 7.84 (d, 7.2 Hz) (*o*-tol).	25.5 (Me), 119.8 (C-Te), 127.4, 130.2, 130.3, 138.4, 142.4 (*o*-tol).	637
trans-$[PdCl_2\{MesTetol\text{-}o)_2]$	2.31, 2.46, 2.76 (each s, Me), 7.01(s), 7.15-7.25 (m).		
$[Pd_2(\mu\text{-}Cl)_2Cl_2(TeMes_2)_2]$	2.24 (s, 1Me); 2.65 (s, 2Me), 6.88 (s, 2H).	20.9, 26.8 (Me), 116.8 (C-Te), 130.1 (3,5-CH), 141.0, 143.3.	575
$[Pd_2(\mu\text{-}Cl)_2Cl_2(MesTePh)_2]$	2.34 (s,1Me), 2.81 (s, 2Me), 7.04 (s, 3,5-CH, Mes), 7.19-7.44 (m, Ph).		704
$[Pd_2(\mu\text{-}Cl)_2Cl_2(TePh_2)_2]$	7.38 (t, 7.5 Hz), 7.49 (t, 7.2 Hz), 7.78 (d, 7.2 Hz).		823
$[Pd_2(\mu\text{-}Cl)_2\{CH_2C_6H_2(4,6\text{-}Me_2)TeMes\}_2]$	2.04 (s, 1Me), 2.25 (s, 1Me), 2.53 (s, 2Me), 3.38 (br, CH_2), 6.94 (s, 1H), 6.78 (s, 1H), 6.87 (s, 2H) (CH, Mes).	20.9, 21.0, 22.9, 25.7, 27.2 (1Me), 29.7 (CH2, metallated), 127.4, 128.8 (3/5- CH of metallated), 129.1 (3,5-CH non-metallated), 140.3, 140.8, 141.2, 143.9 (quaternary carbons).	644

cis-[$PdCl_2${$MesTeCH_2C_6H_2(Me_2$-4,6)TeMes}]	2.02, 2.22, 2.27, 2.50 (each s, 1Me), 2.47, 2.63 (br, s, each 2Me, 2,6-Me of Mes), 3.55 (AX pattern, CH_2 metallated, $\Delta\nu_{AX}$ = 169 Hz, J_{AX} = 11 Hz), 6.25, 6.83 (each s, 1H, 3,5-CH, metallated), 6.93 (s, 3,5-CH, Mes).	20.5, 20.8, 25.3, 26.5 (1Me), 27.5, 28.5 (br, 2Me), 117.0, 117.6 (C-Te), 129.0, 129.2, 130.4, 130.9, 140.6, 140.9, 141.1, 142.3, 142.7, 144.3	428
[Pd_2(μ-$OAc)_2${$CH_2C_6H_2$(4,6-Me_2)TeMes }$_2$]	1.95-2.53 (overlapping singlets due to methyl groups of mesityl and acetate groups), 3.36 (AB pattern, CH_2 metallated, $\Delta\nu_{AB}$ = 71 Hz, J_{AB} = 13 Hz), 6.43, 6.60, 6.64, 6.77, 6.81, 6.86 (each br s of 3,5-CH of mesityl).		554
[Pd_2(μ-$OAc)_2${$CH_2C_6H_2$(4,6-Me_2)Tetol-*o*}$_2$]	1.88 (s, OAc), 2.04, 2.14, 2.29 (each s, 1Me), 3.09 (AB pattern, CH_2 metallated, $\Delta\nu_{AB}$ = 24.6 Hz, J_{AB} = 12.7 Hz), 6.60 (s, 3,5-CH, Mes), 6.70-6.91 (m), 7.18 (br) (o-tol).	21.2, 22.2, 23.4, 24.0, 24.2, (for Me, CH_2), 118.9 (C-Te), 126.6, 127.2, 128.7, 128.9, 130.4, 132.6, 140.6, 141.0, 142.2, 179.8 (C=O)	592
[Pd_2(μ-$OAc)_2${$CH_2C_6H_2$(4,6-Me_2)TePh}$_2$]			690

Table 18. Selected bond lengths (Å) and bond angles (°) for monoclinic form of *trans*-$[PdCl_2(TeMes_2)_2]$.2MeCN

Pd1-Cl1	2.3006(14)	Te1-C1	2.130(5)
Pd1-Te1	2.5817(3)	Te1-C10	2.137(5)
$Cl1\text{-}Pd1\text{-}Cl1^{i}$	180.00(11)	C1-Te1-Pd1	110.36(13)
Cl1-Pd1-Te1	83.78(4)	C10-Te1-Pd1	106.71(13)
$Cl1\text{-}Pd1\text{-}Te1^{i}$	96.22(4)	C1-Te1-C10	102.5(2)
$Cl1^{i}\text{-}Pd1\text{-}Te1$	96.22(4)	$Te1\text{-}Pd1\text{-}Te1^{i}$	180.000(15)
$Cl1^{i}\text{-}Pd1\text{-}Te1^{i}$	83.78(4)		

Table 19. Selected bond lengths (Å) and bond angles (°) for triclinic form of *trans*-$[PdCl_2(TeMes_2)_2]$.toluene

Pd1-Cl1	2.290(2)	Te1-C1	2.149(6)
Pd1-Cl2	2.292(2)	Te1-C10	2.137(6)
Pd1-Te1	2.5951(6)	Te2-C19	2.143(8)
Pd1-Te2	2.5908(6)	Te2-C28	2.126(8)
Cl1-Pd1-Cl2	177.61(10)	C1-Te1-Pd1	109.92(17)
Cl1-Pd1-Te1	83.86(5)	C10-Te1-C1	100.2(3)
Cl1-Pd1-Te2	95.50(5)	C10-Te1-Pd1	113.57(18)
Cl2-Pd1-Te1	95.78(6)	C19-Te2-Pd1	112.0(2)
Cl2-Pd1-Te2	84.19(6)	C28-Te2-C19	100.2(3)
Te2-Pd1-Te1	163.97(3)	C28-Te2-Pd1	114.2(2)

Table 20. Selected bond lengths (Å) and bond angles (°) for $[Pd_2(\mu\text{-}Cl)_2Cl_2(TeMes_2)_2]$.2acetone.

Cl1-Pd1	2.310(4)	C1-Te1	2.156(13)
Cl1-Pd1^{i}	2.403(4)	C10-Te1	2.119(14)
Cl2-Pd1	2.290(4)	Pd1-Te1	2.5067(13)
		Pd1-−-Pd1^{i}	3.421
Cl1-Pd1-Cl1^{i}	86.96(13)	Cl2-Pd1- Te1	83.47(11)
Cl1-Pd1-Te1	96.25(10)	Pd1-Te1-C1	108.4(3)
Cl1^{i}-Pd1- Te1	174.08(12)	C1-Te1-C10	97.6(5)
Cl1-Pd1-Cl2	177.78(17)	Pd1-Te1-C10	111.0(4)
Cl1^{i}-Pd1-Cl2	93.14(13)	Pd1-Cl1-Pd1^{i}	93.04(13)

Table 21. Selected bond lengths (Å) and bond angles (°) for *cis*-$[PdCl_2\{MesTeCH_2C_6H_2(4,6\text{-}Me_2)TeMes\}]$.

Pd1-Te1	2.5402(3)	C1-Te1	2.151(4)
Pd1-Te2	2.5137(3)	C10-Te1	2.135(4)
Pd1-Cl1	2.3419(10)	C16-Te2	2.166(4)
Pd1-Cl2	2.3389(9)	C19-Te2	2.133(3)
Cl1-Pd1-Te1	85.97(3)	C1-Te1-Pd1	110.96(10)
Cl1-Pd1-Te2	172.31(3)	C10-Te1-Pd1	97.38(9)
Cl1-Pd1-Cl2	93.85(4)	C10-Te1-C1	100.76(14)
Cl2-Pd1-Te1	177.01(3)	C16-Te2-Pd1	105.18(9)
Cl2-Pd1-Te2	85.30(3)	C19-Te2-Pd1	113.44(9)
Te2-Pd1-Te1	95.278(11)	C19-Te2-C16	94.41(13)

Table 22. Selected bond lengths (Å) and bond angles (°) for $[Pd_2(\mu\text{-}OAc)_2\{CH_2C_6H_2(4,6\text{-}Me_2)TeMes\}_2]$.toluene.

Pd1-O1	2.108(7)	Pd2-O2	2.097(7)
Pd1-O3	2.238(7)	Pd2-O3	2.272(8)
Pd1-C7	2.027(9)	Pd2-C27	1.999(10)
Pd1-Te1	2.4706(10)	Pd2-Te2	2.4845(9)
Te1-C1	2.133(10)	Te2-C19	2.090(10)
Te1-C10	2.140(11)	Te2-C28	2.152(9)
Pd1…Pd2	3.0831(10)		
O1-Pd1-C7	86.5(4)	O2-Pd2-C27	86.9(3)
O3-Pd1-O1	87.6(3)	O3-Pd2-O2	89.4(3)
Te1-Pd1-O1	172.29(19)	Te2-Pd2-O2	173.0(2)
Te1-Pd1-O3	98.8(2)	Te2-Pd2-O3	97.0(2)
O3-Pd1-C7	173.9(4)	O3-Pd2-C27	175.7(3)
Te1-Pd1-C7	86.9(3)	Te2-Pd2-C27	86.8(3)
Pd1-Te1-C1	94.0(3)	Pd2-Te2-C19	93.7(3)
Pd1-Te1-C10	107.4(3)	Pd2-Te2-C28	105.8(3)
Pd1-C7-C2	122.2(7)	Pd2-C27-C20	122.9(7)
Pd1-O1-C37	124.9(7)	Pd2-O2-C37	129.4(7)
Pd1-O3-C39	130.4(11)	Pd2-O3-C39	116.7(13)
		Pd2-O3-Pd1	86.3(3)

Table 23. Selected bond lengths (Å) and bond angles (°) for $[Pd_2(\mu\text{-}OAc)_2\{CH_2C_6H_2(4,6\text{-}Me)_2Tetol\text{-}o\}_2]$.

Te1-Pd1	2.4979(13)	Te2-Pd2	2.4926(13)
C7-Pd1	1.980(15)	C23-Pd2	2.007(14)
O1-Pd1	2.142(10)	O2-Pd2	2.097(10)
O4-Pd1	2.103(11)	O3-Pd2	2.164(10)
C1-Te1	2.120(13)	C17-Te2	2.104(12)
C10-Te1	2.122(12)	C26-Te2	2.152(13)
O1-C33	1.261(15)	O3-C35	1.248(18)
O2-C33	1.225(16)	O4-C35	1.246(18)
		Pd1…Pd2	2.8677(14)
O1-Pd1-O4	91.7(4)	O2-Pd2-O3	91.5(4)
O1-Pd1-C7	177.6(5)	O2-Pd2-C23	87.1(5)
O1-Pd1-Te1	94.2(3)	O2-Pd2-Te2	168.5(3)
O4-Pd1-C7	89.7(5)	O3-Pd2-C23	178.4(5)
O4-Pd1-Te1	173.9(3)	O3-Pd2-Te2	95.1(3)
C7-Pd1-Te1	84.4(4)	C23-Pd2-Te2	86.2(4)
Pd1-Te1-C1	92.4(4)	Pd2-Te2-C17	93.3(3)
Pd1-Te1-C10	106.6(3)	Pd2-Te2-C26	100.9(3)
Pd1-O1-C33	123.3(9)	Pd2-O2-C33	128.0(9)
Pd1-O4-C35	124.2(9)	Pd2-O3-C35	124.7(10)
C1-Te1-C10	99.6(5)	C17-Te2-C26	98.1(5)

Table 24. Selected bond lengths (Å) and bond angles (°) of $[Pd(\mu\text{-}OAc)(\mu\text{-}TeMes)]_4$

Pd1-O1	2.130(5)	Pd2-O2	2.117(5)
Pd1-O3	2.104(5)	Pd2-O4	2.100(5)
Pd1-Te1	2.5404(7)	Pd2-Te2	2.5299(6)
Pd1-Te2^{i}	2.5448(6)	Pd2-Te1^{i}	2.5374(7)
Te1-C1	2.149(7)	Te2-C10	2.154(7)
Te2^{i}-C10^{i}	2.154(7)	Te1i-C1^{i}	2.149(7)
Pd1^{i}-O1^{i}	2.130(5)	Pd2i-O2^{i}	2.117(5)
Pd1^{i}-O3^{i}	2.104(5)	Pd2i-O4^{i}	2.100(5)
Pd1^{i}-Te1^{i}	2.5404(7)	Pd2^{i}-Te1	2.5374(7)
Pd1^{i}-Te2	2.5448(6)	Pd2^{i}-Te2^{i}	2.5299(6)
Pd1···Pd2	2.9474(7)	Pd2^{i}-Pd1^{i}	2.9474(7)
Pd1…Pd2^{i}	3.695	Pd2-Pd1^{i}	3.695
O1-Pd1-O3	87.7(2)	O2-Pd2-O4	88.3(2)
O1-Pd1-Te1	176.59(15)	O2-Pd2-Te2	177.60(15)
O1-Pd1-Te2^{i}	96.00(15)	O2-Pd2-Te1^{i}	96.20(16)
O3-Pd1-Te1	94.85(19)	O4-Pd2-Te2	93.78(17)
O3-Pd1-Te2^{i}	175.54(17)	O4-Pd2-Te1^{i}	175.42(18)
Te1-Pd1-Te2^{i}	81.347(19)	Te2-Pd2-Te1^{i}	81.694(19)
Pd1-Te1-C1	102.82(17)	Pd2-Te2-C10	103.63(17)
Pd1-Te2^{i}-C10^{i}	106.78(18)	Pd2-Te1^{i}-C1^{i}	107.59(18)
Pd1-Te1-Pd2	93.40(2)	Pd2-Te2-Pd1^{i}	93.47(2)
Pd1-Te2^{i}-Pd2^{i}	93.47(2)	Pd2-Te1^{i}-Pd1^{i}	93.40(2)
O1^{i}-Pd1^{i}-O3^{i}	87.7(2)	O2^{i}-Pd2^{i}-O4^{i}	88.3(2)
O1^{i}-Pd1^{i}-Te2	96.00(15)	O2^{i}-Pd2^{i}-Te1	96.20(16)
O1^{i}-Pd1^{i}-Te1^{i}	176.59(15)	O2^{i}-Pd2^{i}-Te2^{i}	93.78(17)
O3^{i}-Pd1^{i}-Te2	175.54(17)	O4^{i}-Pd2^{i}-Te1	175.42(18)
O3^{i}-Pd1^{i}-Te1^{i}	94.85(19)	O4^{i}-Pd2^{i}-Te2^{i}	93.78(17)
Te2-Pd1^{i}-Te1^{i}	81.347(19)	Te1-Pd2^{i}-Te2^{i}	81.694(19)

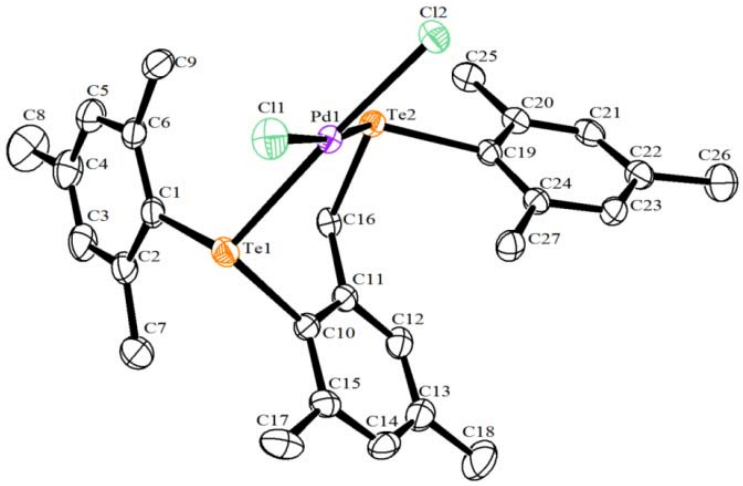

Figure 10. ORTEP diagram of *cis*-[$PdCl_2${$MesTeCH_2C_6H_2(4,6\text{-}Me_2)TeMes$}] (25% probability). Hydrogen atoms are omitted for clarity.

The complex *cis*-[$PdCl_2${$MesTeCH_2C_6H_2(Me_2\text{-}4,6)TeMes$}] (Figure 10) is a discrete monomer in which coordination around palladium is defined by two *cis* chlorides and a chelating telluro ether ligand. The Pd-Te and Pd-Cl distances are slightly shorter and longer, respectively than *trans*-[$PdCl_2(TeMes_2)_2$] owing to weak *trans* influencing chloride ligand *trans* to Te. The six-membered "PdTeCCCTe" ring is puckered. The Cl1 lies slightly (0.391Å) out of the Pd1 mean square plane.

The molecular structure of [$Pd_2(\mu\text{-}OAc)_2${$CH_2C_6H_2(4,6\text{-}Me_2)TeMes$}$_2$] (Figure 11) is unique and distinctly different from bis acetato-bridged binuclear palladium complexes, [$Pd_2(\mu\text{-}OAc)_2X_2Y_2$] reported thus far [102]. The molecule adopts a *sym-cis* configuration in which tellurium atoms are *trans* to anisobidentate acetate group. The Pd-Te distances are shorter than the one observed for mono- and bi-nuclear complexes described above and also from those found in [$Pd_3(o\text{-}tol)_2(\mu\text{-}OAc)_4${$Te(o\text{-}tol)_2$}$_2$] (Pd-Te = 2.5054(5)Å) [152]. The Pd...Pd separation is longer than those reported in acetate-bridged binuclear complexes but is significantly shorter

than the sum of the van der Waal radii (3.08 Å vs 3.26 Å, respectively) [102]. In [Pd_2(μ-OAc)$_2${$CH_2C_6H_2$(4,6-Me_2)TeMes}$_2$] two palladium atoms are held together by two different types of bridging acetate groups; one acting in an anisobidentate fashion while the other bridges through only one oxygen atom, so as to give a six-membered "Pd(μ-OAc)(μ-O)Pd" ring rather than an eight-membered boat shaped "Pd_2(μ-OAc)$_2$" ring usually observed. The second acetate group (O3-C39-C40-O4) is almost coplanar with Pd1 but almost perpendicular to Pd2 square planes. The distances between the O4 and Te1 and Te2 are 3.447 and 2.989 Å, respectively. The latter (O4-Te2) is significantly shorter than the sum of the van der Waal radii of oxygen and tellurium (3.58Å) indicating short secondary Te2...O4 interaction. Also the O4 is placed almost equidistant to neighbouring methyl groups in the unit cell (O4···H36C-C36 = 2.440 Å; O4···H16C-C16 = 2.663 Å; O4···H9B-C9 = 2.591 Å (adjacent molecule). Both Te1 and Te2 atoms are nearly coplanar with the bridging acetate group.

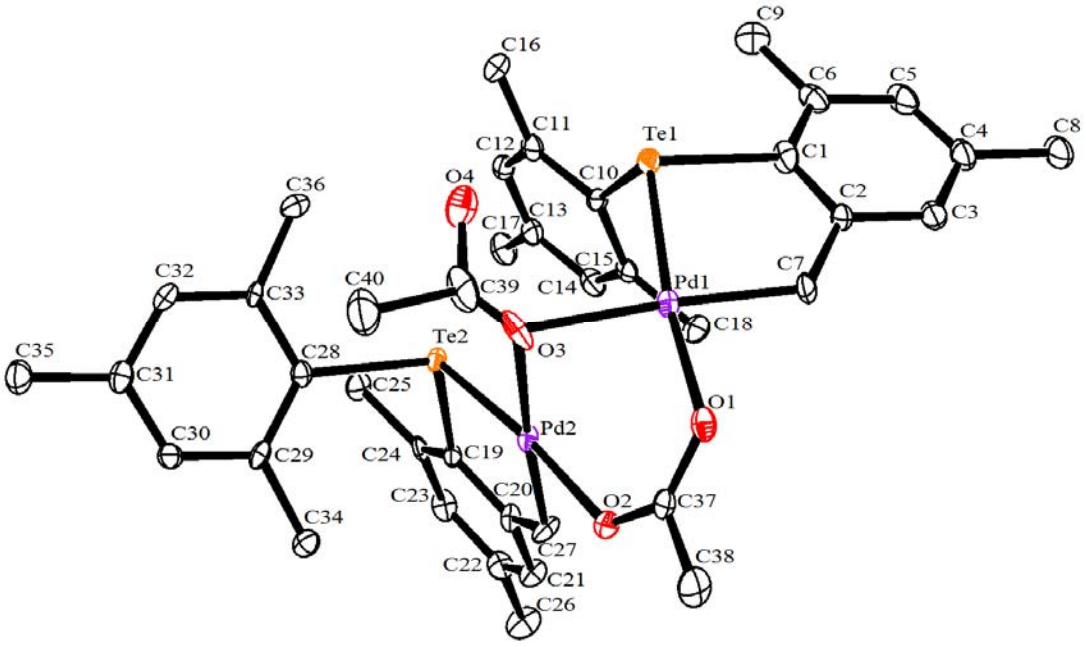

Figure 11. ORTEP diagram of [Pd_2(μ-OAc)$_2${$CH_2C_6H_2$(4,6-Me_2)TeMes}$_2$].toluene(25% probability). Hydrogen atoms and toluene molecule are omitted for clarity.

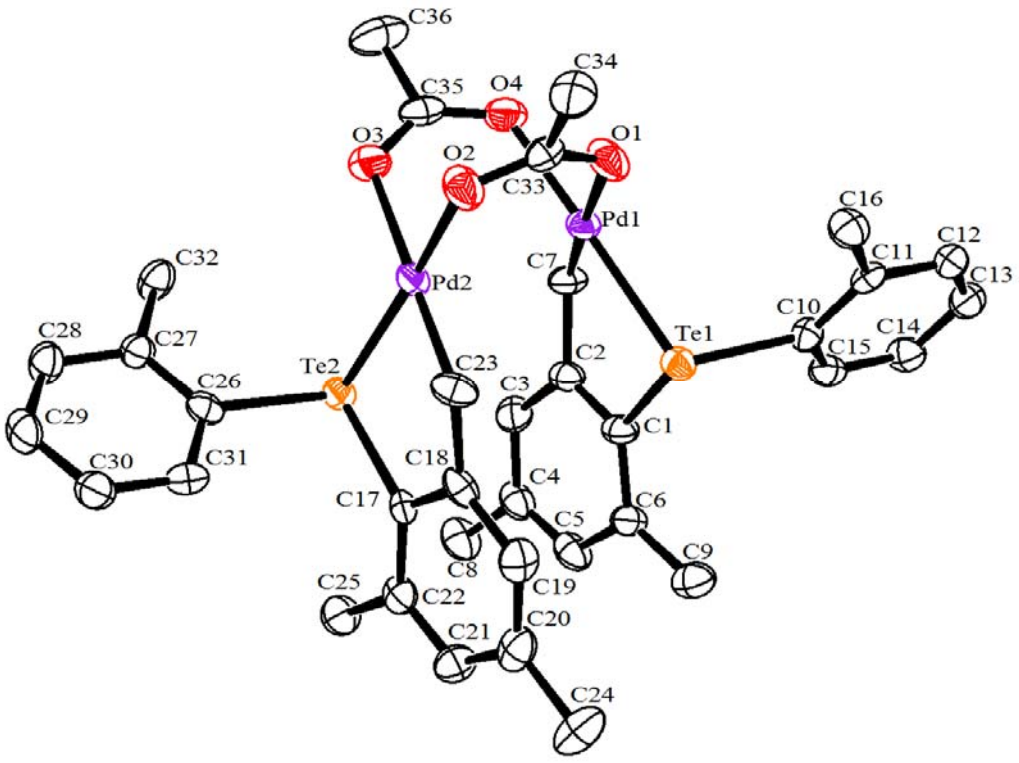

Figure 12. ORTEP diagram of $[Pd_2(\mu\text{-}OAc)_2\{CH_2C_6H_2(4,6\text{-}Me_2)Tetol\text{-}o\}_2]$ (25% probability). Hydrogen atoms are omitted for clarity.

In contrast to $[Pd_2(\mu\text{-}OAc)_2\{CH_2C_6H_2(4,6\text{-}Me_2)TeMes\}_2]$, the complex, $[Pd_2(\mu\text{-}OAc)_2\{CH_2C_6H_2(4,6\text{-}Me_2)Tetol\text{-}o\}_2]$ (Figure 12) adopts an usual acetate bridged structure with short Pd···Pd distance 2.8677(14)Å and boat shaped eight-membered "$Pd_2(\mu\text{-}OAc)_2$" ring. The two tellurium ligands are mutually *trans*. Methyl of tolyl rings and oxygen atoms show short contacts (C16-H16A···O1 = 2.749 Å and C32-H32A···O3 = 2.763 Å). The O2-Pd2 (2.097 Å) and O4-Pd1 (2.104 Å) (*trans* to the Te atom) distances are shorter than the O1-Pd1 (2.142 Å) and O3-Pd2 (2.164 Å) (*trans* to methylene groups).

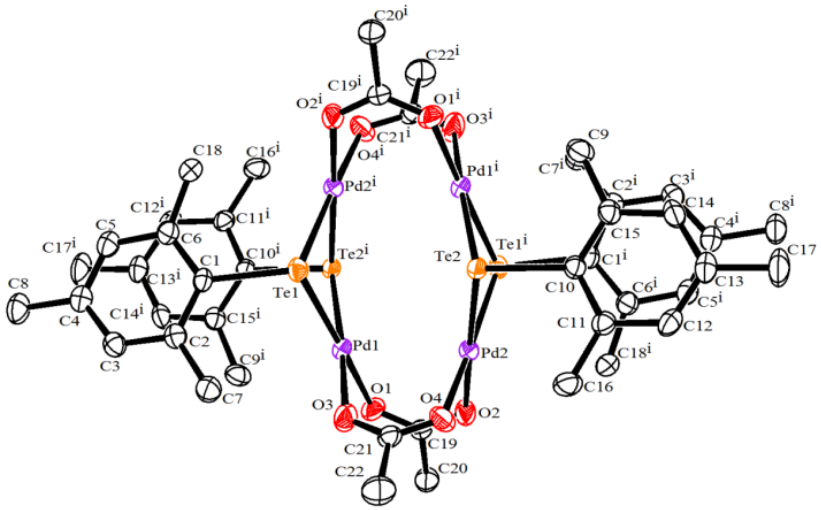

(a)

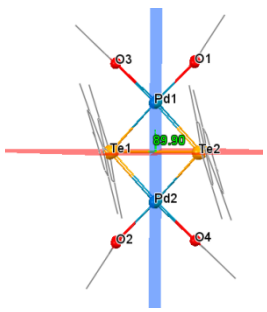

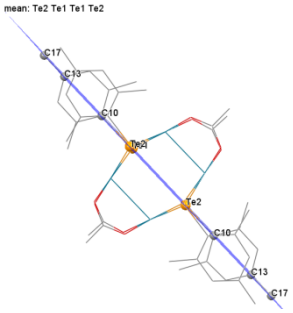

(b) (c)

Figure 13. (a) ORTEP diagram of $[Pd(\mu\text{-}OAc)(\mu\text{-}TeMes)]_4$ (25% probability). Hydrogen atoms are omitted for clarity (b and c) orientations of atomic planes within the molecule

The complex $[Pd(\mu\text{-}OAc)(\mu\text{-}TeMes)]_4$ (Figure 13) obtained as a minor product during the preparation of $[Pd_2(\mu\text{-}OAc)_2\{CH_2C_6H_2(4,6\text{-}Me_2)TeMes\}_2]$ via the Te-C bond cleavage is a tetramer and adopts a paddle-wheel geometry. Two pairs of orthogonal acetate groups and two pairs of mesityl tellurolate ligands hold two different pairs of palladium atoms. The molecule contains two almost rectangular planes formed by Pd1-Pd2-Pd1^i-Pd2^i (Pd2-Pd1-Pd2^i = 93.17°, Pd1-Pd2-Pd1^i = 86.83; Pd1-Pd2^i = 3.696 Å, Pd1-Pd2 = 2.947 Å) and Te1-Te2-Te1^i-Te2^i (Te2-

Te1-Te2^{i} = 89.42, Te1-Te2-Te1^{i} = 90.58, Te1-Te2 = 3.314 Å, Te1-Te2^{i} = 4.009 Å) which are nearly perpendicular (89.90°). The geometry around each palladium atom is defined by two oxygen atoms from two different acetate groups and two tellurolate ligands. The four palladium atoms form a rectangular plane with short Pd···Pd distances (bridged by two acetate groups) varying in the range 2.947 - 3.695Å, which lie well within the range reported in iso-structural chalcogenolate complexes, $[Pd(\mu\text{-}OAc)(\mu\text{-}EAr)]_n$ (EAr = SePh, Pd···Pd = 2.864(18)Å [171], EAr = *o*-tolSe, Pd···Pd = 2.8805(8)Å [152], EAr = SEt, Pd···Pd = 3.036, 3.194 Å [172]). The structures of palladium acetate complexes of composition $[Pd(\mu\text{-}OAc)(\mu\text{-}EAr)]_n$ are influenced by the nature of Ar groups and ranges from bi-nuclear to tetra-nuclear. For example, $[Pd(OAc)(ECH_2CH_2CH_2NMe_2)]_2.H_2O$ (E = S or Se) [157] and $[Pd(OAc)(SCH_2CH_2NMe_2)]_3.3H_2O$ [173] are di- and tri-meric, respectively with terminal monodentate acetate groups and chelating bridging chalcogenlate ligands. In contrast complexes with chacogenolate ligands without internal functionalized organic group yield tetrameric derivatives.

3.3 Chemistry of platinum complexes wih telluroethers

Although a myraid of organic compounds containg N, P, As, S donor atoms undergo cyclometalation, the mechanism for such is not clearly known. It is generally belived that initially, a ligand is coordinated to the metal center and in this intermediate species, the C-H bond is activated only when it is within the metal coordination plane. Though such intermediates are seldom isolated, their existence can be inferred. In the previous section metalation of telluroether ligands has been demonstrated. In general cyclometalation with palladium is quite facile whereas similar reactions with metals like platinum are often sluggish. Thus the recation of platinum precursors with tellurium ligands may provide an opportunity to get insight about the nature of possible intermediates involved in cyclometalation reactions and would also allow to assess the generality of cyclometalation of telluroethers.

Synthesis and spectroscopy

The reactions of K_2PtCl_4 with telluroethers afforded $[PtCl_2\{TeArAr'\}_2]$ (Ar = Ar′ = Ph; *o*-tol; Mes; Ar ≠ Ar′ =Ph, Mes and *o*-tol, Mes) (Scheme 18). The complex, *trans*-$[PtCl_2(TeMes_2)_2]$ on refluxing in THF converted into a mononuclear cycloplatinated complex, $[PtCl\{(CH_2C_6H_2Me_2\text{-}4,6)TeMes\}(TeMes_2)]$ in which one of the telluroether ligand is cyclometalated (Scheme 18) while the complexes *cis*-$[PtCl_2(TePh_2)\}_2]$, *trans*-$[PtCl_2\{(Te(tol\text{-}o)_2\}_2]$, *trans*-$[PtCl_2(PhTeMes)_2]$ and *trans*-$[PtCl_2(o\text{-}tolTeMes)_2]$ did not show any change under similar condition. The complex $[PtCl\{(CH_2C_6H_2Me_2\text{-}4,6)TeMes\}(TeMes_2)]$ showed dynamic equilibrium with the dimeric complex $[Pt_2(\mu\text{-}Cl)_2\{(CH_2C_6H_2Me_2\text{-}4,6)TeMes\}_2]$ formed by dissociation of the coordinated telluroether ligand from complex $[PtCl\{(CH_2C_6H_2Me_2\text{-}4,6)TeMes\}(TeMes_2)]$. Such dynamic equilibrium was arrested by substituting the coordinated

telluroether in [PtCl{($CH_2C_6H_2Me_2$-4,6)TeMes}($TeMes_2$)] by $PPh_3$to give [PtCl{($CH_2C_6H_2Me_2$-4,6)TeMes}(PPh_3)]. The complex, *trans*-[$PtCl_2(TeMes_2)_2$]**,** however, remained unchanged in refluxing toluene-methanol mixture in contrast to analogous palladium derivative which cyclometalate under these conditions (**Section 3.2**). Surprisingly, metalation of the mesityl methyl group in *trans*-[$PtCl_2$(o-tolTeMes)$_2$] does not take place even in refluxing toluene-methanol mixture. Such contrasting behaviour of *trans*-[$PtCl_2(TeMes_2)_2$], *trans*-[$PtCl_2$(PhTeMes)$_2$] and *trans*-[$PtCl_2$(o-tolTeMes)$_2$] is evident from the non-bonding Pt---H interactions known as the anagostic interactions [97, 174]) **(see later)**.

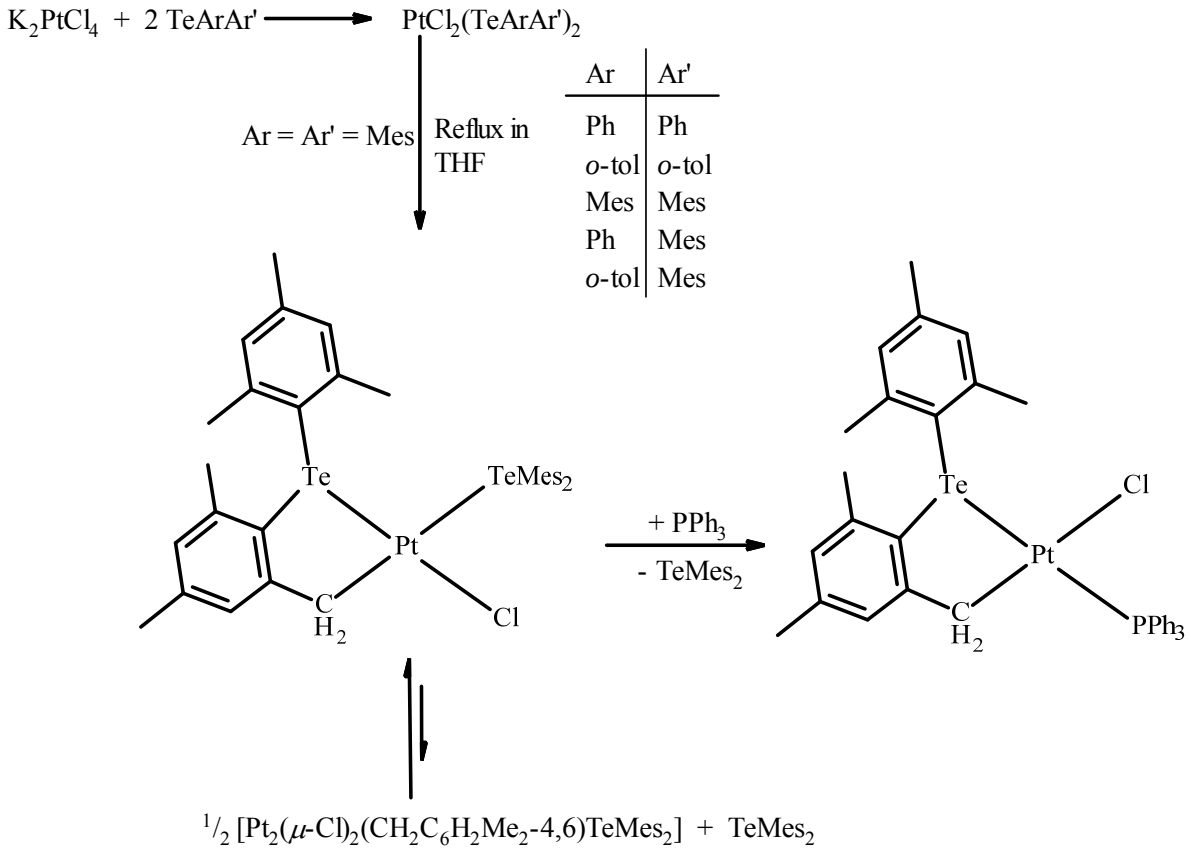

Scheme 18. Synthetic routes for platinum telluroether complexes

Monodentate telluroether complexes, $[PtCl_2(TeArAr')_2]$ (Ar = Ar′ = Me, Et, ^nPr, CH_2CH_2Ph, CH_2SiMe_3, Ph) are known to be formed as *cis* isomer which in solution exists as a mixture of *cis* and *trans* isomers [175-180]. The relative ratio of *cis* and *trans* isomers in solution depends on the nature of the organic groups attached to tellurium and the solvent.^{1}H NMR spectra of all the complex showed expected sinlge set of resonances whereas $^{125}Te\{^1H\}$ and $^{195}Pt\{^1H\}$ NMR spectra of *cis*-$[PtCl_2(TePh_2)\}_2]$ and *trans*-$[PtCl_2\{(Te(tol\text{-}o)_2\}_2]$ in $CDCl_3$ of exhibits two sets of resonances attributable to *cis* and *trans* isomeric forms, the *cis* being the predominant (Table 25). Such behaviour in solution is in accordance with the earlier observations [175].

The $^{125}Te\{^1H\}$ and $^{195}Pt\{^1H\}$ NMR spectra of *trans*-$[PtCl_2(TeMes_2)_2]$ displayed single resonances. The magnitude of $^1J(^{195}Pt\text{-}^{125}Te)$ is in accordance with the *trans* form [175, 176, 180]. The spectra of *trans*-$[PtCl_2(PhTeMes)_2]$ and *trans*-$[PtCl_2(o\text{-}tolTeMes)_2]$ (Figures 14 and 15), however, exhibited two closely spaced resonances. This is due to the fact that tellurium with stereo-chemically active lone pair of electrons is chiral and therefore four enantiomers (*viz.* RR / SS and RS / SR) are expected for each (*cis* and *trans*) isomeric forms. The observed magnitude of $^1J(^{195}Pt\text{-}^{125}Te)$ coupling constants for two resonances are in conformity with the *trans* form [175, 176] and are assigned to the expected enantiomers.

Table 25. ^{1}H, $^{125}Te\{^{1}H\}$ and $^{195}Pt\{^{1}H\}$ NMR data of platinu telluroether complexes in $CDCl_3$.

Complex	^{1}H NMR δ in ppm	$^{125}Te\{^{1}H\}$ NMR δ in ppm	$^{195}Pt\{^{1}H\}$ NMR δ in ppm
cis-$[PtCl_2(TePh_2)\}_2]$	7.22-7.27 (m), 7.35-7.40 (m), 7.61-7.64 (m) [Ph]	717 (major, $^{1}J(^{195}Pt\text{-}^{125}Te)$ = 1329 Hz) and 728 (minor) ppm.	-3650 (major), -3653 (minor)
trans-$[PtCl_2\{(Te(tol\text{-}o)_2\}_2]$	2.25, 2.56 (each s); 7.08-7.15 (m), 7.24-7.36 (m); 7.79 (dd, 1.2, 7.5Hz); 7.88 (d,d, 1.2, 7.5 Hz)	622 ($^{1}J(^{195}Pt\text{-}^{125}Te)$ = 793 Hz);	-3717, -4324
trans-$[PtCl_2(TeMes_2)_2]$	2.24 (s, 4-Me); 2.61 (s, 2,6-Me); 6.85 (s, 3,5-CH).	467 ($^{1}J(^{195}Pt\text{-}^{125}Te)$ = 379 Hz)	-3449 ($^{1}J(^{195}Pt\text{-}^{125}Te)$ = 359 Hz)
trans-$[PtCl_2(PhTeMes)_2]$	2.29 (s, 4-Me), 2.68 (s, 2,6-Me); 6.96 (s, 3,5-CH); 7.30 (br, m); 7.59 (br) (Ph).	575 ($^{1}J(^{195}Pt\text{-}^{125}Te)$ = 366 Hz), 576 (^{1}J(Pt-Te) = 369 Hz)	-3555, -3557
trans-$[PtCl_2(o\text{-}tolTeMes)_2]$	2.29, 2.30 (each s, 4-Me of Mes), 2.45, 2.48 (each s, 2-Me of tol); 2.72, 2.74 (each s, 2,6-Me of Mes); 6.95, 6.97 (each s, 3,5-CH of Mes); 7.02-7.22 (m, tol); 7.51, 7.64 (each d, 7.8 Hz, tol)	541; 543 ($^{1}J(^{195}Pt\text{-}^{125}Te)$ = 515 Hz)	-3611, -3615
$[PtCl\{(CH_2C_6H_2Me_2\text{-}4,6)TeMes\}(TeMes_2)]$	2.02, 2.19, 2.24, 2.27, 2.34, 2.53 (each s for Me); 4.0 (J_{AX} = 16.8, $\Delta\nu_{AX}$=105.8 Hz; metalated CH_2); 6.66 (s, 4,6-CH of Mes of metalated); 6.71 (s, 4,6-CH, Mes_2Te); 6.86, 7.04 (CH of metalated ring)	336 ($^{1}J(^{195}Pt\text{-}^{125}Te)$ = 612 Hz); 592 ($^{1}J(^{195}Pt\text{-}^{125}Te)$ = 1528 Hz); for the dimer: 424 ($^{1}J(^{195}Pt\text{-}^{125}Te)$ = 788 Hz) and 600 ($^{1}J(^{195}Pt\text{-}^{125}Te)$ = 1192 Hz); 260(s, $TeMes_2$)	-4286 (minor); -4450 (major).
$[PtCl\{(CH_2C_6H_2Me_2\text{-}4,6)TeMes\}(PPh_3)]$	2.12, 2.26, 2.28 (each s, 1 Me), 2.58 (s, 2Me);2.89 (br, CH_2),6.47, 6.68 (each s; 1CH); 6.87 (s, 2CH); 7.44 (m, 7.74-7.81 (m) (Ph).	555 ($^{1}J(^{195}Pt\text{-}^{125}Te)$ = 677 Hz; $^{2}J(^{125}Te\text{-}^{31}P)$ = 455 Hz)	

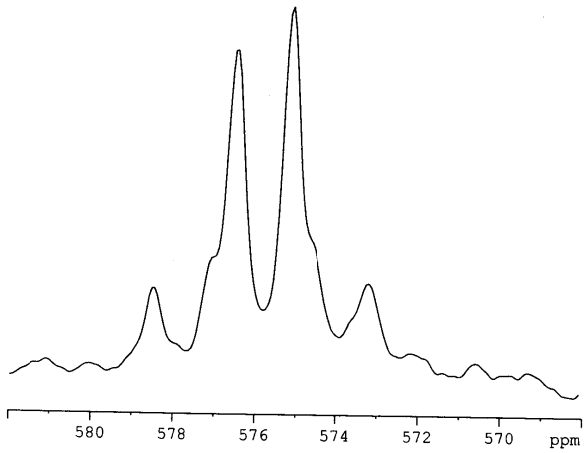

Figure 14. $^{125}Te\{^{1}H\}$ NMR spectrum of *trans*-$[PtCl_2\{Te(Ph)Mes\}_2]$ in $CDCl_3$

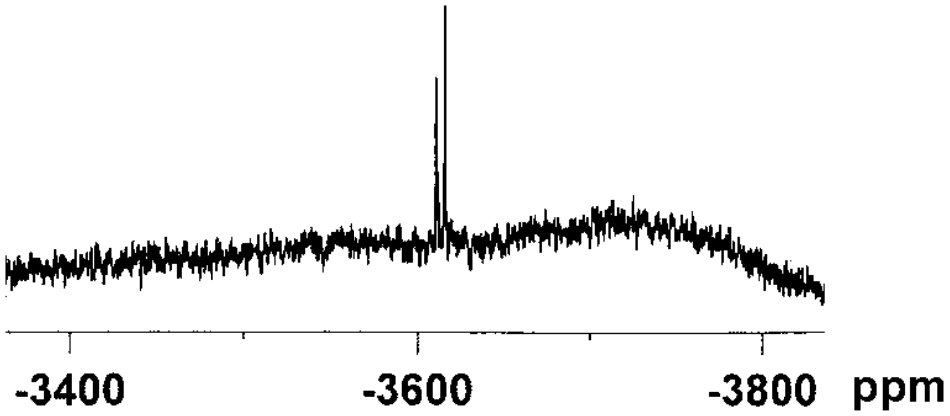

Figure 15. $^{195}Pt\{^{1}H\}$ NMR spectrum of *trans*-$[PtCl_2\{Te(o\text{-tol})Mes\}_2]$ in $CDCl_3$

The $^{125}Te\{^{1}H\}$ NMR spectrum (Figure 16) of $[PtCl\{(CH_2C_6H_2Me_2\text{-}4,6)TeMes\}(TeMes_2)]$ displayed five signals including one for free telluroether ligand ($TeMes_2$ at δ 260 ppm). The other four resonances were flanked with platinum satellites. The

$^{195}Pt\{^{1}H\}$NMR spectrum exhibited two signals at δ: -4286 (major) and δ: -4450 (minor) ppm. The observed spectral pattern is indicative of existence of two species in solution, viz. [PtCl{($CH_2C_6H_2Me_2$-4,6)TeMes}($TeMes_2$)] and a dimeric complex [Pt_2(μ-Cl)$_2${($CH_2C_6H_2Me_2$-4,6)TeMes}$_2$] formed by dissociation of the coordinated telluroether ligand from [PtCl{($CH_2C_6H_2Me_2$-4,6)TeMes}($TeMes_2$)] (Scheme 18). Thus the $^{125}Te\{^{1}H\}$ NMR resonance at δ : 336 ppm with $^{1}J(^{195}Pt\text{-}^{125}Te)$ of 612 Hz is assigned to the coordinated $TeMes_2$ while the resonance at δ 592 ppm with $^{1}J(^{195}Pt\text{-}^{125}Te)$ of 1528 Hz is attributed to metalated tellurium ligand of [PtCl{($CH_2C_6H_2Me_2$-4,6)TeMes}($TeMes_2$)]. The remaining ^{125}Te NMR signals at 600 ppm with $^{1}J(^{195}Pt\text{-}^{125}Te)$ of 1192 Hz and 424 with $^{1}J(^{195}Pt\text{-}^{125}Te)$ of 788 Hz could be due to *cis* and *trans* isomers of [Pt_2(μ-Cl)$_2${($CH_2C_6H_2Me_2$-4,6)TeMes}$_2$]. Dissociation of $TeMes_2$ from [PtCl{($CH_2C_6H_2Me_2$-4,6)TeMes}($TeMes_2$)] could be due to weakening of Pt-Te linkage owing to the presence of strong *trans* influencing metalated carbon atom *trans* to it.

The complex [PtCl{($CH_2C_6H_2Me_2$-4,6)TeMes}(PPh_3)] displayed a single $^{31}P\{^{1}H\}$ resonance with associated platinum satellites ($^{1}J(^{195}Pt\text{-}^{31}P)$ = 3945 Hz). The ^{125}Te NMR spectrum exhibited a doublet at δ 555ppm due to coupling with phosphorus nucleus ($^{2}J(^{125}Te\text{-}^{31}P)$ = 455 Hz) (Figure 17). The doublet was flanked by platinum satellites with $^{1}J(^{195}Pt\text{-}^{125}Te)$ = 677 Hz. The observed magnitude of coupling constants is indicative of a configuration with the neutral ligands (P and Te) *trans* to each other which is further confirmed by X-ray structural analysis (see later). It is worth noting that in [PtCl{($CH_2C_6H_2Me_2$-4,6)TeMes}($TeMes_2$)] the neutral ligands (two Te donor atoms) are *cis* disposed.

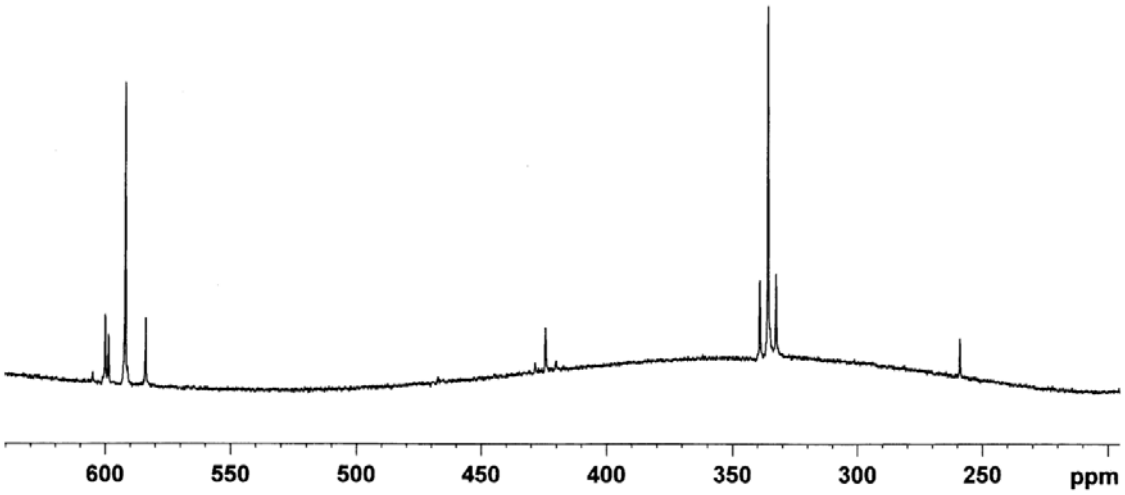

Figure 16. $^{125}Te\{^{1}H\}$ NMR spectrum of$[PtCl\{(CH_2C_6H_2Me_2\text{-}4,6)TeMes\}(TeMes_2)]$ in $CDCl_3$

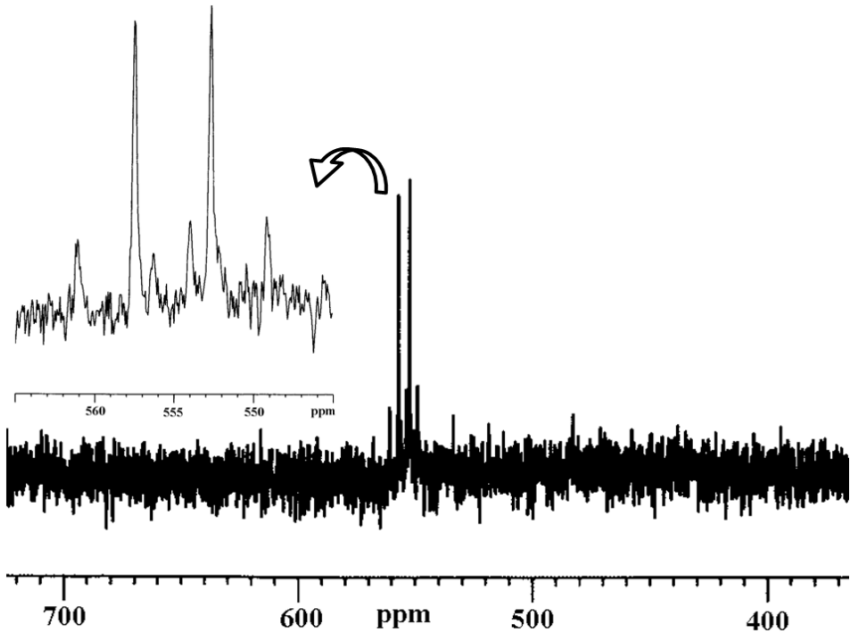

Figure 17. $^{125}Te\{^{1}H\}$ NMR spectrum of $[PtCl\{(CH_2C_6H_2Me_2\text{-}4,6)TeMes\}(PPh_3)]$ in $CDCl_3$

X-ray Crystallography

The molecular structures of *trans*-[$PtCl_2(TeMes_2)_2$], *trans*-[$PtCl_2${Te(Ph)Mes}$_2$],*trans*-[$PtCl_2${Te(*o*-tol)Mes}$_2$], [PtCl{($CH_2C_6H_2Me_2$-4,6)TeMes}($TeMes_2$)] and [PtCl{($CH_2C_6H_2Me_2$-4,6)TeMes}(PPh_3)] were established by single crystal X-ray diffraction analyses and the ORTEP diagrams with the numbering schemes are shown in Figures 18-22. Selected inter-atomic parameters are summarized in Tables 26-29. The central metal atom in these complexes adopts a square planar configuration. The Te-C distances (2.107 (12) – 2.151 (14) Å) are as expected [181-183].

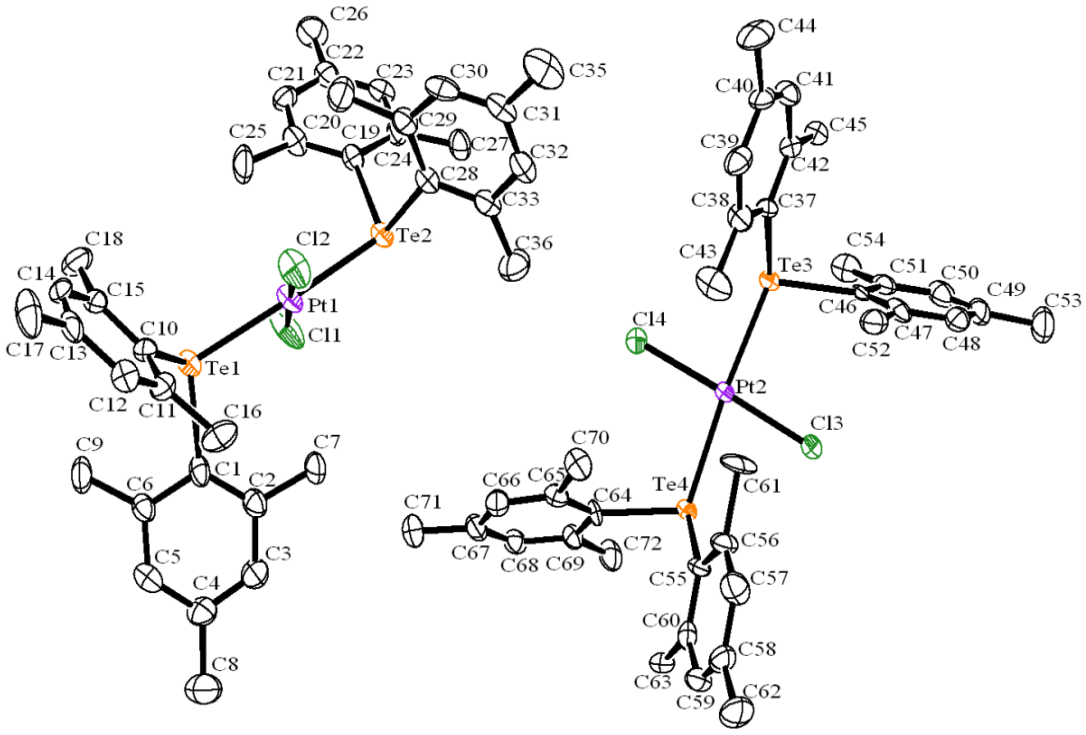

Figure 18. ORTEP drawing of *trans*-[$PtCl_2(TeMes_2)_2$] with atomic numbering (H atoms omitted for clarity)

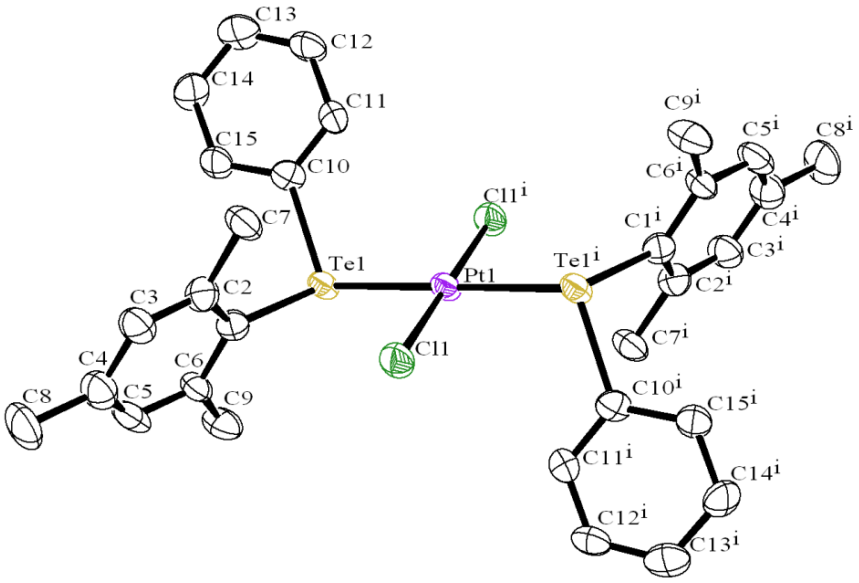

Figure 19. ORTEP drawing of *trans*-[$PtCl_2${Te(Ph)Mes}$_2$] with atomic numbering scheme (H atoms omitted for clarity)

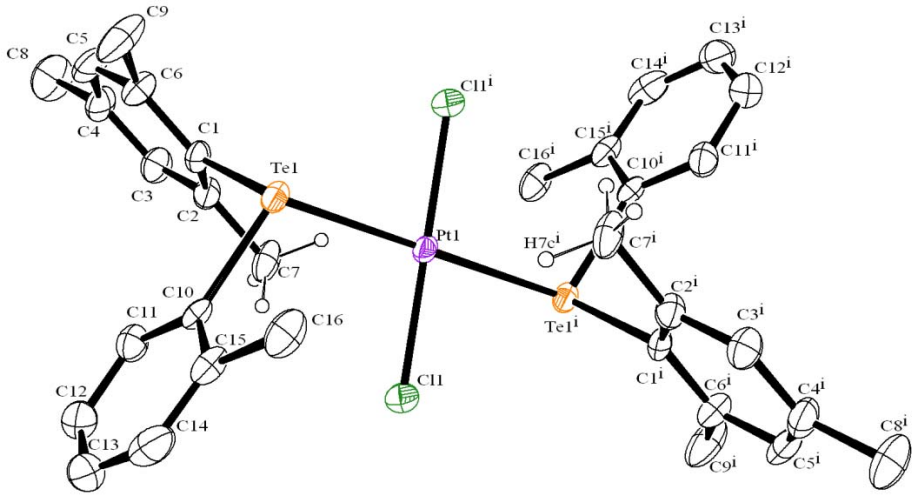

Figure 20. ORTEP drawing of *trans*-[$PtCl_2${Te(*o*-tol)Mes}$_2$] with atomic numbering scheme(H atoms omitted for clarity)

Table 26. Selected inter-atomic parameters (Å, °) for*trans*-[$PtCl_2(TeMes_2)_2$]

Pt1-Te1	2.5717(13)	Pt2-Te3	2.5786(11)
Pt1-Te2	2.5589(12)	Pt2-Te4	2.5763(11)
Pt1-Cl1	2.320(5)	Pt2-Cl3	2.289(5)
Pt1-Cl2	2.275(5)	Pt2-Cl4	2.301(5)
Te1-C1	2.14(2)	Te3-C37	2.161(16)
Te1-C10	2.143(18)	Te3-C46	2.115(13)
Te2-C19	2.150(18)	Te4-C55	2.168(19)
Te2-C28	2.110(17)	Te4-C64	2.121(13)
Cl1-Pt1-Cl2	179.1(3)	Cl3-Pt2-Cl4	174.1(2)
Cl1-Pt1-Te1	84.07(14)	Cl3-Pt2-Te3	94.66(12)
Cl1-Pt1-Te2	83.19(13)	Cl3-Pt2-Te4	80.63(12)
Cl2-Pt1-Te1	96.25(15)	Cl4-Pt2-Te3	85.99(12)
Cl2-Pt1-Te2	96.56(15)	Cl4-Pt2-Te4	97.62(13)
Te1-Pt1-Te2	166.41(5)	Te3-Pt2-Te4	168.39(5)
Pt1-Te1-C1	113.8(4)	Pt2-Te3-C37	115.7(5)
Pt1-Te1-C10	109.2(4)	Pt2-Te3-C46	107.4(4)
Pt1-Te2-C19	108.2(4)	Pt2-Te4-C55	113.6(4)
Pt1-Te2-C28	113.8(5)	Pt2-Te4-C64	111.9(4)
C1-Te1-C10	99.8(7)	C37-Te3-C46	98.5(6)
C19-Te2-C28	101.6(7)	C55-Te3-C64	97.7(6)
Pt1-Te1-C1-C2	1.58	Pt2-Te3-C37-C38	-2.74
Pt1-Te1-C1-C6	-176.94	Pt2-Te3-C37-C42	-177.98
Pt1-Te1-C10-C11	-77.75	Pt2-Te3-C46-C47	-65.69
Pt1-Te1-C10-C15	102.23	Pt2-Te3-C46-C51	112.65
Pt1-Te2-C19-C20	6.33	Pt2-Te4-C55-C56	3.01
Pt1-Te2-C19-C24	-164.71	Pt2-Te4-C55-C60	-170.04
Pt1-Te2-C28-C29	-67.03	Pt2-Te4-C64-C65	-67.4
Pt1-Te2-C28-C33	113.81	Pt2-Te4-C64-C69	115.06

Table 27. Selected bond length (Å) and angles (°) of *trans*-[$PtCl_2${Te(Ph)Mes}$_2$] and *trans*-[$PtCl_2${Te(*o*-tol)Mes}$_2$]

	trans-[$PtCl_2${Te(Ph)Mes}$_2$]	*trans*-[$PtCl_2${Te(*o*-tol)Mes}$_2$]
Pt1-Te1	2.5785(13)	2.5771(7)
Pt1-Cl1	2.287(6)	2.309(3)
Te1-C1	2.10(2)	2.131(12)
Te1-C10	2.11(2)	2.107(12)
Te1-Pt1-Te1^i	180	180
Te1-Pt1-Cl1	93.75(16)	95.81(8)
Cl1-Pt1-Te1^i	86.25(16)	84.19(8)
(Cl1-Pt1-Te1)		
Cl1-Pt1-Cl1^i	180	180
Pt1-Te1-C1	110.4(6)	109.4(4)
Pt1-Te1-C10	106.3(6)	108.2(3)
C1-Te1-C10	95.9(9)	96.7(5)
Pt1-Te1-C1-C2	-58.31	31.47
Pt1-Te1-C1-C6	121.65	-147.69
Pt1-Te1-C10-C11	-19.50	-101.12
Pt1-Te1-C10-C15	-163.58	79.54

There are two different types of molecules in the crystal lattice of *trans*-[$PtCl_2(TeMes_2)_2$] which differ slightly in the relative orientation of the mesityl rings in the two molecules. Interestingly different polymorphic forms for the corresponding palladium complex, [$PdCl_2(TeMes_2)_2$] have been isolated and structurally characterized (**section 3.2**). The dichloro complexes, *trans*-[$PtCl_2${Te(Ph)Mes}$_2$] and *trans*-[$PtCl_2${Te(*o*-tol)Mes}$_2$] are iso-structural and adopt a *trans* configuration defined by two neutral telluroether ligands and two chloro ligands. The Pt-Te and Pt-Cl distances in all these complexes are in accordance with the *trans* configured telluroether complexes, such as *trans*-[$PtCl_2${Te(CH_2CH_2)$_2$O}$_2$] (Pt-Te = 2.5945 (3)Å), [181, 182] *trans*-[$PtCl_2${Te(CH_2SiMe_3)$_2$}$_2$] (Pt-Te = 2.5807 (6) Å; Pt-

Cl= 2.309 (2) Å [176] and [PtCl{(TeC_6H_4OEt-4)CH_2CH_2}$_2$NH)]Cl (Pt-Te_{av}= 2.56 Å; Pt-Cl = 2.306 (4) Å) [184]. However in *cis* configured complexes the Pt-Te bond is shortened as a consequence the Pt-Cl bond is elongated (*e.g.cis*-[$PtCl_2${(Bu^nTeCH_2)$_2SiMe_2$}]; Pt-Te_{av} = 2.50Å, Pt-Cl_{av} = 2.34 Å [185]. Lengthening of Pt-Te distance in the *trans* complexes is in accordance with the stronger *trans* influence of tellurium than that of chloride. One of the Te-C bonds is marginally shorter than the other Te-C bond in the coordinated telluroether. The mesityl rings of telluroether ligands in *trans*-[$PtCl_2${Te(Ph)Mes}$_2$] and *trans*-[$PtCl_2${Te(*o*-tol)Mes}$_2$] lie opposite each other with respect to the metal square plane.

The interesting feature in the structure of *trans*-[$PtCl_2(TeMes_2)_2$] is the Pt…H-C interactions which are significantly longer in the case of *trans*-[$PtCl_2${Te(Ph)Mes}$_2$] and *trans*-[$PtCl_2${Te(*o*-tol)Mes}$_2$]. These interactions can be characterized as anagostic interactions which have M···H distances of ~2.3 - 2.9Å and M-H-C angles of ~110-170° [97] and have implication in C-H bond activation. In general, based on the M···H distance and the M···H-C angle three different types of M···H-C interaction are encountered, viz. i) agostic, ii) anagostic and iii) hydrogen bonding. The former is usually encountered in the case of d^6 metal complexes while the anagostic interactions are noted with d^8 square planar complexes.

The platinum atom in [PtCl{($CH_2C_6H_2Me_2$-4,6)TeMes}($TeMes_2$)] adopts a distorted square planar configuration and is defined by "Te_2CCl" donor set with the neutral telluroether ($TeMes_2$) ligand *trans* to the Pt-Carbon bond. The Pt-Te distance of metalated telluroether ligand is shorter than the neutral $TeMes_2$ due to the strong *trans* influence of the cyclometalated carbon and weak *trans* influence of the chloride. The Pt-C distance (2.084(12) Å) is well in agreement with the values reported for metalated platinum complexes [102]. The C-Te-C angle (~101°) on coordination is little influenced from its value for the free ligand, $TeMes_2$ (101.0(1)°) [144]. The mesityl ring on Te is nearly perpendicular to this ring.

The metalated mesityl ring plane lies at an angle of 14.06° with the metal square plane rendering the metalated five-membered "PtTeCCC" ring in puckered conformation.

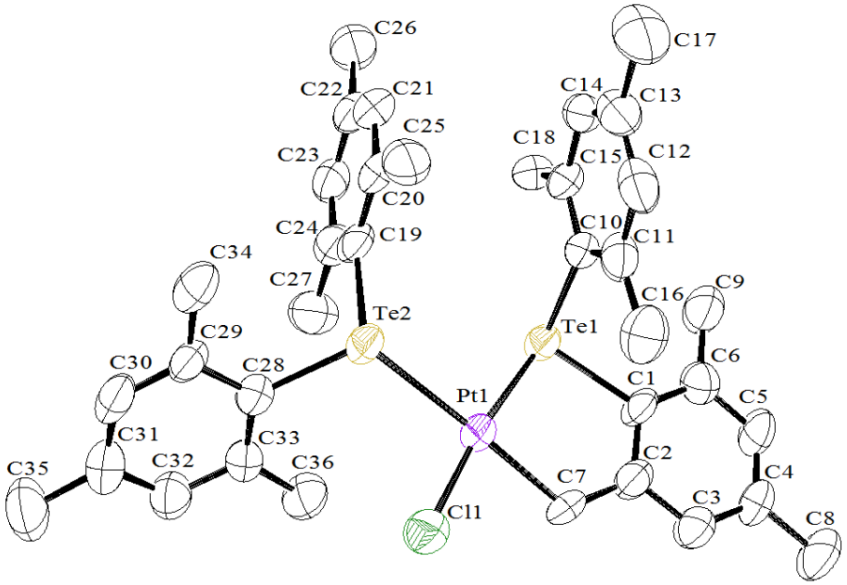

Figure 21. ORTEP drawing of [PtCl{($CH_2C_6H_2Me_2$-4,6)TeMes}($TeMes_2$)] with atomic numbering scheme (H atoms omitted for clarity)

Table 28. Selected bond length (Å) and angles (°) for [PtCl{($CH_2C_6H_2Me_2$-4,6)TeMes}($TeMes_2$)]

Pt1-Te1	2.4870(11)	Te1-C1	2.121(12)
Pt1-Te2	2.6138(10)	Te1-C10	2.141(13)
Pt1-Cl1	2.342(4)	Te2-C19	2.151(14)
Pt1-C7	2.084(12)	Te2-C28	2.112(14)
C7-Pt1-Cl1	87.3(4)	C1-Te1-C10	100.8(5)
C7-Pt1-Te1	86.7(4)	C1-Te1-Pt1	93.4(4)
Cl1-Pt1-Te1	173.59(10)	C10-Te1-Pt1	105.9(4)
C7-Pt1-Te2	172.4(4)	C28-Te2-C19	100.9(5)
Cl1-Pt1-Te2	86.46(9)	C28-Te2-Pt1	112.7(4)
Te1-Pt1-Te2	99.34(3)	C19-Te2-Pt1	113.7(3)

The R-factor of [PtCl{($CH_2C_6H_2Me_2$-4,6)TeMes}(PPh_3)] is large due to presence of disordered aromatic rings, but the overall chemical structure supports the conclusions drawn from NMR data. The crystal lattice of [PtCl{($CH_2C_6H_2Me_2$-4,6)TeMes}(PPh_3)] shows two independent molecules which differ slightly in their interatomic parameters. The platinum(II) center in each molecule adopts a distorted square planar geometry with a "TeCPCl" coordination core [186]. The neutral ligands (Te and P) are mutually *trans* with P-Pt-Te angle of 175.50(11) and 177.37(12) °. The five-membered cyclometalated ring is almost planar.

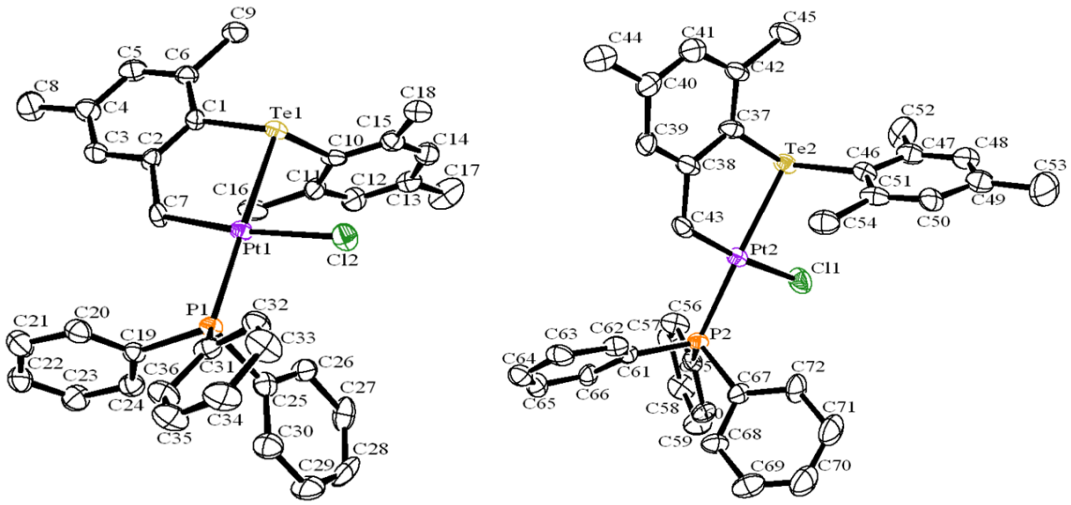

(a) **(b)**

Figure 22. ORTEP drawing of [PtCl{($CH_2C_6H_2Me_2$-4,6)TeMes}(PPh_3)] with atomic numbering scheme (H atoms omitted for clarity)

Table 29. Selected bond length (Å) and angles (°) for[PtCl{($CH_2C_6H_2Me_2$-4,6)TeMes}(PPh_3)]

molecule a		**molecule b**	
Pt1-P1	2.268(4)	Pt2-P2	2.273(4)
Pt1-Cl2	2.412(5)	Pt2-Cl1	2.410(5)
Pt1-Te1	2.5504(11)	Pt2-Te2	2.5410(12)
Pt1-C7	2.029(14)	Pt2-C43	2.09(2)
Te1-C1	2.080(17)	Te2-C37	2.15(2)
Te1-C10	2.161(17)	Te2-C46	2.13(2)
P1-Pt1-Cl2	94.49(15)	P2-Pt2-Cl1	91.07(17)
P1-Pt1-Te1	175.50(11)	P2-Pt2-Te2	177.37(12)
P1-Pt1-C7	91.8(4)	P2-Pt2-C43	94.8(5)
Cl2-Pt1-Te1	86.25(11)	Cl1-Pt2-Te2	86.35(13)
Cl2-Pt1-C7	173.4(5)	Cl1-Pt2-C43	174.0(5)
Te1-Pt1-C7	87.6(4)	Te2-Pt2-C43	87.8(4)
Pt1-C7-C2	119.2(10)	Pt2-C43-C38	119.1(12)
Pt1-Te1-C1	92.5(5)	Pt2-Te2-C37	93.0(4)
Pt1-Te1-C10	104.2(4)	Pt2-Te2-C46	107.7(4)
C1-Te1-C10	102.2(7)	C37-Te2-C46	103.0(7)

A comparison of all the above structures (Table 30) shows increase in steric bulkiness of the groups on tellurium leads to gradually decrease of the torsion angles Pt1-Te-C1-C2 from *trans*-$PtCl_2(PhTeMes)_2$ to *trans*-$PtCl_2$(o-tolTeMes)$_2$ to *trans*-$PtCl_2(TeMes_2)_2$ leading to increase in proximity of the methyl group C7 with the metal centre. This may lead to favourable anagostic interactions resulting in cyclometalation of ligands with bulky groups

while others despite the presence of bulky mesityl group show reluctance under similar conditions. Therefore, it is clear that the presence of anagostic interaction in *trans*-$PtCl_2(TeMes_2)_2$ facilitate C-H bond activation leading to cyclometalation, while the absence of such interaction, as in *trans*-$PtCl_2(PhTeMes)_2$ and *trans*-$PtCl_2$(o-tolTeMes)$_2$, does not result in cyclometalation. A similar situation has been reported for palladium complexes. The $[PdCl_2(TeMes_2)_2]$ cyclometalate in refluxing toluene-methanol solution while $[PdCl_2$(Te(*o*-tolMes)$_2$] and $[PdCl_2$(*o*-tol$_2$Te)$_2$] fail to metalate under similar conditions (**section 3.2**).

Table 30. Secondary C-H···M interactions with the metal centre(Å/°)

	trans-$PtCl_2(PhTeMes)_2$	*trans*-$PtCl_2$(*o*-tolTeMes)$_2$	*trans*-$PtCl_2(TeMes_2)_2$	
			molecule A	**molecule B**
C7-H7c…Pt1	3.114	2.850	2.794	2.689
∠C7-H7c-Pt1	157.06	119.37	122.89	134.74
Pt1-Te1-C1-C2	-58.31	31.47	1.58	-2.74
Pt1-Cl1	2.286	2.309	2.320	2.289
∠Cl1-Pt1-Cl2	180	180	179.06	174.08
Pt1-Te1	2.578	2.577	2.572	2.579
∠Te1-Pt1-Te2	180	180	166.41	168.39
Mean sq. plane-M			0.042	0.180

3.4 Reactivity of platinum organonitrile complexes with telluroethers

Recent developments in the coordination chemistry of tellurium ligands have defied the general belief that it would be similar to that of sulfur and selenium [187]. Of late several dissimilarities between tellurium coordination chemistry and sulfur / selenium have not only been recognized, but numerous unprecedented results have also been reported. Isolation of $[Pt(Te)(TeC_5H_4N)_2(PPh_3)]$, containing bare Te^0 as a ligand, from the reaction of $Pt(PPh_3)_4$ with py_2Te_2 is an example of unprecedented formation of such complexes[188]. The general preparative route of palladium / platinum complexes are either by the reaction between M'_2MCl_4 with a telluroether in water (eq. 2) [126, 180, 189] or by treatment of $[MCl_2(Ar'CN)_2]$ (Ar′ = Me or Ph) with a telluroether in an organic solvent (CH_2Cl_2 or THF) (eq. 3) [175, 176, 185]. Since the separation of the final products from the biphasic reaction medium was a bit tedious process, it was considered to employ reaction route involving $[PtCl_2(PhCN)_2]$ and telluroether in an organic solvent. While the reaction with simple telluroethers gave the desired products, as has been discussed in earlier section [section 3.2, 175, 176, 185], but with bulky telluroether (e.g., $TeMes_2$) formation of other intermediate complexes could be detected by ^{125}Te NMR spectroscopy. Thus in this section, a detailed study of the reaction of platinum benzonitrile complexes with telluroethers together with the isolation of various intermediates leading to cycloplatination is presented.

$$M'_2MCl_4 + 2\ TeAr_2 \xrightarrow{H_2O} [MCl_2(TeAr_2)_2] + 2\ M'Cl \qquad ...(2)$$

$$MCl_2\ (R'CN)_2 + 2\ TeAr_2 \xrightarrow{\text{organic solvent}} [MCl_2(TeAr_2)_2] + 2\ R'CN \qquad ...(3)$$

Synthesis and spectroscopy

Reactions of $[PtCl_2(PhCN)_2]$ with telluroethers TeArAr′ in 1:2 stoichiometry in dichloromethane over 48 hrs afforded the expected *cis/trans*-$[PtCl_2(TeArAr')_2]$ (Ar/Ar′ =

Ph/Ph, Ph/Mes, *o*-tol/tol-*o*, *o*-tol/Mes, Mes/Mes) in 60-83% yield as isolated from the reaction of K_2PtCl_4 with the telluroether in water-acetone mixture. With asymmetric telluroethers diastereomers were formed. As the steric demand of organic group on tellurium increases, the reactions tend to be slower. Thus in the case of $TeMes_2$, unreacted $[PtCl_2(PhCN)_2]$ was noted in solution by ^{195}Pt NMR spectroscopy even after 48 hrs of reaction.

Since the reactions involving bulky telluroethers were sluggish in dichloromethane, another commonly used solvent, viz. THF was used. Surprisingly the reactions were more complex giving several products formed by the initial attack of telluroether on the coordinated benzonitrile rather than the platinum center. To understand the reaction profile, reactions between $[PtCl_2(PhCN)_2]$ and telluroethers in 1:1 and 1:2 stoichiometry in THF were examined under different reaction conditions.

Reactions of $[PtCl_2(PhCN)_2]$ with TeArMes (Ar = mesityl, *o*-tolyl, phenyl) in 1:1 ratio in THF afforded different products depending on the steric demand of the Ar group (Scheme 19). When Ar is phenyl, expected mononuclear complex *trans*-$[PtCl_2\{Te(Ph)(Mes)\}_2]$ was formed exclusively. When the steric demand of the Ar group increases from phenyl to *o*-tolyl, two products, viz. *trans*-$[PtCl_2\{Te(o\text{-tol})(Mes)\}_2]$, as a minor fraction and *trans*-$[PtCl_2(PhCN)\{NC(O)Ph(Te(Mes)tol\text{-}o)\}]$ (see later for structure), formed by the attack of telluroether on one of the coordinated benzonitrile, as a major fraction, were isolated. On further increasing the steric demand of Ar group from *o*-tolyl to mesityl, again two products, *trans*-$[PtCl_2(TeMes_2)_2]$ as a minor fraction and a product formed by the attack of telluroether on both the coordinated benzonitrile, *trans*-$[PtCl_2\{NC(O)Ph(TeMes_2)\}_2]$ as a major fraction (see later for structure) were isolated. When this reaction was carried out in refluxing THF, different products were isolated depending on the duration of refluxing. The reaction mixture on refluxing for 30 minutes yielded a single

product, *trans*-[$PtCl_2${NC(Ph)C_4H_7O}{NC(O)Ph($TeMes_2$)}] (see later for structure) wherein one of the coordinated benzonitrile is activated by THF molecule (C-H *ortho* to oxygen) while the other coordinated benzonitrile is attacked by the telluroether. When refluxing prolonged for three hours, a mixture of products were formed which were separated using diethyl ether. The ether soluble component was characterized by NMR spectroscopy as cycloplatinated complex [$PtCl(TeMes_2)${Te(Mes)$CH_2C_6H_2Me_2$}] while the ether insoluble part contained [$PtCl_2(PhCN)_2$] and [$Pt_2Cl_2(\mu\text{-}Cl)_2(TeMes_2)_2$] as confirmed by ^{125}Te and ^{195}Pt NMR spectroscopy. The formation of [$PtCl(TeMes_2)${Te(Mes)$CH_2C_6H_2Me_2$}] from *trans*-[$PtCl_2(TeMes_2)_2$] in refluxing THF has also been observed in the previous section (**section 3.3**).

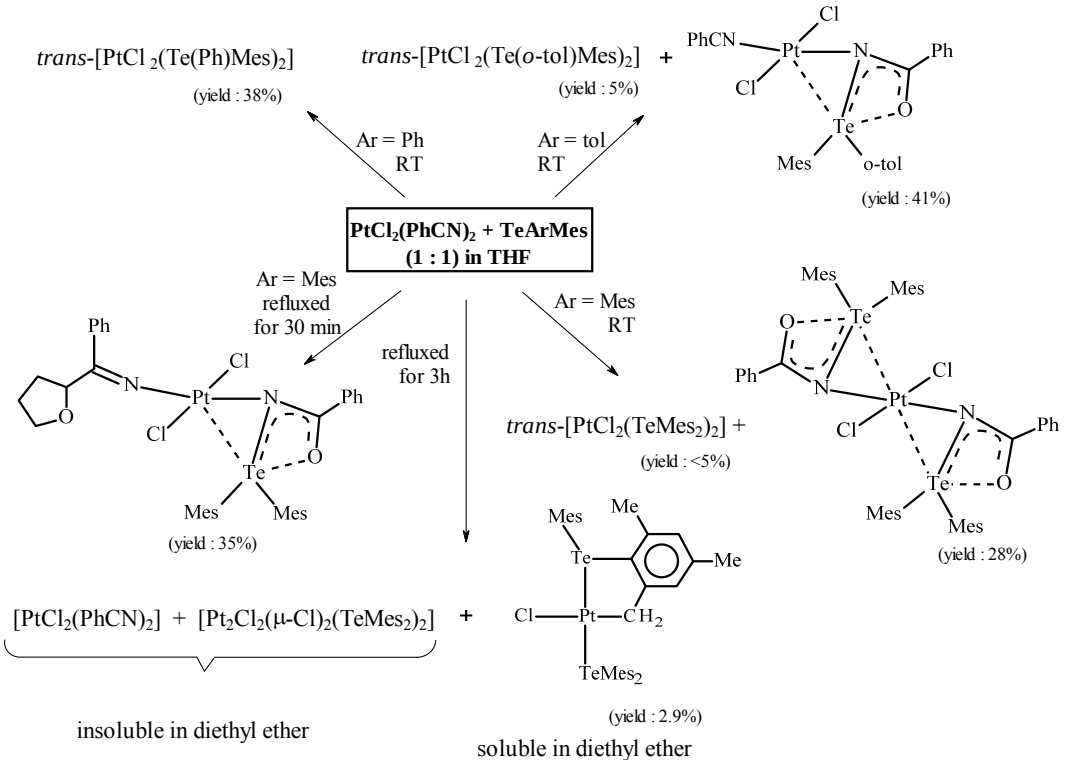

Scheme 19. Reactions between [$PtCl_2(PhCN)_2$] and Te(Ar)Mes in 1:1 stoichiometry in THF

The reaction of $[PtCl_2(PhCN)_2]$ with Te(Ar)Mes in 1:2 stoichiometry has also been carried out (Scheme 20). The reaction of $[PtCl_2(PhCN)_2]$ with TePhMes in 1:2 in THF at room temperature afforded expected complex, *trans*-$[PtCl_2(Te(Ph)Mes)_2]$. The reaction of Te(*o*-tol)Mes with $[PtCl_2(PhCN)_2]$ gave two products, viz. $[PtCl_2\{Te(o\text{-tol})Mes\}_2]$ as a minor fraction and a complex formed by the attack of telluroether on both the coordinated benzonitrile *trans*-$[PtCl_2\{NC(O)Ph\{Te(o\text{-tol})Mes\}\}_2]$ (see later for structure) as a major constituent. The complex, *trans*-$[PtCl_2\{NC(O)Ph\{Te(o\text{-tol})Mes\}\}_2]$ decomposes slowly in solution. Thus when *trans*-$[PtCl_2\{NC(O)Ph\{Te(o\text{-tol})Mes\}\}_2]$ was left for recrystallization in acetone at room temperature along with the crystals of *trans*-$[PtCl_2\{NC(O)Ph\{Te(o\text{-tol})Mes\}\}_2]$, $[PtCl_2\{Te(o\text{-tol})Mes\}_2]$ was also formed as precipitate together with the colorless crystals of $[PtCl(Tetol\text{-}o)\{NC(O)Ph\}_2]$. This indicates that in the reaction medium initially the complex, *trans*-$[PtCl_2(NC(O)Ph\{Te(tol\text{-}o)Mes\})_2]$ is formed, which is converted gradually into the more stable $[PtCl_2\{Te(o\text{-tol})Mes\}_2]$ via the cleavage of Pt-N bond with concomitant formation of stable Pt-Te linkage. All the three complexes ($[PtCl_2\{Te(o\text{-tol})Mes\}_2]$, *trans*-$[PtCl_2(NC(O)Ph\{Te(tol\text{-}o)Mes\})_2]$ and $[PtCl(Tetol\text{-}o)\{NC(O)Ph\}_2]$) were separated manually. Interestingly the reaction of $[PtCl_2(PhCN)_2]$ with $TeMes_2$ yielded different products depending on the duration of the reaction which was monitored by ^{125}Te NMR spectroscopy (Figure 23). Initially a complex generated by telluroether attack on coordinated benzonitrile, was formed in 24 hrs, although other products, viz. *trans*-$[PtCl_2(TeMes_2)_2]$ and *trans*-$[PtCl_2(TeMes_2)\{NC(O)Ph(TeMes_2)\}]$ also existed in solution (Figure 23). When this reaction continued for 72 hrs, in addition to *trans*-$[PtCl_2(TeMes_2)\{NC(O)Ph(TeMes_2)\}]$ and *trans*-$[PtCl_2(TeMes_2)_2]$, the concentration of *trans*-$[PtCl_2(TeMes_2)\{NC(O)Ph(TeMes_2)\}]$ increased significantly and could be isolated from solution (see later for structure). On prolonging the reaction for a week, bis-telluroether complex *trans*-$[PtCl_2(TeMes_2)_2]$ existed in more than 90% yield (Figure 23). Therefore, from

the above time dependent complexation history it is clear that initial reaction of telluroether takes place at the coordinated benzonitrile rather than at platinum center followed by stepwise rearrangement. All these intermediate complexes could be isolated and characterized with sterically demanding telluroether whereas with non-steriaclly hindered telluroethers such intermediates, might have formed, could not be detected and only the substitution products, *trans*-$[PtCl_2(TeArAr')_2]$ were isolated.

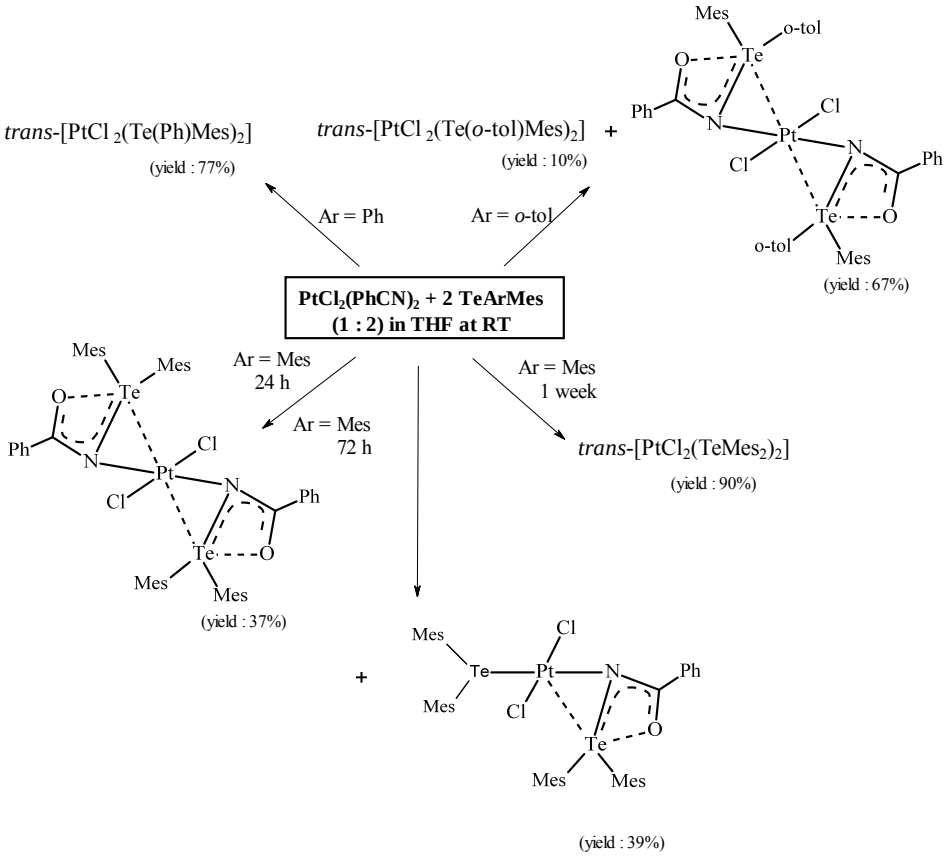

Scheme 20. Reactions between $[PtCl_2(PhCN)_2]$ and Te(Ar)Mes in 1:2 stoichiometry in THF at room temperature

The generality of the reaction was also examined by carring out the reactions with organonitriles differeing in the the nature of organic substituents. Thus the reactions between $[PtCl_2(RCN)_2]$ (R = Me, 4-MeC_6H_4, 4-$CF_3C_6H_4$) with two equivalents of $TeMes_2$ in THF at

room temperature were carried out and were monitored by ^{125}Te NMR spectroscopy. In every case, reaction proceeds in a manner similar to benzonitrile. In the ^{125}Te NMR spectra resonances due to *trans*-[$PtCl_2${NC(O)R($TeMes_2$)}$_2$] and *trans*-[$PtCl_2$($TeMes_2$){NC(O)R($TeMes_2$)}] (Figures 24-26) were observed.

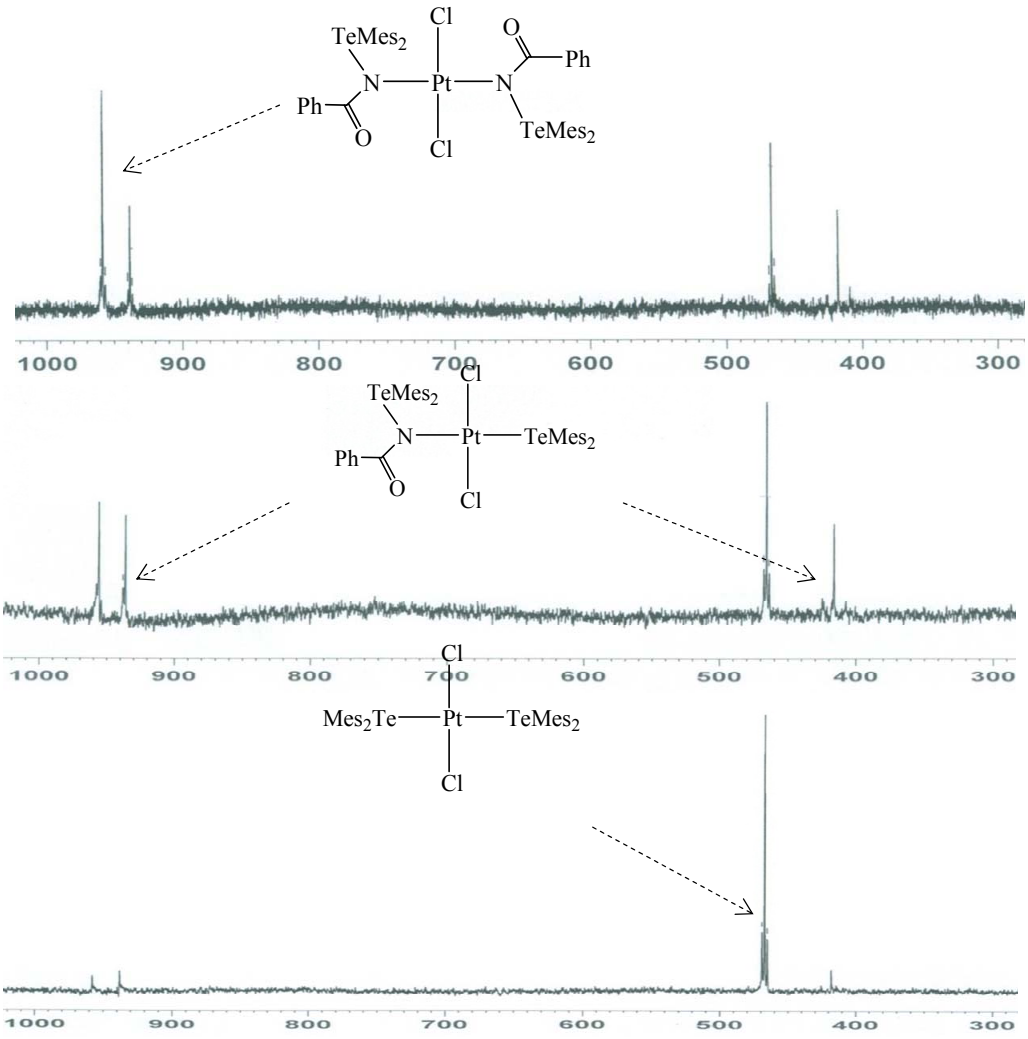

Figure 23. ^{125}Te NMR spectra of a reaction between [$PtCl_2(PhCN)_2$] and $TeMes_2$ in 1:2 molar ratio in THF monitored with time (a) 24 Hrs, (b) 3 days and (c) 7 days. Spectra were recorded in $CDCl_3$

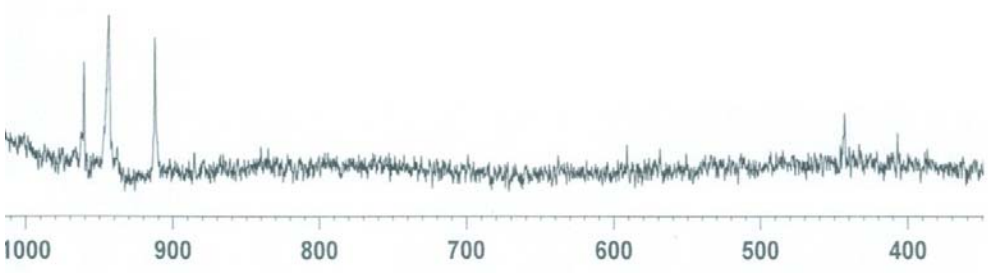

Figure 24. ^{125}Te NMR spectrum of a reaction between $[PtCl_2(MeCN)_2]$ and $TeMes_2$ in 1:2 molar ratio in THF (after 60 Hrs). Spectra were recorded in $CDCl_3$

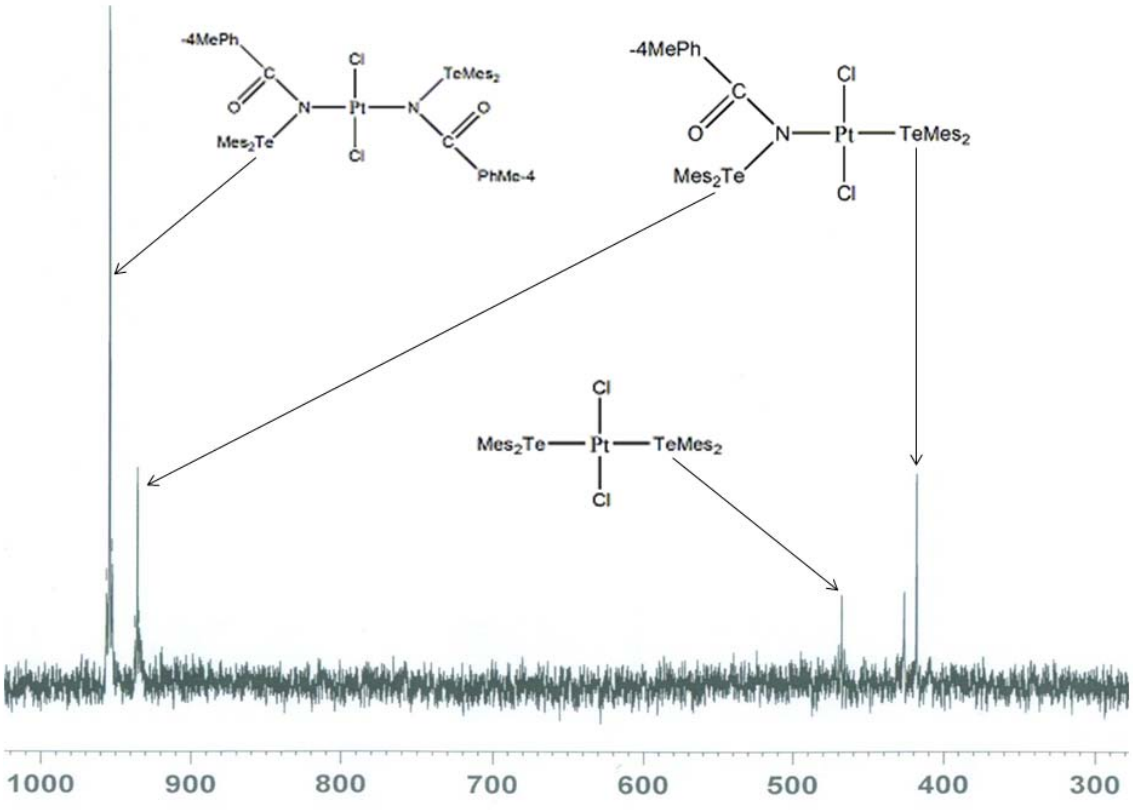

Figure 25. ^{125}Te NMR spectrum of a reaction between $[PtCl_2(4\text{-}MeC_6H_4CN)_2]$ and $TeMes_2$ in 1:2 molar ratio in THF (after 65 Hrs). Spectra were recorded in $CDCl_3$

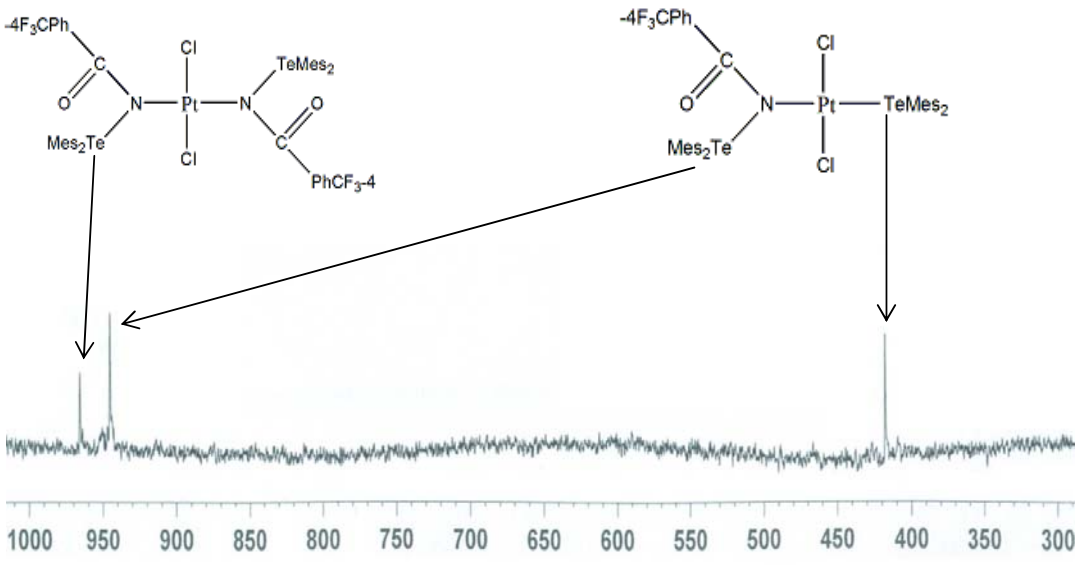

Figure 26. ^{125}Te NMR spectrum of a reaction between $[PtCl_2(4\text{-}CF_3C_6H_4CN)_2]$ and $TeMes_2$ in 1:2 molar ratio in THF (after 135 Hrs). Spectra were recorded in $CDCl_3$

To compare the reactivity of telluroether with palladium benzonitrile complex, reaction of $[PdCl_2(PhCN)_2]$ with $TeMes_2$ in 1:2 molar ratio in THF at room temperature was also carried out. The reaction afforded expected product *trans*-$[PdCl_2(TeMes_2)_2]$ as revealed by ^{1}H and ^{125}Te NMR spectroscopy.

Activation of C-N bond of metal ligated organonitriles by a variety of nucleophiles, and to a lesser extent with electrophiles, have been investigated extensively during the past two decades or so [190-196]. Both protic (e.g., ROH, RSH, oximes, etc) and aprotic nucleophiles have been shown to react with coordinated organonitrile to yield a variety of compounds containing new C-C and C-X (X = N, P, O, S) bonds. Activation of nitriles by telluroethers in THF to give kinetically labile imidecomplexes, described here, represents the first example of the formation of $N{=}TeR_2$ linkage. A possible route could be the initial attack of telluroether on nitrile carbon atom to give Te-C=N-Pt linkage. The latter is attacked by

THF oxygen on carbon and simultaneous migration of TeArAr' to nitrogen leads to Pt-N(TeArAr')C(=O)R linkage. Since Pt-N(TeArAr')C(=O)R linkage does not form in moist dichloromethane, the source is attributed to THF. The C-H actiation of the *ortho*-position of THF [197] as noted for *trans*-[$PtCl_2${$NC(Ph)C_4H_7O$}{$NC(O)Ph(TeMes_2)$}] and extrusion of oxygen from THF [198, 199] is well documented in literature.

The NMR spectral data (^1H, ^{125}Te and ^{195}Pt) for [$PtCl_2(TeArAr')_2$] and for [$PtCl(TeMes_2)${$Te(Mes)CH_2C_6H_2Me_2$}] are in accord with those prepared in **section 3.3**. The ^1H NMR spectra of *trans*-[$PtCl_2(PhCN)${$NC(O)Ph[Te(tol\text{-}o)Mes]$}], *trans*-[$PtCl_2${$NC(O)Ph(TeMes_2)$}$_2$], *trans*-[$PtCl_2${$NC(Ph)C_4H_7O$}{$NC(O)Ph(TeMes_2)$}], [$PtCl(TeMes_2)${$Te(Mes)CH_2C_6H_2Me_2$}], *trans*-[$PtCl_2(NC(O)Ph${$Te(tol\text{-}o)Mes$}$)_2$] and *trans*-[$PtCl_2(TeMes_2)${$NC(O)Ph(TeMes_2)$}] displayed resonances and peak multiplicities as expected (Table 31). Both the ortho protons of phenyl of benzonitrile resonances are significantly deshielded (δ: ~ 8.25 ppm, ~7.2 Hz). The ^{13}C NMR spectra (Table 31) exhibited, in addition to the expected resonances, a signal at ~180 ppm due to C=O group. The ^{125}Te NMR spectra (Table 31) of the complexes containing "NC(O)Ph(TeAr′Mes)" as a ligand exhibited a resonance in the region, δ 907–959 ppm and were flanked by ^{195}Pt satellites with J(^{195}Pt-^{125}Te) in the range, 309-347 Hz. The ^{125}Te NMR resonances are significantly deshielded from the corresponding signal for both coordinated telluroethers as well as cyclometalated telluroether ligands. The magnitude of platinum-tellurium coupling is comparable to the *trans*-[$PtCl_2(TeArAr')_2$]. The observed ^{125}Te NMR chemical shift range for *trans*-[$PtCl_2(PhCN)${$NC(O)Ph[Te(tol\text{-}o)Mes]$}], *trans*-[$PtCl_2${$NC(O)Ph(TeMes_2)$}$_2$], *trans*-[$PtCl_2${$NC(Ph)C_4H_7O$}{$NC(O)Ph(TeMes_2)$}], *trans*-[$PtCl_2(NC(O)Ph${$Te(tol\text{-}o)Mes$}$)_2$], *trans*-[$PtCl_2(TeMes_2)${$NC(O)Ph(TeMes_2)$}] are indicative of tellurium in higher formal oxidation state as has been noted for organotellurium(IV) complexes [200], such as ($Et_2NCOCH_2)_2TeCl_2$ ($\delta^{125}Te$ = 806 ppm) [201]; ($5,7\text{-}Cl_2\text{-}8\text{-}Me_2NC_{10}H_4)_2TeCl_2$ (δ ^{125}Te =

1031.3 ppm) [202]. Recently Lin and Gabbaï described several platinum complexes of Te(*o*-$C_6H_4PPh_2)_2$ (δ^{125}Te = 580 ppm) in which tellurium undergoes oxidation with formal oxidation state III/IV and showed ^{125}Te NMR chemical shift >1000 ppm [203]. The ^{195}Pt NMR resonances for these complexes are also deshielded with respect to the corresponding signal for $[PtCl_2(TeArAr')_2]$.

The X-ray photoelectron spectra of *trans*-$[PtCl_2\{NC(O)Ph(TeMes_2)\}_2]$ were recorded with an aim to find out the chemical state of tellurium and platinum. Figure 27 showed the core level Te 3d and Pt 4f spectra. Two groups of peaks at 575.1 and 585.5 eV were assigned to Te($3d_{5/2}$) and Te($3d_{3/2}$), respectively. Similarly, the peaks for Pt($4f_{7/2}$) and Pt($4f_{5/2}$) were observed at 72.4 and 75.7 eV, respectively. The binding energies of Te(3d) and Pt(4f) indicate that the chemical state of tellurium and platinum are Te(IV) [204] and Pt(II) [205], respectively.

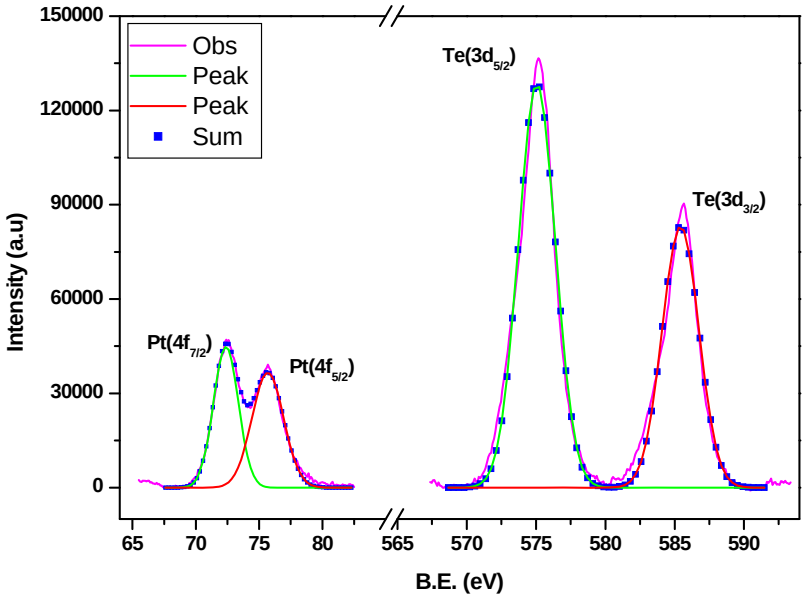

Figure 27. Te **3d** and Pt **4f** X-ray photoelectron spectrum of *trans*-$[PtCl_2\{NC(O)Ph(TeMes_2)\}_2]$

Table 31. ^{1}H, $^{125}Te\{^{1}H\}$ and $^{195}Pt\{^{1}H\}$ NMR data of platinum telluroether complexes recorded in $CDCl_3$.

Complex	^{1}H NMR δ in ppm	$^{13}C\{^{1}H\}$ NMR δ in ppm	$^{125}Te\{^{1}H\}$ NMR δ in ppm	$^{195}Pt\{^{1}H\}$ NMR δ in ppm
trans-[$PtCl_2$(PhCN){NC(O)Ph[Te(tol-*o*)Mes]}]	2.29 (s, 4-Me of Mes), 2.38 (s, 2-Me of tol), 2.64 (s, 2,6-Me of Mes), 6.98 (s, 3,5-CH of Mes),7.38-7.86 (m), 8.73-8.77(m) (aryl)		937 ($J(^{195}Pt-^{125}Te)$ = 317 Hz)	
trans-[$PtCl_2${NC(O)Ph($TeMes_2$)}$_2$]	2.21 (s, 4-Me), 2.39 (s, 2,6-Me_2); 6.70 (s, 3,5-CH); 7.16 (t, 7.8 Hz), 7.36 (m), 8.24 (d, 7.2 Hz)	21.0, 22.4 (s, Me), 127.4, 128.6, 130.2, 130.3, 130.7, 133.9 (56 Hz), 140.6, 143.6, 182.3 (C=O)	959 ($J(^{195}Pt-^{125}Te)$ = 347 Hz)	- 3079
trans-[$PtCl_2${NC(Ph)C_4H_7O}{NC(O)Ph($TeMes_2$)}]	2.21, 2.27 (each s, Me); 2.60 (br), 3.54-3.78 (m), 5.18 (br) (C_4H_7O); 6.95 (s, $C_6H_2Me_3$); 7.28-7.50 (m); 8.58-8.65 (m) (aryl)		946	- 1861
[PtCl($TeMes_2$){Te(Mes)$CH_2C_6H_2Me_2$}]	2.02, 2.19, 2.24, 2.27, 2.34, 2.53 (each s for Me) , 4.0 (J_{AX} = 16.8, $\Delta\nu_{AX}$=105.8 Hz; metalated CH_2); 6.66 (s, 3,5-CH of Mes of metallated); 6.71 (s, 3,5-CH of $TeMes_2$); 6.86, 7.04 (CH of metallated ring)		336 ($^{1}J(^{195}Pt-^{125}Te)$ = 622 Hz), 592 ($^{1}J(^{195}Pt-^{125}Te)$ = 1545 Hz), 598 (~ 5% due to dimer), 259 ($TeMes_2$)	
trans-[$PtCl_2$(NC(O)Ph{Te(tol-*o*)Mes})$_2$]	2.13 (s, 4-Me of Mes), 2.18 (s, 2-Me of tol), 2.43 (s, 2,6-Me of Mes), 6.64 (s, 3,5-CH of Mes), 7.09-7.23 (m), 7.30-7.35 (m), 7.90 (d, 7.8Hz), 8.18 (d, 7.5Hz) [tol]		907	- 1525
trans-[$PtCl_2$($TeMes_2$){NC(O)Ph($TeMes_2$)}]	2.21 (s, 2,4,6-Me of –N$TeMes_2$), 2.29 (s, 4-Me of $TeMes_2$), 2.59 (br, s, 2,6-Me of $TeMes_2$)), 6.70 (s, 3,5-CH of N$TeMes_2$), 6.91 (s, 3,5-CH of $TeMes_2$), 7.41-7.54 (m, 3,4,5-CH of Ph), 8.49 (d, 7.2 Hz, 2,6-CH of Ph)	20.8, 21.0, 22.8, 26.1, 127.8, 128.9, 129.3, 130.2, 130.7, 134.7, 139.3, 141.5, 143.4, 183.4 (C=O)	418 ($^{1}J(^{195}Pt-^{125}Te)$ = 1638 Hz), 939 ($J(^{195}Pt-^{125}Te)$ = 309 Hz)	- 2701

X-ray Crystallography

The molecular structures of *trans*-[$PtCl_2$(PhCN){NC(O)Ph(TeMestol-*o*)}], *trans*-[$PtCl_2${NC(O)Ph($TeMes_2$)}$_2$].$4H_2O$, *trans*-[$PtCl_2${NC(Ph)C_4H_7O}{NC(O)Ph($TeMes_2$)}], *trans*-[$PtCl_2${NC(O)Ph{Te(tol-*o*)Mes}}$_2$], *trans*-[$PtCl_2$($TeMes_2$){NC(O)Ph($TeMes_2$)}], *trans*-[$PtCl_2${NC(O)Me($TeMes_2$)}$_2$] and [PtCl(*o*-tolTe){NC(O)Ph}$_2$].CH_2Cl_2 were established unambiguously by single crystal X-ray diffraction analyses. ORTEP drawings are shown in Figures 28-34 while the selected interatomic parameters are summarized in Tables 32-38.

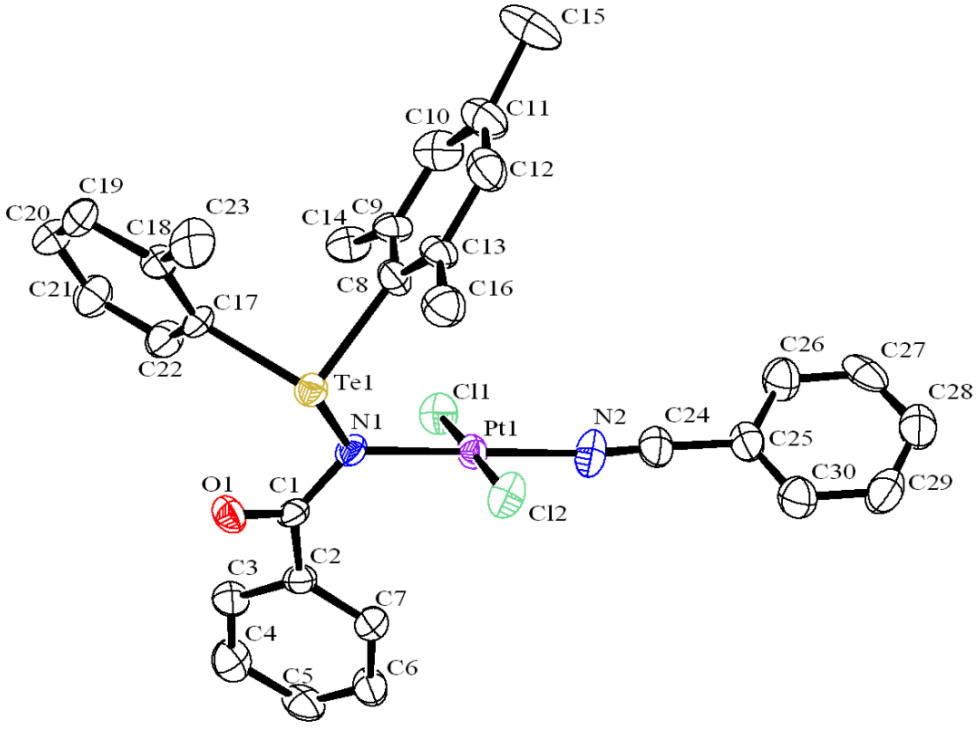

Figure 28. ORTEP drawing of *trans*-[$PtCl_2$(PhCN){NC(O)Ph(TeMestol-*o*)}] with atomic numbering scheme (drawn with 25% probablility ellipsoids and H atoms omitted for clarity)

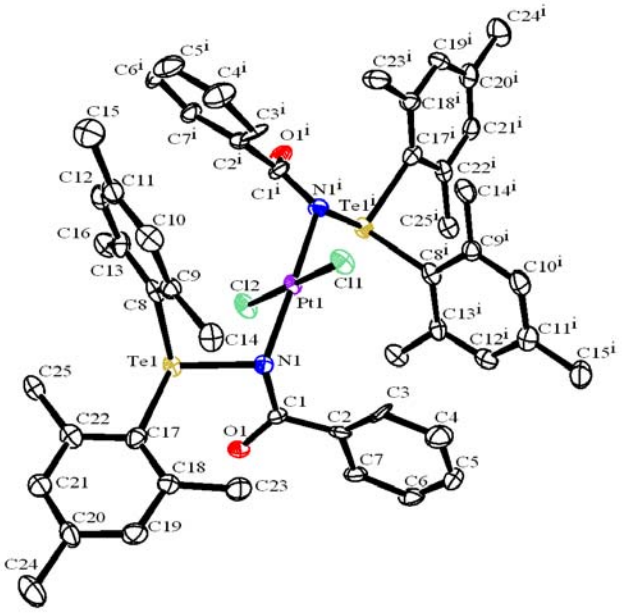

Figure 29. ORTEP drawing of *trans*-[$PtCl_2${$NC(O)Ph(TeMes_2)$}$_2$].$4H_2O$ with atomic numbering scheme (drawn with 25% probablility ellipsoids and H atoms and solvent molecules are omitted for clarity)

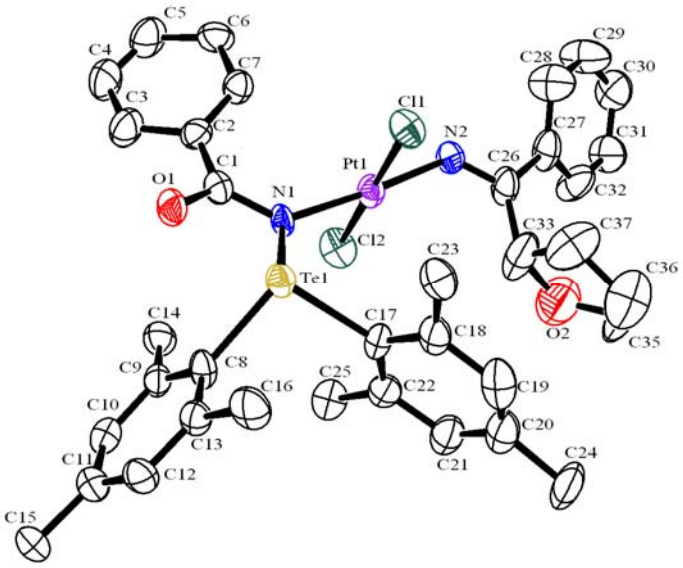

Figure 30. ORTEP drawing of *trans*-[$PtCl_2${$NC(Ph)C_4H_7O$}{$NC(O)Ph(TeMes_2)$}] with atomic numbering scheme (drawn with 25% probablility ellipsoids and H atoms omitted for clarity)

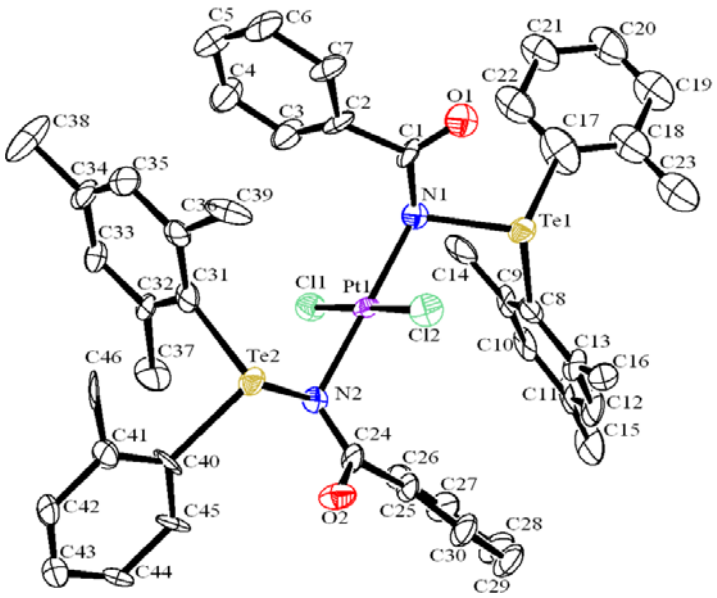

Figure 31. ORTEP drawing of *trans*-[$PtCl_2${NC(O)Ph{Te(tol-*o*)Mes}}$_2$] with atomic numbering scheme (drawn with 25% probablility ellipsoids and H atoms omitted for clarity)

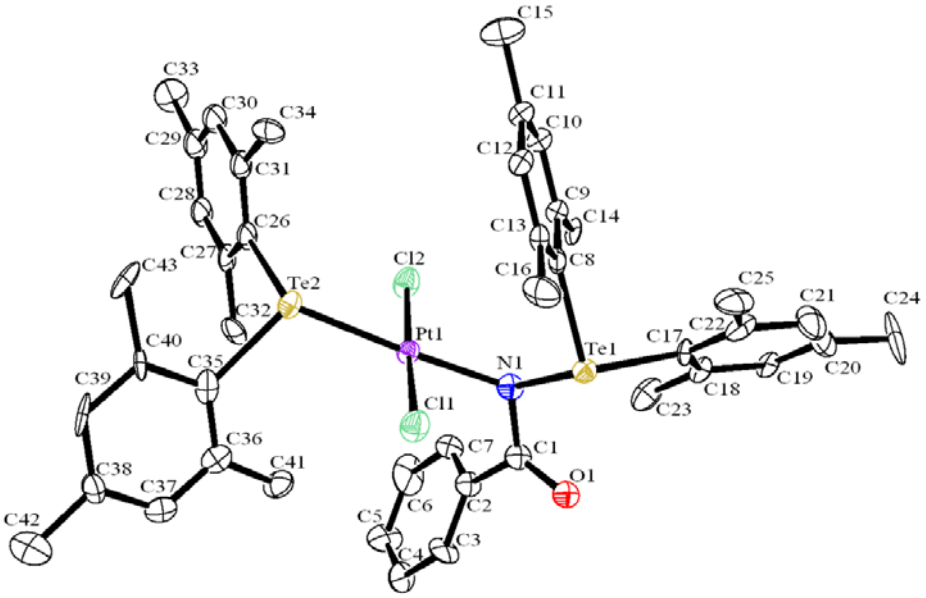

Figure 32. ORTEP drawing of *trans*-[$PtCl_2(TeMes_2)${NC(O)Ph($TeMes_2$)}] with atomic numbering scheme (drawn with 25% probablility ellipsoids and H atoms omitted for clarity)

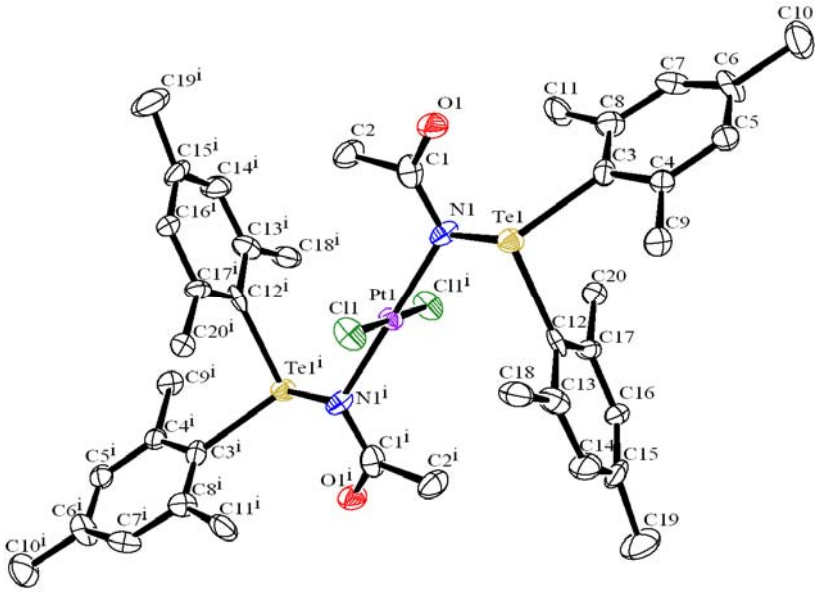

Figure 33. ORTEP drawing of *trans*-[$PtCl_2${$NC(O)Me(TeMes_2)$}$_2$].$2CH_2Cl_2$ with atomic numbering scheme (drawn with 25% probablility ellipsoids and H atoms omitted for clarity)

Table 32. Selected interatomic parameters (Å / °) for *trans*-[$PtCl_2$(PhCN){NC(O)Ph[Te(tol-*o*)Mes]}]

Pt1-Cl1	2.289 (6)	C1-O1	1.241(19)
Pt1-Cl2	2.280(6)	C1-N1	1.35(2)
Pt1-N1	2.000(13)	Te1-N1	2.025(14)
Pt1-N2	1.962(18)	Te1-C8	2.132(17)
N2-C24	1.10(2)	Te1-C17	2.099(18)
Pt1…Te1	3.501(13)	Te1-O1	2.532(12)
Cl1-Pt1-Cl2	178.9(2)	Pt1-N1-Te1	120.9(7)
Cl1-Pt1-N2	91.5(6)	N1-C1-O1	118.8(15)
Cl1-Pt1-N1	92.4(4)	N1-C1-C2	123.5(15)
Cl2-Pt1-N1	86.8(4)	N1-Te1-C8	98.6(7)
Cl2-Pt1-N2	89.2(6)	N1-Te1-C17	105.5(7)
N1-Pt1-N2	176.0(7)	C8-Te1-C17	94.4(7)
Pt1-N2-C24	174(2)	Te1-N1-C1	101.6(10)
Pt1-N1-C1	128.4(11)	O1-C1-C2	117.7(16)

Table 33. Selected interatomic parameters (Å / °) for *trans*-[$PtCl_2\{NC(O)Ph(TeMes_2)\}_2$]

Pt1-Cl1	2.283(4)	Te1-C8	2.128(13)
Pt1-Cl2	2.321(5)	Te1-C17	2.183(13)
Pt1-N1	2.059(9)	C1-N1	1.371(15)
Te1-N1	2.051(10)	C1-O1	1.236(14)
Pt1-Te1	3.3440(16)	Te1-O1	2.618(9)
Cl1-Pt1-Cl2	180.0	N1-C1-C2	117.3(10)
Cl1-Pt1-N1	91.6(3)	O1-C1-N1	121.0(11)
Cl2-Pt1-N1	88.4(3)	O1-C1-C2	121.3(10)
N1-Pt1-$N1^i$	176.7(6)	N1-Te1-C8	97.8(4)
Pt1-N1-C1	121.2(8)	N1-Te1-C17	109.3(4)
Pt1-N1-Te1	108.9(4)	C8-Te1-C17	97.5(4)
		C1-N1-Te1	102.2(8)

Table 34. Selected interatomic parameters (Å / °) for

trans[$PtCl_2\{NC(Ph)C_4H_7O\}\{NC(O)Ph(TeMes_2)\}$]

Pt1-Cl1	2.308(5)	N1-C1	1.345(19)
Pt1-Cl2	2.282(5)	C1-O1	1.291(18)
Pt1-N1	1.989(10)	Te1-C8	2.130(16)
Pt1-N2	1.969(11)	Te1-C17	2.110(14)
N1-Te1	2.028(11)	N2-C26	1.27(2)
Te1-O1	2.500(11)	C26-C27	1.49(2)
Pt1-Te1	3.5150(13)	C26-C33	1.52(3)
Cl1-Pt1-Cl2	179.46(18)	N1-Te1-C8	111.8(5)
Cl1-Pt1-N1	89.1(4)	N1-Te1-C17	99.0(5)
Cl1-Pt1-N2	91.9(4)	N1-C1-O1	117.0(15)
Cl2-Pt1-N1	90.6(4)	N1-C1-C2	125.3(15)
Cl2-Pt1-N2	88.5(4)	C8-Te1-C17	98.1(6)
N1-Pt1-N2	175.3(5)	N2-C27-C34	116.1(17)
Pt1-N1-C1	130.2(11)	N2-C27-C28	118.4(18)
Pt1-N1-Te1	122.1(6)	C28-C27-C34	125.5(18)
Pt1-N2-C27	132.3(13)	N1-Te1-O1	58.4(4)
O1-C1-C2	117.8(13)	Te1-N1-C1	101.9(10)

Table 35. Selected interatomic parameters (Å / °) for *trans*-[$PtCl_2${NC(O)Ph[Te(tol-*o*)Mes}$_2$]

Pt1-Cl1	2.281(6)	N1-C1	1.38(3)
Pt1-Cl2	2.286(6)	Te1-C8	2.113(13)
Pt1-N1	2.03(2)	Te1-C17	2.145(17)
Pt1-N2	2.04(2)	C24-O2	1.27(4)
Te1-N1	2.06(2)	N2-C24	1.34(3)
Te2-N2	2.07(2)	C1-O1	1.23(3)
Pt1-Te1	3.320(3)	Te2-C31	2.110(12)
Pt1-Te2	3.320(3)	Te2-C40	2.085(17)
Te1-O1	2.576(18)	Te2-O2	2.593(15)
Cl1-Pt1-Cl2	179.1(3)	N1-C1-O1	122(3)
C11-Pt1-N1	92.4(5)	N1-Te1-C8	99.6(8)
Cl1-Pt1-N2	91.0(5)	N1-Te1-C17	103.2(11)
Cl2-Pt1-N1	88.5(5)	C8-Te1-C17	96.1(9)
Cl2-Pt1-N2	88.1(5)	O1-C1-C2	119(2)
N1-Pt1-N2	175.9(7)	N2-C24-O2	123(3)
Pt1-N1-C1	124(2)	N2-C24-C25	119(2)
Pt1-N1-Te1	108.5(9)	O2-C24-C25	118(2)
Pt1-N2-C24	121(2)	N2-Te2-C31	97.5(8)
Pt1-N2-Te2	107.8(9)	N2-Te2-C40	105.3(9)
Te2-N2-C24	99.7(16)	C31-Te2-C40	95.1(8)

Table 36. Selected interatomic parameters (Å / °) for *trans*-[$PtCl_2(TeMes_2)\{NC(O)Ph(TeMes_2)\}$]

Pt1-Cl1	2.322(6)	N1-C1	1.40(2)
Pt1-Cl2	2.273(6)	C1-O1	1.24(2)
Pt1-N1	2.098(16)	C1-C2	1.50(2)
Pt1-Te2	2.5158(18)	Te1-C8	2.104(9)
Te1-N1	1.998(15)	Te1-C17	2.181(10)
Pt1-Te1	3.4150(19)	Te2-C26	2.142(10)
Te1-O1	2.690(12)	Te2-C35	2.139(11)
Cl1-Pt1-Cl2	177.3(2)	N1-C1-O1	121.8(19)
Cl1-Pt1-N1	87.5(5)	N1-C1-C2	117.5(17)
Cl1-Pt1-Te2	87.33(15)	O1-C1-C2	120.7(18)
Cl2-Pt1-N1	91.3(5)	C1-N1-Te1	104.1(12)
Cl2-Pt1-Te2	93.62(15)	N1-Te1-C8	95.6(6)
N1-Pt1-Te2	171.7(4)	N1-Te1-C17	108.8(6)
Pt1-N1-Te1	112.9(7)	C8-Te1-C17	97.3(5)
Pt1-N1-C1	117.5(13)	C26-Te2-C35	100.2(5)
Pt1-Te2-C26	110.1(4)		
Pt1-Te2-C35	112.7(5)		

Table 37. Selected interatomic parameters (Å / °) for *trans*-[$PtCl_2\{NC(O)Me(TeMes_2)\}_2$]

Pt1-Cl1	2.305(5)	Te1-C3	2.174(16)
Pt1-N1	2.051(14)	Te1-C12	2.142(18)
Te1-N1	1.973(13)	C1-N1	1.35(2)
Pt1-Te1	3.476(3)	C1-O1	1.241(19)
Te1-O1	2.612(12)		
$Cl1\text{-}Pt1\text{-}Cl^{i}$	180.0(18)	N1-C1-C2	119.1(16)
Cl1-Pt1-N1	94.0(4)	O1-C1-N1	120.0(16)
Cl^{i}-Pt1-N1	86.0(4)	O1-C1-C2	120.7(18)
$N1\text{-}Pt1\text{-}N1^{i}$	180.0	N1-Te1-C3	109.2(6)
Pt1-N1-C1	120.6(12)	N1-Te1-C12	97.0(6)
Pt1-N1-Te1	119.5(6)	C3-Te1-C12	98.2(6)
		C1-N1-Te1	103.8(11)

The two *trans* chloride and two neutral donor (N or / and Te) ligands define the coordination environment around platinum. There is slight deviation of various angles involving platinum from idealized square planar configuration of central platinum atom in these complexes. The Pt-Cl distances (2.281(6)-2.318(7)Å) are well in agreement with those reported in mono-nuclear *trans*-$PtCl_2L_2$ complexes, such as *trans*-$[PtCl_2\{Te(CH_2SiMe_3)_2\}_2]$ (2.309(2)Å) [176] and *trans*-$[PtCl_2(Te\{(CH_2CH_2)O\}_2)]$ (2.3169 (9)Å) [181, 182]. The Pt-N distances (1.966(13)-2.06(2)Å) are in accord with the values reported for $[Pt_2(\mu\text{-}Br)_2(diimine)_2]^{2+}$ (Pt-N = 1.992(2), 2.001(2) Å [206], but are longer than those found in complexes in which nitrogen is *trans* to the strong *trans* influencing ligands, e.g. $[PtCl(ECH_2CH_2NMe_2)(PR_3)]$ (E/PR_3= Se/PEt_3 (2.160(7)Å; $Te/PMePh_2$ (2.182(4)Å) [207]. The Pt-Te distance (2.520(2) Å) is well in agreement with our previous data of *trans*-$[PtCl_2(TeArAr')_2]$ (**section 3.3**).

The Te-C distances (2.08(3) – 2.18(13) Å) are as expected. The Te-N bond lengths (1.97-2.06Å) in these complexes can be compared with those reported in diorganotellurimides ($R_2Te{=}NR'$) [208]. The observed distances indicate dipolar character as is usually observed in tellurium imides [208]. These distances are significantly shorter than those found for intramolecular Te···N secondary bonding interactions [209]. The Te-O distances (2.510(13)–2.690(12)Å) are significantly longer than those expected for single tellurium-oxygen bond lengths but are indicative of intramolecular secondary Te···O bonding interactions [209]. The Pt---Te distances fall in the range 3.320(3)–3.5150(13) Å which are shorter than the sum of van der Waals radii of platinum and tellurium (3.81 Å). This suggests that there is platinum- tellurium non-bonding interaction which facilitates the formation of Pt-telluroether linkage.

The C-Te-C angles (94.4–100.2°) are reduced from the free telluroether (e.g. $TeMes_2$ 101.0(1)° [144].This angle is little influenced on coordination with platinum (**section 3.3**).

The Te-N-C angles showed little variation (101.6–104.1°) and the Pt-N-C (120(2)-130.4(12)°) angles fall in a rather large range. The carbon –oxygen bond lengths (1.23(4)-1.30(2) Å) are of double bond character.

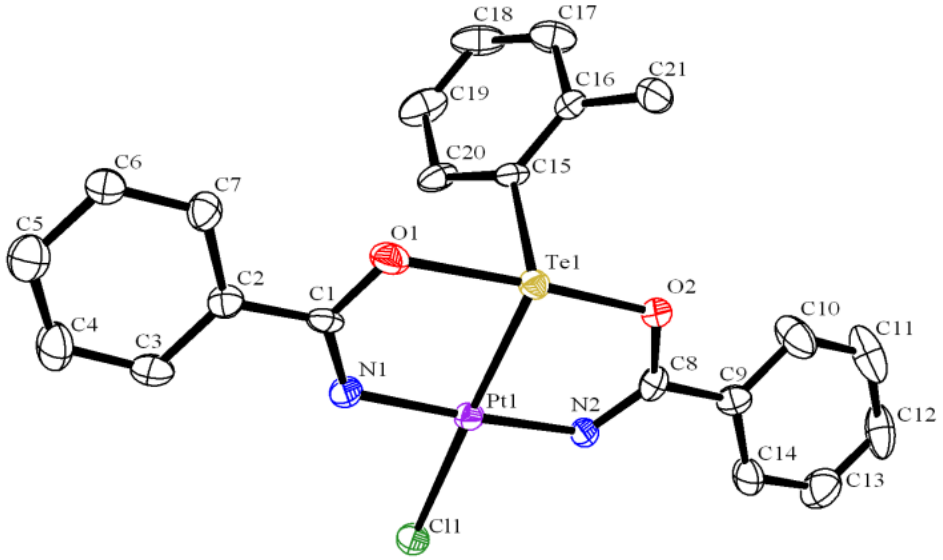

(a)

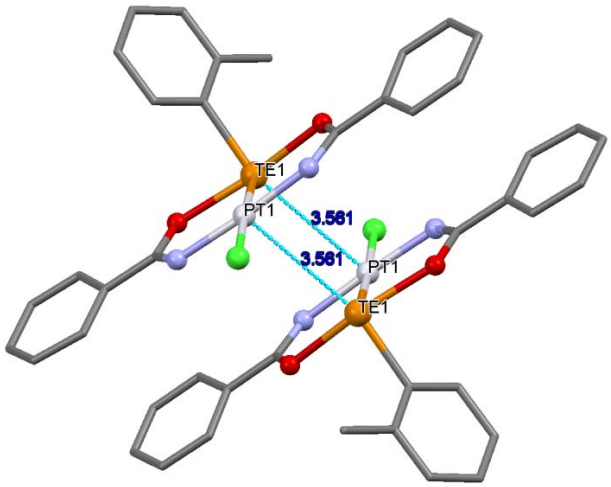

(b)

Figure 34. (a) ORTEP drawing of [PtCl(*o*-tolTe){NC(O)Ph}$_2$].CH_2Cl_2 (drawn with 25% probablility ellipsoids). H atoms and Solvent molecule omitted for clarity (b) inter molecular interaction π-π stacking

Table 38. Selected inter-atomic parameters (Å / °) for [PtCl(Tetol-*o*){NC(O)Ph}$_2$]

Pt1-Cl1	2.340 (3)	N1-C1	1.313 (14)
Pt1-Te1	2.4503 (10)	C1-O1	1.308 (13)
Pt1-N1	2.001 (10)	C1-C2	1.481 (17)
Pt1-N2	1.982 (10)	N2-C8	1.302 (15)
Te1-O1	2.196 (10)	C8-O2	1.309 (15)
Te1-O2	2.187 (9)	C8-C9	1.476 (17)
Te1-C15	2.122 (12)		
Cl1-Pt1-Te1	177.03 (10)	Te1-O1-C1	118.6 (8)
Cl1-Pt1-N1	90.5 (13)	O1-C1-C2	115.7 (11)
Cl1-Pt1-N2	91.3 (3)	O1-C1-N1	121.5 (13)
N1-Pt1-N2	176.7 (5)	N1-C1-C2	122.8 (11)
N1-Pt1-Te1	89.6 (3)	Te1-O2-C8	116.7 (8)
N2-Pt1-Te2	88.8 (3)	O2-C8-C9	114.4 (13)
Pt1-Te1-C15	106.4 (3)	O2-C8-N2	122.7 (12)
Pt1-Te1-O1	85.8 (2)	N2-C8-C9	122.8 (13)
Pt1-Te1-O2	86.6 (2)	O1-Te1-O2	169.2 (3)

The complex [PtCl(Tetol-*o*){NC(O)Ph}$_2$] (Figure 34) comprises of a distorted square planar platinum atom with a 'N2ClTe' coordination core. The two nitrogen atoms of the amide group are mutually *trans*. The deviations of the N1-Pt1-N2 and Cl1-Pt1-Te1 angles from linearity are rather small. The two five- membered chelate rings 'Pt1Te1O1C1N1' and 'Pt1Te1O2C8N2' are co-planar. The phenyl rings of the amide groups are slightly out of the

plane and are little tilted in the opposite directions from this plane. The co-planarity of the two chelate rings and short bite angle of the amide ligands appear to be responsible for unusually short Pt-Te distance (2.4503(10)Å) reported thus far [187]. The other bond distances involving platinum (Pt-N and Pt-Cl) are normal. The tellurium atom adopts a distorted trigonal bipyramidal configuration defined by the platinum, *o*-tolyl ring and a lone pair of electrons at the equatorial positions while the two oxygen atoms occupying the axial sites. The Te-C and Te-O distances are as expected. Tellurium(IV) as a ligand has been described recently and complexes in general have Te-Cl linkages [203, 210]. The present complex represents the first example where organotellurium(IV) acetoxy compound acts as a ligand. Recently Singh and co-workers have isolated a palladium complex [{(*o*-tolylTe)$_2$O}Pd(μ-OAc)$_2$] containing tellurenic anhydride as a ligand [152]. The complex shows π-π stacking with the separation of 3.56 Å (Figure 34(b)) due to extensive delocalization of electron density along the "PtCl(Te){NC(O)Ph}$_2$" unit.

3.5 Thermal behavior cyclometalated palladium complexes

The interest in the preparation of platinum group metal chalcogenides (M_xE_y) has grown considerably during the last decads due to extensive applications in numerous areas such as catalyst in organic transformation [211-213], low resistance ohmic contacts of semiconducting electronic devices [213], high temperature acid resistance electrode [214], light image receiving materials with silver halides [215], recording films in optical discs and lithographic films [213], etc. Palladium chalcogenolates are gaining importance as molecular precursorsfor moderately low temperature synthesis of palladium chalcogenides [105, 146, 213]. These palladium chalcogenides (Pd_xE_y) are also believed to be formed during several catalytic processes involving palladium chalcogenolate complexes [216, 217]. Depending on auxiliary ligands on palladium and the nature of Ar group on chalcogenolate ligand, a variety of palladium chalcogenides are formed. With that aim various molecular precursors with varring auxiliary ligands have been synthesized and their thermal decomposition into palladaium chalcogenides have been carried out and presented in this section.

Synthesis and spectroscopy

The reaction of $[Pd_2(\mu\text{-}Cl)_2(Me_2NCH_2C_6H_4\text{-}C,N)_2]$ with lead salt of 2-mercapto or selenopyridine in dichloromethane afforded 2-chalcogenopyridine-bridged binuclear palladium complexes, $[Pd_2(\mu\text{-}Epy)_2(Me_2NCH_2C_6H_4\text{-}C,N)_2]$ (E = S or Se) in fairly good yield (Scheme 21). Interestingly similar reaction with simple arylthiolate groups gave mixed chloro/mercapto-bridged derivatives, $[Pd_2(\mu\text{-}Cl)(\mu\text{-}SAr)(Me_2NCH_2C_6H_4\text{-}C,N)_2]$ (Ar = Ph or Mes). Contrary to this, the analogous arylselenolate ligand yielded the expected bis selenolato-bridged complexes, $[Pd_2(\mu\text{-}SeAr)_2(Me_2NCH_2C_6H_4\text{-}C,N)_2]$ (Ar = Ph or Mes).

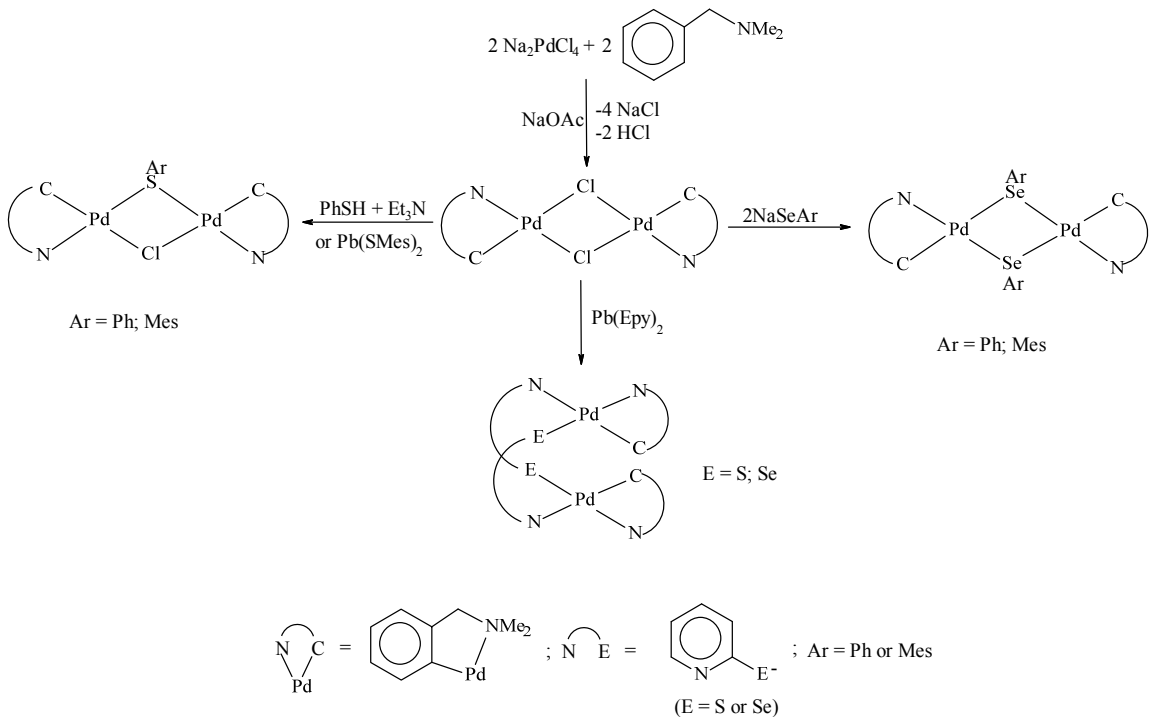

Scheme 21

The mass spectra of $[Pd_2(\mu\text{-}Epy)_2(Me_2NCH_2C_6H_4\text{–}C,N)_2]$ (E = S or Se) did not show any molecular ion peak, instead a peak due to M-Epy fragment with expected isotopic pattern was observed. The mass spectra of $[Pd_2(\mu\text{-}Cl)(\mu\text{-}SPh)(Me_2NCH_2C_6H_4\text{–}C,N)_2]$, $[Pd_2(\mu\text{-}Cl)(\mu\text{-}SMes)(Me_2NCH_2C_6H_4\text{–}C,N)_2]$, $[Pd_2(\mu\text{-}SePh)_2(Me_2NCH_2C_6H_4\text{–}C,N)_2]$ and $[Pd_2(\mu\text{-}SeMes)_2(Me_2NCH_2C_6H_4\text{–}C,N)_2]$ displayed molecular ion peaks. The ^1H NMR spectral (Table 39) data for $[Pd_2(\mu\text{-}Spy)_2(Me_2NCH_2C_6H_4\text{–}C,N)_2]$ are consistent with the one reported earlier [155]. Deeming et.al. described temperature independent ^1H NMR spectra of $[Pd_2(\mu\text{-}Spy)_2(Me_2NCH_2C_6H_4\text{–}C,N)_2]$ while the analogous complex, $[Pd_2(\mu\text{-}SC_5H_3(Me\text{-}6)N)_2(Me_2NCH_2C_6H_4\text{-}C,N)_2]$ is fluxional at room temperature [155]. Unlike $[Pd_2(\mu\text{-}Spy)_2(Me_2NCH_2C_6H_4\text{–}C,N)_2]$, the ^1H NMR spectrum of $[Pd_2(\mu\text{-}Sepy)_2(Me_2NCH_2C_6H_4\text{–}C,N)_2]$ showed broad resonances indicative of fluxional nature of the complex in solution.

The spectrum displayed a singlet for NMe_2 protons and two separate resonances for CH_2 protons, i.e. a singlet at 2.97 ppm and a broad AB pattern in the region 3.13- 3.37 ppm in the ratio of 1:1.6 at room temperature. On lowering the temperature, two separate signals for NMe_2 protons appeared. At -30 ºC the spectrum showed two separate signals for NMe_2 at 2.49 and 2.52 ppm while the NCH_2 protons showed a singlet at 2.97 ppm and an AB pattern in the region 3.05-3.14 ppm in the ratio of 1:8.8. The singlet at 2.97 ppm may be attributed to the *sym-cis* isomeric form. The spectra of $[Pd_2(\mu\text{-}Cl)(\mu\text{-}SPh)(Me_2NCH_2C_6H_4\text{–}C,N)_2]$, $[Pd_2(\mu\text{-}Cl)(\mu\text{-}SMes)(Me_2NCH_2C_6H_4\text{–}C,N)_2]$, $[Pd_2(\mu\text{-}SePh)_2(Me_2NCH_2C_6H_4\text{–}C,N)_2]$ and $[Pd_2(\mu\text{-}SeMes)_2(Me_2NCH_2C_6H_4\text{–}C,N)_2]$ exhibited singlets for NMe_2 and CH_2 protons at ~2.75 and ~3.85 ppm, respectively indicating magnetic equivalence of protons of methyl and methylene groups. This suggests that these groups of both the metalated ligands are *trans* to the similar bridging ligands. Recent X–ray analysis of $[Pd_2(\mu\text{-}Cl)(\mu\text{–}SMes)(Me_2NC_{10}H_6\text{-}C,N)_2]$ [105] and $[Pd_2(\mu\text{-}Cl)(\mu\text{–}SBu^n)\{(Bu^nO)C_6H_3CH{=}NC_6H_4(OBu^n\text{–}4)\}_2]$ [218] have shown a *sym-cis* configuration with the nitrogen atom of the metalated ligands *trans* to the bridging thiolate group. The ^1H NMR spectra of $[Pd_2(\mu\text{-}Cl)(\mu\text{-}SPh)(Me_2NCH_2C_6H_4\text{–}C,N)_2]$ and $[Pd_2(\mu\text{-}Cl)(\mu\text{-}SMes)(Me_2NCH_2C_6H_4\text{–}C,N)_2]$ can be interpreted in terms of *sym-cis* configuration. The ^{77}Se NMR spectrum (Table 39) of $[Pd_2(\mu\text{-}SePh)_2(Me_2NCH_2C_6H_4\text{–}C,N)_2]$ showed a singlet at 181 ppm indicating that both the bridging selenolates are magnetically equivalent as is expected for *sym-trans* configuration.

Table 39. ^{1}H and $^{77}Se\{^{1}H\}$ NMR data for cyclopalladated complexes in $CDCl_3$

Complex	^{1}H NMR δ in ppm	$^{77}Se\{^{1}H\}$ NMR δ in ppm
$[Pd_2(\mu\text{-Spy})_2(Me_2NCH_2C_6H_4\text{–}C,N)_2]$	2.39, 2.55 (each s, NMe_2); 2.84–3.10 (AB pattern CH_2N); 6.65–6.69 (m), 6.91 (br, C_6H_4); 6.99 (t, 6.6 Hz, CH–5), 7.30 (d, 7.5Hz, CH–4), 7.66 (d, 7.5 Hz, CH–3), 8.60 (d, 6Hz, CH–6) (Spy).	
$[Pd_2(\mu\text{-Sepy})_2(Me_2NCH_2C_6H_4\text{–}C,N)_2]$	(at room temperature) 2.53 (s, NMe_2), 2.97 (s), 3.13-3.37 (AB pattern) (NCH_2), 6.68 (br) 6.76 (t, 6 Hz), 6.87 (m), 6.94 (m), 7. 45 (d, 8 Hz), 7.69 (br), 8.73 (d, 5 Hz); (at -30 ºC): 2.49, 2.52 (each s, NMe_2), 2.97 (s) 3.05-3.14 (AB pattern) (NCH_2), 6.68 (t, 1H, C_6H_4), 6.81 (t, 6.5 Hz,1H, C_5H_4N), 6.89 (t, 4.5 Hz, 2H, C_6H_4), 6.98 (t,7 Hz, 1H, C_5H_4N), 7.46 (d, 8 Hz, 1H, C_5H_4N), 7.75 (t,5 Hz, 1H, C_6H_4), 8.73 (d, 5Hz, 1H, C_5H_4N)	311
$[Pd_2(\mu\text{-Cl})(\mu\text{-SPh})(Me_2NCH_2C_6H_4\text{–}C,N)_2]$	2.77 (s, 12H, NMe_2); 3.89 (s, 4H, $-CH_2-$); 6.94–6.97 (m), 7.13 (m) (SPh); 7.60–7.63 (m),8.15–8.18 (m) (C_6H_4).	
$[Pd_2(\mu\text{-Cl})(\mu\text{-SMes})(Me_2NCH_2C_6H_4\text{–}C,N)_2]$	2.16 (s, 3H, 4-Me); 2.71 (s, 12H, NMe_2); 3.14 (s, 6H ,2,6-Me); 3.85 (s, 4H, $-CH_2-$); 6.44(s); 6.47 (s) ($C_6H_2Me_3$); 6.54–6.60 (m); 6.79–6.82 (m) (C_6H_4).	
$[Pd_2(\mu\text{-SePh})_2(Me_2NCH_2C_6H_4\text{–}C,N)_2]$	2.76 (s, 12H, NMe_2); 3.91 (s, 4H, $-CH_2-$); 6.89–6.97 (m), 7.12–7.15 (m), 7.63 (d, 6.6 Hz); 8.81 (d, d, 1.8, 7.8 Hz) (Ph + C_6H_4)	181
$[Pd_2(\mu\text{-SeMes})_2(Me_2NCH_2C_6H_4\text{–}C,N)_2]$	2.17 (s, 3H, 4-Me); 2.73 (s, 12H, NMe_2); 3.20 (s, 6H, 2,6-Me); 3.86 (s, 4H, NCH_2); 6.60-7.37 (m, 3,5-Mes + C_6H_4).	30, -11

X-ray Crystallography

Molecular structures of $[Pd_2(\mu\text{-}Spy)_2(Me_2NCH_2C_6H_4\text{–}C,N)_2]$ and $[Pd_2(\mu\text{-}Sepy)_2(Me_2NCH_2C_6H_4\text{–}C,N)_2]$ were established by X–ray diffraction analysis and the ORTEP diagrams with the numbering schemes are shown in Figures 35 and 36, while the selected inter-atomic parameters are given in Tables 40 and 41. The coordination around each palladium atom, defined by C, N, E, N, donor set, is nearly planar. The sulfur or selenium atoms in the two bridging pyridine-chalcogenolate ligands occupy the *trans* position to the N atoms of the metalated ligands resulting in an *anti* configuration (head-to-tail arrangement) which is usually observed for this type of complexes [104, 159, 160]. The eight-membered ring adopts a distorted twist-boat conformation. The methyl groups of NMe_2 of the metallated rings are mutually *anti* but differ in their conformation in two complexes. In the case of Spy bridged complex they are *exo* with resepect to the eight membered boat configurations while in the case of Sepy bridged complex they adopt an *endo* configuration. The Pd–C and Pd–$N_{(metalated)}$ are well in agreement with those reported for $[Pd_3(\mu\text{–}Spy)_2(Me_2NCH_2C_6H_4\text{–}C,N)_3][BF_4]$ [155] and other related cyclometalated palladium complexes [218]. The two Pd–S distances are essentially similar and can be compared with those reported in $[Pd_3(\mu\text{–}Spy)_2(Me_2NCH_2C_6H_4\text{–}C,N)_3][BF_4]$ [155], $[Pd_2(\mu\text{–}Spy)_2(Bzq)_2]$ [104] and $[Pd_2(\mu\text{–}Spy)_2(4,4'\text{–}Bu^t{}_2bipy)_2][ClO_4]_2$ [219]. The Pd–Se distance (2.410Å) is as expected and can be compared with the one *trans* to nitrogen atom as observed in $[Pd_2(\mu\text{–}SePh)_2(C_{10}H_6NMe_2\text{–}C,N)_2]$ [105].

The Pd···Pd separation in Spy bridged complex (2.976(2) Å) is significantly longer than those reported in $[Pd_2(Spy)_4]$ (2.677(1) Å) [220], $[Pd_2(\mu\text{–}Spy)_2(4,4'\text{–}Bu^t{}_2bipy)_2][ClO_4]_2$ (2.891(4)Å) [219], $[Pt_2(Spy)_2(ppy)_2]$ (2.8491(4) Å) [221], but only marginally longer than the one reported in $[Pd_2(\mu\text{–}Spy)_2(Bzq)_2]$ (2.929(4) Å) [104]. However, it is shorter than sum of the van der Waals radii of Pd atoms (3.26Å) and is within the acceptable value for a Pd···Pd intra-molecular interaction. The Pd···Pd separation in the corresponding Sepy bridged

complex (3.420Å) is much longer than the analogous thio derivative and is also longer than the sum of van der Waals radii of Pd atoms indicative of absence of Pd···Pd interaction.

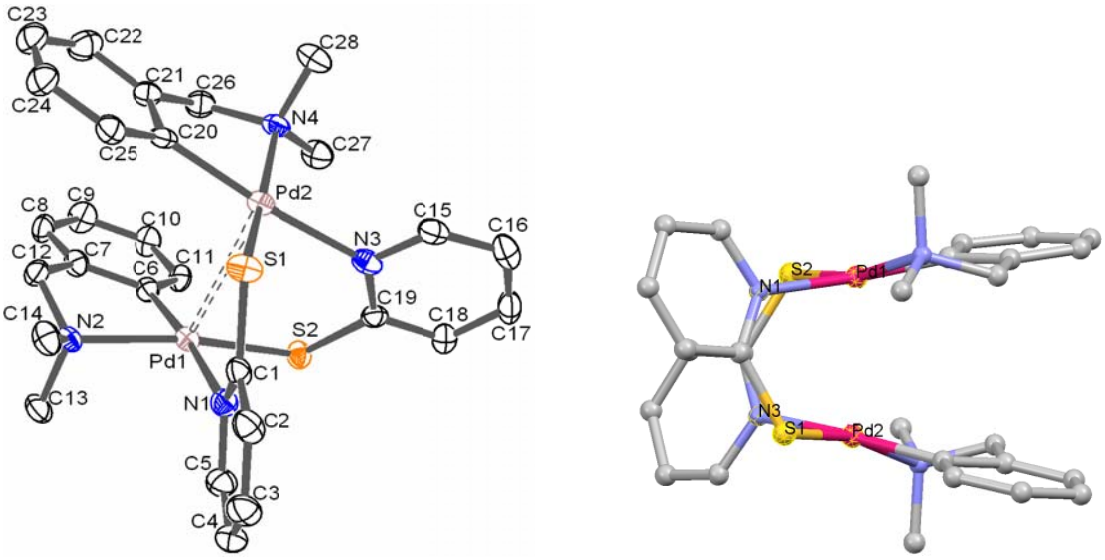

Figure 35. ORTEP drawing of $[Pd_2(\mu\text{-}Spy)_2(Me_2NCH_2C_6H_4\text{–}C,N)_2]$.

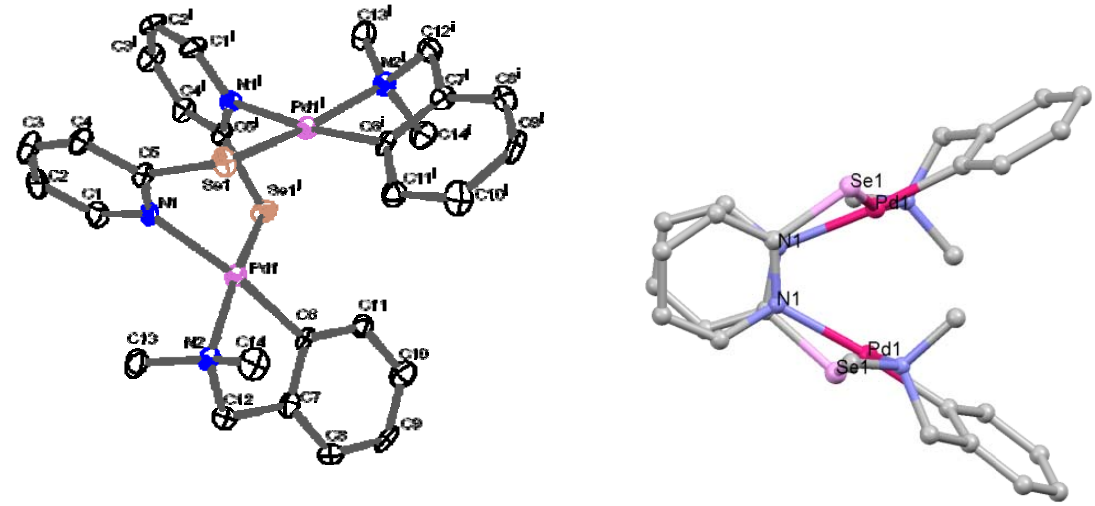

Figure 36. ORTEP drawing of $[Pd_2(\mu\text{-}Sepy)_2(Me_2NCH_2C_6H_4\text{–}C,N)_2]$.

Table 40. Selected bond lengths (Å) and angles (°) for $[Pd_2(\mu\text{-}Spy)_2(Me_2NCH_2C_6H_4\text{–}C,N)_2]$

Pd1 – C11	2.028 (8)	Pd2 – C20	2.004 (8)
Pd1 – N2	2.184 (7)	Pd2 – N1	2.157 (7)
Pd1 – N3	2.143 (6)	Pd2 – N4	2.163 (6)
Pd1 – S1	2.295 (2)	Pd2 – S2	2.305 (2)
S1 – C1	1.728 (9)	S2– C6	1.732 (8)
		Pd1---Pd2	2.976 (2)
N2 – Pd1 – N3	92.7 (2)	N1 – Pd2 – N4	93.4 (2)
N2 – Pd1 – S1	92.81 (18)	N1 – Pd2 – S2	91.37 (18)
N2 – Pd1 – C11	174.0 (3)	N1 – Pd2 – C20	174.7 (3)
N3 – Pd1 – C11	81.6 (3)	N4 – Pd2 – C20	82.1 (3)
N3 – Pd1 – S1	166.84 (19)	N4 – Pd2 – S2	167.55 (17)
C11 – Pd1 – S1	92.2 (2)	C20 – Pd2 – S2	92.5 (2)
N1 – C6 – S2	122.2 (6)	N1 – C1 – S1	122.4 (6)
C11 – Pd1 – Pd2	98.6 (2)	C20 – Pd2 – Pd1	98.5 (2)

Table 41. Selected bond lengths (Å) and angles (°) for $[Pd_2(\mu\text{-}Sepy)_2(Me_2NCH_2C_6H_4\text{–}C,N)_2]$

Pd1 – C6	1.994 (9)	Pd1 – $Se1^{i}$	2.410 (2)
Pd1 – N1	2.189 (8)	Se1 – C5	1.906 (10)
Pd1 – N2	2.140 (8)	Pd1---$Pd1^{i}$	3.420
N1 – Pd1 – N2	94.3 (3)	N2 – Pd1 – C6	81.4 (4)
N1 – Pd1 –$Se1^{i}$	94.7 (2)	N2 – Pd1 –$Se1^{i}$	165.2 (2)
N1 – Pd1 – C6	173.6 (4)	C6 – Pd1 –$Se1^{i}$	88.5 (3)
		N1 – C5 –Se1	118.3 (7)

Thermal behavior

Thermal behaviour of these molecular precurssors was investigated both by thermogravimetric analysis (TGA) and by furnace heating. The final residues were

characterized by powder XRD analysis. The TG-DTG curves and the XRD pattern of the decomposed products are given in Figures 37-42. The TG-DTG curves revealed that these complexes undergo a multi-step decomposition in the temperature range 200-300 ºC leading to the formation of palladium chalcogenides. The thiolato-bridged complexes decomposed to single phase Pd_4S (JCPD file No 73-1387) (Figure 37-39). The TG curve (Figure 37(a)) of $[Pd_2(\mu\text{-}Spy)_2(Me_2NCH_2C_6H_4\text{–}C,N)_2]$ appears to be a single step decomposition but the DTG clearly shows overlapping of closely spaced two-step decomposition (weight loss 30, 28%) at ~ 215 °C with the formation of Pd_4S (from XRD pattern, Figure 37(b)). This complex converted into single phasic Pd_4S even at low temperature (210 °C) as seen during the conventional furnace heating under dynamic argon flow condition.

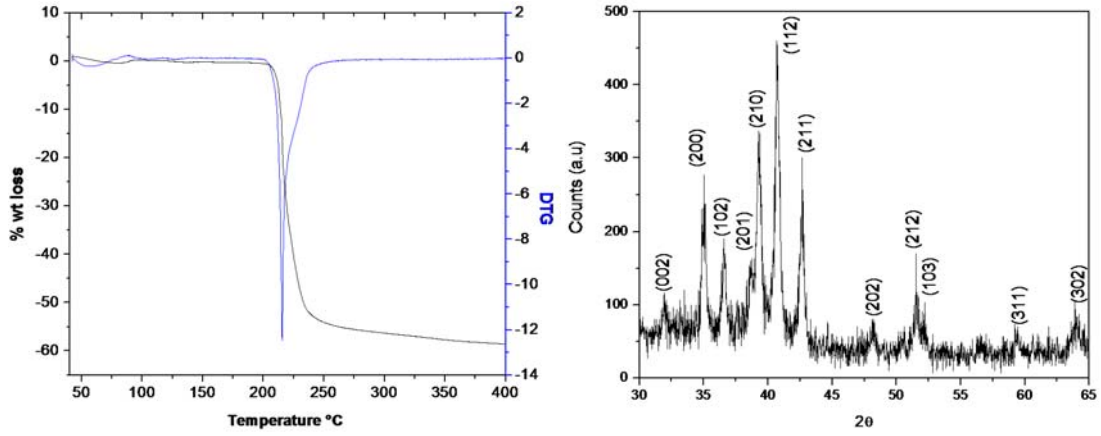

(a) **(b)**

Figure 37. (a) TG-DTG curve of $[Pd_2(\mu\text{-}Spy)_2(Me_2NCH_2C_6H_4\text{–}C,N)_2]$; **(b)** XRD pattern of Pd_4S obtained from $[Pd_2(\mu\text{-}Spy)_2(Me_2NCH_2C_6H_4\text{–}C,N)_2]$.

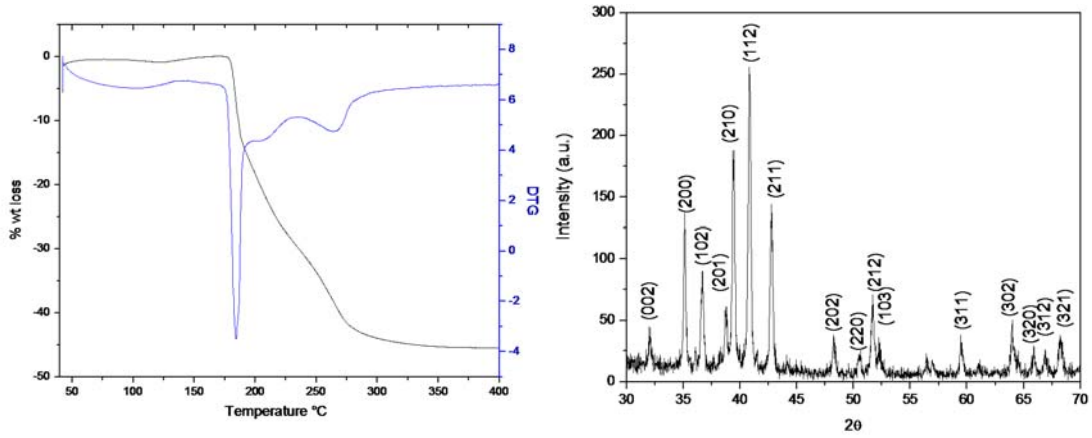

(a) (b)

Figure 38(a). TG-DTG curve of $[Pd_2(\mu\text{-}Cl)(\mu\text{-}SPh)(Me_2NCH_2C_6H_4\text{-}C,N)_2]$; **(b)** XRD of TG residue (Pd_4S, JCPDS -73-1387) obtained from $[Pd_2(\mu\text{-}Cl)(\mu\text{-}SPh)(Me_2NCH_2C_6H_4\text{-}C,N)_2]$.

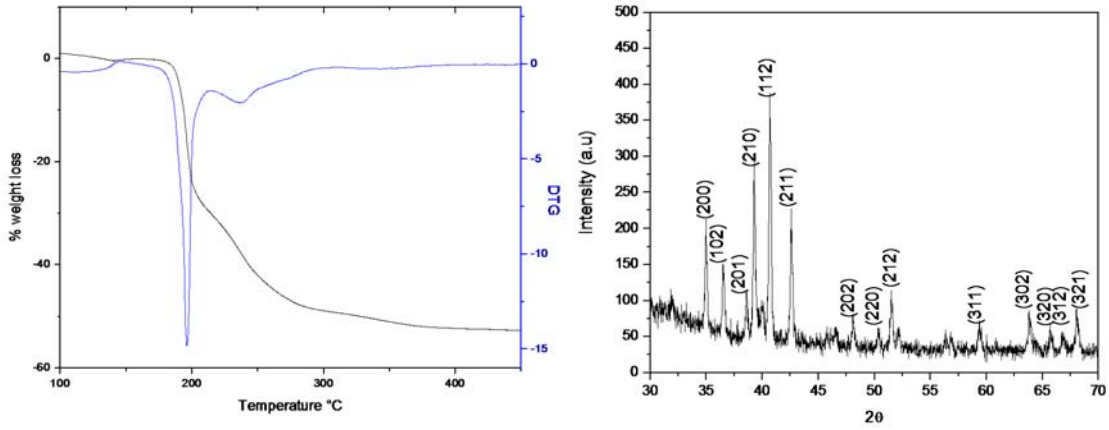

(a) (b)

Figure 39(a). TG-DTG curve of $[Pd_2(\mu\text{-}Cl)(\mu\text{-}SMes)(Me_2NCH_2C_6H_4\text{-}C,N)_2]$; **(b)** XRD of TG residue (Pd_4S, JCPDS -73-1387) obtained from $[Pd_2(\mu\text{-}Cl)(\mu\text{-}SMes)(Me_2NCH_2C_6H_4\text{-}C,N)_2]$.

The selenolato-bridged complexes in general gave a mixture of palladium selenides on decomposition. The TG curve of $[Pd_2(\mu\text{-}SePh)_2(Me_2NCH_2C_6H_4\text{-}C,N)_2]$ (Figure 40(a)) showed that the complex decomposed at ~290°C into single phasic Pd_7Se_4 (Figure 40(b)). Attempts were made to identify the low temperature decomposition product by carrying out the decomposition of the complex at 200°C in a furnace under flowing argon, air and H_2 atmospheres. However, in every case, Pd_4Se was the major product together with Pd_7Se_4 as confirmed from their powder XRD patterns.

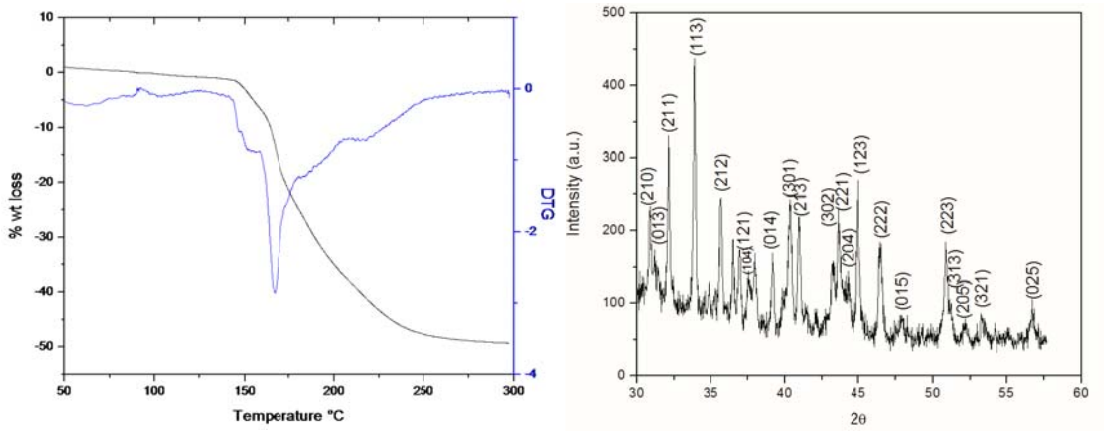

Figure 40(a). TG-DTG curve of $[Pd_2(\mu\text{-}SePh)_2(Me_2NCH_2C_6H_4\text{-}C,N)_2]$; **(b)** XRD of TG residue (Pd_7Se_4, JCPDS 44-0875) obtained from $[Pd_2(\mu\text{-}SePh)_2(Me_2NCH_2C_6H_4\text{-}C,N)_2]$.

Similarly, $[Pd_2(\mu\text{-}SeMes)_2(Me_2NCH_2C_6H_4\text{-}C,N)_2]$ decomposed into a biphasic mixture of $Pd_{34}Se_{11}$ (JCPDS file No: 79-0140) and Pd_4Se_7 (JCPDS file No: 31-0939) at ~350°C (Figure 41(a) and 41(b)). The complex, $[Pd_2(\mu\text{-}Sepy)_2(Me_2NCH_2C_6H_4\text{–}C,N)_2]$ undergoes a multi-step decomposition (Figure 42(a)) at 225°C to yield $Pd_{17}Se_{15}$ as confirmed by the XRD pattern (Figure 42(b)) (JCPDS file No 73-1424).

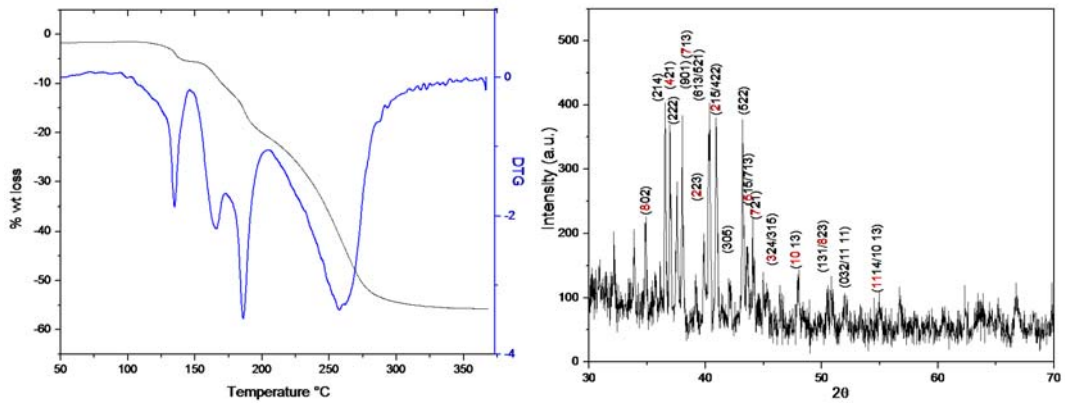

(a) (b)

Figure 41(a). TG-DTG curve of $[Pd_2(\mu\text{-}SeMes)_2(Me_2NCH_2C_6H_4\text{-}C,N)_2]$; **(b)** XRD of TG residue obtained from $[Pd_2(\mu\text{-}SeMes)_2(Me_2NCH_2C_6H_4\text{-}C,N)_2]$

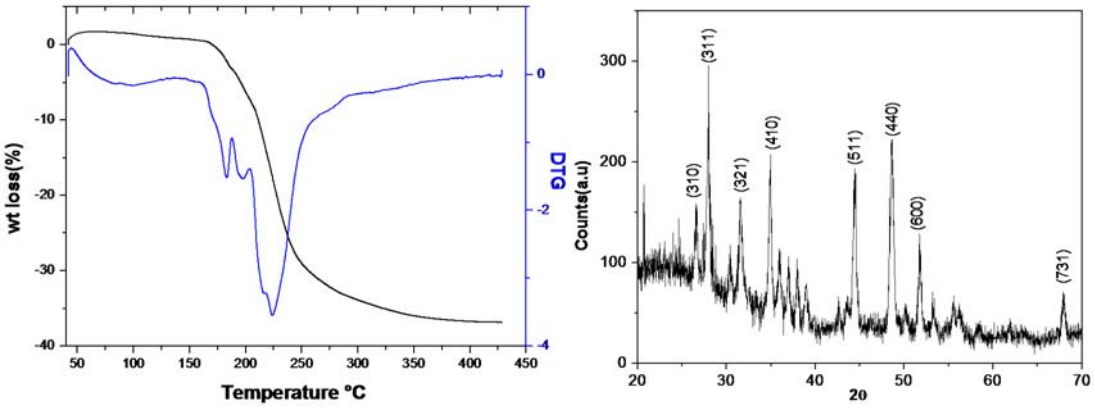

(a) **(b)**

Figure 42(a). TG-DTG curve of $[Pd_2(\mu\text{-}Sepy)_2(Me_2NCH_2C_6H_4\text{–}C,N)_2]$; **(b)** XRD pattern of $Pd_{17}Se_{15}$ obtained from $[Pd_2(\mu\text{-}Sepy)_2(Me_2NCH_2C_6H_4\text{–}C,N)_2]$.

To develop precursors for ternary palladium chalcogenides, 1, 1-dithiolate complexes derived from cyclopalladated selenoether ligand have been considered. Metal xanthates are known to undergo clean cleavage of the xanthate group to yield metal sulfides. Keeping this in mind, reactions of $[Pd_2(\mu\text{-}Cl)_2\{MesSeC_6H_2(Me_2)CH_2\}_2]$ with sodium xanthates in dichloromethane–methanol mixture were carried out (eq. 4) and complexes of composition

$[Pd(S_2COR)\{(CH_2C_6H_2Me_2\text{-}4,6)SeMes\}]$ (R = Me, Et, n-propyl and *iso*-propyl) were isolated as yellow-reddish, low melting crystalline solids in 60-70% yield. These complexes are soluble in common organic solvents. A similar reaction between $[Pd_2(\mu\text{-}Cl)_2\{MesSeC_6H_2(Me_2)CH_2\}_2]$ and sodium diethyl dithiocarbamate, however, afforded a bis chelate, $[Pd(S_2CNEt_2)_2]$.

$[Pd_2(\mu\text{-}Cl)_2MesSeC_6H_2(Me_2)CH_2{}_2]$ + 2 NaS_2COR ⟶ 2 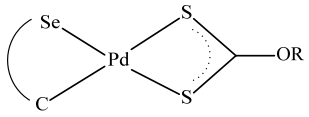 ...(4)

R = Me, Et, Pr^n, Pr^i

^1H NMR spectra of these complexes exhibited expected resonances and peak multiplicities assignable to metalated selenoether and xanthate fragments. The ^{13}C NMR resonance for CS_2 group is deshielded (~ 3 ppm) in the complexes with respect to its position in the corresponding sodium xanthate. This could be due to chelation of the xanthate group. The ^{77}Se NMR spectra displayed a single resonance at ~ 390 ppm and is shielded with respect to the parent chloro-bridged precursor $[Pd_2(\mu\text{-}Cl)_2\{MesSeC_6H_2(Me_2)CH_2\}_2]$ (^{77}Se NMR δ: 408 ppm).

The molecular structure of $[Pd(S_2COPr^i)\{(CH_2C_6H_2Me_2\text{-}4,6)SeMes\}]$ has been unambiguously established by single crystal X-ray analysis (Figure 43). Selected interatomic parameters are summarized in Table 42. The palladium atom in the complex acquires a distorted square planar configuration defined by ′CSeS2′ donor set. Various inter atomic parameters involving metalated selenoether are similar to the parent chloro-bridged complex. The non-metalated mesityl ring is nearly perpendicular to the metal square plane. The xanthate ligand binds to palladium in an anisobidentate fashion; accordingly the two Pd-S distances are dissimilar (Table 42). The Pd-S distance *trans* to metalated carbon is longer than the one *trans* to Se. This is owing to the strong *trans* influence of the metalated carbon atom and is consistent with organopalladium dithiolates [222-224]. The two C-S distances are

similar and are intermediate between single (1.81 Å) and double (1.62 Å) bond values indicating delocalization of double bond over OCS^{-}_{2} group. The strain caused by four-membered PdS_2C ring results into compression of S-Pd-S angle (74.21 (11)°) which is similar to [Pt(S_2COEt)(ppy)] (S-Pt-S = 74.28 (6)°) [225].

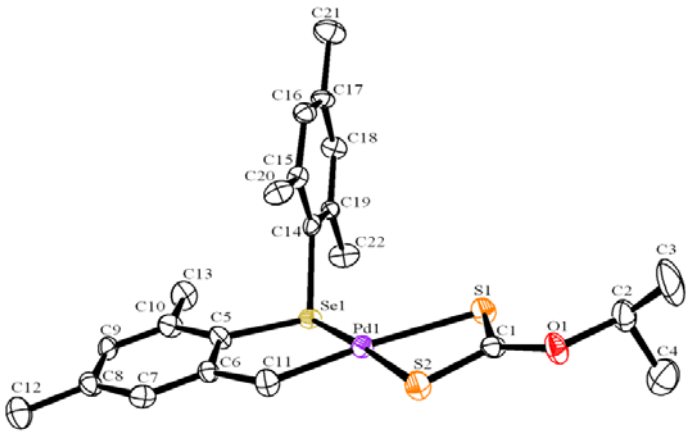

Figure 43. ORTEP drawing of [Pd(S_2COPr^{i}){($CH_2C_6H_2Me_2$-4,6)SeMes}], elipsoids are drawn with 25% probability.

Table 42. Selected bond lengths (Å) and angles (°) of [Pd(S_2COPr^{i}){($CH_2C_6H_2Me_2$-4,6)SeMes}]

Pd1-C11	2.021 (9)	Se1-C5	1.924 (10)
Pd1-Se1	2.389 (2)	Se1-C14	1.959 (9)
Pd1-S1	2.452 (3)	S1-C1	1.700 (10)
Pd1-S2	2.319 (3)	S2-C1	1.678 (10)
C1-O1	1.330 (10)		
S1-Pd1-S2	74.21 (11)	Pd1-S1-C1	82.0 (3)
S2-Pd1-C11	91.5 (3)	Pd1-S2-C1	86.7 (3)
S2-Pd1-Se1	176.21 (9)	S1-C1-S2	117.0 (5)
S1-Pd1-C11	165.6 (3)	Pd1-Se1-C5	97.5 (3)
S1-Pd1-Se1	107.75 (9)	Pd1-Se1-C14	109.9 (3)
C11-Pd1-Se1	86.6 (3)		

The thermal behaviour of both $[Pd_2(\mu\text{-}Cl)_2\{MesSeC_6H_2(Me_2)CH_2\}_2]$ and its xanthate derivatives, $[Pd(S_2COR)\{(CH_2C_6H_2Me_2\text{-}4,6)SeMes\}]$ (R = Et or *iso*-propyl) has been investigated. TG-DTG curve (Figure 44) of $[Pd_2(\mu\text{-}Cl)_2\{MesSeC_6H_2(Me_2)CH_2\}_2]$ revealed that the complex undergoes a multi-step decomposition. The weight loss in TG (observe weight loss: 61.3%; calculated weight loss: 61.5%) is consistent with the formation of $Pd_{17}Se_{15}$. The XRD pattern (Figure 45a) is well in agreement with the pattern for $Pd_{17}Se_{15}$ (JCPDS: 73-1424). The thermolysis of this complex in diphenyl ether at 250°C, however, gave Pd_7Se_4 (JCPDS: 31-0939) (Figure 45b).

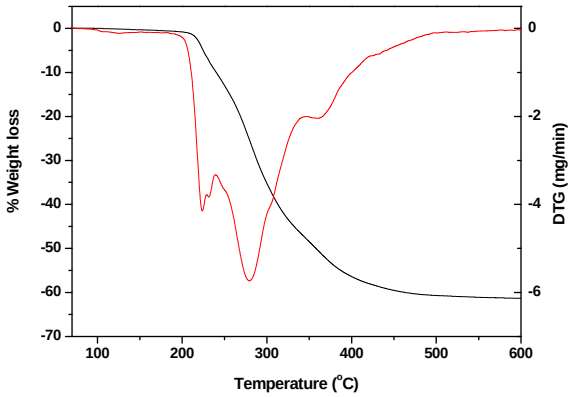

Figure 44. TG-DTG curve of $[Pd_2(\mu\text{-}Cl)_2\{MesSeC_6H_2(Me_2)CH_2\}_2]$.

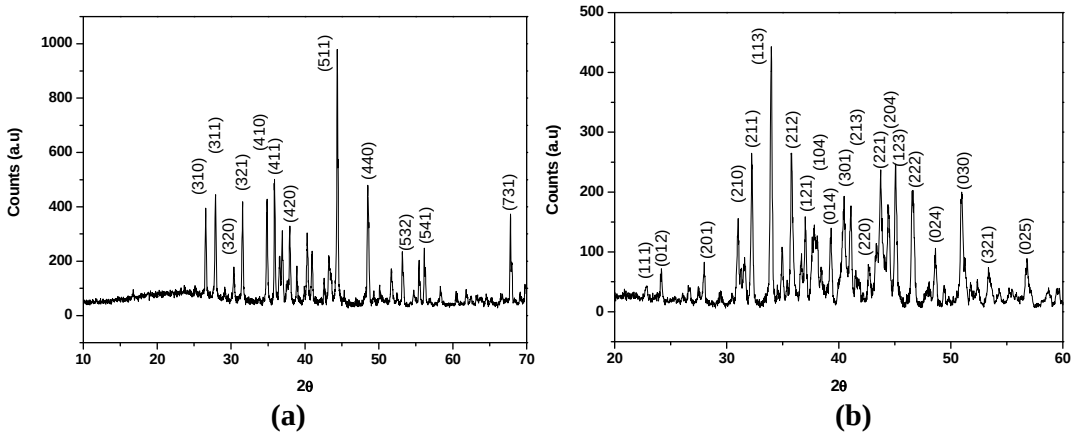

Figure 45. (a) XRD of $Pd_{17}Se_{15}$ (JCPDS -73-1424) and (**b**) XRD of Pd_7Se_4 (JCPDS: 31-0939) obtained from $[Pd_2(\mu\text{-}Cl)_2\{MesSeC_6H_2(Me_2)CH_2\}_2]$ in TG and in diphenyl ether at 250°C, respectively.

The TG-DTG curves (Figure 46) of xanthate complexes [Pd(S_2COR){($CH_2C_6H_2Me_2$-4,6)SeMes}] (R = Et or *iso*-propyl) showed a two-step decomposition with the weight loss indicative of the formation of PdSSe (observed weight loss: 59.3 % (R = Et); 59.3 % (R = *iso*-propyl); calculated weight loss: 60% (R = Et), 61% (R = *iso*-propyl)). The XRD pattern (Figure 47) of the residue showed peaks closely similar to that reported for cubic $Pd_{17}Se_{15}$ (JCPDS: 73-1424). However all the peaks are shifted to higher angle. All the peaks and intensity distributions could be explained by considering structural model of $Pd_{17}Se_{15}$ and a unit cell parameter: a = 10.4998(5) Å. The observed unit cell parameter is smaller in comparison to the reported unit cell parameters of $Pd_{17}Se_{15}$ (a = 10.606 Å). This may be due to either partial substitution of S in the lattice or deviation of composition from $Pd_{17}Se_{15}$. In order to see the possible substitution, the refinements of occupation of various atoms were attempted. However, the occupation of various atoms could be refined separately. At least two of Se sites appear to have under occupation. This may be due to a partial substitution of S (Z = 16) at Se (Z = 34) sites. But the exact composition of the sites cannot be unequivocally obtained due to poor quality of the diffraction data.

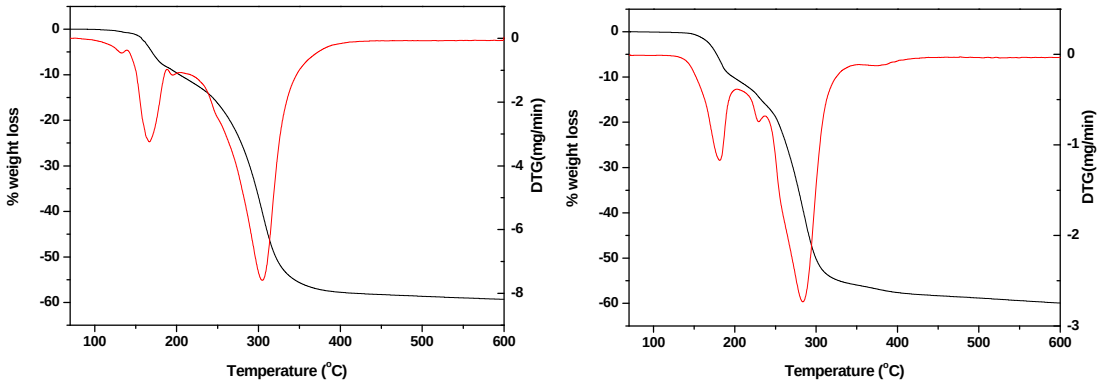

(a) (b)

Figure 46. (a) TG-DTG curve of [Pd(S_2COEt){($CH_2C_6H_2Me_2$-4,6)SeMes}] and **(b)** TG-DTG curve of [Pd(S_2CO^iPr){($CH_2C_6H_2Me_2$-4,6)SeMes}].

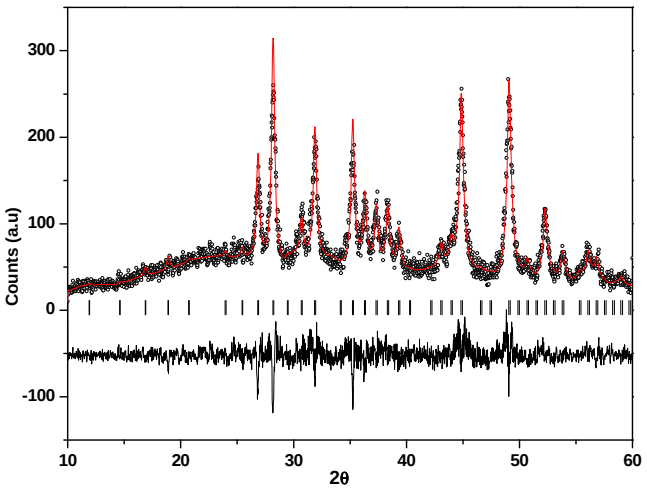

Figure 47. Powder XRD pattern of the TG-residue modelled with structural model of $Pd_{17}Se_{15}$ (black sphere: observed data; red and black continuous lines: calculated pattern and difference between observed and calculated data; vertical ticks: Bragg positions).

The solvothermal decomposition of $[Pd(S_2CO^iPr)\{(CH_2C_6H_2Me_2\text{-}4,6)SeMes\}]$ in diphenyl ether at 250°C, however, yielded a new ternary system of composition $PdSe_{0.45}S_{0.83}$ as confirmed from EDAX data (Figure 48).

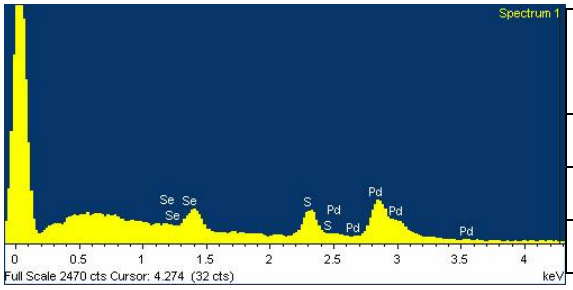

Element	Weight %	Weight % (Sigma)	Atomic %
S K	15.89	1.08	36.59
Se K	20.93	1.88	19.57
Pd K	63.18	2.01	43.84

Figure 48. EDAX data of the residue obtained from the solvothermal decomposition of $[Pd(S_2CO^iPr)\{(CH_2C_6H_2Me_2\text{-}4,6)SeMes\}]$ in diphenyl ether at 250°C.

Chapter 4

Summary and Conclusions

The present thesis consists of four chapters, *viz* Introduction, Experimental, Results and Discussion and Summary and Conclusion followed by references.

Chapter 1 deals with the general introduction about palladium and platinum metals and their chemistry with chalcogen ligands. Discussion about cyclometalation reactions, effect of various factors like source of metal precursor, nature of metalacycle, hybridization of carbon center undergoing metalation, experimental conditions, etc is included in this chapter. Applications of cyclometalated complexes are briefly covered in this chapter. The scope of the present work is discussed at the end of the chapter.

Chapter 2, "Experimental", describes different experimental techniques and synthetic methods employed during the course of present work and characterization techniques used. Details of synthesis and characterization of various ligands, metal precursors, and their complexation are discussed. The complexes were characterized by elemental analyses, IR, NMR, UV/Vis spectroscopy, TG-DTA, XPS and single crystal X-ray analysis. The physical and analytical data of all the complexes and structure refinement details of the complexes studied by crystallography are given in this chapter.

Chapter 3 deals with the results obtained during the present investigation and discussion on the present work. This chapter is further divided into five sections.

Section 3.1 deals with cyclopalladation of dimesitylselenide in mild reaction conditions. The cyclopalladated complex, $[Pd_2(\mu\text{-}Cl)_2\{MesSeC_6H_2(Me_2)CH_2\}_2]$ has been isolated from the reaction of Na_2PdCl_4 with dimesitylselenide in refluxing ethanol. The above complex can also be obtained by refluxing $[Pd_2(\mu\text{-}Cl)_2(Mes_2Se)_2]$ in ethanol. The complex $[Pd_2(\mu\text{-}Cl)_2\{MesSeC_6H_2(Me_2)CH_2\}_2]$ on treatment with $Pb(Epy)_2$ in dichloromethane afforded Epy-bridged binuclear complexes, $[Pd_2(\mu\text{-}Epy)_2\{MesSeC_6H_2(Me_2)CH_2\}_2]$ (E = S or Se). The molecular structures of all the complexes were established by X–ray diffraction analyses. All the complexes are dimeric with the palladium atoms acquiring a distorted

square planar configuration. There are intra-molecular C–H···Pd interaction (d_{M-H}: 2.75Å and $<_{C-H\cdots Pd}$: 111.23°) known as agostic interaction in $[Pd_2(\mu\text{-}Cl)_2(Mes_2Se)_2]$ which facilitates activation of C–H (sp^3) bond leading to metalation.

Section 3.2 describes the reaction of various telluroethers with Pd(II) precursors. By subtle variation in reaction conditions a variety of complexes, such as addition complexes (e.g. *trans*-$[PdCl_2(TeMes_2)_2]$), complexes showing secondary Pd···H interactions (e.g. $[Pd_2(\mu\text{-}Cl)_2Cl_2(TeMes_2)_2]$), cyclometalated complexes (e.g. $[Pd_2(\mu\text{-}OAc)_2\{CH_2C_6H_2(4,6\text{-}Me_2)TeMes\}_2]$), complexes formed by Te-C bond cleavage (e.g. $[Pd(\mu\text{-}OAc)(\mu\text{-}TeMes)]_4$) and finally leading to palladium telluride (Pd_7Te_3), have been isolated and structurally characterized. The favourable conditions for cyclopalladation *via* benzyl C-H bond activation has also been demonstrated with the modification of telluroethers of varying steric crowding and with varying palladium precursors. Thus, the reaction of $[PdCl_2(PhCN)_2]$ with diaryl telluride in 1:2 molar ratio gave mononuclear palladium complexes, *trans*-$[PdCl_2(TeAr_2)_2]$ (Ar = Mes (Mes = 2,4,6-trimethylphenyl); Ph; *o*-tol (*o*-tol = *ortho*-tolyl)). Reaction of $[PdCl_2(TeMes_2)_2]$ with one equivalent of $[PdCl_2(PhCN)_2]$ or Na_2PdCl_4 with TeArAr′ afforded chloro-bridged binuclear complexes, $[Pd_2(\mu\text{-}Cl)_2Cl_2(TeRR')_2]$ (Ar/Ar′ = Mes/Mes; Mes/Ph; Ph/Ph). Toluene-methanol solution of *trans*-$[PdCl_2(TeMes_2)_2]$ on refluxing for 30 minutes yielded a binuclear cyclopalladated complex, $[Pd_2(\mu\text{-}Cl)_2\{CH_2C_6H_2(4,6\text{-}Me_2)TeMes)\}_2]$. When the refluxing was prolonged, a mononuclear complex *cis*-$[PdCl_2\{MesTeCH_2C_6H_2(4,6\text{-}Me_2)TeMes\}]$ was isolated. Treatment of palladium acetate with $TeMes_2$ afforded an acetato-bridged cyclopalladated complex, $[Pd_2(\mu\text{-}OAc)_2\{CH_2C_6H_2(4,6\text{-}Me_2)TeMes\}_2]$ together with a very minor component, a tetranuclear complex, $[Pd(\mu\text{-}OAc)(\mu\text{-}TeMes)]_4$. This reaction with unsymmetrical tellurides, MesTeAr also gave cyclopalladated complexes $[Pd_2(\mu\text{-}OAc)_2\{CH_2C_6H_2(4,6\text{-}Me_2)TeR\}_2]$ (Ar = *o*-tolorPh) in which 2-methyl of mesityl group of the telluride was exclusively metalated. The complex *trans*-$[PdCl_2(TeMes_2)_2]$ on refluxing in

xylene gave palladium telluride, Pd_7Te_3.These complexes were characterized by elemental analyses, IR and NMR (^1H, ^{13}C and ^{125}Te) spectroscopy.

The molecular structures of *trans*-$[PdCl_2(TeMes_2)_2]$, $[Pd_2(\mu\text{-}Cl)_2Cl_2(TeMes_2)_2]$, *cis*-$[PdCl_2\{MesTeCH_2C_6H_2(4,6\text{-}Me_2)TeMes\}]$, $[Pd_2(\mu\text{-}OAc)_2\{CH_2C_6H_2(4,6\text{-}Me_2)TeMes)\}_2]$, $[Pd_2(\mu\text{-}OAc)_2\{CH_2C_6H_2(4,6\text{-}Me_2)Tetol\text{-}o\}_2]$ and $[Pd(\mu\text{-}OAc)(\mu\text{-}TeMes)]_4$ were established by single crystal X-ray diffraction analyses. The mononuclear complex *trans*-$[PdCl_2(TeMes_2)_2]$ exist in two polymorphic forms; which could be isolated on recrystallizing the complex from different solvents.

Section 3.3 discusses the cycloplatination of telluroethers. The reactions of K_2PtCl_4 with TeArAr′ gave complexes of composition $[PtCl_2(TeArAr')_2]$ (Ar/Ar′ = Ph_2; *o*-tol_2; Mes_2; Ph/Mes; *o*-tol/Mes). The complex $[PtCl_2(TeMes_2)_2]$ in refluxing THF afforded a mononuclear cyclometalated complex $[PtCl\{(CH_2C_6H_2Me_2\text{-}4,6)TeMes\}(TeMes_2)]$ and tends to remain in equilibrium with a binuclear derivative $[Pt(\mu\text{-}Cl)\{(CH_2C_6H_2Me_2\text{-}4,6)TeMes\}]_2$ in $CDCl_3$ solution. $[PtCl_2(MesTePh)_2]$ and $[PtCl_2(o\text{-}tolTeMes)_2]$ did not undergo cyclometalation reaction under similar reaction conditions. $[PtCl\{(CH_2C_6H_2Me_2\text{-}4,6)TeMes\}(TeMes_2)]$ on treatment with PPh_3 gave $[PtCl\{(CH_2C_6H_2Me_2\text{-}4,6)TeMes\}(PPh_3)]$. All the complexes have been characterized by elemental analysis and NMR (^1H, ^{31}P, ^{125}Te, ^{195}Pt) spectroscopy. The complexes with sterically bulky organic groups on tellurium tend to exist as *trans* isomers, while ligands with smaller Ar groups yield *cis* isomers which isomerise to *trans* form in solution. The complexes with asymmetric telluroethers exist as diastereomers which has been identified from their $^{125}Te/\ ^{195}Pt$ NMR spectra. The molecular structures of *trans*-$[PtCl_2(TeMes_2)_2]$, *trans*-$[PtCl_2(PhTeMes)_2]$, *trans*-$[PtCl_2(o\text{-}tolTeMes)_2]$, $[PtCl\{(CH_2C_6H_2Me_2\text{-}4,6)TeMes\}(TeMes_2)]$ and $[PtCl\{(CH_2C_6H_2Me_2\text{-}4,6)TeMes\}(PPh_3)]$ have been established unambiguously by single crystal X-ray diffraction analyses. The reason behind the benzylic C-H activation leading to cyclometalation only in case of $TeMes_2$ and not

for other cases has been evaluated from molecular arrangements of the complexes. A comparison of all the structures showed increase in steric bulkiness of the groups on tellurium leads to gradually decreases of the torsion angels of Pt-Te-C1-C2 from $[PtCl_2(PhTeMes)_2]$ to $[PtCl_2(o\text{-tolTeMes})_2]$ to $[PtCl_2(MesTeMes)_2]$ leading to increase in proximity of the methyl group C7 with the platinum centre.

In **Section 3.4** reactivity of telluroethers with coordinated organonitrile with platinum(II) have been described. The reactions of $[PtCl_2(NCR)_2]$ with telluroethers (ArAr'Te) in dichloromethane yielded $[PtCl_2(TeArAr')_2]$ (Ar/Ar' = Ph/Ph; tol/Mes; Mes/Mes) while in THF gave different products like $[PtCl_2(TeArAr')_2]$ (Ar/Ar' = Ph/Ph; tol/Mes; Mes/Mes), $[PtCl_2(PhCN)\{NC(O)Ph[TeMes(tol\text{-}o)]\}]$ and $[PtCl_2\{NC(O)Ph(TeMes_2)\}_2]$ depending on the steric demands of the aryl groups on tellurium, molarity of the reactants and the reaction conditions. The reaction with $TeMes_2$ in refluxing THF gave $[PtCl_2\{NC(Ph)C_4H_7O\}\{NC(O)Ph(TeMes_2)\}]$ and $[PtCl(TeMes_2)\{Te(Mes)CH_2C_6H_2Me_2\}]$ depending on the duration of heating. Reaction of $[PtCl_2(PhCN)_2]$ with MesTeAr afforded $[PtCl_2(MesTeAr)_2]$ (Ar = Ph, *o*-tol and Mes) formation of which decreases with increasing steric demand of Ar group, together with $[PtCl_2\{NC(O)Ph(TeArMes)\}_2]$. The telluroether in the latter binds to nitrogen and tellurium exists in the formal oxidation state of +4 (confirmed from XPS study). The tellurium in these complexes exhibits secondary interaction with platinum ($J(^{195}Pt\text{-}^{125}Te)$ = 309-347 Hz) and with the carbonyl oxygen. These complexes slowly dissociate in solution to give $[PtCl_2(TeMesAr)\{NC(O)Ph(TeMesAr)\}]$ finally leading to the formation of $[PtCl_2(TeMesAr)_2]$. Molecular structures of *trans*-$[PtCl_2(PhCN)\{NC(O)Ph[TeMes(tol\text{-}o)]\}]$, *trans*-$[PtCl_2\{NC(O)Ph(TeMes_2)\}_2]$, *trans*-$[PtCl_2\{NC(Ph)C_4H_7O\}\{NC(O)Ph(TeMes_2)\}]$, *trans*-$[PtCl_2\{NC(O)Ph[TeMes(tol\text{-}o)]\}_2]$, *trans*-$[PtCl_2(TeMes_2)\{NC(O)Ph(TeMes_2)\}]$, *trans*-$[PtCl_2\{NC(O)Me(TeMes_2)\}_2]$ and $[PtCl(Tetol\text{-}o)\{NC(O)Ph\}_2]$ have been unambiguously established by single crystal X-ray

diffraction analyses. From the forgoing results it can be concluded that the reactions of telluroether with commonly used platinum precursor, $[PtCl_2(RCN)_2]$ in dichloromethane yield the desired substitution products, $[PtCl_2(TeAr_2)_2]$, but in tetrahydrofuran such reactions proceed through a complex intermediate species which can be isolated and structurally characterized in case of telluroethers containing sterically demanding organic groups.

Section 3.5 describes the thermochemical behavior of cyclopalladated complexes. Organochalcogenolate-bridged cyclometalated palladium(II) complexes of the formulae, $[Pd_2(\mu\text{-}Epy)_2(Me_2NCH_2C_6H_4\text{-}C,N)_2]$ (E = S or Se), $[Pd_2(\mu\text{-}SAr)(\mu\text{-}Cl)(Me_2NCH_2C_6H_4\text{-}C,N)_2]$ (Ar = Ph, Mes (Mes = 2,4,6-$Me_3C_6H_2$)) and $[Pd_2(\mu\text{-}SeAr)_2(Me_2NCH_2C_6H_4\text{-}C,N)_2]$ (Ar = Ph, Mes) have been synthesized by the reactions of $[Pd_2(\mu\text{-}Cl)_2(Me_2NCH_2C_6H_4\text{-}C,N)_2]$ with lead or sodium salts of the chalcogenolate ligand. These complexes have been characterized by elemental analysis, mass spectral data and NMR (^1H and $^{77}Se\{^1H\}$) spectroscopy. The molecular structure of $[Pd_2(\mu\text{-}Epy)_2(Me_2NCH_2C_6H_4\text{-}C,N)_2]$ (E = S or Se) have been determined by single crystal X-ray diffraction analysis and revealed a Epy-bridged head-to-tail arrangement in which the 8-membered "$(PdECN)_2$" ring adopts a distorted twist boat conformation. The thermal behavior of these complexes has been studied by thermogravimetric analysis. The thiolato-bridged complexes decomposed to single phase Pd_4S.The selenolato-bridged complexes in general gave a mixture of palladium selenides on decomposition. $[Pd_2(\mu\text{-}SePh)_2(Me_2NCH_2C_6H_4\text{-}C,N)_2]$ decomposed into single phasic Pd_7Se_4 at ~290°C whereas$[Pd_2(\mu\text{-}SeMes)_2(Me_2NCH_2C_6H_4\text{-}C,N)_2]$ decomposed into a biphasic mixture of $Pd_{34}Se_{11}$ and Pd_4Se_7 at ~350°C. The thermal decomposition of molecular precursor, $[Pd(S_2COR)\{(CH_2C_6H_2Me_2\text{-}4,6)SeMes\}]$ (R = Et, *iso*-propyl) gave ternary PdSeS.

From the forgoing work the following conclusions can be drawn:

- For the synthesis of cyclopalladated complex via benzylic C-H bond activation using Na_2PdCl_4 as the palladating agent, the presence of polar solvent like ethanol or methanol is essential to stabilize the HCl formed as byproduct via solvation. The intra-molecular Pd···H-C agostic interaction is important for cyclometalation reaction to take place. Cyclopalladated complex serves as a useful precursor for the synthesis of other derivative containing metalated selenium ligand.
- $[Pd(OAc)_2]_3$ is a better palladating precursor than Na_2PdCl_4. Due to η^2-bridging mode of OAc^- ion a cyclic transition state is formed by coordinating palladium with one oxygen and at the same time bringing one of the *ortho* C-H bond of methyl group of mesityl into the close proximity of palladium using other oxygen atom through C-H···O interaction and leads to activation of the C-H bond with the generation of HOAc as the by-product. HOAc being a weak conjugate of OAc^- also makes metalation energetically more feasible than strong acid; HCl generated in the case of Na_2PdCl_4 and have a strong interference with the formed M-C bond than HOAc. The above advantages of OAc^- ion helps in the activation of a wide variety of telluroethers like MesTePh, MesTetol-o in addition of MesTeMes.
- Platinum(II) telluroether complexes with sterically bulky organic groups on tellurium tend to exist as *trans* isomers, while ligands with smaller Ar groups yield *cis* isomers which isomerise to *trans* form in solution. The complexes with asymmetric telluroethers exist as diastereomers which can readily be identified from their $^{125}Te/^{195}Pt$ NMR spectra. The role of anagostic interaction in cycloplatination reactions has been demonstrated.
- The reactions of telluroether with commonly used platinum precursor, $[PtCl_2(RCN)_2]$ in dichloromethane yield the desired substitution products, $[PtCl_2(TeAr_2)_2]$, but in

tetrahydrofuran such reactions proceed through a complex intermediate species which can be isolated and structurally characterized in case of telluroethers containing sterically demanding organic groups. These intermediate species are formed by sequential attack of telluroether on coordinated nitrile, mediated by the platinum center, to generate $[PtCl_2(RCN)(NC(O)R\{TeAr_2\})]$ and $[PtCl_2(NC(O)R\{TeAr_2\})_2]$. Tellurium in these species is in the formal oxidation state of +4 and shows intra-molecular interactions both with oxygen as well as platinum. The interaction with platinum exists in solution as one can observe J(Pt-Te) coupling in ^{125}Te NMR spectra. These species slowly decompose again in stepwise manner to generate $[PtCl_2(TeAr_2)\{NC(O)R(TeAr_2)\}]$ and $[PtCl_2(TeAr_2)_2]$.

- Cyclopalladated molecular precursors are suitable source for the synthesis of single phasic palladium chalcogenide at comparatively low temperature. The stoichiometry of the palladium chalcogenide can be easily tuned with the variation of the auxiliary group attached to organochalcogen ligands. Xanthate complexes have been successfully used as precursors for the synthesis of ternary palladium chalcogenides.

References

1. H. Gavin, Platinum Met. Rev., 54 (2010) 166-171.
2. W.C. Zeise, Mag. Pharm., 35 (1830) 105.
3. B. Rosenberg, L. Vancamp, L. Grimley, E. B. A. Thompson, Biol. Chem., 242 (1967**)** 1347-1352.
4. H. C. Clark, V. K. Jain, Coord. Chem. Rev., 55 (1984) 151-204.
5. V. K. Jain, G. S. Rao, L. Jain, Adv. Organomet. Chem., 27 (1987) 113-168.
6. I. I. Chernyaev, Ann. Inst. Platine USSR, 4 (1926) 243-275; Chem. Abst, 21 (1927) 2620.
7. J. Simdt, Chem. Ind. (London), (1962) 54-61; P. M. Henry, J. Am. Chem. Soc., 86 (1964) 3246-3250.
8. D. C. Harris, L. J. Cabri, The Canadian Mineralogist, 29 (1991) 231-237.
9. E. M. Wise in Metals Handbook, ed. T. Lyman, American Society of Metals, Cleveland, (1968).
10. F. E. Beamish, W. A. E. McBryde, R. R. Barefoot, Rare Metals Handbook, ed. C. A. Hampel, Reinhold, New York, (1954) p. 291.
11. F. R. Hartley, The chemistry of platinum and palladium, John Wiley & Sons, New York (1973).
12. S. E. Livingstone, Comprehensive Inorganic Chemistry, ed. J. C. Bailar, Pergamon Press, 3 (1973) 1274.
13. R. J. Puddephat, Chem. Soc. Rev., 12 (1983) 99-127.
14. J. M. Davidson, C. Triggs, J. Chem. Soc (A), (1968) 1324-1300.
15. M. Yamashita, I. Takamiya, K. Jin, K. Nozaki, Organometallics, 25 (2006) 4588-4595.
16. V. G. Albano, G. Natile, A. Panunzi, Coord. Chem. Rev., 133 (1994) 67-114.
17. H. C. Clark, R. J. Puddephat, Inorg. Chem., 10 (1971) 18.
18. T. Mizuta, A. Okano, T. Sasaki, H. Nakazawa, K. Miyoshi, Inorg. Chem., 36 (1997) 200-203.
19. R. Uson, J. Fornies, M. Thomas, B. Menjon, R. Bau, K. Suenkel, E. Kuwabara, Organometallics, 5 (1986) 1576-1581.
20. D. M. Roundhill, H. B. Gray, Chi. M. Che, Acc. Chem. Res., 22 (1989) 55-61.
21. V. K. Jain, Rev. Inorg. Chem., 9 (1988) 299.
22. A. J. Canty, Handbook of Organopalladium Chemistry for organic synthesis, ed. E. Negishi, John Wiley & Sons 189.
23. U. Belluco, Organometallic and coordination chemistry of Platinum, Academic, New York, (1974).
24. D. M. Roundhill, Comprehensive Coordination Chemistry, ed. G. Willkinson, Pergamon Press 5 (1987) 353.
25. P. M. Maitlis, The Organic Chemistry of Palladium, Academic Press, (1971) 1-2.
26. P. M. Maitlis, P. Espinet, M. J. H. Russell, Comprehensive Organometallic Chemistry, eds. G. Willkinson, F. G. A. Stone and E. W. Ebel, Pergamon Press, Oxford, 6 (1982), Chap 38-39.

27. C. F. J. Barnard, M. J. H. Russell, Comprehensive Coordination Chemistry, eds. G. Willkinson, R. D. Gillard and J. A. M. Cleverty, Pergamon Press, Oxford, 5(1987) 1099.
28. B. Cornils, W. A. Hermann, Applied Homogenous Catalysis with Organometallic Compound, VCH (1996).
29. A. A. Zinn, L. Brandet, H. D. Kaisz, R. F. Hicks, Chemistry of Metal CVD, eds. T. K. Kodas and M. J. Kampden-Smith, VCH, **7** (1994) 329.
30. E. Wong and C. M. Giandomenico, Chem. Rev., 99 (1999) 2451-2466.
31. F. Bosolo, R. G. Pearson, Prog. Inorg. Chem., 4 (1962) 381-453.
32. F. Basolo, R.G. Pearson, Mechanisms of Inorganic Reactions, 2nd Edition, Wiley, New York (1967).
33. A. C. Cope, R. W. Siekman, J. Am. Chem. Soc., 87 (1965) 3272-3273.
34. S. Trofimenko, Inorg. Chem., 12 (1973) 1215-1221.
35. J. Campora, P. Pala, E. Carmona, Coord. Chem. Rev., 207 (1999) 193-195.
36. I. Omae, Organometallic IntramolecularCoodination Compounds; Elsevier: Amsterdam, The Netherlands, 1986.
37. J. Dehand, M. Pfeffer, Coord. Chem. Rev., 18 (1976) 327-352.
38. I. Omae, Chem. Rev., 79 (1979) 287-321.
39. M. I. Bruce, Angew. Chem., Int. Ed. Engl. 16 (1977) 73-86.
40. I.Omae, Coord. Chem. Rev., 28 (1979) 97-115.
41. I. Omae, Coord. Chem. Rev., 32 (1980) 235-271.
42. I. Omae, Coord. Chem. Rev., 42 (1982) 245-257.
43. I. Omae, Coord. Chem. Rev., 53 (1984) 261-291.
44. E. C. Constable, Polyhedron, 3 (1984) 1037-1057.
45. I. P. Rothwell, Polyhedron, 4 (1985) 177-200.
46. G. R. Newkome, W. E. Puckert, V. K. Gupta, G. E. Kiefer, Chem. Rev.,86 (1986) 451-489.
47. M. Albrecht, Chem. Rev., 110 (2010) 576-623.
48. I. Omae, J. Organomet. Chem., 692 (2007) 2608–2632.
49. M. Beller, H. Fischer, W. A. Herrmann, K. Öfele, C. Brossmer, Angew. Chem., Int. Ed. Engl., 34 (1995) 1848–1849.
50. D. Zim, A. S. Gruber, G. Ebeling, J. Dupont, A. L. Monteiro, Org. Lett., 2 (2000) 2881–2884.
51. Q. Yao, E. P. Kinney, C. Zheng, Org. Lett., 6 (2004) 2997–2999.
52. J. Dupont, C. S. Consorti, J. Spencer, Chem. Rev., 105 (2005) 2527–2571.
53. M. Ghedini, I. Aiello, A. Crispini, A. Golemme, M. La Deda, D. Pucci, Coord. Chem. Rev., 250 (2006) 1373–1390.
54. D. A. Alonso, C. Najera, Chem. Soc. Rev., 39 (2010) 2891–2902.
55. M. Albrecht, G. van Koten, Adv. Mater., 11 (1999) 171-174.

56. Q. Zhao, T. Cao, F. Li, X. Li, H. Jing, T. Yi, C. Huang, Organometallics,26 (2007) 2077-2081.
57. I. M. Dixon, J. –P. Collin, J. –P. Sauvage, L. Flamigni, S. Encinas, F. Barigelletti, Chem. Soc. Rev., 29 (2000) 385-391.
58. M. E.Thopson, P. E. Djurovich, S.Barlow, S. Marder, Comprehensive Organometallic Chemistry III; eds. D. M. P. Mingos, R. H. Crabtree, Elsevier: Amsterdam, The Netherlands, 2007; Vol. 12, p 145.
59. J. A. G. Williams, Chem. Soc. Rev., 93 (1993) 861.
60. S. H. Wadman, M. Lutz, D. M.Tooke, A. L. Spek, F. Hartl, R. W. A. Havenith, G. P. M. van Klink, G. van Koten, Inorg. Chem., 48 (2009) 1887-1900.
61. K. Severin, R. Bergs, W. Beck, Angew. Chem. Int. Ed., 37 (1998) 1634-1654.
62. A. D. Ryabov, V. S. Sukharev, L. Alexandrova. R. Le Lagadee, M. Pfeffer, Inorg. Chem., 40 (2001) 6529-6532.
63. P. J. Dyson, G. Sava, Dalton Trans., (2006) 1929-1933.
64. S. A. Kurzeev, A. S.Vilesov, T. V. Fedorova, E. V. Stepanova, O. V. Koroleva, C. Bukh, M. J. Bjerrum, I. V. Kurnikov, A. D. Ryabov, Biochemistry, 48 (2009) 4519-4527.
65. A. D. Ryabov, Chem. Rev., 90 (1990) 403-424.
66. J. Dupont, M. Pfeffer, Eds. Palladacycles; Wiley-VCH: Weinheim, Germany, 2008.
67. D. L. Davis, S. M. A. Donald, S. A. Macgregor, J. Am. Chem. Soc., 127 (2005) 13754-13755.
68. R. F. Jordan, A. S. Guram, Organometallics, 9 (1990) 2116-2123.
69. A. C. Cope, E. C. Friedrich, J. Am. Chem. Soc., 90 (1968) 909-913.
70. J. A. M. van Beek, G. van Koten, M. J. Ramp, K. Vrieeze, Inorg. Chem., 30 (1991) 3059-3068.
71. G. Van Koten, Pure Appl. Chem., 61 (1989) 1681-1694.
72. J. Vicente, I. Saura-Liamas, Comments Inorg. Chem., 28 (2007) 39-72.
73. V. V. Dunina, O. N. Gorunova, Russ. Chem. Rev., 74 (2005) 871-913.
74. W. A. Herrmann, C. Brossmer, K. öfele, C. –P. Reisinger, T. Priermeier, M. Beller, H. Fischer, Angew. Chem., Int. Ed. Engl., 34 (1995) 1844-1848.
75. B. L. Shaw, J. Organomet. Chem., 200 (1980) 307-318.
76. V. V. Dunina, O. A. Zalevskaya, V. M. Potapov, Russian Chemical Review, 57 (1988) 250-269.
77. A. J. Klaus, P. Rys, Helv. Chim. Acta, 64 (1981) 1452-1466.
78. M. Hugentobler, A. J. Klaus, H. Mettler, P. Rys, G. Wehrle, Helv. Chim. Acta, 65 (1982) 1202-1211.
79. K. Gehrig, M. Hugentobler, A. J. Klaus, P. Rys, Inorg. Chem., 21 (1982) 2493-2494.
80. S. Matsuda, Sh. Kikkawa, I. Omae, Kogyo Kagaku Zasshi., 69 (1966) 646; Chem. Abs., 65 (1966) 18612.

81. H. Werner, H. J. Kraus, J. Organometal. Chem., 204 (1981) 415-422.
82. R. G. Goel, R. G. Montemyor, Inorg. Chem., 16 (1977) 2183-2186.
83. H. C. Clark, A. B. Goel, S. Goel, Inorg. Chem., 18 (1979) 2803-2808.
84. H. C. Clark, A. B.Goel, R. G. Goel, S. Goel, W. O. Ogini,Inorg. Chim. Acta, 31 (1978) L441-L442.
85. A. J. Deeming, I. P. Rothwell, J. Organometal. Chem., 205 (1981) 117-131.
86. A. J. Deeming, I. P. Rothwell, Pure Appl. Chem., 52 (1980) 649-655.
87. G. R. Newkome, T. Kawato, D. K. Kohli, W. E. Puckett, B. D. Olivier, G. Chiari, F. R. Fronczek, W. A. Deutsch, J. Am. Chem. Soc., 103 (1981) 3423-3429.
88. G. R. Newkome, W.E. Puckett, G. E. Kiefer, V. K. Gupta, F. R. Fronczek, D. C. Pantaleo, G. L. McClure, J. B. Simpson, W. A. Deutsch, Inorg. Chem., 24 (1985) 811-826.
89. J. M. Duff, B. E. Mann, B. L. Shaw, B. Turtle, J. Chem. Soc., Dalton Trans., (1974) 139-145.
90. H. Onous, K. Minami, K. Nakagawa, Bull. Chem. Soc. Japan, 43 (1970) 3480-3485.
91. D. F. Gill, B. E. Mann, B. L. Shaw, J. Chem. Soc. Dalton Trans., (1973) 270-278.
92. Y. Tamaru, M. Kagotani, Z. Yoshida, Angew. Chem., 93 (1981) 1031-1032.
93. S. Baba, S. Kawaguchi, Inorg. Nucl. Chem. Lett., 11 (1975) 415-420.
94. A. J. Deeming, J. P. Rothwell, J. Chem. Soc. Chem. Comm., (1978) 344-345.
95. G. W. Parshall, Acc. Chem. Res., 3 (1970) 139-144.
96. A. J. Canty, G. van Koten, Acc. Chem. Res., 28 (1995) 406-413.
97. M. Brookhart, M. L. H. Green, G. Perkin, Proc. Natt. Acad. Sci. U.S.A, 104 (2007) 6908-6914.
98. H. V. Huynth, L. R. Wong, P. S. Ng, Organometallics, 27 (2008) 2231-2237.
99. A. T. Colak, O. Z. Yesilel, O. Büyükgüngör, J. Molecular Struct., 991 (2011) 68-72.
100. W. Scherer, A. C. Dunbar, J. E. Barquera-Lozada, D. Schmitz, D. Schmitz, G. Eickerling, J. Ebad-Allah, C. Kuntscher, Angew. Chem., Int. Ed., 54 (2015) 2505-2509.
101. W. I. Sundquist, D. P. Bancroft, S. J. Lippard, J. Am. Chem. Soc., 112 (1990) 1590-1596.
102. V. K. Jain, L. Jain, Coord. Chem. Rev., 249 (2005) 3075-3197.
103. P. Espinet, M. A. Esteruelas, L. A. Oro, J. L. Serrano, E. Sola,Coord. Chem. Rev., 117 (1992) 215-274.
104. M. D. Santana, R. Garcia-Bueno, G. Garcia, G. Sanchez, J. Garcia, J. Perez, L. Garcia, J. L. Serrano,Dalton Trans., 40 (2011) 3537-3546.
105. N. D. Ghawale, S. Dey, V. K. Jain, M. Nethaji, Inorg. Chim. Acta, 361 (2008) 2462-2470.
106. M. A. Baldo, M. E. Thompson, S. E. Forrest, Nature, 403 (2000) 750-753.
107. J. Slinker, D. Bernards, P. L. Houston, H. D. Abruňa, S. Bernhard, G. G. Malliaras, Chem. Commun., (2003) 2392-2399 .
108. J. D. Slinker, A. A. Gorodetsky, M. S. Lowry, J. wang, S. Parker, R. Rohl, S. Bernhard, G. G. Malliaras, J. Am. Chem. Soc., 126 (2004)2763-2767 .

109. Y. Byun, W. S. jeon, T. W. Lee, Yi-Y. Lyu, S. Chang, O. Kwon, E. Han, H. Kim, M. Kim, Ha-J. Lee, R. R. Das, Dalton Trans., (2008) 4732-4741.
110. P. J. Spellane, M. Gouterman, A. Antipas, S. Kim, Y. C. Liu, Inorg. Chem., 19 (1980) 386-391.
111. D. S. Lawrence, D. G. Whitten, Photochemistry and Photobiology, 64 (1996) 923 -935.
112. M. Hissler, J. E. McGarrah, W. B. Connick, D. K. Geiger, S. D. Cummings, R. Eisenberg, Coord. Chem. Rev., 208 (2000) 115-137.
113. J. A. G. Williams, S. Develay, D. L. Rochester, L. Murphy, Coord. Chem. Rev., 252 (2008) 2596-2611.
114. M. A. Baldo, S. Lamansky, P. E. Burrows, M. E. Thompson, S. R. Forrest, Appl. Phys. Lett., 75 (1999) 4-6.
115. R. Gimenez, D. P. Lydon, J. L. Serrano, Curr. Opin. Solid State Mater. Sci., 6 (2002) 527-535.
116. A. P. Polishchuk, T. V. Timofeeva, Russian Chem. Rev., 62 (1993) 291-321.
117. K. Hallman, C. Moberg, Adv. Syn. Cat., 343 (2001) 260-263.
118. S. Paavola, K. Zetterberg, T. Privalov, I. Csöregh, Adv. Syn. Cat., 346 (2004)237-244.
119. T. Privalov, C. Linde, K. Zetterberg, C. Moberg, Organometallics, 24 (2005) 885-893.
120. S. G. Murray, F. R. Hartley, Chem. Rev., 81 (1981) 365-414.
121. H. J. Gysling, The Chemistry of Organoselenium and Organotellurium Compounds, S. Patai (ed), 1(18), Wiley, N. -Y., (1986), 679.
122. W. Levason, S. D. Orchard, G. Reid, Coord. Chem. Rev., 225 (2002) 159-199.
123. W. Levason, G. Reid, J. Chem. Soc., Dalton Trans., (2001) 2953-2960.
124. A. M. Masdeu-Bulto, M. Diegez, E. Martin, M. Gomez, Coord. Chem. Rev., 242 (2003) 159-201.
125. K. G. Orrell, Coord. Chem. Rev., 96 (1989) 1-48.
126. J. Chatt, L. M. Venanzi, J. Chem. Soc., (1957) 2351-2356.
127. J. Chatt, L. M. Venanzi, J. Chem. Soc., (1955) 2787-2793.
128. K. Öfele, E. Dotzauer, J. Organomet. Chem., 42 (1972) C87-C90.
129. D. D. Perrin, W. L. F. Armarego, D. R. Perrin, Purifiaction of Laboratory Chemicals, Pergamon, Oxford, 2nd ed.(1980).
130. NMR and Periodic Table, Eds. R. K. Harris and B. E. Mann, Academic Press, (1978).
131. SIR92 –A. Altomare, G. Gascarano, C. Giacovazzo, A. Guagliardi, M. C. Burla, G. Polidori, M. Camalli, J. Appl. Crystallogr., 27 (1994) 435.
132. SHELX-G. M. Sheldrick, Acta Cryst. Sect. A: Found. Crystallogr., 64 (2008) 112-122;G. M. Sheldrick, “Program for Absorption Correction of Area Detector Frames”, BRUKER AXS Inc., 5465 East Cheryl Parkway, Madison, WI 53711–5373 USA.

133. O. V. Dolomanov, L. J. Bourhis, R. J. Gildea, J. A. K. Howard, H. Puschmann, "OLEX2: A Complete Structure Solution, Refinement and Analysis Program", J. Appl. Cryst., 42 (2009) 339-341.

134. A. L. Spek, "PLATON - A Multipurpose Crystallographic Tool",J. Appl. Cryst., 36 (2003) 7-13; b) A. L. Spek, Utrecht University, Utrecht, The Netherlands 2008.

135. Crystal structure 3.7.0: Crystal structure Analysis Package, Rigaku, Rigaku/MSC 2000–2005, 9009 New Trials Dr., The Wood, TX 77381, USA.

136. D. J. Watkins, C. K. Prout, J. R. Carruthers, P. W. Betteridge,CAMERON–A Molecular Graphics Package, Chemical Laboratory, Oxford (U.K.), (1996).

137. PSISCANS- A. C. T. North, D. C. Phillips, F. S. Mathews, Acta Crystallography., A24 (1968) 351-359.

138. C. K. Johnson, ORTEP-II, Report ORNL-5136, Oak ridge National Laboratory, Oak Ridge, TN (1976).

139. L. J. Farrugia, J. Appl. Crystallography, 30 (1997) 565-566. APEX2 "Program for Data Collection on Area Detectors" BRUKER AXS Inc., 5465 East Cheryl Parkway, Madison, WI 53711–5373 USA.

140. A. J. Costanza, R. J. Coleman, R. M. Pierson, C. S. Marvel, C. King, J. Poly. Sci., 17 (1955) 319-340.

141. M. Bochmann, K. J. Webb, M. B. Hursthouse, M. Mazid, J. Chem. Soc. Dalton Trans., (1991) 2317-2323.

142. K. K. Bhasin, V. Arora, T. M. Klapotke, M. J. Crawford, Eur. J. Inorg. Chem., (2004) 4781-4788.

143. M. Akiba, M. V. Lakshmikantham, K. Y. Jen, M. P. Cava., J. Org. Chem., 49 (1984) 4819-4821.

144. T. M. Klapotke, B. Krumm, P. Mayer, K. Polborn,I. Schwab, Z. Ang. Allg. Chem., 631(2005) 2677-2682.

145. S. Ghoshal, N. P. Kushwah, D. P. Dutta, V. K. Jain, Appl. Organometal. Chem., 19 (2005) 1257-1262.

146. N. Ghavale, S. Dey, A. Wadawale, V.K. Jain, Organometallics, 27 (2008) 3297-2302.

147. N. Ghavale, S. Dey, A. Wadawale, V. K. Jain, J. Organomet. Chem., 696 (2011) 3491-3498.

148. G. B. Kauffmann, J. H. Tsai, Inorg. Synth., 8 (1966) 234.

149. T. A. Stephenson, S. M. Morehouse, A. R. Powell, J. P. Heffer, G. Willkinson, J. Chem. Soc.,(1995) 3632-3640.

150. V. I. Bakhmutov, J. F. Berry, F. A. Cotton, S. Ibragimov, C. A. Murillo, Dalton Trans., (2005) 1989-1992.

151. A.D. Ryabov, V.A. Polyakov, A.K. Yatsimirsky, J. Chem. Soc. Perkin Trans. II, (1983) 1503-1509.

152. T. Chakraborty, S. Sharma, H. B. Singh, R. J. Butcher, Organometallics, 30 (2011) 2525-2530.
153. A. Kumar, M. Agarwal, A. K. Singh, R. J. Butcher, Inorg. Chim. Acta, 362 (2009) 3208-3218.
154. S. Kolay, N. Ghavale, A. Wadawale, D. Das, V. K. Jain, Phosphorus, Sulfur, and Silicon, 188 (2013) 1449-1461.
155. A. J. Deeming, M. N. Meah, P. A. Bates, M. B. Hursthouse, J. Chem. Soc., Dalton Trans., (1988) 2193-2199.
156. S. Dey, V. K. Jain, S. Chaudhury, A. Knoedler, F. Lissner, W. Kaim, J. Chem. Soc., Dalton Trans., (2001) 723-728.
157. S. Dey, V. K. Jain, B. Varghese, T. Schurr, M. Niemeyer, W. Kaim, R. J. Butcher, Inorg. Chim. Acta, 359 (2006) 1449-1457.
158. E. C. Constable, A. M. W. C. Thompson, T. A. Leese, D. G. F. Reese, D. A. Tocher, Inorg. Chim. Acta, 182 (1991) 93-100.
159. M. Kato, A. Omura, A. Toshikawa, S. Kishi, Y. Sugimoto, Angew. Chem., Int. Ed., 41 (2002) 3183-3185.
160. J. Ruiz, F. Florenciano, G. Lopez, P. A. Chaloner, P. B. Hitchcock, Inorg. Chim. Acta, 281 (1998) 165-173.
161. J. Dupont, N. Beydoun and M. pfeffer, J. Chem. Soc., Dalton Trans., (1989) 1715-1720.
162. R. S. Chauhan, G. Kedarnath, A. Wadawale, A. L. Rheingold, A. M. Castro, R. A. Perez, V. K. Jain, Organometallics, 31 (2012) 1743-1750.
163. R. S. Chauhan, G. Kedarnath, A. Wadawale, A. M. Z. Slawin, V. K. Jain, Dalton Trans., 42 (2013) 259-269.
164. L. B. Han, N. Choi, M. Tanaka, J. Am. Chem. Soc., 119 (1997) 1795-1796.
165. G. K. Rao, A. Kumar, M. P. Singh, A. K. Singh, J. Organomet. Chem., 749 (2014) 1-6.
166. A. Kumar, M. Agarwal, A. K. Singh, J. Organomet. Chem., 693 (2008) 3533-3545.
167. K. N. Sharma, H. Joshi, A. K. Sharma, O. Prakash, A. K. Singh, Chem. Commun., 49 (2013) 9344-9346.
168. M. Risto, E. M. Jahr, M. S. Hannu-Kuure, R. Oilunkaninemi, R. S. Laitinen, J. Organomet. Chem., 692 (2007) 2193-2204.
169. S. Kolay, A. Wadawale, D. Das, H. Kisan, R. B. Sunoj, V. K. Jain, Dalton Trans., 42 (2013) 10828-10837.
170. M. Bochmann, A. P. Coleman, K. J. Webb, M. B. Hursthouse, M. Mazid, Angew. Chem., Int. Ed., 30 (1991) 973-975.
171. H. P. Nayek, H. Niedermeyer, S. Dehnen, Dalton Trans., (2009) 4208-4212.
172. A. I. Stash, T. I. Pereplkova, Yu. G. Noskov, T. M. Buslaeva, I. P. Romm, Russ. J. Coord. Chem., 27 (2001) 585-590.
173. D. K. Palura, S. Dey, A. Wadawale, V. K. Jain, J. Organomet. Che., 728 (2013) 52-56.

174. H. V. Huynth, L. R. Wong, P. S. Ng. Organometallics, 27 (2008) 2231-2237; A. T. Colak, O. Z. Yesilel, O. Büyükgüngör, J. Molecular Struct., 991 (2011) 68-72.
175. T. Kemmitt, W. Levason, Inorg. Chem., 29 (1990) 731-735.
176. L. Vigo, R. Oilunkaniemi, R. S. Laitinen, Eur. J. Inorg. Chem., (2008) 284-290.
177. J. R. Allkins, P. J. Hendra, J. Chem. Soc. (A) (1967) 1325-1329.
178. R. J. Cross, T. H. Green, R. Keat, J. Chem. Soc. Chem. Commun., (1974) 207-208.
179. R. J. Cross, T. H. Green, R. Keat, J. Chem. Soc. Dalton Trans., (1967) 1150-1152.
180. H. J. Gysling, N. Zumbulyadis, J. A. Robertson, J. Organomet. Chem., 209 (1981) C41-C44.
181. A. K. Singh, M. Kadarkaraisamy, S. Husebye, K. W. Tomroos, J. Chem. Res., (2000) 64-65.
182. A. K. S. Chauhan, S. N. Bharti, R. C. Srivastava, R. J. Butcher, A. Dutthie, J. Organomet. Chem., 708-709 (2012) 75-81.
183. A. K. Singh, J. S. Kumar, R. J. Butcher, Inorg. Chim. Acta., 312 (2001) 163-169.
184. J. E. Drake, J. H. E. Bailey, A. K. Singh, V. Srivastava, Acta Cryst. C 49 (1993) 684-687.
185. M. Knorrr, F. Guyon, I. Jourdain, S. Kneifel, J. Frenzel, C. Strohmann, Inorg. Chim. Acta, 350 (2003) 455-466.
186. K. V. Vivekananda, S. Dey, A. Wadawale, N. Bhuvanesh, V. K. Jain, Dalton Trans., 42 (2013) 14158-14167.
187. V. K. Jain, R. S. Chauhan, Coord. Chem. Rev., 306 (2016)270-301.
188. R. S. Chauhan, G. Kedarnath, A. Wadawale, A. Munoz-Castro, R. Arratia-Perez, V. K. Jain, W. Kaim, Inorg. Chem., 49 (2010) 4179-4185.
189. D. M. Adams, J. Chatt, J. Gerratt, A. D. Westland, J. Chem. Soc., (1964) 734-739.
190. R. A. Michelin, M. Mozzon, R. Bertani, Coord. Chem. Rev., 147 (1996) 299-338.
191. V. Y. Kukushkin, A. J. L. Pombeiro, *Chem. Rev*., 102 (2002**)** 1771-1802.
192. A. J. L. Pombeiro, V. Y. Kukushkin, Comprehensive Coordination Chemistry-II. (2004**)** vol-I, pp: 639, Vol ed. A. B. P. Lever.
193. D. S. Bolotin, N. A. Bokach, M. Haukka, V. Y. Kukushkin, Inorg. Chem., 51 (2012**)** 5950-5964.
194. J. Lasri, M. L. Kuznetsov, M. F. C. G. d. Silva, A. J. L. Pombeiro, Inorg. Chem., 51 (2012) 10774-10786.
195. D. S. Bolotin, N. A. Bokach, A. S. Kritchenkov, M. Haukka, V. Y. Kukushkin, Inorg. Chem., 52 (2013) 6378-6389.
196. V. Gupta, V. Karthik, G. Anantharaman, Dalton Trans., 44 (2015) 758-766.
197. F. Pünner, G. Hilt, Chem. Commun., 50 (2014) 7310-7313.
198. I. Korobkov, S. Gambarotta, G. P. A. Yap, Organometallics, 20 (2001) 2552-2559.
199. J. Clayden, Nat. Chem., 2 (2010) 523-524.
200. H. Duddeck, A. Biallaβ, Magn. Reson. Chem., 32 (1994) 303-311.

201. S. Misra, A. K. S. Chauhan, P. Singh, R. C. Srivastava, A. Duthie, R. J. Butcher, Dalton Trans., 39 (2010) 2637-2643.
202. J. Beckmann, J. Bolsinger, A. Duthie, P. Finke, Dalton Trans., 42 (2013) 12193-12203.
203. T. P. Lin, F. P. Gabbaï, J. am. Chem. Soc., 134 (2012) 12230-12238.
204. H. Konno, Y. Yamamoto, Bull. Chem. Soc. Jpn., 61 (1988) 2990-2992.
205. J. S. Hammond, N. Winograd, J. Electroanal. Chem. Interfacial Electrochem., 78 (1977) 55-69.
206. P. F. Oblad, J. E. Bercaw, N. Hazari, A. J. Labinger, Organometallics, 29 (2010) 789-794.
207. S. Dey, V. K. Jain, A. Knödler, A. Klein, W. Kaim, S. Záliš, Inorg. Chem., 41 (2002) 2864-2870.
208. T. Chivers, J. Chem. Soc. Dalton Trans., (1996) 1185-1194.
209. N. Sudha, H. B. Singh, Coord. Chem. Rev., 135/136 (1994) 469-515.
210. Y. Torubaev, A. Pasynskii, P. Mathur, Coord. Chem. Rev., 256 (2012) 709-721.
211. L. Y. Chiang, J. W. Sioirczeweki, R. Kastrup, C. S. Hsu, R. B. Upasani, J. Am. Chem. Soc., 113 (1991) 6574-6584.
212. S. Eijsbouts, V. H. J. DeBeer, R. Prins, J. Catal., 109 (1988) 217-220.
213. S. Dey, V. K. Jain, Platinum Met. Rev, 48 (2004) 16-19.
214. B. Radha, G. U. Kulkarni, Adv. Funct. Mater., 20 (2010) 879-884.
215. H. Kyama, T. Iwata, Japanese Patent, 08 /095, 209; Mitsubishi Paper Mills Ltd, 1996; O. Tanabe, U. S. Patent, 5, 030, 545; Fuji Photo Film Co Ltd, 1991.
216. P. Singh, D. Das, A. Kumar, A. K. Singh, Inorg. Chem. Commun., 15 (2012) 163-166.
217. V. Singh, G. K. rao, A. Kumar, A. K. singh, Dalton Trans., 41 (2012) 1142-1145.
218. J. Buey, G. A. Diez, P. Espinet, S. Garcia-Granda, E. Perez-Carreno, Eur. J. Inorg. Chem., 1235-1241.
219. B. C. Tzeng, W. F. Fu, C. M. Che, H. Y. Chao, K. K. Cheung, S. M. Peng, J. Chem. Soc. Dalton Trans., (1999) 1017-1023.
220. K. Umakoshi, A. Ichimura, I. Kinoshita, S. Ooi, Inorg. Chem., 29 (1990) 4005-4101.
221. T. Koshiyama, A. Omura, M. Kato, Chem. Lett., 33 (2004) 1386-1387.
222. S. Narayan, V. K. Jain, S. Chaudhury, J. Organomet. Chem., 530 (1997) 101-104.
223. S. Narayan, V. K. Jain, R. J. Butcher, J. Organomet. Chem., 549 (1997) 73-80.
224. K. P. Chaudhury, S. Dey, A. P. Wadawale, V. K. Jain, J. Organomet. Chem., unpublish.
225. N. Ghavale, A. Wadawale, S. Dey, V. K. Jain, J. Organomet. Chem., 695 (2010) 1237-1245.